Orexin A in the Central Control of Cardiorespiratory Regulation

Mst. Israt Zahan Shahid
B.Pharm (Hons)

A thesis submitted to Macquarie University in fulfilment of the requirements for the degree of Doctor of Philosophy.

TABLE OF CONTENTS

ABSTRACT

Presympathetic neurons in the rostral ventrolateral medulla (RVLM) provide a monosynaptic excitatory drive to sympathetic preganglionic neurons (SPN) of the spinal cord and are involved in the differential regulation of sympathetic outflows to different target tissues. Neurons in the RVLM integrate information from the centre and periphery, including: respiration, and baro-, chemo- and somatosympathetic reflex afferent neurons. Metabotropic transmitters including neuropeptides, apart from basic neurotransmitters (e.g. glutamate and GABA), with long-term effects play important roles in the regulation of RVLM neurons. This thesis investigates the role of one such neuropeptide, orexin A (OX-A), in the control of blood pressure and breathing and to see if its role is altered in diseases such as hypertension. Results of this work will provide a better understanding of the way that the brain controls blood pressure and breathing, and may also lead to the development of new therapies for hypertension.

In the first set of experiments (chapter 3, Shahid *et al.,* 2011), the effects of OX-A in the spinal cord on vasomotor tone and adaptive reflexes were investigated. Intrathecal (i.t.) administration of OX-A caused a prolonged and dose-dependent increase in mean arterial pressure (MAP), heart rate (HR) and splanchnic sympathetic nerve activity (sSNA). OX-A also dose-dependently increased respiratory drive, as indicated by a rise in phrenic nerve amplitude (PNamp) and a fall in phrenic nerve frequency (PNf), an increase in neural minute ventilation, a lengthening of the expiratory period, and a shortening of the inspiratory period. All cardiorespiratory effects of OX-A were attenuated by the orexin 1 (OX_1) receptor antagonist SB 334867. I.t. OX-A significantly reduced both the sympathoexcitatory peaks of somatosympathetic reflex but increased baroreflex sensitivity.

In the second set of experiments (chapter 4, Shahid *et al.,* 2012a), immunohistochemistry was performed to detect the presence of OX-A and it's receptors in the RVLM. Tyrosine hydroxylase immunoreactive (TH-ir) neurons in the RVLM frequently expressed OX_1 and orexin 2 (OX_2) receptors and closely apposed to OX-A-ir terminals. OX_1 receptor immunoreactivity was found in 78 ± 2% of TH-ir neurons in the RVLM and OX_2 receptor in 77 ± 3% of TH-ir neurons. In addition, within the RVLM, about 51% of OX_1 receptors and 56% of OX_2 receptors were expressed in non-TH-ir or non-C1 neurons, suggesting that both C1 and non-C1 neurons in the RVLM contain both OX receptors.

In the third set of experiments (chapter 4, Shahid *et al.,* 2012a), OX-A was injected bilaterally into the RVLM of normotensive Sprague-Dawley rats and the effects on cardiorespiratory function and sympathetic reflexes were observed. Microinjection of OX-A into the RVLM elicited a pressor and sympathoexcitatory response. Responses to OX-A were attenuated by the OX_1 receptor antagonist, SB 334867, and reproduced by the OX_2 receptor agonist, [Ala11, D-Leu15]orexin B indicating that both OX receptors are involved in OX-A mediated response in the RVLM. OX-A increased baroreflex sensitivity but attenuated the somatosympathetic reflex. OX-A injection into the RVLM also increased or reduced sympathoexcitation following hypoxia or hypercapnia respectively.

A fourth set of experiments (chapter 5) were conducted to investigate whether OX-A responses in the RVLM of normotensive rats are exaggerated in hypertensive animal models. OX-A injected into the RVLM elicited hypertension, tachycardia and sympathoexcitation in both hypertensive and normotensive rat models. The pressor and sympathoexcitatory responses evoked by OX-A were exaggerated in spontaneously hypertensive rats (SHR). OX-A also increased PNamp in both strains. The sympathoexcitatory peaks of somatosympathetic reflex were attenuated following OX-A injection in both SHR and Wistar-Kyoto rats (WKY). The attenuation of the sympathoexcitatory peaks of the somatosympathetic reflex was potentiated in SHR. OX-A injection into the RVLM increased baroreflex sensitivity in both SHR and WKY. An interesting finding is that the extent of increase in the barosensitivity evoked by OX-A was reduced in SHR as compared to WKY.

Taken together, the presence of OX receptors in C1 bulbospinal sympathoexcitatory neurons of the rostral RVLM and the effects of OX-A in the RVLM and spinal cord on basal cardiorespiratory parameters and adaptive reflexes suggest that OX receptor activation plays a key role in mediating the sympathoexcitatory responses. These data also suggest a role for OX-A in the development and maintenance of essential hypertension. The precise physiological circumstances in which OX-A is released to exert the effects described in this thesis remains to be established.

DECLARATION OF CONTRIBUTION TO CHAPTERS

Chapter 3

The author was the major contributor to this work. Conception, design and conduction of experiments, data analysis and drafting of manuscript were performed by the author. AA Rahman contributed to some experiments.

Chapter 4

The author was a major contributor to this work. Conception and design of experiments, data acquisition and analysis were performed by both the author and AA Rahman. The author wrote the manuscript. AA Rahman was involved in the critical revision of the manuscript.

Chapter 5

The author was the major contributor to this work. Conception, design and conduction of experiments, data analysis and drafting of manuscript were performed by the author. AA Rahman assisted with some data acquisition.

PUBLICATIONS ARISING FROM THIS THESIS

REFEREED JOURNAL ARTICLES

Shahid IZ*, Rahman AA* & Pilowsky PM. (2012). Orexin A in rat rostral ventrolateral medulla is pressor, sympathoexcitatory, increases barosensitivity and attenuates the somatosympathetic reflex. ***Br J Pharmacol*** 167, 2292-2303.
***Equal first authors.**

Shahid IZ, Rahman AA & Pilowsky PM. (2011). Intrathecal orexin A increases sympathetic outflow and respiratory drive, enhances baroreflex sensitivity and blocks the somato-sympathetic reflex. ***Br J Pharmacol*** 162, 961-973.

SCHOLARLY BOOK CHAPTER

Shahid, IZ, Rahman, AA & Pilowsky, PM. (2012). Orexin and central regulation of cardiorespiratory system. ***Vitam Horm*** 89, 159-184.

PUBLICATIONS DURING THE PERIOD OF CANDIDATURE

Rahman AA, **Shahid IZ** & Pilowsky PM (2013). Neuromedin U causes biphasic cardiovascular effects and impairs baroreflex function in rostral ventrolateral medulla of spontaneously hypertensive rat. ***Peptides*** 44,15-24.

Rahman AA*, **Shahid IZ*** & Pilowsky PM. (2012b). Differential cardiorespiratory and sympathetic reflex responses to microinjection of neuromedin U in rat rostral ventrolateral medulla. ***J Pharmacol Exp Ther*** 341, 213-224.
***Equal first authors.**

Rahman AA, **Shahid IZ,** Fong AY, Hammond AM & Pilowsky PM. (2012a). Vasostatin I (CgA_{17-76}) vasoconstricts rat splanchnic vascular bed but does not affect central cardiovascular function. ***Auton Neurosci*** 166, 22-28.

Rahman AA, **Shahid IZ** & Pilowsky PM. (2011). Intrathecal neuromedin U induces biphasic effects on sympathetic vasomotor tone, increases respiratory drive and attenuates sympathetic reflexes in rat. ***Br J Pharmacol*** 164, 617-631.

IN PREPARATION

Shahid, IZ, Rahman, AA & Pilowsky, PM. (2012). Role of orexin A in rostral ventrolateral medulla in regulation of sympathetic nerve activity and reflexes in wistar-kyoto and spontaneously hypertensive rats.

REFEREED CONFERENCE ABSTRACTS

Shahid IZ, Rahman AA & Pilowsky PM. (2011). Both orexin 1 and 2 receptors mediate orexin a induced sympathoexcitaton and increase in phrenic nerve activity. ***Hypertension*** 58, 123-123.

Rahman AA, **Shahid IZ,** Fong AY & Pilowsky PM. (2011). Effects of centrally administered vasostatin I on the modulation of cardio-respiratory function and sympathetic reflexes. ***Hypertension*** 58, 123-123.

COMMUNICATIONS

Rahman, AA, **Shahid, IZ,** Pilowsky, PM. (2012). Differential sympathetic reflex responses to microinjection of neuromedin U in rat rostral ventrolateral medulla. 32nd Annual Meeting of Australian Neuroscience Society, Gold Coast, Queensland. Poster presentation.

Shahid, IZ, Rahman, AA, Pilowsky, PM. (2011). Orexin A in the rostral ventrolateral medulla is hypertensive, sympathoexcitatory and increases phrenic nerve activity. 41st Annual Meeting of Society for Neuroscience (SfN), Washington DC, USA. Poster presentation.

Shahid, IZ, Rahman, AA, Pilowsky, PM. (2011). Localisation of orexin receptor 1 and 2 in the rostral ventrolateral medulla of rat. 31st Annual Meeting of Australian Neuroscience Society, Auckland, New Zealand. Poster Presentation.

Rahman, AA, **Shahid, IZ,** Pilowsky, PM. (2011). Neuromedin U in the spinal cord differentially modulates sympathetic outflow and adaptive sympathetic reflexes. 41st Annual Meeting of Society for Neuroscience (SfN), Washington DC, USA. Poster presentation.

Rahman, AA, **Shahid, IZ,** Pilowsky, PM. (2011). Neuromedin U causes biphasic effects on sympathetic vasomotor tone and increases respiratory drive in rat rostral ventrolateral medulla. 33rd Annual Scientific Meeting of High Blood Pressure Research Council of Australia (HBPRCA), Perth, Western Australia. Melbourne. Moderated Poster Presentation.

Rahman, AA, **Shahid, IZ,** Pilowsky, PM. (2011). Intrathecal neuromedin U causes sympathetically mediated biphasic changes in blood pressure and increases respiratory drive. 31st Annual Meeting of Australian Neuroscience Society, Auckland, New Zealand. Poster Presentation.

Shahid, IZ & Pilowsky, PM. (2010). Intrathecal orexin A increases sympathetic outflow and respiratory drive and modulates physiological reflexes. 30th Annual Meeting of Australian Neuroscience Society, Sydney, Australia. Poster Presentation.

INVITED SEMINAR

“Neural Regulation of the Cardiorespiratory System: Role of Orexin A” at the Institute of Membrane and Systems Biology, University of Leeds, UK (2011).

ACKNOWLEDGEMENTS

Firstly I would like to thank my greatest supervisor Prof Paul Pilowsky for taking me on board, your endless hardwork, patience, guidance and absolutely for everything you have done for me over last four years. You have given me the freedom to pursue my own research interests while also teaching me a great deal, and I am profoundly grateful. Your academic advice and support has been invaluable. I appreciate the time and energy you contributed towards my dissertation, without you I would never be what I am today.

I gratefully acknowledge the support of Macquarie University for providing Macquarie University Research Excellence Scholarship (MQRES), Post Graduate Research Fund (PGRF) and also to ASAM for top-up fund and world class research facility.

I would like to extend special thanks to my co-supervisor Dr Angelina Y Fong for having been very supportive and understanding. You never hesitate to drop whatever you do to help me. You are a great mentor and thank you very much for all your support.

I would like to express my gratitude to Drs Peter Burke and Simon McMullan. Pete I am really grateful to you for the immense amount of training and assistance you have provided me. I learned so many things from you. Thanks Simon for developing my electrophysiological techniques and giving all sort of rig troubleshooting support.

I thank Drs Mandy Lung and Natasha Kumar for helping me with molecular biology and microscopy techniques and for keeping me good company in the lab.

Thanks to Dr Branimir Zogovic for showing me the surgical preparation for the *in vivo* electrophysiological experiments. To all those in the Pilowsky's team: Drs Qi-Jian Sun, Mellisa F, Andrea, Andrew, Temi, Tara, Dan, Mel I, Willy, Darko, Lei, Sarah and also Newsha, Miok, Belinda, Mojtaba, Omar, Ibrahim, and everyone else at ASAM. Thank you so much for the help you guys gave; you have made all the difference to make this journey enjoying.

And of course I'd like to thank my family, friends, teachers and colleagues back in Bangladesh. Thanks Abba, Amma, Boro vai, Ligy, Bhaia and Shammi for understanding and allowing me to pursue my dream and I am proud of having you as my family. Abba and Amma, I would like to take this opportunity to dedicate this thesis to you.

Last but certainly not least, my soul mate Sajal (Dr Ahmed Rahman). You are just the best. You are everything to me. There is no word to express my love and gratitude to you. You were always, are always and hope will be always, with me till the end of my life.

Adyan, my little angel, you are the best blessing from Allah. I am eagerly waiting to play with you.

LIST OF FIGURES

Chapter 1

Chapter 3

Chapter 4

Chapter 5

Chapter 6

LIST OF TABLES

LIST OF ABBREVIATIONS

Abbreviation	Elaboration
2-DG	2-deoxyglucose
5-HT	5-Hydroxy tryptamine
ACh	Acetylcholine
AIH	Acute intermittent hypoxia
ANS	Autonomic nervous system
Arc	Arcuate nucleus
AT1	Angiotensin receptor 1
AUC	Area under the curve
BötC	Bötzinger complex
BP	Blood pressure
bpm	Beats (bursts) per minute
C1	Catecholaminergic
CART	Cocaine- and amphetamine-regulated transcript
CNS	Central nervous system
CommNTS	Commissural NTS
CO_2	Carbon dioxide
CVLM	Caudal ventrolateral medulla
cVRG	Caudal ventral respiratory group
DMH	Dorsomedial hypothalamus
DR	Dorsal raphé
DRG	Dorsal respiratory group
DβH	Dopamine-β-hydroxylase
E	Expiratory
EAA	Excitatory amino acid
ECG	Electrocardiogram

ENK	Enkephalin
EPSPs	Excitatory post synaptic potentials
GABA	Gamma-amino butyric acid
GPCR	G-protein coupled receptor
HR	Heart rate
icv	Intracerebroventricular
i.p.	Intraperitoneal
i.t.	Intrathecal
i.v.	Intravenous
IHC	Immunohistochemistry
IML	Intermediolateral cell column
KCl	Potassium chloride
KF	Kölliker-fuse
LC	Locus coeruleus
LHA	Lateral hypothalamic area
LSNA	Lumbar sympathetic nerve activity
LTF	Long term facilitation
MCH	Melanin concentrating hormone
MAP	Mean arterial pressure
MCPA	Medullo-cervical pressor area
NA	Noradrenaline
NAc	Nucleus accumbens
NK1	Neurokinin receptor 1
NO	Nitric oxide
non-C1	Non-catecholaminergic
NMDA	N-methyl-D-aspartate
NOS	Nitric oxide synthetase
NPY	Neuropeptide Y

NTS	Nucleus tractus solitarius
O_2	Oxygen
OX	Orexin
OX-A	Orexin A
OX_1	Orexin receptor 1
OX_2	Orexin receptor 2
PACAP	Pituitary adenylyl cyclase activating polypeptide
PAG	Periaqueductal grey
PBN	Parabrachial nucleus
PBS	Phosphate buffered saline
PE	Phenylephrine hydrochloride
PI	Post inspiratory
PNA	Phrenic nerve activity
PNamp	Phrenic nerve amplitude
PNf	Phrenic nerve frequency
PNMT	Phenylethanolamine-n-methyltransferase
PNS	Parasympathetic nervous system
POMC	Proopiomelanocortin
PPE	Preproenkephalin
PPT	Preprotachykinin
preBötC	Prebötzinger complex
PRG	Pontine respiratory group
PRN	Pontine respiratory nuclei
PVN	Paraventricular nucleus
RARs	Rapidly-adapting pulmonary stretch receptors
RAS	Renin-angiotensin system
rSNA	Renal sympathetic nerve activity
RTN	Retrotrapezoid nucleus

RVLM	Rostral ventrolateral medulla
RVMM	Rostral ventromedial medulla
SB 334867	(*N*-(2-methyl-6-benzoxazolyl)-*N*′-1,5-naphthyridin-4-yl-urea
SE	Standard error
SHR	Spontaneously hypertensive rats
SNA	Sympathetic nerve activity
SNP	Sodium nitroprusside
SNS	Sympathetic nervous system
SON	Supraoptic nucleus
Sp5	Spinal trigeminal tract
SPN	Sympathetic preganglionic neurons
sSNA	Splanchnic ympathetic nerve activity
T_E	Expiratory period
TH	Tyrosine hydroxylase
T_I	Inspiratory period
TMN	Tuberomammillary nucleus
TRH	Thyrotropin releasing hormone
VGLUT2	Vesicular glutamate transporter2
VIP	Vasoactive intestinal peptide
VLPO	Ventrolateral preoptic area
VMH	Ventromedial hypothalamus
VRC	ventral respiratory column
VRG	Ventral respiratory group
VTA	Ventral tegmental area

STATEMENT OF CANDIDATE

I certify that the work in this thesis entitled “Orexin A in the Central Control of Cardiorespiratory Regulation” has not previously been submitted for a degree nor it has been submitted as part of requirements for a degree to any other university or institution other than Macquarie University.

I also certify that the thesis is an original piece of research and it has been written by me. Any help and assistance that I have received in my research work and the preparation of the thesis itself have been appropriately acknowledged (see “Declaration of contribution to published work”). In addition, I certify that all information sources and literature used are indicated in the thesis.

The research presented in this thesis was approved by Macquarie University Ethics Review Committee, reference numbers: #**2009-016** (Full Approval Duration: 08 September 2009 to 07 September 2012) (see Appendix 3).

MST. ISRAT ZAHAN SHAHID
Student ID: 41596455

Chapter 1.

Literature Review

Literature Review

Part of this chapter has been published in Vitamins and Hormones (see **Appendix 2**) Shahid, IZ, Rahman, AA, Pilowsky, PM (2012b). Orexin and central regulation of cardiorespiratory system. *Vitam Horm* **89**: 159-184.

1.1 Introduction

Life is maintained by the proper functioning of the cardiorespiratory system which ensures the required delivery of oxygen (O_2) and nutrients to, and removal of carbon dioxide (CO_2) and other wastes from, the tissues and organs. The cardiovascular system principally comprises the heart and blood vessels (arteries, veins and capillaries). The blood vessels form an integrated network that supply all cells with nutrients, thus allowing cellular homeostasis. To maintain homeostasis, the cardiovascular system needs to provide a continuous and controlled flow of blood keeping arterial blood pressure (BP) relatively stable. Although long term BP is regulated by hormonal and renal mechanisms, short term minute-to-minute regulation depends on central neural mechanisms involving both the sympathetic and parasympathetic branches of the autonomic nervous system (ANS). Heart rate (HR) is predominantly controlled by the parasympathetic nervous system (PNS) whereas sympathetic nerves regulate resistance of the arteries and hence total peripheral resistance. Thus, changes in HR combined with total peripheral resistance determine mean arterial pressure (MAP). Several regions within the central nervous system (CNS) are essential for the regulation of the sympathetic nervous system (SNS) and therefore sympathetic tone, with the brainstem playing a particularly important role (Bianchi *et al.*, 1995; Sun, 1995).

The respiratory system regulates the intake of O_2 and the expiration of excess CO_2 by the rhythmic movement of the main pump muscle, the diaphragm, which is innervated by the phrenic nerve. The central control of respiratory rhythm and pattern is governed by a network of neurons within the brainstem (Dobbins & Feldman, 1994).

Among the brainstem nuclei, the rostral ventrolateral medulla (RVLM) is essential for maintaining the vasomotor tone. In anaesthetised animals, acute chemical or electrical lesion of RVLM neurons causes hypotension due to removal of sympathetic vasomotor tone (Guertzenstein & Silver, 1974; Dampney & Moon, 1980). Similarly in conscious animals, inhibition of the RVLM evokes a profound reduction in BP and sympathetic nerve activity (SNA) (Sakima *et al.*, 2000). In normotensive animals, there is no other site within the CNS whereby a lesion alters sympathetic vasomotor tone to such an extent. In the hypertensive rat, some excitatory contribution arises from the paraventricular nucleus (PVN) of the hypothalamus which is in fact mediated via the RVLM (Allen, 2002).

Viral and retrograde tracing studies show that neurons directly projecting to the sympathetic preganglionic neurons (SPN) in the spinal cord are found in the RVLM and these are known as RVLM presympathetic neurons (Schramm *et al.*, 1993). It is generally accepted that the basal level of sympathetic vasomotor tone is maintained by barosensitive RVLM presympathetic neurons due to the fact that maximal activation of baroreceptors abolishes sympathetic vasomotor activity.

SPN, located in the intermediolateral cell column (IML) of the thoracolumbar spinal cord, are the only line of communication between central sympathetic outflow and the peripheral ganglia. SPN receive input from the RVLM and different discrete regions of the brain and participate in controlling cardiovascular responses via projections to the adrenal medulla and sympathetic autonomic ganglia in the periphery (Pilowsky & Goodchild, 2002; Guyenet, 2006).

The RVLM is also essential for the integration of afferent, from the central nuclei or the periphery, to efferent signals, relaying the necessary output. Glutamate and γ-amino butyric acid (GABA) contribute, largely, to the short-term regulation of RVLM neurons. Different metabotropic neurotransmitters, including neuropeptides, that have long term effects on cell function, are expressed in and/or released on RVLM neurons to modulate the activity of fast-acting neurotransmitters (Pilowsky *et al.*, 2008; Pilowsky *et al.*, 2009).

This thesis is focused on the autonomic control of the cardiorespiratory system, and the effects of the peptide orexin A (OX-A) on the tonic and reflex regulatory control of this system. OX-A is a neuropeptide solely produced by a group of neurons in the hypothalamic region of the brain. From the hypothalamus, OX-A producing cells communicate with many different regions of the brain that are critical for regulating BP and breathing including PVN, RVLM, retrotrapezoid nucleus (RTN), caudal raphé, and spinal cord. OX-A is generally excitatory, acting via two G-protein coupled receptors (GPCRs) (coupled to $G\alpha_{q/11}$ and/or $G\alpha_{i}$), orexin 1 (OX_1) and orexin 2 (OX_2) receptors. Stimulation of OX receptors activate several intracellular signalling pathways including: activation of adenylate cyclase and phospholipase C, to exert short- and long- term changes on neuronal activity (for review see Sakurai, 2007; Kuwaki *et al.*, 2008).

In this chapter, the current knowledge concerning the sympathetic control of the circulation, brainstem cardiovascular reflexes, and central control of breathing is discussed. Finally, the role played by the neuropeptide OX-A in modulating cardiorespiratory function is addressed.

1.2 Autonomic control of cardiovascular system

The conventional concept of the ANS was described by Langley almost a century ago, as primarily a motor, or efferent, branch of the peripheral nervous system which transmits signal from the CNS to effector tissues thereby regulating function. The ANS, in concert with the endocrine system, plays a vital role in controlling visceral tone, BP, HR, respiration and temperature regulation, and maintaining general homeostasis (Langley, 1916; Morrison, 2001; McCorry, 2007; Powley *et al.*, 2008). Therefore the maintenance of homeostatic balance depends on the afferent input from peripheral receptors and central drives, and the corresponding efferent outflow. The ANS has two major components: the SNS and PNS.

Both the sympathetic and parasympathetic divisions consist of parallel but differentially regulated pathways made up of preganglionic neurons located in the thoracolumbar regions of the spinal cord and craniosacral regions, respectively. Preganglionic neurons synapse with postganglionic neurons and hence transduce

the subsequent outcome onto the effector organs. Parasympathetic cholinergic preganglionic neurons innervate peripheral ganglia, from which in turn, postganglionic cholinergic neurons innervate, and regulate limited organs, such as the heart, lung, kidneys and stomach, in a more precise and target-focused manner (Morrison, 2001; Guyenet, 2006). In contrast to the parasympathetic division, the SNS is the most diverse autonomic system and exhibits an exquisite differential regulation of the vasculature and all of its other target organs (Malpas, 2010).

Autonomic control of the circulation depends both on parasympathetic neurons innervating mainly the heart, and sympathetic neurons innervating blood vessels, heart, kidneys and the adrenal medulla (Guyenet, 2006). The PNS innervates the heart via the vagus nerve and plays a major role in the control of HR, contractility and speed of conduction of impulses in the conducting system of the heart. Conversely, sympathetic nerve fibers increase HR and cause vasoconstriction, directing blood flow to skeletal muscle, preparing the body for a “fight or flight” response. Thus the actions of the two systems complement each other to control visceral organs and blood vessels (Malpas, 2010).

1.2.1 Sympathetic control of cardiovascular system

Mass activation of the SNS is recognized as the “fight or flight response” whereby there is an increase in HR, BP, energy expenditure, mobilization of fats and glycogen and a reduction in the blood flow to the gut (Guyenet, 2006). The SNS is responsible for homeostasis of cardiovascular function such as resting state changes in HR, cardiac contractility, venous capacitance and constriction of resistance vessels, as well as responding to stressful conditions such as exercise and disease (Guyenet, 2006; Kishi, 2012). These functions are coordinated via a complex network operating through SPN in the spinal cord. In general, sympathetic control of the blood vessels and heart occurs from excitatory noradrenergic cell populations localised in the pre- and para-vertebral ganglia (Janig & Habler, 2003). These postganglionic nerve fibres travel through the body to reach their effector organs and control smooth muscle and other visceral targets (e.g. kidneys, stomach, intestine and liver). These cells receive excitatory inputs from cholinergic SPN in the spinal cord (Strack *et al.*, 1988). The SPN are discussed in section 1.2.3.

1.2.2 Cardiovascular presympathetic nuclei

Presympathetic neurons are, by definition, neurons that synapse with SPN. The properties of these higher autonomic nuclei have been investigated by electrophysiological and immunohistochemical approaches (e.g. Dampney *et al.*, 1984; Card *et al.*, 1990). Retrograde labelling of SPN in the IML of the spinal cord with neurotropic viruses demonstrated inputs originating from the hypothalamus and the brainstem (Strack *et al.*, 1988). The ongoing synaptic activity in SPN arises predominantly from excitatory monosynaptic inputs, mediated over both fast and slow-conducting pathways (Barman & Gebber, 1985; Dembowsky *et al.*, 1985; Morrison, 1993), from at least six regions, namely, RVLM, rostral ventromedial medulla (RVMM), A5 neurons, caudal raphé, PVN (Strack *et al.*, 1989a) and the medullo-cervical pressor area (MCPA) (Seyedabadi *et al.*, 2006) (Fig 1.1). Certainly there are other sites in the CNS that contribute to cardiovascular regulation but their action is predominantly relayed through one or more of these nuclei. Presympathetic neurons differentially regulate the activity of sympathetic nerves (Morrison, 2001; Janig & Habler, 2003). For instance, RVLM presympathetic neurons regulate cardiovascular target tissues to control BP, whereas some medullary raphé presympathetic neurons selectively control the sympathetic outflow involved in thermoregulatory and metabolic control (Morrison, 1999; Cao & Morrison, 2003). All these six areas are discussed below.

1.2.2.1 Paraventricular nucleus of the hypothalamus

The hypothalamic PVN is a convergence point for various regions involved in bodily homeostasis (for example, fluid regulation, metabolism, immune responses and thermoregulation) (Benarroch, 2005). The parvocellular subdivision of the nucleus innervates the lower brainstem (for example, the nucleus tractus solitarius (NTS), and RVLM) and spinal cord (Benarroch, 2005; Coote, 2005), and is involved in the regulation of cardiovascular function as well as sympathetic outflow. The PVN also innervates other autonomic nuclei, including the midbrain periaqueductal gray (PAG), parabrachial region, dorsal vagal nucleus, and the nucleus ambiguus (Luiten *et al.*, 1985; Dampney *et al.*, 1987). However the specific role of these pathways in cardiovascular regulation is poorly understood. The autonomic neurons of the PVN use glutamate as well as peptides as transmitters (for example, vasopressin, oxytocin and corticotropin releasing factor (CRF)) (Benarroch, 2005; Stocker *et al.*,

2006). The PVN also receive inputs from autonomic nuclei, including NTS and RVLM (Sawchenko & Swanson, 1982; Card *et al.*, 2006). Spinally projecting PVN neurons express oxytocin, vasopressin, enkephalin (ENK), galanin, substance P, neurotensin, and cholecystokinin (Cechetto & Saper, 1988). Angiotensin receptor 1 (AT1) expressing neurons do not project to the RVLM or the spinal cord but most of them project to neurons of the median eminence (Oldfield *et al.*, 2001). As neurons of the median eminence release CRF, AT1 expressing PVN neurons are suggested to be involved in stress regulation (Oldfield *et al.*, 2001).

Experiments conducted to reveal the role of PVN on sympathetic outflow have yielded conflicting results. For example, electrical stimulation, as well as chemical stimulation by microinjection of excitatory amino acids (EAAs), of the PVN increases or decreases BP and SNA (Gilbey *et al.*, 1982; Porter & Brody, 1985; Yamashita *et al.*, 1987; Katafuchi *et al.*, 1988; Kannan *et al.*, 1989). PVN stimulation with glutamate elicits an increase in adrenal nerve activity and a decrease in renal nerve activity (Katafuchi *et al.*, 1988). Such differential control by PVN neurons of different sympathetic outflows may be attributed to the differential projection of different subgroups of PVN neurons to different types of SPN (Dampney, 1994) or the influence of other autonomic nuclei receiving inputs from PVN neurons. However, the PVN has little or no effect in the generation or maintenance of sympathetic vasomotor tone.

Despite the autonomic PVN neurons playing a minor role in the moment-to-moment regulation of BP, they are inhibited by baroreceptor inputs provided that their basal firing rate is artificially increased (Lovick & Coote, 1988). Lesions of the PVN increase the baroreceptor-induced inhibition of lumbar sympathetic activity, but have little effect on the cardiac component of the baroreceptor reflex (Darlington *et al.*, 1988; Patel & Schmid, 1988). Some evidence also shows that the hyperactivity of RVLM barosensitive neurons in some models of hypertension depends partly on the increased excitatory drive from the autonomic PVN neurons (Allen, 2002; Ito *et al.*, 2003), indicating that the integrity of the PVN is essential for the production of certain types of neurogenic hypertension (Ciriello *et al.*, 1984; Zhang & Ciriello, 1985).

1.2.2.2 A5 noradrenergic cell groups in the pons

The A5 region in the pons receives inputs from the perifornical area and PVN in the hypothalamus, Kolliker-Fuse (KF) nucleus, lateral parabrachial nucleus (PBN), and NTS (Woodruff *et al.*, 1986; Byrum & Guyenet, 1987). Although the A5 cell group is one of the major sources of noradrenergic input to SPN (Byrum *et al.*, 1984; Strack *et al.*, 1989b), its role in controlling the sympathetic outflow is not clearly established due to the contradictory results obtained from different types of physiological and pharmacological studies.

Chemical stimulation of the A5 region results in a decrease in BP and HR (Loewy *et al.*, 1986; Drye *et al.*, 1990) which may be due to the direct inhibition of vasomotor SPN. In contrast, another study has shown that stimulation of the A5 region produces an increase in renal SNA (rSNA) and splanchnic SNA (sSNA), an effect that is abolished by administration of the neurotoxin 6-hydroxydopamine (Huangfu *et al.*, 1992). Spinally projecting A5 cells are inhibited by baroreceptor inputs suggesting that they are more likely to be excitatory rather than inhibitory to SPN (Andrade & Aghajanian, 1982; Byrum *et al.*, 1984; Guyenet, 1984; Huangfu *et al.*, 1991).

Byrum and Guyenet (1987) suggested that A5 cells may affect integrated cardiovascular responses by widespread actions on cardiovascular nuclei located in several different regions. This hypothesis is supported by the widespread projections of A5 cells to autonomic nuclei distributed throughout the CNS, including the medulla oblongata, pons, midbrain, hypothalamus, and the limbic system (Loewy *et al.*, 1986; Byrum & Guyenet, 1987). However, more information on the physiological properties of A5 cells is required to make any conclusions about their precise role in cardiovascular regulation.

1.2.2.3 Rostral ventrolateral medulla

It is now well established that the presympathetic neurons in the RVLM are essential for the generation and maintenance of sympathetic vasomotor tone. The RVLM is also involved in the reflex regulation of BP and is one of the major concerns of this thesis and will be discussed in greater detail in section 1.2.4.

1.2.2.4 Rostral ventromedial medulla

Presympathetic neurons of the RVMM lie in the ventral medullary region just lateral to the pyramidal tract and project directly to SPN innervating the adrenal medulla and all the major sympathetic ganglia in the rat (Strack *et al.*, 1989a; Strack *et al.*, 1989b) (Fig 1.1). RVMM neurons differ in both chemical and functional properties from RVLM neurons. These neurons use glutamate as their main neurotransmitter, while they also contain and release other neurotransmitters such as 5-hydroxytryptamine (5-HT), substance P, thyrotropin releasing hormone (TRH), and ENK (Strack *et al.*, 1989b).

Electrical and chemical stimulation of RVMM neurons evoke a pressor effect, at least in rats (Minson *et al.*, 1987; Zhuo & Gebhart, 1990) that is abolished by pre-treatment with 5,7-dihydroxytryptamine, a selective neurotoxin for 5-HT neurons indicating that the response is solely mediated by 5-HT neurons. On the other hand, microinjection of lignocaine into RVMM decreases BP and SNA. More interestingly, microinjection of glycine in the same regions of the RVMM where N-methyl-D-aspartate (NMDA) had a pressor effect, also resulted in pressor effect in anaesthetised rats (Varner *et al.*, 1992). However the role of RVMM in the tonic and reflex regulation of vasomotor tone is poorly understood. RVMM neurons also modulate nociception (Heinricher *et al.*, 2009), thermogenesis (Smith *et al.*, 1998; Morrison *et al.*, 2008) and the chemoreflex (Miura *et al.*, 1996).

1.2.2.5 Caudal (medullary) raphé

The caudal raphé nuclei (raphé obscurus and pallidus) are located in the midline of the medulla, extending ventrally to the pyramids at the level of RVLM (Figure 1.1). These nuclei directly project to, and their axons synapse with, SPN that innervate the adrenal medulla and all major sympathetic ganglia (Amendt *et al.*, 1979; Loewy, 1981; Miura *et al.*, 1983; Strack *et al.*, 1989a). The caudal raphé also sends inputs to the RVLM (Bacon *et al.*, 1990; Heslop *et al.*, 2004) as well as receiving inputs from the NTS, RVLM, and the hypothalamus (Loewy & Burton, 1978; Hosoya, 1985; Luppi *et al.*, 1989), although it is not clear whether these inputs project specifically to cardiovascular neurons in the raphé or to neurons subserving other functions.

Electrical or chemical stimulation of the medullary raphé nuclei elicit either an increasing or decreasing effect on BP and sympathetic activity, depending on the site of stimulation and the experimental conditions (Adair *et al.*, 1977; Futuro-Neto & Coote, 1982; Haselton *et al.*, 1988; McCall, 1988; Dreteler *et al.*, 1991). These variable patterns of response are likely due to the presence of both sympathoexcitatory and sympathoinhibitory neurons in the raphé, as revealed by single-cell recording experiments. The sympathoinhibitory action of the caudal raphé is mediated primarily by GABA (McCall & Humphrey, 1985; McCall, 1988). Gebber and co-workers (Morrison & Gebber, 1982, 1985; Barman & Gebber, 1989) demonstrated that presympathetic raphé neurons are excited by baroreceptor stimulation, indicating that they are sympathoinhibitory. In contrast, Pilowsky *et al.,* (1995) reported that at least some bulbospinal neurons in the rat caudal raphé are inhibited by activation of arterial baroreceptors (Pilowsky *et al.*, 1995). However, the reflex is maintained following lesions of the midline medulla including the caudal raphé, indicating that they are not a crucial component of the baroreceptor reflex pathway (McCall & Harris, 1987).

1.2.2.6 Medullo-cervical pressor area

The existence of the MCPA was first reported by Jansen and Lowey (1997) as neurons in the cervical spinal cord white matter that innervate SPN (Jansen & Loewy, 1997). Subsequently, Seyedabadi *et. al.,* (2006) provided functional evidence for a cardiovascular role of this presympathetic nuclei that extend caudally from the medulla at the level of the caudal pole of the inferior olive, to the fourth cervical segment and termed as “MCPA” (Seyedabadi *et al.*, 2006) (Figure 1.1).

Chemical stimulation of the MCPA with glutamate microinjection evokes large sympathetically mediated pressor responses that do not depend on the RVLM and may be mediated by glutamatergic neurons. This region is distinct from the caudal pressor area (CPA), as blockade of the RVLM with muscimol inhibited this pressor response, but not that evoked from the MCPA (Seyedabadi *et al.*, 2006). However, the MCPA is not involved in maintaining vasomotor tone as it does not act to restore BP after chemical lesion of the RVLM. Hence, the physiological role of this sympathoexcitatory region in circulatory control remains to be determined.

1.2.3 Sympathetic preganglionic neurons

The sympathetic division of the ANS emerges bilaterally from the last cervical, entire thoracic and the upper lumbar segments (C8-L2 levels) of the spinal cord. SPN cell bodies are located in four regions of these segments: the IML, lateral funiculus, intercalated nucleus, and central autonomic nucleus (Coote, 1988; Strack *et al.*, 1988; Pyner & Coote, 1994). However, the majority of SPN are found in the IML (~85% of total SPN) and in the adjacent lateral funiculus (Oldfield & McLachlan, 1981; Strack *et al.*, 1988; Pyner & Coote, 1994).

1.2.3.1 Morphology of SPN

SPN cell bodies in the IML are organized into four groups: nucleus intermediolateralis thoracolumbalis - pars funicularis (ILf) and pars principalis (ILp), nucleus intercalatus spinalis and nucleus intermediomedialis (central autonomic nucleus) (Petras & Cummings, 1972; Oldfield & McLachlan, 1981). Due to the different autonomic innervations, the distribution of cells within groups varies within spinal cord levels (Lichtman *et al.*, 1979). ILf cells are scattered within the lateral funiculus and medially, join the cells of the principal part of the nucleus; ILf cells are multipolar or round, are normally larger than ILp cells, and form longitudinal series of cell nests (Petras & Cummings, 1972; Pilowsky *et al.*, 1994). The nucleus intercalatus, located medial to the ILp, is composed of large elongated fusiform neurons (Petras & Cummings, 1972). There are two groups of neurons found in the central autonomic nucleus: the first group of neurons appear in clusters and surrounding the central canal; the second group of neurons (the nucleus intercalatus paraependymalis) contain medium-sized, small fusiform cells located between the central canal and the Clarke column (Petras & Cummings, 1972). Axons of SPN exit the spinal cord through the ventral roots to the white communicating rami and onto the sympathetic ganglia. The dendrites of SPN in the IML have an extensive mediolateral orientation (Bacon & Smith, 1988; Vera *et al.*, 1990b) that would provide a way by which SPN are innervated by axons descending through the lateral funiculus on both sides of the spinal cord. SPN synapse with noradrenergic sympathetic postganglionic neurons in the paravertebral and prevertebral ganglia which, in turn, innervate peripheral target organs (Pick, 1970; Baron *et al.*, 1985). The only exception is the chromaffin cells of the adrenal medulla which are directly innervated by SPN (Strack *et al.*, 1989a).

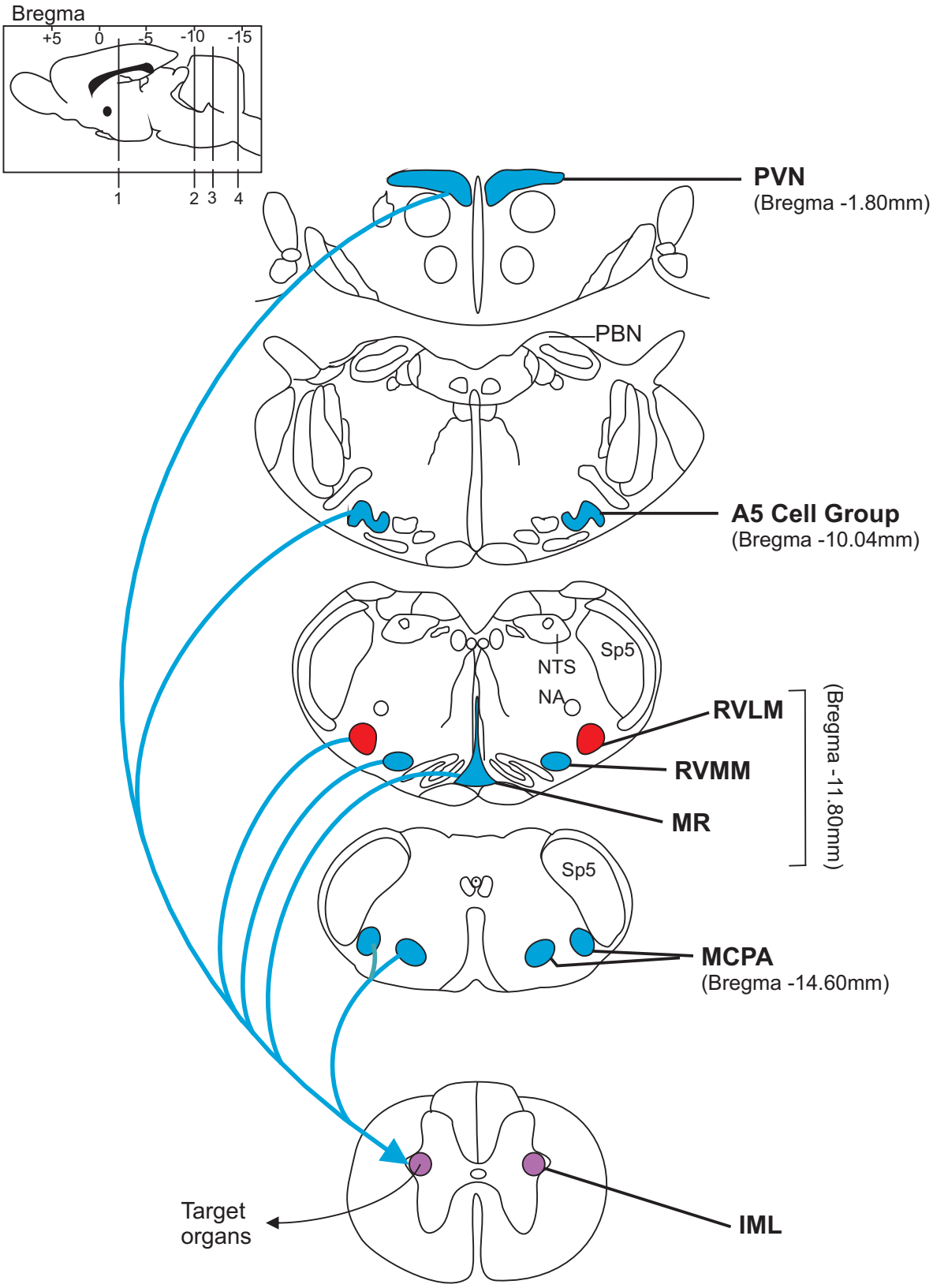

Figure 1.1. Presympathetic neurons projecting to the spinal cord.

The six regions of the brain that project to sympathetic preganglionic neurons (SPN) in the intermediolateral cell column (IML) of the spinal cord: the paraventricular nucleus (PVN) of hypothalamus, the A5 cell group in the pons, rostral ventrolateral medulla (RVLM), rostral ventromedial medulla (RVMM), medullary raphe (MR) and medullo-cervical pressor area (MCPA). Adapted from Strack *et al.*, 1989a; Seyedabadi *et al.*, 2006. Abbreviations: NA, nucleus ambiguus; NTS, nucleus tractus solitarius; PBN, parabrachial nucleus; Sp5, spinal trigeminal nucleus.

1.2.3.2 Organization of SPN

SPN have a particular organization through the spinal segments of the IML. For example, there is an approximate rostrocaudal organization of the SPN that corresponds with the rostrocaudal position of ganglia (Strack & Loewy, 1990). There is also columnar organization of the SPN. For example, the neurons innervating the stellate ganglion are located in the intermediate IML, those innervating the adrenal medulla are in the lateral portion of the IML and those innervating the superior cervical ganglion are in the medial portion of the IML (Pyner & Coote, 1994). However this organization may not be identical throughout all species (Funakoshi *et al.*, 1996).

SPN are also topographically organized, albeit with considerable overlap, according to their peripheral targets. For example, the cell bodies of SPN innervating the cervical sympathetic nerve are located between C8 and T5 and those innervating the adrenal gland are located between T4 and T12 (Strack *et al.*, 1988). In addition, SPN which innervatine adrenaline- and noradrenaline (NA) - secreting adrenal chromaffin cells are histologically and electrophysiologically distinct populations in rat and cat (Edwards *et al.*, 1996; Morrison & Cao, 2000). For example, SPN regulating adrenaline secreting chromaffin cells are sensitive to 2-deoxyglucose (2-DG), a glucoprivic agent, but are not sensitive to baroreceptor activation. Alternatively, SPN that project to NA secreting chromaffin cells are not affected by 2-DG, but are excited by baroreceptor activation (Morrison & Cao, 2000). However, functional specificity of SPN is not observed in the lumbar spinal cord of the cat, where intracellular recordings from vasomotor SPN show that they are dispersed throughout the IML (Pilowsky *et al.*, 1994). These differences in functional state and topographical orientation within SPN reflect the differences in the central circuits that determine the activity of SPN and underlie the concept of differential control of sympathetic outflow (for review see Morrison, 2001; Guyenet, 2006).

In addition to supraspinal regulation, SPN are also regulated by a network of spinal interneurons (Poree & Schramm, 1992; Chizh *et al.*, 1998). Interneurons are multipolar neurons that do not project to spinal nerves (Deuchars *et al.*, 2001). Electrical and chemical (glutamate) stimulation of the central autonomic nucleus

containing interneurons causes inhibitory postsynaptic potentials to SPN. Since bicuculline ($GABA_A$ antagonist) blocks the excitatory effects of glutamate in the central autonomic nucleus, it is suggested that the inhibitory effect of interneurons that synapse with SPN is mediated via $GABA_A$ receptors (Deuchars *et al.*, 2005). On the other hand, interneurons can also be excitatory, this is observed in certain cases of brainstem-provoked sympathoexcitation (for review see Deuchars, 2007). Electrophysiological recordings have shown that the firing frequency of the interneurons is higher than that of the SPN, potentially allowing for a greater level of regulation of the SPN (Brooke *et al.*, 2002). However, spinal interneurons are not considered to be vital for the generation and maintenance of sympathetic tone because acute C1 spinal transection eliminates efferent sympathetic nerve activity (Alexander, 1946; Taylor & Schramm, 1987).

1.2.3.3 Neurochemistry of the SPN

The SPN receive inputs from a number of sources including local interneurons (see above), central respiratory nuclei, and other higher centres including the six supraspinal cardiovascular sites that have significant bulbospinal projections (section 1.2.2). All SPN are cholinergic (Schafer *et al.*, 1998) and they are identified by immunoreactivity to choline acetyltransferase (ChAT) (Fenwick *et al.*, 2006), the enzyme required to synthesize acetylcholine (ACh). Anatomical and pharmacological studies have shown diverse chemical phenotypes of neurotransmitters and neuropeptides in the varicosities that surround SPN. The most important neurotransmitters released from nerve terminals which synapse with SPN are the amino acids such as glutamate (Morrison *et al.*, 1989a; Morrison *et al.*, 1989b; Llewellyn-Smith *et al.*, 1992), GABA (Bacon & Smith, 1988; Bogan *et al.*, 1989; Chiba & Semba, 1991; Llewellyn-Smith *et al.*, 1998), glycine (Chiba & Semba, 1991; Cabot *et al.*, 1992), and 5-HT (Bacon & Smith, 1988; Chiba, 1989; Vera *et al.*, 1990a; Poulat *et al.*, 1992). In fact, it has been demonstrated that two-thirds of all terminals apposing SPN in the thoracic spinal cord of the rat contain glutamate (Llewellyn-Smith *et al.*, 1992) which acts as the major neurotransmitter and plays crucial role in the maintenance of vasomotor tone. Moreover, other studies illustrate that about one-third of all axons making contact with SPN are GABAergic (Bacon & Smith, 1988; Llewellyn-Smith *et al.*, 1998). However, glutamate and GABA are not colocalized in the same nerve terminals (Llewellyn-Smith *et al.*, 1992).

In addition to neurotransmitter, axon terminals synapsing with SPN are also immunoreactive for a wide variety of neuropeptides including substance P (Bacon & Smith, 1988; Vera *et al.*, 1990a; Pilowsky *et al.*, 1992), neuropeptides Y (NPY) (Chiba, 1989), angiotensin II (Galabov, 1992), ENK (Vera *et al.*, 1990a), TRH (Poulat *et al.*, 1992), pituitary adenylate cyclase activating polypeptide (PACAP) (Chiba *et al.*, 1996), somatostatin (Chiba, 1989) and orexin (Geerling *et al.*, 2003; Llewellyn-Smith *et al.*, 2003). Synapses have also been demonstrated between both noradrenergic and adrenergic, terminals and SPN (Chiba & Masuko, 1986, 1987; Milner *et al.*, 1988a; Bernstein-Goral & Bohn, 1989). Although various neurotransmitters and neuropeptides are colocalized with glutamate or GABA in terminals synapsing on SPN, the exact physiological condition at which these colocalized neurotransmitters are co-released and the effects they produce are still not clear.

Based on peptide immunoreactivity, SPN fibres can be divided according to their function, into, cardiac, vascular (vasoconstrictor) and non-cardiovascular. In general two groups of cardiac SPN exist: calretinin (calcium-binding protein), and non-calretinin containing (Anderson, 1998; Richardson *et al.*, 2006). Nitric oxide (NO) synthetase (NOS), which is present in the majority of SPN, coexists with a significant number of calretinin- and neurokynin receptor 1 (NK-1)- positive SPN (Anderson, 1992; Anderson *et al.*, 1993; Grkovic & Anderson, 1996; Anderson, 1998). The distribution of chemically distinctive terminals surrounding SPN in the different spinal segments is non-uniform. For instance, some SPN are densely innervated by catecholamine terminals while others are sparsely innervated by catecholamine terminals (McLachlan & Oldfield, 1981). In addition, glycine immunoreactive terminals are associated particularly with SPN in the central autonomic area and intercalated nuclei (Cabot *et al.*, 1992).

SPN have many cell surface receptors, including the substance P receptor (Benoliel *et al.*, 2000), ENK 1 receptor (Llewellyn-Smith *et al.*, 2005), angiotensin II type 1a receptor (Ahmad *et al.*, 2003), 5-HT receptor (Nakamura *et al.*, 2004) and OX receptors (van den Top *et al.*, 2003). The findings suggest multiple levels and types of transmission in the spinal cord in regards to SPN activity. Lewis and Coote (1990) proposed that the function of co-released compounds may be quite different from that

observed when a compound is applied in isolation (Lewis & Coote, 1990). For instance, in the presence of low concentrations of an EAA (DL-homocysteic acid), NA has an inhibitory effect, but the opposite effect (excitation) is exhibited when the concentration of the amino acid is increased (Lewis & Coote, 1990). A growing body of evidence suggests that co-stored and co-released neurotransmitters or neuropeptides might modulate the responses of classical neurotransmitters such as glutamate or GABA.

The effects of OX-A in the spinal cord on the cardiorespiratory response and responses to arterial baroreceptor, somatic receptor, and peripheral chemoreceptor stimulation are detailed in chapter 3.

1.2.4 Rostral ventrolateral medulla

The RVLM is the most comprehensively studied sympathetic premotor cell groups in the brain, particularly in relation to cardiovascular control. The RVLM plays a key role in the regulation of basal cardiac and vasomotor sympathetic tone and in mediating the sympathetic responses to baroreceptor, chemoreceptor and somatic receptor activation. Anatomically, the RVLM is now most commonly accepted as the region that extends (approximately 1mm) caudally from the caudal pole of the facial nucleus, ventral to the compact formation of the nucleus ambiguus and Bötzinger Complex (BötC), rostral to the pre-Bötzinger Complex (preBötC), and lateral to the spinal trigeminal nucleus (Ruggiero *et al.*, 1994; Goodchild & Moon, 2009). In the context of cardiovascular regulation, the most rostral 500 µm of the RVLM is considered the ‘hot spot’ because this area evokes the largest pressor response to glutamate microinjection (Goodchild & Moon, 2009) (chapters 4 and 5).

1.2.4.1 Identification of the vasomotor centre and the RVLM

The importance of the ventrolateral medulla in the regulation of BP was first made by Carl Friedrich Wilhelm Ludwig, the head of the Leipzig Physiological Institute, during the 1870’s. Ludwig with his co-workers Owsjannikow and Dittmar, suggested that a vasomotor centre in the brainstem controls the contraction of arterial blood vessels by receiving inputs from the periphery via a ‘depressor nerve’ (for overview see Pagani *et al.*, 1982; Gillis *et al.*, 1983; Seller, 1996). In 1873 Dittmar showed that destruction of the ventral but not the dorsal medulla around the level of the facial

nucleus, pertaining to the RVLM, resulted in a profound fall in BP (Sun, 1995). After a century, in 1972, Feldberg and Guertzenstein revitalized the idea of a vasomotor centre in the brainstem. Feldberg and Guertzenstein observed a transient pressor effect even with the slightest mechanical (cannula) manipulation of 'a small area at the ventral surface of the medulla oblongata' (Feldberg & Guertzenstein, 1972). An extreme decline in BP was observed following local application of sodium pentobarbitone to the area 'situated lateral to the pyramids and just caudal to the trapezoid bodies' (Feldberg & Guertzenstein, 1972). In addition, the activity of RVLM neurons was suppressed by the application of glycine to the surface of the ventral medulla or by microinjection of glycine into the RVLM in the cat (Guertzenstein & Silver, 1974; Wennergren & Oberg, 1980; Hilton *et al.*, 1983; Dean & Coote, 1986) which suggests that these neurons are tonically active. Under stereotaxic guidance, chemical inhibition or electrical lesions of the RVLM in the anaesthetised rabbit (Dampney & Moon, 1980; Pilowsky *et al.*, 1985), rat (Willette *et al.*, 1983b; Ross *et al.*, 1984b) and cat (McAllen, 1985), evoked hypotension and sympathoinhibition to the same extent as that seen following C1 spinal transection or ganglionic blockade. The excitation of the RVLM by electrical or chemical stimulation caused hypertension and a powerful increase in sympathetic drive to the heart, blood vessels and adrenal medulla (Goodchild *et al.*, 1982; Willette *et al.*, 1983a; Ross *et al.*, 1984b; McAllen, 1986) and monosynaptically excited SPN (Deuchars *et al.*, 1995). The effects of inhibition or excitation of RVLM neurons on sympathetic vasomotor tone (described above) were observed in anaesthetised animals. Similarly in conscious animals, inhibition of the RVLM by microinjection of the neuroinhibitory compound glycine, evoked a profound reduction in rSNA as well as BP (Sakima *et al.*, 2000). These data further support the idea that RVLM neurons play a critical role in the maintenance of sympathetic vasomotor tone in the conscious as well as the anaesthetised state. Around the same time (1980s), studies illustrated that the RVLM is the critical center in the control of adaptive autonomic reflexes, particularly the baroreflex (Willette *et al.*, 1983b) (see section 1.3.1) and somatosympathetic reflex (McAllen, 1985) (see section 1.3.2). These studies, and many others, recognized the RVLM as a key brainstem site responsible for the tonic and reflex control of cardiovascular function.

1.2.4.2 Classification of RVLM neurons

The RVLM consists mainly of two groups of neurons: the catecholaminergic (C1) and the non catecholaminergic (non-C1) neurons. The C1 population is defined by the presence of the enzymes required for the synthesis of adrenaline (tyrosine hydroxylase (TH), dopamine β-hydroxylase (DβH) and phenylethanolamine-N-methyltransferase (PNMT)) (Hokfelt *et al.*, 1973; Blessing *et al.*, 1981; Ross *et al.*, 1981; Goodchild *et al.*, 1984; Phillips *et al.*, 2001; Stornetta *et al.*, 2002). Bulbospinal and non-bulbospinal RVLM neurons are anatomically and neurochemically distinct groups of neurons. Retrograde tracing studies have shown that RVLM presympathetic neurons display bilateral spinal projections making monosynaptic connections with SPN in the thoracolumbar spinal cord, with an ipsilateral predominance (Jeske & McKenna, 1992; Moon *et al.*, 2002). Spinal projections were also demonstrated by antidromic activation of RVLM neurons (Lipski, 1981; Brown & Guyenet, 1985; Lipski *et al.*, 1995b). Most barosensitive bulbospinal neurons reside at the rostral pole of the RVLM (0-300μm caudal to the facial nucleus in rat) and project to SPN at all levels of the spinal cord (Strack *et al.*, 1989a; Jansen *et al.*, 1995; Pyner & Coote, 1998). Whereas neurons concentrated in the caudal half of the RVLM (600-800 μm caudal to the facial nucleus in the rat) send projections to higher brain regions (Sawchenko & Swanson, 1982; Tucker *et al.*, 1987; Petrov *et al.*, 1993). Immunohistochemistry studies show that, RVLM neurons that project to the spinal cord and hypothalamic area, form completely separate subpopulations (Tucker *et al.*, 1987). Approximately 60–70% of bulbospinal neurons are phenotypically defined as C1 neurons. Bulbospinal C1 neurons comprise ~25-33% of all C1 neurons, whereas C1 neurons projecting to the hypothalamus make up more than 50% of the total C1 population (Minson *et al.*, 1990; Stornetta *et al.*, 1999; Verberne *et al.*, 1999; Phillips *et al.*, 2001). Many C1 neurons are sympathoexcitatory (Abbott *et al.*, 2009a), barosensitive (Sartor & Verberne, 2003) and are activated by a fall in BP (Sved *et al.*, 1994). Bulbospinal and non-bulbospinal RVLM neurons also exhibit differences in expression of neurochemicals. For instance, using retrograde labelling, NPY mRNA was visualized in 96% of C1 neurons with hypothalamic projections, but only in 9% of spinally projecting C1 neurons (Stornetta *et al.*, 1999). This suggests that C1 neurons may not have a major synaptic input to all SPN. In addition, Pilowsky *et al*.,(1994) reported in cat, that only approximately 8% of SPN were of a vasoconstrictor type (Pilowsky *et al.*, 1994).

Depending on the conduction velocity of the axon, the barosensitive bulbospinal RVLM neurons are further classified as either fast or slow conducting (Brown & Guyenet, 1984). Approximately 80% of bulbospinal RVLM neurons are lightly myelinated, and have a high axonal conduction velocity (average of 3m/s), while 20% are unmyelinated, and have a slow axonal conduction velocity (<1m/s) (Morrison *et al.*, 1988). The conduction velocity is correlated with the basal activity of RVLM neurons; the highest spontaneous activity is observed in neurons with the fastest conduction velocity (Schreihofer & Guyenet, 1997). Lipski and colleagues gave a similar classification of bulbospinal RVLM neurons based on *in vivo* intracellular recordings. The first criterion was barosensitivity, as demonstrated by an inhibitory response to aortic nerve stimulation (in rats the aortic nerve is exclusively barosensitive while in humans and rabbits it also contains chemosensitive properties) (Lipski *et al.*, 1995a; Lipski *et al.*, 1996a). The second criterion was the antidromic response of efferent pathways to near-threshold stimulation that does not significantly alter BP, or the amplitude of synaptic responses (Lipski *et al.*, 1995a; Lipski *et al.*, 1996a). Later Lipski *et al.,* (1996) confirmed the observation that the majority of barosensitive bulbospinal RVLM neurons are fast conducting, however the study failed to identify neurons with slow-conducting velocity (i.e. the non-myelinated fibres). The reasons behind the inability to identify neurons with slow-conducting activity were also explained in the study. The first reason was the difficulty of recording intracellular activity from small cell bodies of unmyelinated fibres, while the second reason was the 'masking effect' of faster conducted afferent fibres that masked the antidromic action potentials of slower conducting fibres (Lipski *et al.*, 1996a). The physiological difference and contribution of the slow and fast conducting spinally projecting RVLM neurons in the regulation of sympathetic tone and reflexes is unclear and remains to be investigated.

For many years, C1 neurons were thought to be the generators of vasomotor tone. Now the importance of C1 neurons in cardiovascular regulation, particularly in the long term, has been questioned: the elimination of up to 90% of C1 neurons by neurotoxin lesion of C1 cells (Madden *et al.*, 1999; Madden & Sved, 2003) or lesion of the bulbospinal C1 subpopulation (Schreihofer *et al.*, 2000) reduced BP by less than 10 mmHg, if at all, and had no significant effects on tonic SNA. However,

lesioning studies have revealed that RVLM C1 neurons are important for the sympathetic responses to baroreceptor loading and unloading (Schreihofer & Guyenet, 2000; Guyenet *et al.*, 2001) and other sympathoexcitatory reflexes including the chemoreflex (Schreihofer & Guyenet, 2000) and somatosympathetic reflex (McAllen, 1985; Morrison & Reis, 1989). In contrast, a recent study has shown that C1 neurons do not appear to mediate the sympathoexcitation evoked by hypercapnia (Marina *et al.*, 2011). Perhaps the most plausible explanation for the stability of BP following C1 destruction, is that the non C1 neurons and other regulatory sites may compensate or that there is such redundancy that only 10% of the C1 neurons are required to maintain basal levels of vasomotor tone.

The function of presympathetic cardiovascular non-C1 neurons in the RVLM is not well studied. Although these neurons are differentiated from the C1 population by the absence of the markers for catecholamines, they share similar electrophysiological properties (Lipski *et al.*, 1995a; Lipski *et al.*, 1995b), anatomical projections (Ross *et al.*, 1984b; Card *et al.*, 2006) and express many, but not all, of the same neurotransmitters and neuropeptides (see section 1.2.4.5). There is an obvious difference between C1 and non-C1 neurons in terms of their conduction velocity. Schreihofer and Guyenet (1997) demonstrated that the conduction velocity of bulbospinal RVLM neurons is correlated with TH content; C1 and non-C1 neurons display fast conducting bulbospinal axons, whereas slow conducting axons originate only from C1 neurons (Schreihofer & Guyenet, 1997). However the functional significance of non-C1 neurons is important to know to identify subpopulation of the RVLM neurons that are critical in generating sympathetic vasomotor tone.

1.2.4.3 Connectivity of the RVLM

1.2.4.3.1 Inputs

The RVLM receives and integrates information from diverse regions of the brain. Electrophysiological and neuroanatomical studies confirm that neurons in the RVLM receive inputs from other brain regions including the PVN of the hypothalamus (Coote *et al.*, 1998), lateral hypothalamus (Ciriello *et al.*, 1985; Sun & Guyenet, 1986a), RVMM (Farkas *et al.*, 1998; Sartor & Verberne, 2003), NTS (Ross *et al.*, 1985; Ciriello & Caverson, 1986) and caudal ventrolateral medulla (CVLM) (Li *et al.*, 1992). They also receive inputs from cardiovascular reflexes, including:

baroreceptors, chemoreceptors and somatic receptors, either directly or indirectly (Stornetta *et al.*, 1989; Koshiya *et al.*, 1993; Pilowsky & Goodchild, 2002). Inputs can be described by their place of origin, function and/or by chemical identification. For instance, CVLM to RVLM input is divided into: baroreceptor and non-baroreceptor sensitive inhibitory input. These two inputs may be from the same and/or separate neuronal populations within the CVLM. For example, microinjection of kainic acid into the rostral CVLM causes an increase in BP and SNA, as well as an inhibition of baroreceptor silencing of SNA. This disruption to the baroreceptor reflex response is not found following caudal CVLM injection of kainic acid. This differential effect reflects the heterogeneous organization in the CVLM, such that, the barosensitive input from CVLM to RVLM originates from the rostral part of the CVLM (Cravo *et al.*, 1991). However, the barosensitive and non-barosensitive CVLM outputs may be integrated without anatomical segregation (Schreihofer & Guyenet, 2002). Most of the cardiovascular and reflex responses that originate from other brain regions are known to relay and integrate in the RVLM. For instance, damage to the RVLM eliminates the rise in BP produced by lesions in the NTS (Benarroch *et al.*, 1986).

1.2.4.3.2 Outputs

It is well accepted that the RVLM projects to all levels of the thoracic IML (Dampney, 1994). This was initially demonstrated using retrograde tracers injected at different levels of the thoracic spinal cord (Amendt *et al.*, 1979; Ross *et al.*, 1984a; Jeske & McKenna, 1992). Direct synaptic contact between the terminals of RVLM neurons in the IML and SPN retrogradely labelled from the adrenal medulla or superior cervical ganglion was also demonstrated with this technique (Zagon & Smith, 1993; Coote *et al.*, 1998). Electrical stimulation of the spinal cord combined with single unit recordings of RVLM neurons confirmed spinal projections (Brown & Guyenet, 1985; Lipski *et al.*, 1995b) that are monosynaptic (Oshima *et al.*, 2006; Oshima *et al.*, 2008). Caudal RVLM neurons send projections to higher brain regions, including the PVN, supraoptic nucleus (SON) of the hypothalamus and basal forebrain (Sawchenko & Swanson, 1982; Tucker *et al.*, 1987; Petrov *et al.*, 1993). Rostral projections are believed to drive aspects of central cardiovascular control that are regulated by the hypothalamic-pituitary axis, including osmolality and blood volume. RVLM neurons that project to arcuate and raphé nuclei are involved in feeding, circadian rhythms and thermogenesis (Card *et al.*, 2006), while neurons projecting to

the PAG (Herbert & Saper, 1992) and locus coeruleus (LC) (Pieribone & Aston-Jones, 1991) are involved in sleep and pain regulation.

1.2.4.4 Morphology and electrophysiological properties of RVLM neurons

The cell bodies of RVLM neurons come in a variety of shapes and sizes, there may be a presence or absence of spinal projections and/or rostral ipsilateral and contralateral brainstem communications (Lipski et al., 1995b). Cell bodies of RVLM neurons are spindle shaped, and multipolar with the average area of the soma being approximately ~20-30 μm^2 (Lipski et al., 1995b; Schreihofer & Guyenet, 1997). Multiple dendrites arise from the cell bodies, and project mainly in the coronal plane, although many do project to the ventral medullary surface and terminate immediately beneath the pia mater (Lipski et al., 1995b; Schreihofer & Guyenet, 1997). The axons of barosensitive bulbospinal neurons project dorsomedially before turning in a caudal direction to project to the spinal cord (Schreihofer & Guyenet, 1997).

RVLM neurons have a wide range of firing frequencies and patterns which may be associated with differential release of neurotransmitters (Morris, 1999; Todorov *et al.*, 1999; Fulop *et al.*, 2005). In some cases, the firing pattern is dependent on conduction velocities, which is in turn related to the size and myelination of the axon (Morrison *et al.*, 1988). For instance, RVLM neurons with myelinated axons have increased firing rates (Schreihofer & Guyenet, 1997). Two criteria for the identification of presympathetic vasomotor neurons have been recommended during *in vivo* intracellular recording; 1) that they should have an inhibitory post synaptic potential (IPSP) following low frequency electrical stimulation of the aortic depressor nerve while avoiding large changes in BP and 2) that they should be antidromically activated when stimulated from the thoracic spinal cord (Lipski *et al.*, 1996b). Other key features of RVLM neurons are: (i) RVLM neurons have irregular firing discharges that are maintained by ongoing excitatory and inhibitory inputs; (ii) these irregular firing discharges become regular when induced with a large depolarising current or injury, thereby showing that the inhibitory inputs modulate the excitability of the RVLM neurons (Lipski *et al.*, 1996b).

Experiments conducted *in vitro* to characterize RVLM neurons gave rise to a debate on the origin of their activity. RVLM neurons in medullary slices from neonatal rats,

which were deprived of synaptic inputs, were found to evoke a pacemaker like discharge (Sun *et al.*, 1988b). This pacemaker activity was not inhibited when the slice was treated with glutamate receptor antagonists, further strengthening the idea that RVLM neurons have an intrinsic pacemaker property and thus led to the pacemaker theory (Sun *et al.*, 1988a). The intrinsic pacemaker property of RVLM neurons was further confirmed by several other *in vitro* studies (Sun *et al.*, 1988c; Kangrga & Loewy, 1995; Li *et al.*, 1995). This pacemaker theory has been opposed and the network theory advocated by other groups due to the absence of any pacemaker properties in RVLM neurons in *in vivo* experiments with adult rats (Lipski *et al.*, 1996b). It has since been concluded, based on *in vivo* and *in vitro* intracellular recordings, that the cells in the RVLM lack known pacemaker currents and that all action potentials in the RVLM neurons are preceded by excitatory post synaptic potentials (EPSP) produced by synaptic inputs (Lipski *et al.*, 2002). An argument was also made that only cells in slice preparations of neonatal rat brains show pacemaker properties and the actual activity of RVLM neurons is produced by a summed effect of excitatory and inhibitory inputs to these neurons under normal physiological conditions in an adult rat (Dampney *et al.*, 2000).

1.2.4.5 Neurotransmitters / neuromodulators and signal transduction in the RVLM

A great deal of effort has been devoted to determining the neurochemical and receptor phenotype of RVLM neurons since these will determine the potential function and downstream/upstream targets of RVLM neurons. Neurotransmitters and neuromodulators that are suggested to act on the RVLM neurons range from classical amino acids (GABA, glycine) and glutamate to gases (NO, O_2) and neuropeptides (ENK, substance P, PACAP, orexin, somatostatin, galanin etc).

Accumulating evidence suggests that glutamate and GABA receptors are essential for the excitation and tonic inhibition of RVLM neurons. Glutamate is considered to be the principal excitatory neurotransmitter of RVLM presympathetic neurons projecting to the spinal cord (Morrison, 2003). Markers for glutamate transmission such as phosphate-activated glutaminase (a glutamate-synthesizing enzyme) (Minson *et al.*, 1991) and the vesicular glutamate transporter 2 (VGLUT2) mRNA (Stornetta *et al.*, 2002) are expressed in most of the RVLM presympathetic neurons.

In addition, the excitatory response to the stimulation of C1 cells in the RVLM is completely abolished by blockade of ionotropic glutamate transmission with kynurenic acid in the spinal cord (Mills *et al.*, 1990; Bazil & Gordon, 1993; Morrison, 2003). Furthermore, stimulation of the RVLM causes an immediate increase in the release of glutamate and aspartate as measured by dialysis (Kapoor *et al.*, 1992). On the other hand, GABA receptors, expressed on presympathetic RVLM neurons (Li & Guyenet, 1996), are proposed to be involved in the tonic inhibition of these neurons by GABA despite the expression of precursors for GABA or glycine (Stornetta *et al.*, 2004) being rare in the RVLM. Moreover, GABA terminals synapse with PNMT immunoreactive cell bodies and dendrites in the RVLM (Milner *et al.*, 1987) and injection of a GABA antagonist into the RVLM resulted in an increase in BP indicating tonic inhibition of the RVLM by endogenous GABA (Amano & Kubo, 1993).

Neurotransmitters / neuromodulators other than glutamate and GABA are also found within subpopulations of RVLM neurons, and participate in the modulation of RVLM responses. PACAP mRNA is found in both C1 (82%) and non-C1 (10%) bulbospinal neurons in the RVLM (Farnham *et al.*, 2008). Both C1 and non-C1 neurons also express cocaine- and amphetamine-regulated transcript (CART) that has been suggested to be a histological marker for all RVLM neurons (Dun *et al.*, 2002; Burman *et al.*, 2004; Wittmann *et al.*, 2004). Other peptides or their precursors differentially expressed in the subpopulations of RVLM neurons include substance P (Pilowsky *et al.*, 1986; Milner *et al.*, 1988b; Li *et al.*, 2005), NPY (Stornetta *et al.*, 1999), preprogalanin (Sweerts *et al.*, 1999), ENK (Sasek & Helke, 1989), TRH (Helke *et al.*, 1986; Hirsch & Helke, 1988), somatostatin (Burke *et al.*, 2008) and opiates (Stornetta *et al.*, 2001). For instance, NPY is expressed by 95% of hypothalamic projecting C1 neurons but is absent from most spinally projecting RVLM neurons (Sawchenko *et al.*, 1985; Stornetta *et al.*, 1999; Schreihofer *et al.*, 2000). Preproenkephalin (PPE) is expressed by ~29% of bulbospinal C1 neurons (Stornetta *et al.*, 2001), while the substance P precursor, preprotachykinin (PPT), is expressed in ~20% of bulbospinal C1 neurons (Li *et al.*, 2005). 80% of non-C1 bulbospinal neurons express PPE (Stornetta *et al.*, 2001). In addition to expressing different neurotransmitters RVLM neurons are closely apposed to, and make synapses with many other neurotransmitters that act via GPCRs. For example, the RVLM receives projections which utilize different neuropeptides (e.g. angiotensin II (Lind *et al.*,

1985), PACAP (Das *et al.*, 2007), substance P (Milner *et al.*, 1989; Milner *et al.*, 1996), orexin (Machado *et al.*, 2002)), amines (ACh (Giuliano *et al.*, 1989; Padley *et al.*, 2007), serotonin (Bago *et al.*, 2002)), and gases (NO (Iadecola *et al.*, 1993)).

Subpopulations of RVLM neurons also show diversity in their receptor content. Receptors for a variety of neurotransmitters and neuropeptides, apart from glutamate and GABA, that are also pre- or post-synaptically expressed within the RVLM (Ruggiero *et al.*, 1989) include angiotensin II (Song *et al.*, 1992), ACh (Padley *et al.*, 2007), substance P (Helke *et al.*, 1984; Nakaya *et al.*, 1994; Makeham *et al.*, 2001), somatostatin (Burke e*t al.,* 2008), opiates (Stasinopoulos *et al.*, 2000), serotonin (Polson *et al.*, 1992; Helke *et al.*, 1997), and adenosine (Jiang *et al.*, 2011). However, the role played by most of these receptors in the RVLM under normal physiological conditions is not clearly understood. Antagonism of metabotropic receptors including NK1 receptors (Makeham *et al.*, 2005), cannabinoid 1 receptor (Padley *et al.*, 2003), 5-HT1A receptor (Miyawaki *et al.*, 2001), and somatostatin 2A receptor (Burke *et al.*, 2008) in the RVLM in the anaesthetised rat has little effect on resting BP and SNA. However, there are a few exceptions, blockade of delta (δ) opioid receptors (Morilak *et al.*, 1990b, a) and muscarinic receptors (Padley *et al.*, 2007) in the RVLM of an anaesthetised preparation produce changes in the resting BP and SNA. Possible explanations for the lack of metabotropic transmission under resting conditions are that; i) only classical neurotransmitters (i.e. glutamate, GABA) are required for the maintenance of BP in a resting state, ii) anaesthesia obscures the role of these neurotransmitters, or iii) neuropeptides require repetitive action potentials at high frequencies (10-40 Hz) to mobilise and fuse the dense core vesicles storing them to the membrane (Hokfelt *et al.*, 2000; Mansvelder & Kits, 2000).

Recent studies provide evidence for the role of metabotropic transmitters / peptides on the modulation of differential reflex responses integrated within bulbospinal presympathetic RVLM neurons. For instance, activation of the δ-opioid receptor in the RVLM impairs somatosensory inputs, but has no effect on baroreceptor or chemoreceptor inputs; μ-opioid receptors activation blocks sympathetic baroreflex, but has no effect on somatosympathetic or peripheral chemoreceptor reflexes (Miyawaki *et al.*, 2002a; Kasamatsu & Sapru, 2005). AT1 receptor activation increases the maximum range of the SNA baroreflex, but has no effect on baroreflex

gain (Head & Mayorov, 2001); whereas activation of the muscarinic cholinergic receptor increases the range and gain of the sympathetic baroreflex, but attenuates somatosensory and chemoafferent inputs (Padley *et al.*, 2007). Injection of 5-HT1A agonists (Miyawaki *et al*, 2001), NK1 agonists (Makeham *et al.*, 2005), and somatostatin 2A agonists (Burke *et al.*, 2008) have also shown differential effects on sympathetic vasomotor tone and reflexes. All the accumulated evidence suggests that, different neuropeptides cause differential modulation of the subpopulations of bulbospinal presympathetic RVLM neurons that are also activated differentially by different reflex stimuli. This apparent functional specificity is investigated further in chapters 4 and 5, with sympathetic baroreflex, somatosympathetic reflex and sympathetic chemoreflex responses following administration of OX-A in the RVLM.

1.3 Central pathways mediating sympathetic reflexes

Autonomic reflexes are important in order to provide minute-to-minute alterations in sympathetic activity to various vascular beds which enables all organs to meet their nutritional requirements and thus maintain homeostasis. The most extensively studied autonomic reflexes are the sympathetic baroreflex, somatosympathetic reflex, and peripheral and central chemoreceptor reflexes that are integrated in, and mediated through the RVLM and finally relayed via SPN. These are discussed in some detail below.

1.3.1 The baroreceptor reflex

The primary role of the baroreflex is to normalize any deviations in baseline arterial BP. Therefore the aim of the baroreflex is to lower sympathetic outflow, in response to an increase in arterial BP, by inhibiting the excitation of sympathoexcitatory RVLM neurons. Similarly, a decrease in BP results in a reflex increase in SNA that elevates BP to baseline (Figure 1.2).

Although the basic understanding of the baroreflex was described in 1866 when Ludwig and Cyon performed experiments showing that electrical stimulation of the aortic nerve resulted in acute hypotension and bradycardia via brainstem mechanisms (for review see Green & Heffron, 1966). However the current concept of

the baroreflex involved in short-term control of BP was first illustrated in denervated dogs by Cowley and colleagues who observed that denervation of arterial baroreceptors caused a pressor effect that persisted for several weeks until BP finally returned to pre-denervation levels (Cowley *et al.*, 1973). Baroreceptors are slowly adapting specialised mechanoreceptors that originate primarily in the adventitia of the carotid sinus and the aortic arch whose cell bodies are located in the petrosal ganglion and nodose ganglion respectively (Andersen *et al.*, 1978; Donoghue *et al.*, 1984; Kumada *et al.*, 1990; Chapleau *et al.*, 1995).

An increase in arterial pressure stretches the baroreceptors and mechanical deformation of the vessel wall leads to the opening of mechanosensitive cation channels resulting in baroreceptor afferent depolarization, increased firing and subsequent generation of an action potential (Brown, 1980; Chapleau *et al.*, 2001). The nerve signal is then transmitted via the aortic depressor nerves (arising from the aortic arch) that join the vagus nerve, and Hering's nerve (arising from the carotid sinus), which joins the glossopharyngeal nerve (Ciriello, 1983; Housley *et al.*, 1987). However in terms of baroreceptor reflex control, the aortic baroreceptors have a dominant role over carotid baroreceptors since the reflex bradycardia which occurrs after baroreflex is reduced by 85% following denervation of the aortic depressor nerve (Pickering *et al.*, 2008). The primary baroreceptor afferent nerves first synapse with neurons of the medial and dorsolateral subdivision of the NTS (Lipski *et al.*, 1975; Ciriello, 1983; Zhang & Mifflin, 1998). Glutamate is presumably the primary neurotransmitter in relaying the baroreceptor information to the NTS since bilateral blockade of EAA receptors eliminates the baroreflex in anaesthetised rats (Guyenet *et al.*, 1987; Leone & Gordon, 1989). The NTS have a number of outputs influencing many regions of nervous system. However, the most critical output in terms of baroreflex is the excitatory projection of the NTS to the GABAergic neurons in the CVLM via a combination of NMDA and AMPA/kainate receptors (Chalmers *et al.*, 1994; Dampney, 1994; Sun, 1995; Pilowsky & Goodchild, 2002).

The CVLM is thought to be a sympathoinhibitory region as lesions or inhibitions of the CVLM neurons evoke long lasting pressor and sympathoexcitatory responses. Further, stimulation of the CVLM results in depressor and sympathoinhibitory responses (Pilowsky *et al.*, 1987; Cravo & Morrison, 1993; Schreihofer & Guyenet,

2002). Barosensitive GABAergic CVLM neurons are concentrated in the most rostral part of the CVLM, while tonically active non-barosensitive GABAergic neurons are more common in the caudal CVLM (Cravo *et al.*, 1991; Sved *et al.*, 2000; Horiuchi & Dampney, 2002). Barosensitive inhibitory neurons of the CVLM project monosynaptically to bulbospinal sympathoexcitatory neurons in the RVLM (Masuda *et al.*, 1991) and inhibit their activity by releasing GABA as the principal neurotransmitter (Li *et al.*, 1991; Minson *et al.*, 1997). Barosensitive CVLM neurons exhibit tonic baroreceptor related discharges (Schreihofer & Guyenet, 2003) which are crucial for the arterial baroreflex (Dampney, 1994). After acute lesions of the NTS combined with CVLM inhibition, administration of bicuculline results in a larger increase in BP both in baroreceptor intact and barodenervated rats indicating baro-insensitive neuronal control of the RVLM (Sved *et al.*, 2000; Schreihofer & Guyenet, 2003). The RVLM is the final central site for integration of the baroreflex. Both the C1 and non-C1 cells in the RVLM influence the baroreflex. As previously mentioned, approximately 70% of electrophysiologically identified bulbospinal barosensitive neurons of the RVLM are catecholaminergic. Although these barosensitive C1 neurons are not essential for the maintenance of resting sympathetic tone, they are involved in the baroreflex as evidenced by the approximately 40% reduction in baroreflex gain following chemical depletion of these bulbospinal C1 neurons (Schreihofer & Guyenet, 2000; Guyenet *et al.*, 2001). Thus inhibition of RVLM activity results in decreased sympathetic output to SPN causing a reduction in cardiac output and heart activity, as well as a reduction in peripheral vascular resistance (Sved *et al.*, 2001; Pilowsky & Goodchild, 2002; Guyenet, 2006), which ultimately result in a reduction in MAP.

In addition to the baroreflex-sympathoinhibitory pathway, there is also a baroreflex-cardioinhibitory pathway that involves a direct input from the NTS to a group of vagal (parasympathetic) preganglionic neurons (cholinergic) in the nucleus ambiguus. These cardiac vagal preganglionic motoneurons are activated to reduce HR (McAllen & Spyer, 1976, 1978; Simms *et al.*, 2007). In normotensive rats, the SNS is dominant at lower BP levels, in contrast to the parasympathetic, which is dominant at higher BP levels (Simms *et al.*, 2007).

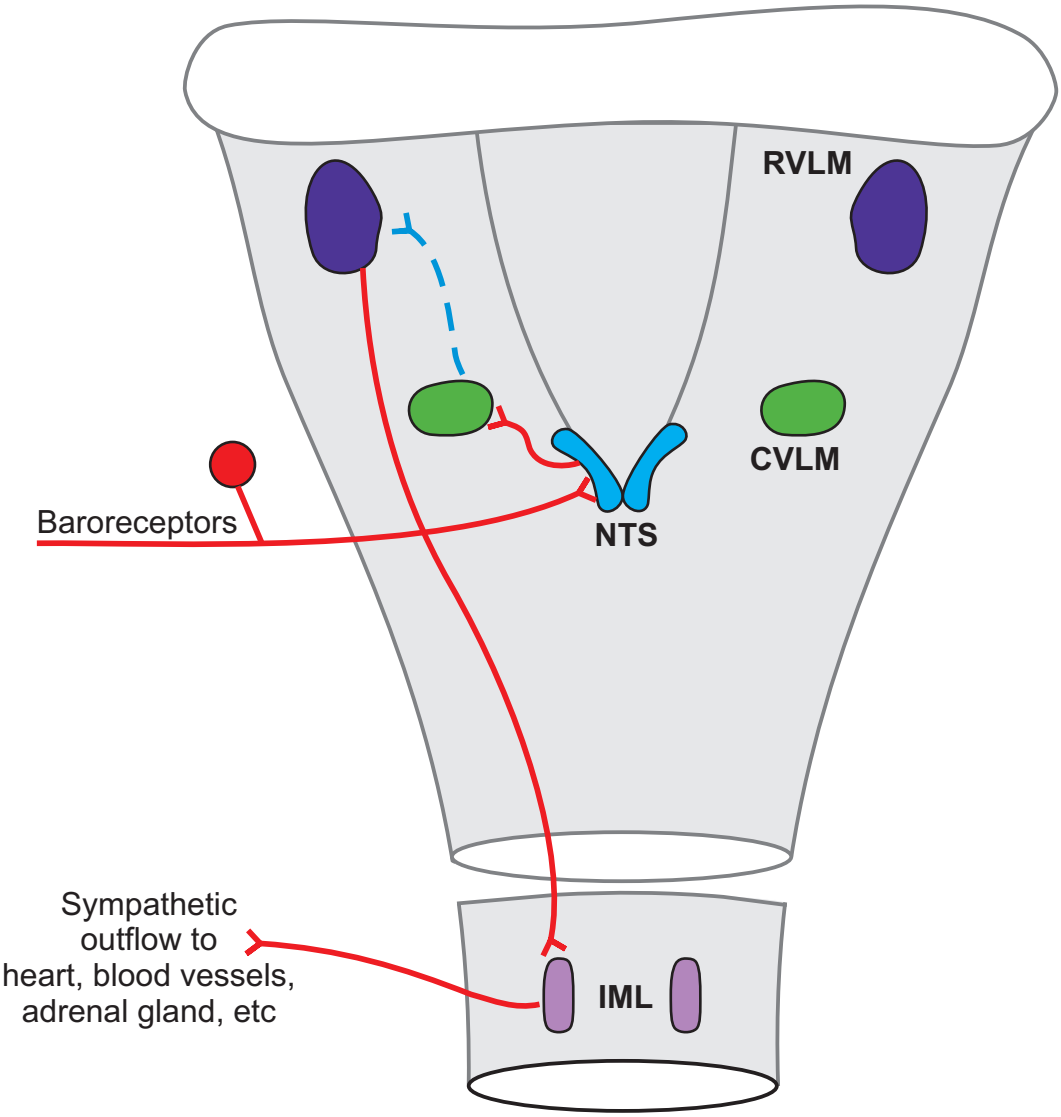

Figure 1.2. Central pathways involved in the sympathetic baroreceptor reflex.

Elevated blood pressure (BP) causes reflex sympathoinhibition to return BP to normal level. Arterial baroreceptors, when activated by elevated BP, send excitatory inputs to NTS. The sympathoinhibition occurs via disinhibition of RVLM neurons by GABA-ergic projection from CVLM that receives excitatory input from the NTS. Excitatory pathways are indicated by red lines and inhibitory pathways are indicated by dashed blue lines. Abbreviations: NTS, nucleus tractus solitarius; CVLM, caudal ventrolateral medulla; RVLM, rostral ventrolateral medulla; IML, intermediolateral cell column.

Since the major concern of this thesis is the regulation of sympathetic reflexes, the cardiac baroreflex is not discussed in detail here. Moreover the methods (chapter 2) and result chapters (3–5) in this thesis detail experiments conducted in bilaterally atropine treated and vagotomised rats where the PNS controlling the cardiovagal baroreflex is inactive.

1.3.2 The somatosympathetic reflex

The term “somatosympathetic reflex” refers to responses exhibited in the SNA following activation of somatic afferent neurons (Schmidt & Schönfuss, 1970; Sato & Schmidt, 1973). Somatic afferent nerves convey information about temperature, touch, body position, mechanical pressure, and distortion of the muscle (e.g. muscle stretch and tendon tension) and skin, to central autonomic nuclei (Christensen & Perl, 1970; Uchino *et al.*, 1970; Bessou *et al.*, 1971; Kumazawa & Perl, 1977). Activation of sensory pathways leads to appropriate changes in O_2, pH, and energy levels in the skeletal muscle and skin to meet metabolic demands and maintain homeostasis (Potts & Mitchell, 1998).

The afferent limb of the somatosympathetic reflex consists of primary afferent neurons synapsing directly with laminae I and II cells in the dorsal horn of the spinal cord (Light & Perl, 1979). Substance P plays a major role in the transmission of nociceptive somatic afferent input to the spinal cord. Axons of these cells cross the midline and ascend in the spinothalamic tract located in the dorsolateral funiculus on the contralateral side of the spinal cord. They may target autonomic sites in the spinal cord (SPN) (Willis & Westlund, 1997), then brainstem (RVLM, A1, NTS, A5, PBN), midbrain (PAG) and forebrain (hypothalamus, amygdala, thalamus) and, in primates, the cortex (Stornetta *et al.*, 1989; Andrew *et al.*, 2003; Craig, 2003) where the integration of the afferent signal takes place. The efferent limb comprises of presympathetic neurons projecting to, and synapsing with the SPN, which provides the basis for spino-spinal, spino-medullary, and spino-mesencephalic somatosympathetic reflex arcs (Sato & Schmidt, 1973; Craig, 2003) (Figure 1.3).

Intermittent electrical stimulation of somatic nerves (e.g. sciatic nerve) at low voltage in rats, consistently evokes two characteristic excitatory peaks in SNA with latencies

of ~ 70 and 170 ms (Morrison & Reis, 1989; Miyawaki *et al.*, 2001). A third late peak (peak III; ~250 ms) is also observed if the nerve is stimulated electrically at high intensity (Morrison & Reis, 1989; Burke *et al.*, 2011). Based on the conduction velocities of the peaks, it has been suggested that the first two peaks correspond to the lightly myelinated A-δ afferent fibres and the third peak belongs to the unmyelinated C- fibres. Furthermore, A-δ afferent fibres are suggested to be sufficient to produce the somatosympathetic reflex with a limited role for C-fibres in this response (Morrison & Reis, 1989).

Despite extensive studies on somatosympathetic reflex, there is still some debate about the origin of the two peaks observed in the SNA. As per the proposal of Morrison & Reis (1989), somatic afferent fibres (primarily A-δ fibres) course to the contralateral spinal cord with two different conduction velocities. These ascending afferent fibres then evoke direct or indirect excitation of both myelinated and unmyelinated presympathetic RVLM neurons through intermedullary neurons resulting in two excitatory peaks (Morrison & Reis, 1989). This proposal was further supported by Miyawaki *et al.,* (2001) who showed that the time between the two excitatory peaks are identical following electrical stimulation of the sciatic nerve and hypothesised different conduction velocities in efferent neurons to the RVLM . On the other hand, McMullan and colleagues proposed an alternative model to the origin of sympathoexcitatory peaks of somatosympathetic reflex in 2008. According to their study, stimulation of the sciatic nerve activates both A and C fibres which, in turn, drive separate second-order pathways from the contralateral side of the dorsal horn (Figure 1.3). These pathways were hypothesized to remain segregated until convergence on the RVLM neurons, which drive sympathetic nerve output in equal measure (McMullan *et al.*, 2008). However, the hypothesis remains to be confirmed.

The RVLM is crucial for the characteristic sympathoexcitatory response to somatic afferent nerve stimulation. Cooling the ventrolateral medulla (Zanzinger *et al.*, 1994) or neurotoxic lesions of cell bodies in the RVLM (Morrison & Reis, 1989) abolishes late (>50 ms; Schouenborg & Kalliomaki, 1990), but not early sympathetic responses, following stimulation of somatic afferents. Premotor RVLM neurons are suggested to relay the late supraspinal responses seen in the somatosympathetic reflex since

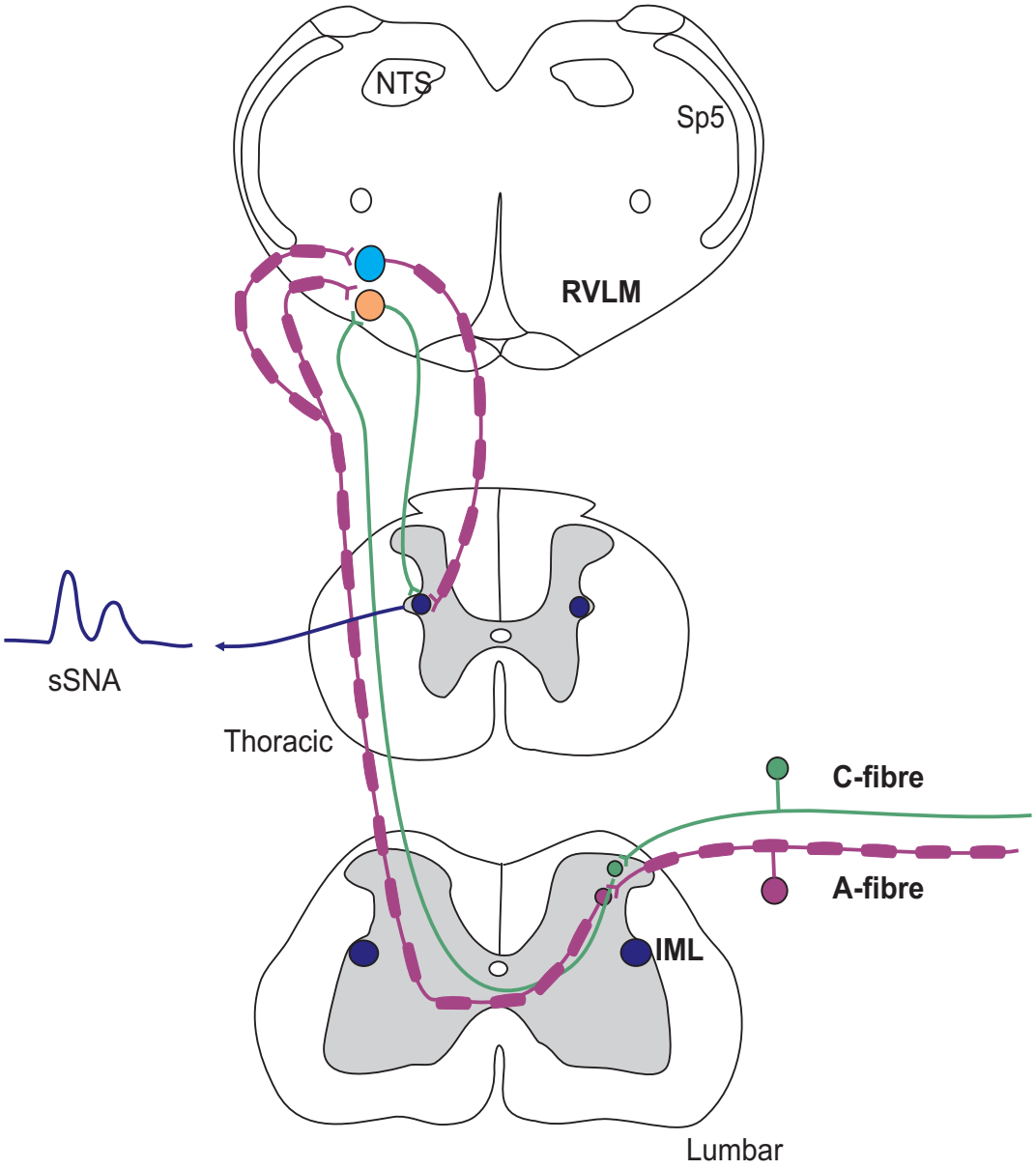

Figure 1.3. Central pathways involved in the somatosympathetic reflex.

Schematic diagram of the somatosympathetic pathway illustrating a possible mechanism by which myelinated and unmyelinated somatic inputs may regulate SNA. The green lines represent unmyelinated pathway and purple represent myelinated pathway. Adapted from McMullan *et al.*, 2008).

Abbreviations: IML, intermediolateral cell column; NTS, nucleus tractus solitarius; RVLM, rostral ventrolateral medulla; sSNA, splanchnic sympathetic nerve activity.

pharmacological blockade of this region has been shown to eliminate the supraspinal component of the reflex (Burke *et al.*, 2008). Extensive evidence supports the idea that glutamate transmission mediates the inputs to RVLM neurons activated in the somatosympathetic reflex. Blockade of glutamate receptors in the RVLM in cats (Zanzinger *et al.*, 1994) or rats (Miyawaki *et al.*, 1997) abolished the late supraspinal somatosympathetic reflex. Although the EAAs are proposed to be the major excitatory neurotransmitters for the somatosympathetic reflex in the RVLM, the reflex can be modulated by many other substances. For instance, selective activation of the γ-opioid receptors or 5-HT1A in the RVLM abolishes the somatosympathetic reflex whereas selective activation of δ -opioid receptors has no effect (Miyawaki *et al.*, 2001, 2002a).

1.3.3 The chemoreceptor reflex

The chemoreceptor reflex is an autonomic reflex that involves the monitoring of arterial O_2 and CO_2 levels on a second-to-second basis and a reflex response of neurally mediated adjustments in cardio-respiratory parameters to maintain homeostasis. Two types of chemoreceptors are implicated in this reflex, peripheral chemoreceptors that detect falls in PaO_2 (also known as the hypoxic chemoreflex), and central chemoreceptors that sense changes in arterial $PaCO_2$ or pH (also known as the hypercapnic chemoreflex).

1.3.3.1 Peripheral (hypoxic) chemoreflex

Peripheral chemoreceptors are located in the carotid bodies (in all mammals) and aortic bodies (in some species like human, cats and dogs). Glomus cells in the carotid bodies sense hypoxia while aortic bodies monitor O_2 saturation (Prabhakar & Peng, 2004). Although peripheral chemoreceptors can also be activated in response to other stimuli, e.g. hypercapnia, hypoglycaemia and pressure, the influence of these secondary reflexes on the sympathetic response is not significant (Morris *et al.*, 1996; Guyenet, 2000; Pardal & Lopez-Barneo, 2002). Sensory information from peripheral chemoreceptors travels via branches of the vagus nerve, and glossopharyngeal nerve together with fibres from baroreceptors (Sapru & Krieger, 1977; Housley *et al.*, 1987).

Chemosensitive afferents primarily terminate in the medial and commissural NTS at the level of the obex (CommNTS) (Lipski *et al.*, 1977; Finley & Katz, 1992; Mifflin, 1992). The major neurotransmitter of the chemoreceptor afferents projecting to the NTS is presumed to be an EAA, likely glutamate (Mizusawa *et al.*, 1994; Zhang & Mifflin, 1998). Glutamate microinjections into the commissural NTS increases phrenic nerve activity (PNA) identical to chemoreceptor activation (Vardhan *et al.*, 1993). An *in vivo* microdialysis study shows that glutamate is released in the NTS during hypoxia and that carotid body denervation abolishes this effect (Mizusawa *et al.*, 1994). The integrity of the NTS is crucial for the sympathoexcitatory effect of hypoxia which is further evidenced by the abolishment of sympathoexcitation by microinjection of EAA receptor antagonists (Vardhan *et al.*, 1993; Moreira *et al.*, 2006).

The NTS is believed to transmit chemoreceptor input from peripheral chemoreceptors to the RVLM, providing a neural substrate for the EAA-dependent excitation of RVLM neurons caused by hypoxia (Sun & Spyer, 1991; McAllen, 1992; Koshiya *et al.*, 1993; Sun & Reis, 1993a, b; Miyawaki *et al.*, 1996b) (Figure 1.4). Under anaesthesia, bilateral microinjection of kynurenic acid (glutamate antagonist) into the RVLM abolishes the sympathoexcitatory and pressor response following peripheral chemoreceptor activation which suggests glutamate mediated neurotransmission (Koshiya *et al.*, 1993; Sun & Reis, 1995).

A robust sympathoexcitatory response synchronized with central respiratory drive and PNA is observed following activation of the hypoxic chemoreflex (Koshiya & Guyenet, 1996b). This supports the notion that some chemoreflex information reaches the RVLM presympathetic neurons via the respiratory network. Electron microscopy studies have illustrated that some NTS neurons make monosynaptic connections with the C1 presympathetic neurons in the RVLM (Aicher *et al.*, 1996) (Figure 1.4). Certain neurons in the commissural NTS are excited by stimulation of the hypoxic chemoreflex and project to the RVLM, but do not display visible respiratory entrainment (Koshiya & Guyenet, 1996a). This suggests that these neurons do not receive central respiratory input. In addition, the neural circuitry subserving the hypoxic chemoreflex beyond the NTS is still unclear. There is evidence that the hypoxia-related changes in respiratory frequency and tidal volume

involve alteration in activity of medullary neurons in the DRG and VRG that are mediated by direct and indirect projections from the chemosensitive caudal NTS (St-John & Bianchi, 1985; Richter *et al.*, 1991; Fortuna *et al.*, 2008). Anatomical studies using tracers as well as functional studies, indicate that other brain regions such as the hypothalamic PVN innervating RVLM, noradrenergic A5 cell groups of the pons and PBN and RTN (Rosin *et al.*, 2006) also contribute in the central neuronal circuitry, along with the RVLM, underlying the processing of the sympathoexcitatory component of the chemoreflex (Guyenet *et al.*, 1993; Olivan *et al.*, 2001; Haibara *et al.*, 2002; Cruz *et al.*, 2008). *Fos* studies further demonstrate c-*fos* (a marker for neural activity) expression in other areas including the medullary raphé, A5, KF, LC, dorsal raphé, and ventrolateral PAG (Hirooka *et al.*, 1997; Teppema *et al.*, 1997). This suggests the involvement of these activated areas in the response to hypoxia (either the ventilatory or cardiovascular responses).

1.3.3.2 Central (hypercapnic) chemoreflex

Central chemoreceptors are stimulated by the acidification of brain extracellular fluid or an increase in the CO_2 level in the CNS. Although the location and phenotype of central chemoreceptors are widely debated, there is general agreement that central chemoreceptors have an intrinsic ability to detect changes in CO_2/H^+ and have the anatomical connections to respiratory centres that would enable them to regulate breathing (Putnam *et al.*, 2004; Guyenet *et al.*, 2005b). Hypercapnia causes powerful augmentation in BP and SNA even after surgical removal of peripheral chemoreceptors and baroreceptors suggesting that the reflex response to an elevated CO_2 is mediated mainly via central chemoreceptors (Millhorn & Eldridge, 1986; Oikawa *et al.*, 2005).

Central chemoreceptors are proposed to exist in various neurons including catecholaminergic neurons, serotonergic neurons, orexinergic neurons and NK-1 expressing neurons in different regions including the RTN, NTS, LC, ventral respiratory group, the A5 region, the raphé and fastigial nucleus (Nattie & Li, 2006a; Huckstepp *et al.*, 2010). For example, regional acidification in putative chemoreceptor sites including RTN (Li *et al.*, 1999; Dias *et al.*, 2008), medullary raphé (Nattie & Li, 2001), NTS (Nattie & Li, 2002a), and preBotC (Solomon *et al.*, 2000; Solomon, 2002) increases ventilation. In addition, local inhibition or destruction of neurons within these

putative neurons reduces the ventilatory response to hypercapnia from 22% to 65% (Nattie & Li, 1994; Nattie & Li, 2000, 2006b). However, the neurons in the RTN are considered to be central respiratory chemoreceptors based on their anatomical location, electrophysiological and chemical properties. For instance, *in vivo* single unit recordings from a subpopulation of glutamatergic, tonically active neurons in the RTN show a significant increase in discharge frequency in response to hypercapnia. This increased discharge frequency of RTN neurons persists even after peripheral chemoreceptor denervation and also after application of kynurenic acid (Mulkey *et al.*, 2004; Guyenet *et al.*, 2005a). Moreover, chemical stimulation of the RTN with glutamate increases PNA in anaesthetised, paralysed, vagotomised, artificially ventilated cats (Nattie & Li, 1994). Bilateral microinjection of muscimol ($GABA_A$ agonist) into the RTN completely abolishes sensitivity to hypercapnia and the drive to breathe in both anaesthetised and conscious rats (Nattie & Li, 2000; Takakura *et al.*, 2006), while bicuculline has no effect on chemosensitivity but promotes breathing under resting conditions (Nattie *et al.*, 2001). The data suggest that RTN neurons are intrinsically chemosensitive and that they also receive tonic inhibitory input originating from early inspiratory, post-inspiratory, and expiratory augmenting neurons via $GABA_A$ receptors that modulate respiration and potentially prevent saturation of neuronal discharge following hypercapnia (Guyenet *et al.*, 2005a). Neurochemical profiling has shown that chemosensitive neurons in the RTN express VGLUT2, a large portion of which co-localise Phox2b (necessary for the development of all types of autonomic ganglia) and the NK-1 receptor (Nattie & Li, 2002b; Mulkey *et al.*, 2004; Stornetta *et al.*, 2006). Unilateral lesion of 70% of Phox2b expressing RTN neurons attenuates central chemosensitivity and abolishes PNA following blockade of the contralateral RTN with muscimol (Takakura *et al.*, 2008). Recently Takakura *et al.,* (2011) showed that inhibition of chemosensitive RTN neurons eliminates resting breathing suggesting that central chemoreceptor-induced PNA is dependent on the RTN (Takakura *et al.*, 2011).

Activation of central chemoreceptors by an increase in brain CO_2 also induces sympathoexcitation. The activity of the RVLM presympathetic neurons is increased by 70% following central chemoreceptor stimulation (Haselton & Guyenet, 1989; Moreira *et al.*, 2006) suggesting that the RVLM contributes to the sympathoexcitation of hypercapnia. RTN neurons are considered as the plausible source of CO_2-dependent

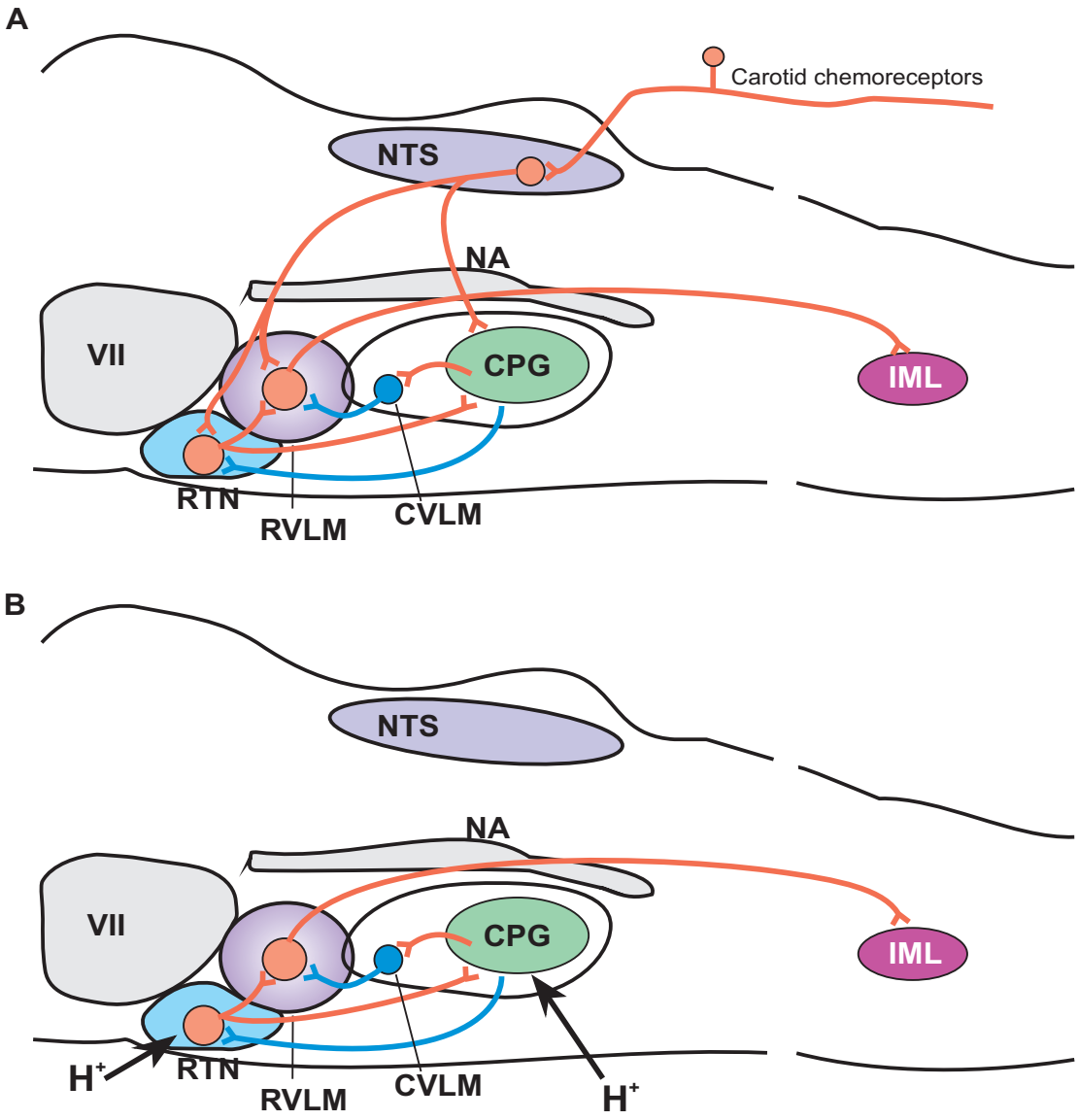

Figure 1.4. Central pathways involved in peripheral and central chemoreflex

A. Peripheral chemoreflex. Low PaO_2 level activates carotid chemoreceptors and causes reflex vasoconstriction, elevates BP and redistributes blood flow to the brain and heart. The increased SNA is mediated primarily by activation of the bulbospinal sympathoexcitatory neurons of the RVLM.

B. Central chemoreflex. CNS acidification (low pH) activates central chemoreceptors located in the RTN, and causes reflex vasoconstriction, elevates BP and redistributes blood flow to the brain and heart. The increased SNA is mediated primarily by activation of the bulbospinal sympathoexcitatory neurons of the RVLM.

Excitatory pathways are indicated by red lines and inhibitory pathways are indicated by blue lines. Blue circle indicate inhibitory neurons and red circles indicate excitatory neurons. Abbreviations: CPG, central/respiratory pattern generator; CVLM, caudal ventrolateral medulla; IML, intermediolateral nucleus; NA, nucleus ambiguus; NTS, nucleus tractus solitarius; RTN, retrotrapezoid nucleus; RVLM, rostral ventrolateral medulla. Adapted from Moreira *et al.*, 2006.

excitatory input to RVLM presympathetic neurons (Takakura *et al.*, 2011) since these neurons are not intrinsically pH-sensitive (Lazarenko *et al.*, 2009). Moreover, recent studies show that inhibition of the chemosensitive neurons located in the RTN reduced the sympathoexcitatory responses produced by central chemoreceptor activation (Takakura *et al.*, 2011) suggesting that sympathoexcitation and pressor responses to hypercapnia are partially mediated by the RTN. The sympathoexcitation produced by hypercapnia is reduced after injection of the NMDA glutamate antagonist (AP-5) into the RTN which might be due to the decrease in the excitability of RVLM presympathetic neurons after removing baseline facilitatory glutamatergic signals from the RTN (Moreira *et al.*, 2011) (Figure 1.4). Furthermore, the activation of RVLM neurons is patterned by the central respiratory cycle in the same manner as is SNA (McAllen, 1987; Haselton & Guyenet, 1989; Miyawaki et al., 1995; Moreira *et al.*, 2006).

1.4 Central regulation of respiration: a brief overview

Respiration (or breathing) is a process that maintains life by ensuring the appropriate delivery of O_2 to, and removal of CO_2 from, body tissues and organs. This autonomic process depends on the coordinated synchronization of the central respiratory neurons and other bodily functions such as swallowing, motion and coughing (St-John, 1998).

Respiratory neurons are organized within longitudinally arranged columns of functional groups in the pons and medulla of the brainstem, in close proximity of the sympathetic cardiovascular neurons (Smith *et al.*, 2009). Several muscle groups including the diaphragm, intercostal muscles and those of the upper airways and abdomen also participate in breathing by displaying a specific pattern of activity during reflex responses. However, these muscles are activated to a lesser extent during normal breathing. Phrenic motoneurons located in the cervical spinal cord at levels C3-C5 receive excitatory monosynaptic input from the inspiratory neurons in the ventral respiratory column (VRC), and innervate the diaphragm (Dobbins & Feldman, 1994; Bianchi *et al.*, 1995). The activity of phrenic nerve fibres is commonly

used as a measure of neural inspiratory drive. The medullary networks that regulate PNA are primarily discussed in this thesis.

1.4.1 Respiratory cycle

Central respiratory output is usually divided into three main phases: inspiration, post inspiration (or early expiration) and late expiration. In the inspiratory period, the diaphragm contracts, resulting in inflation of the lungs. During post-inspiration, the activity of inspiratory muscles decreases while muscles of the upper airways are activated to control the rate of airflow out of the lungs. Finally, in late expiration, contraction of the abdominal and intercostal muscles occurs to force air out of the lungs (Richter, 1982; Bianchi *et al.*, 1995).

1.4.2 Organization of respiratory neurons

Respiratory neural centres located in bilateral columns of nuclei in the pons, and the dorsal and ventral respiratory column of the medulla oblongata (Figure 1.5) are functionally classified into three major groups: (1) rhythm generators that initiate inspiration, (2) premotor neurons that shape and elaborate specific respiratory patterns and (3) motoneurons innervating respiratory muscles.

1.4.2.1 Pontine respiratory nuclei (PRN)

Pontine respiratory neurons comprise the PB / KF complexes and the inter-trigeminal (ITR) area extending rostrocaudally from the dorsolateral pons to the ventrolateral pons and A5. These neurons show reciprocal connection with all the nuclei in the VRC and dorsal respiratory group (DRG) (Herbert *et al.*, 1990; Bianchi *et al.*, 1995; Alheid *et al.*, 2004; Chamberlin, 2004).

PRN are essential to maintain the respiratory cycle, particularly after bilateral vagotomy (Dick *et al.*, 2009). From earlier as well as recent studies, it is evident that removal or lesion of the pons evokes abnormalities in respiration, including apneusis (Lumsden, 1923; O'Sullivan *et al.*, 2008). PRN also serve as vital interface nuclei linking behaviour and environmental cues with rhythm and pattern generating circuits of the VRC. For example, the ventrolateral pons and A5 region initiate adaptive breathing patterns in response to hypoxia (Dick & Coles, 2000). Bilateral inactivation

of pontine nuclei markedly attenuates or abolishes respiratory adjustments to these various reflexes (Coles & Dick, 1996; Jiang *et al.*, 2004).

1.4.2.2 Dorsal respiratory group (DRG)

The DRG is composed largely of inspiratory neurons located at the level of obex in the ventrolateral subnucleus of the NTS and the reticular formation ventral to the NTS. A portion of DRG neurons (66%, in cat) are bulbospinal (n = 31/47; Fedorko *et al.*, 1983) while some show monosynaptic projection to phrenic motoneurons (Bianchi *et al.*, 1995). DRG neurons are second order neurons that receive afferent inputs from pulmonary stretch receptors, and are activated by lung inflation or deflation (Ezure & Tanaka, 2000). These neurons are also reported to be driven by the inspiratory neurons in the VRC (Ezure & Tanaka, 2000).

1.4.2.3 Ventral respiratory column (VRC)

The VRC in the medulla oblongata extends rostrocaudally from the caudal pole of the facial nucleus to the rostral portion of the first cervical spinal segment (Chitravanshi & Sapru, 1999). The column consists of highly interconnected neurons that can be divided into at least four functional groups: the BötC, preBötC and the rostral (rVRG) and caudal (cVRG) parts of the ventral respiratory group (VRG) (Figure 1.5).

1.4.2.3.1 The Bötzinger Complex (BötC)

BötC neurons are located in the most rostral part of the VRC (Figure 1.5) and consist mainly of bulbospinal expiratory neurons and propriobulbar neurons. The BötC neurons are intermingled with ventrally located presympathetic RVLM neurons (Moraes *et al.*, 2011) as well as with the caudally located inspiratory neurons of preBötC (Sun *et al.*, 1998; Zheng *et al.*, 1998, Zheng et al., 1991, 1992). Glycine is the principal neurotransmitter of the BötC (Schreihofer *et al.*, 1999; Ezure *et al.*, 2003) that provide monosynaptic inhibitory projection to a wide variety of area including other respiratory (such as preBötC, rVRG, cVRG, DRG and phrenic motoneurons) (Tian *et al.*, 1998), cardiovascular (such as RVLM and CVLM) (Sun *et al.*, 1997), and chemosensitive neurons (RTN) (Sun *et al.*, 1997; Tian *et al.*, 1999; Rosin *et al.*, 2006). The primary function of the BötC is to terminate the inspiratory phase via its projection to the rhythm generator, preBötC, and to maintain the expiratory phase.

1.4.2.3.2 The preBötzinger Complex (preBötC)

The preBötC, discovered in the early 1990s, is considered as a key site for rhythm generation (Ellenberger & Feldman, 1990; Feldman *et al.*, 1990). This complex lies caudal to the BötC and rostral to the rVRG (Figure 1.5), and the neurons are intermingled with ventral GABAergic CVLM neurons. These neurons also show extensive interconnections with all ponto-medullary respiratory nuclei (Sun *et al.*, 1998; Tan *et al.*, 2009). PreBötC neurons consist of a mixed population of propriobulbar inspiratory, expiratory and phase-spanning neurons. These neurons also show heterogeneity in their neurotransmitter and receptor content. The preBötC neurons contain a glutamate marker (VGLUT2) and are immunoreactive to NK-1 (Gray *et al.*, 2001; Wang *et al.*, 2001; Guyenet *et al.*, 2002), GABA and glycine receptors (Liu *et al.*, 2001; Liu & Wong-Riley, 2002). In addition, recent studies have shown the presence of glycinergic pacemaker neurons in the preBötC that are suggested to be important in the generation and maintenance of the respiratory rhythm (Winter *et al.*, 2009; Morgado-Valle *et al.*, 2010).

Extensive studies have been conducted to reveal the role of preBötC in respiratory rhythm generation and to date at least four different theories have been suggested: the group-pacemaker model (also referred to as the inspiratory-expiratory two oscillator model) (Feldman & Del Negro, 2006), the hybrid pacemaker-network model (Smith *et al.*, 2000; Rybak *et al.*, 2004), the maturational network-burster model (Richter & Spyer, 2001), and the dual pacemaker model (Ramirez *et al.*, 2004). However, the mechanism by which the preBötC generates respiratory related rhythm remains controversial.

1.4.2.3.3 Caudal ventral respiratory group (cVRG)

The cVRG is located caudal to the inspiratory neurons of the rVRG and extends to the level of the pyramidal decussation. This nucleus consists mainly of excitatory, expiratory neurons that project largely to spinal thoracic and lumbar expiratory motoneurons controlling abdominal and internal intercostal muscles (late expiratory musculature), and to a lesser extent, to the phrenic motoneurons (Feldman *et al.*, 1985; Monteau & Hilaire,1991). The cVRG also project to the rVRG, contralateral cVRG, BötC,

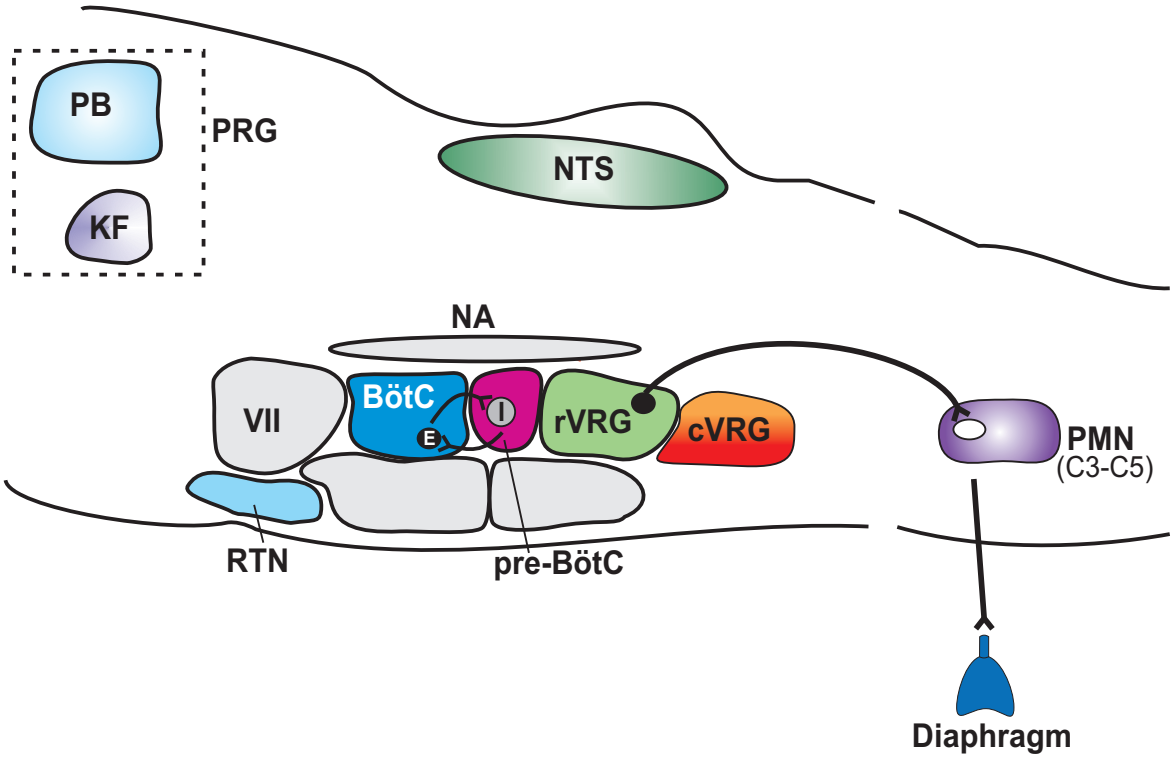

Figure 1.5. Schematic of respiratory related regions of the brainstem.

A simplified representation of spatially arrayed subnuclei of brainstem involved in the regulation of respiration. The pontine respiratory group (PRG) consists of parabrachial nucleus (PB) and Kölliker Fuse (KF). The ventral respiratory column consists of Bötzinger complex (BötC), pre-Bötzinger complex (pre-BötC), rostral ventral respiratory group (rVRG), and caudal VRG (cVRG). See text for descriptions of the functional properties of each nucleus.
Abbreviations: NA, nucleus ambiguus; NTS, nucleus tractus solitarius; PMN, phrenic motoneuron; RTN, retrotrapezoid nucleus.

A5 and KF (Ellenberger & Feldman, 1990; Nunez-Abades *et al.*, 1991; Gaytan *et al.*, 1997; Saito *et al.*, 2002).

1.4.2.4 Retrotrapezoid nucleus (RTN)

RTN neurons are considered to be the key central chemoreceptors and are located on the ventral surface of the medulla, beneath the facial nucleus and extend caudal to the level of the BötC (Figure 1.5). This nucleus is a major central chemosensory site as the firing rate of these neurons are increased in response to local changes in pH as suggested by both *in vivo* and *in vitro* studies (Mulkey *et al.*, 2004; Takakura *et al.*, 2006; Abbott *et al.*, 2009b; Guyenet *et al.*, 2009; Guyenet *et al.*, 2010). The chemosensitive RTN neurons are non-cholinergic but are glutamatergic and express the homeodomain transcription factor Phox2b (Mulkey *et al.*, 2004; Stornetta *et al.*, 2006; Lazarenko *et al.*, 2009; Guyenet & Mulkey, 2010).

The RTN is also involved in the reflex responses to hypoxia (Takakura *et al.*, 2006). The neurons are interconnected with the VRG, DRG, NTS, nucleus ambiguus, KF, and also with the autonomic areas of the spinal cord, brainstem (medulla: RVLM & CVLM), lateral hypothalamus and amygdala (Smith *et al.*, 1989; Weston *et al.*, 2004; Rosin *et al.*, 2006).

1.4.3 Respiratory modulation of SNA

The idea that SNA is coupled to distinct phases of the respiratory cycle was first demonstrated in 1932 (Adrian *et al.*, 1932). This coupling is characterised by a rhythmic fluctuation in SNA in relation to PNA and the exact pattern of this coupling depends on the species, strain, and peripheral nerve (Janig & Habler, 2003). The presence of respiratory-coupling after bilateral vagotomy and paralysis indicates that it originates in the CNS. PNA triggered averaging of the cervical and lumbar nerves commonly reveal only one peak during the post-inspiratory (post-I) phase (Miyawaki *et al.*, 2002b), while the splanchnic nerve displays a biphasic pattern of activity with peaks during both the inspiration and post-I periods (Dick *et al.*, 2004) in the adult rat. This difference in the pattern of respiratory coupling of SNA may be due to functional specificity of sympathetic nerves innervating different tissue beds.

The exact source and target area involved in cardiorespiratory coupling are still not clear. The most likely source of respiratory input is either the putative respiratory rhythm generating centre within the brainstem, the preBötC, or closely associated respiratory related interneurons. Pontine circuits are suggested to be the source of the excitatory post-I input of the modulation (Baekey *et al.*, 2008; Dick *et al.*, 2009). The synaptic interaction between central respiratory drive and vasomotor neurons takes place in the ventrolateral medulla (McAllen, 1987; Pilowsky *et al.*, 1996). As evidence of support, morphological studies show that medullary respiratory neurons project to cardiovascular neurons in the RVLM (Pilowsky *et al.*, 1990; Sun *et al.*, 1997). In addition, microinjection of muscimol in the preBötC abolishes all central respiratory activity including the respiratory related modulation of SNA (Koshiya & Guyenet, 1996b). In bilaterally vagotomised rats, the post-I splanchnic SNA (sSNA) peak is blocked by ionotropic glutamate receptor blockade in the RVLM suggesting that the post-I coupling of sSNA is derived from an excitatory synaptic input to the RVLM (Miyawaki *et al.*, 1996a). Furthermore, blockade of RVLM $GABA_A$ receptors with bicuculline increases the post-I peak of both sSNA and lumbar SNA (Miyawaki *et al.*, 2002b) indicating that excitatory and inhibitory drives are both important for cardiorespiratory coupling.

The pattern of respiratory-modulated SNA is also influenced by reflex changes. For example, central respiratory drive modulates the activity of RVLM neurons to baroreceptor inputs (Miyawaki *et al.*, 1995). An augmented post-I related SNA has been reported in juvenile pre-hypertensive spontaneously hypertensive rats (SHR) (Simms *et al.*, 2009) suggesting an alteration in cardiorespiratory coupling in hypertension. The post-I sSNA peak is greatly increased during acute hypoxic exposure (Dick *et al.*, 2004; Dick *et al.*, 2007) suggesting chemoreceptor-dependent modulation of cardiorespiratory coupling.

1.5 Hypertension

Hypertension is the most prevalent cause of cardiovascular disease leading to heart failure, stroke and ultimately to death. Hypertension currently affects 10%-30% of the Australian population (Briganti *et al.*, 2003). Hypertension is characterised by an

elevation of BP, an increase in vascular resistance to blood flow, cardiac hypertrophy, often an increase in cardiac output, increased activity of SNS, change within vascular smooth muscles, often atherosclerosis, and renal dysfunction (Hennersdorf & Strauer, 2001). Since hypertension and other cardiovascular diseases are the leading causes of death, dedicated research efforts, to elucidate the mechanism of and explore the treatment for hypertension, have been taken. Despite the research efforts taken over the century, the specific mechanisms behind the development of hypertension are poorly understood (Zaiman *et al.*, 2005). It is generally believed that both genetic and environmental factors and their interactions, play a critical role in the pathogenesis of hypertension (Carretero & Oparil, 2000; Touyz, 2000; Oudit *et al.*, 2003). Hypertension is classified into two types: primary or essential hypertension, and secondary hypertension. The aetiology of essential hypertension is largely unknown and the cause of it may be multifactorial (Izawa *et al.*, 2003). Secondary hypertension is caused by known pathological conditions including dysfunction in the renin-angiotensin-aldosterone system, vasopressin, NO and endothelin (Zaiman *et al.*, 2005; Sakao *et al.*, 2009).

1.5.1 Neural mechanisms of hypertension

Much evidence supports the 'neurogenic hypothesis of hypertension' which implies that excessive sympathetic vasomotor activity plays a key pathogenic role in triggering and sustaining the hypertensive state (Fisher & Fadel, 2010; Grassi, 2010). Increased sympathetic outflow to the heart results in elevated cardiac output via increased force and rate of contraction contributing to an elevation in BP. The effect of sympathetic nerve activation to the kidney leads to excessive sodium retention resulting in blood volume expansion. This increase in blood volume will cause BP to elevate via an increase in cardiac output. In addition, increased rSNA results in increased renin secretion which activates the systemic renin – angiotensin system (RAS) leading to angiotensin (Ang) II-induced vasoconstriction. Persistent elevation in sympathetic outflow would also contribute to rise in BP by causing trophic effects on vascular smooth muscle leading to increases in vascular resistance and enhanced responses to vasoconstrictor stimuli (for review see Veerasingham & Raizada, 2003). The neural basis of hypertension is also supported by a high rate of cardiac and renal NA spillover due to an impairment in the neuronal NA reuptake system (Rumantir *et al.*, 2000), which is attributed to increased sympathetic nerve

firing to the heart, kidney and skeletal muscle (Esler *et al.*, 1988; Esler *et al.*, 1990). Muscle SNA measured by microneurography (Yamada *et al.*, 1988) and single unit recording (Grassi *et al.*, 1998; Lambert *et al.*, 2007) in hypertensive patients compared to normotensive patients, revealed elevated sympathetic outflow, supporting the concept of a central neural mechanism for sympathetic activation in hypertension.

The arterial baroreflex is a major control mechanism of arterial pressure and sympathetic vasomotor activity. In particular, alterations in arterial baroreflex function appear to contribute to the pathogenesis of hypertension (Gonzalez *et al.*, 1983; Widdop *et al.*, 1990; Head & Adams, 1992). The arterial baroreflex responds to changes in BP by modulating parasympathetic and SNA and hence, HR and vascular tone. This curtails fluctuations in BP and maintains it close to a particular set point. In response to a static increase in BP, the baroreflex rapidly resets towards a higher pressure (Andresen & Yang, 1989). In hypertensive conditions, resetting of the operational point of the arterial baroreflex may therefore contribute to maintaining an increased BP rather than opposing it. In humans, arterial baroreflex function is significantly related to the prognosis of acute myocardial infarction, arrhythmias, heart failure and stroke. Patients with a lower baroreflex sensitivity exhibit shorter survival times (La Rovere *et al.*, 2002; Guyenet, 2006; Seedat, 2009). The baroreflex resetting by neural mechanisms also contributes to sympathetic overactivity leading to hypertension.

1.5.2 The RVLM in hypertension

The RVLM is the major vasomotor centre that determines basal SNA and is essential for the maintenance of basal vasomotor tone and reflex responses (Pilowsky & Goodchild, 2002; Guyenet, 2006). Accumulating evidence suggests that increased RVLM activity leads to chronic sympathetic hyperactivity in many forms of hypertension. For example, in SHR, excitation of the RVLM vasomotor neurons is increased by L-glutamate-mediated excitation and decreased by GABA-mediated inhibition (Sun & Guyenet, 1986b; Minson *et al.*, 1996; Leenen, 1999; Palatini, 2001; Campese & Krol, 2002; Sved *et al.*, 2003). Thus any imbalance of excitatory or inhibitory inputs to the RVLM could potentially lead to an elevation in the SNA and thus in hypertension. Greater expression of *c-fos* is observed in the RVLM of SHR

compared to Wistar-Kyoto rats (WKY) (Minson *et al.*, 1996) and the reason for the greater *c-fos* expression might be due to augmented neural activity in the RVLM of SHR. In SHR, an upregulation of RVLM catecholaminergic gene expression is found which indicates a higher level of activity of these neurons contributing to the aetiology of neurogenic hypertension (Kumai *et al.*, 1996; Xiong *et al.*, 1998; Reja *et al.*, 2002a; Reja *et al.*, 2002b). Electrophysiological studies also support the notion that RVLM activity is increased in hypertension. For instance, the majority of SHR RVLM neurons (57%) exhibited double (irregular) discharges while 43% of neurons showed single (regular) discharge patterns. In contrast, only 7% of WKY RVLM neurons displayed double discharges and 93% of these neurons showed single discharge pattern (Chan *et al.*, 1991). In addition, intracellular recordings using whole cell patch clamp technique in neonatal SHR found that RVLM neurons had significantly lower membrane potentials and exhibited increased firing rates compared to their normotensive counterparts (Matsuura *et al.*, 2002). Moreover, peptides like apelin (Zhang *et al.*, 2009), AT1 receptors (Allen, 2011), and muscarinic cholinergic receptor (Kumar *et al.*, 2009) mRNA levels are upregulated in the RVLM neurons of the SHR compared to their normotensive counterparts. The understanding of the role of this altered peptidergic mechanism in the development or maintenance of essential hypertension is not clear.

1.5.3 Rodent models of hypertension

Animal models are useful for studying the pathophysiology of hypertension, and seeking new therapies. The first animal model of hypertension was developed by clipping the renal artery in the dog to decrease blood flow to the kidney producing a renovascular hypertension phenotype (Goldblatt, 1964). Since then, a number of hypertensive rat models, according to hypertension etiology, have been developed (Figure 1.6). Although the final common manifestation of all these models is high BP, none of them encompass all traits of human hypertension.

In addition to high BP, various animal models of hypertension are also associated with elevated SNA such as the spontaneously hypertensive rat (SHR) (Cabassi *et al.*, 2002), the renin transgenic rat (TGR mRen2) (Arribas *et al.*, 1996), the Dahl salt sensitive rat (Leenen *et al.*, 2002) and the deoxycorticosterone acetate (DOCA)-salt rat (Takeda & Bunag, 1980). By using different types of experimental hypertensive

models, scientists may identify and evaluate potential risk factors contributing to hypertension and related cardiovascular diseases.

1.5.3.1 Spontaneously hypertensive rats (SHR)

The SHR, genetically derived from the Wistar-Kyoto line with the highest BP (Okamoto & Aoki, 1963), is an inbred strain with heritable hypertension and is widely employed as an animal model of essential hypertension (for review see Sun & Zhang, 2005). SHR develop many features of hypertensive end-organ damage including cardiac hypertrophy, heart failure, and renal dysfunction. Although the mechanisms for producing the hypertension are not clear, different studies seem to indicate the participation of the hypothalamus and the medulla oblongata including RVLM, in the mechanisms underlying the expression or maintenance of hypertension in SHR (Renaud *et al.*, 1979; Miyagawa *et al.*, 1991; Vasquez *et al.*, 1992). In SHR, excitation of RVLM vasomotor neurons is mainly due to increased glutamate mediated excitation and decreased GABA mediated inhibition (Sved *et al.*, 2003; Hirooka *et al.*, 2010). Overactivity of the brain RAS appears to be involved in initiating the development of spontaneous hypertension based on the finding that central injections of angiotensin II receptor antagonists cause greater reductions in BP in SHR than in normotensive rat (Mann *et al.*, 1978; Yang *et al.*, 1992). Interestingly, some hemodynamic alterations which occur during the progression of the disease are similar to human essential hypertension (i.e. a high cardiac output at an early stage, and a normal cardiac output and increased vascular resistance in the adult) (Trippodo & Frohlich, 1981). In the SHR, basal BP is 40–60 mmHg higher than in normotensive rats, and the sigmoid curve demonstrating baroreflex control of MAP and SNA is shifted upward but remains parallel to the normal baroreflex curve (Gonzalez *et al.*, 1983; Hayashi *et al.*, 1993; Yin & Sved, 1996).

Previous studies reported the effects of OX-A on blood pressure and heart rate following injection into the RVLM of rats (Chen *et al*., 2000; Machado *et al*., 2002). But there are no studies prior to this work that reveal the effects of OX-A into the RVLM on sympathetic and phrenic nerve activity, and on sympathetic reflexes. The expression of OX receptors in the RVLM is also unexplored.

Based on the results of previous studies and the presence of OX-A fibres in the RVLM we aimed to evaluate the role of OX-A on cardiorespiratory parameters and sympathetic reflexes following bilateral microinjection into the RVLM.

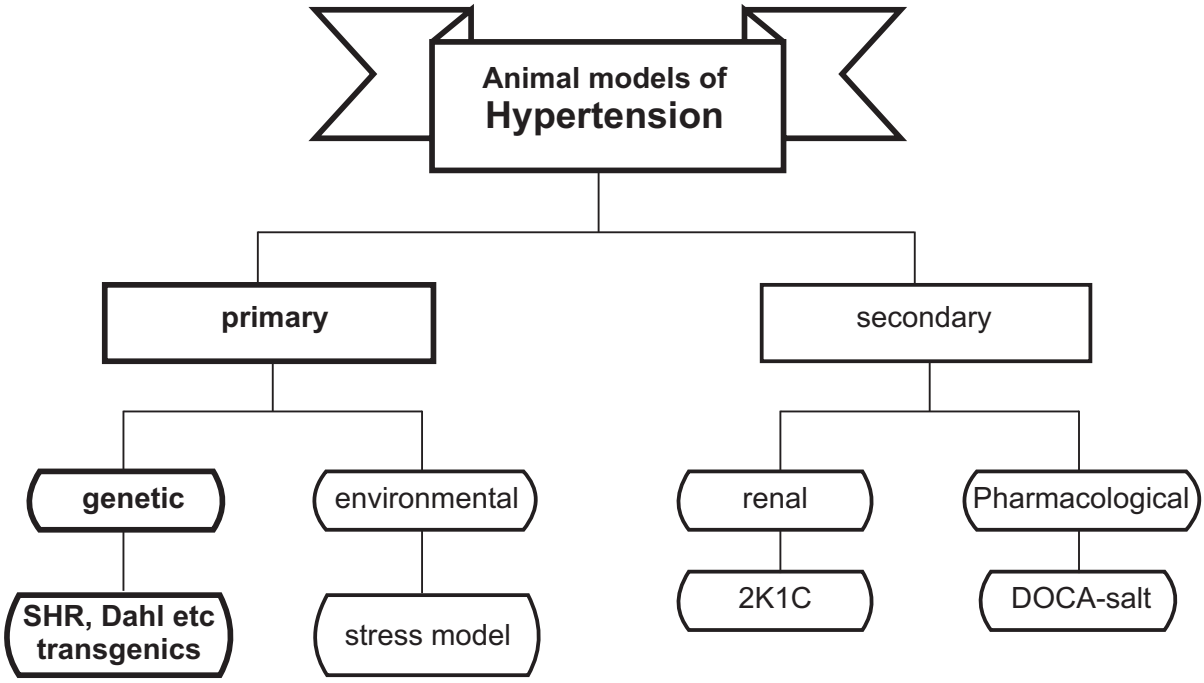

Figure 1.6. Animal models of hypertension.

The classification of major animal models of hypertension. Primary hypertension is the most common form in humans, and is often represented by genetic models of hypertension, such as SHR. This thesis used SHR. Figure and legend adapted from Sun & Zhang, 2005.

1.6 Orexin A

1.6.1 Identification and structure

1.6.1.1 Orexins

OX-A and orexin B (OX-B) (also called hypocretin 1 and hypocretin 2) were first identified in 1998 by two separate groups via two different approaches (de Lecea *et al.*, 1998; Acuna-Goycolea & van den Pol, 2004; Alexander *et al.*, 2011). In the current review we will use the term orexin, which is derived from the Greek word '*orexis'*, meaning 'appetite'. Orexins were so named for their stimulatory role in feeding (Sakurai et al., 1998). Both OX-A and OX-B are produced by proteolytic cleavage of the gene product prepro-orexin.

Mammalian (human, pig, dog, rat, mouse) prepro-orexin, composed of 130-131 amino acid, is highly conserved with 75% amino acid sequence identity (de Lecea *et al.*, 1998; Sakurai *et al.*, 1998; Dyer *et al.*, 1999; Hungs *et al.*, 2001). The human prepro-orexin gene is localized on chromosome 17q21 (Sakurai et al., 1998). The mRNA of this precursor is abundantly and specifically expressed in the lateral hypothalamus and adjacent areas important in the central regulation of feeding behaviour and energy homeostasis (Sakurai et al., 1999).

OX-A is a 33-amino acid peptide of 3562 Da. It consists of an N-terminal pyroglutamyl residue, two intramolecular disulfide bridges between Cys^{6}-Cys^{12} and Cys^{7}-Cys^{14}, and a C-terminal amidation. The primary structure of OX-A is completely conserved among several mammals (human, rat, mouse, dog, cow, sheep and pig) (Figure 1.7A). On the other hand, OX-B is a 28-amino acid linear peptide of 2937 Da with a C-terminal amidation. Human OX-B differs by one amino acid from pig and dog OX-B, and by two amino acids from rat and mouse OX-B (Figure 1.7B). OX-B shares 46% sequence identity with OX-A. The similarity in amino acid sequence lies mainly in C-terminus whereas the N-terminal half is more variable (Figure 1.7A). The free N-terminal can be related to the rapid metabolism and shorter action of OX-B as compared to OX-A. In contrast, post-translational modifications of both termini and two intrachain disulfide bonds may render orexin-A more stable and readily available

in cerebrospinal fluid. OX-A also shows higher lipid solubility than OX-B which makes it more blood brain barrier permeable (Kastin & Akerstrom, 1999).

1.6.1.2 OX receptors

HFGAN72, the orphan GPCR, was identified as an OX receptor when OX was discovered and was named OX receptor 1 (OX_1R) (also called hypocretin 1). An extensive search for amino acid sequence identity with OX_1R resulted in the discovery of a second receptor for OX, another GPCR, named OX receptor 2 (OX_2R) (also known as hypocretin 2) (Sakurai *et al.*, 1998; Alexander *et al.*, 2011). OX receptors show only 20-28% structural similarity with other GPCR neuropeptide receptors such as neuropeptide Y2 receptor, thyrotropin releasing hormone receptor, cholesystokinin type-A receptor and neurokinin 2 receptor (Sakurai et al, 1998).

Human OX_1R is a 425-amino acid long protein and OX_2R is a 444-amino acid long protein sharing 64% sequence identity with each other. OX_1R gene is localized on chromosome 1p33 and OX_2R gene on chromosome 6p11-q11 (Sakurai et al, 1998; De Lecea et al, 1998). Each of the receptors consists of seven putative transmembrane helices, several modifications (glycolysation and phosphorylation) of extracellular and intracellular loops, and are encoded by seven exons. In human OX_1R and OX_2R, all transmembrane segments, extracellular loops and intracellular loops I and II are highly conserved while the N-terminal extracellular domain, intracellular loop III and the C-terminal tail exhibit great variability in amino acid sequence as well as length. The amino acid sequence of human OX_1R and OX_2R are 94% and 95% (respectively) identical to their rat counterparts, respectively, indicating that both receptor genes are highly conserved among species (Peyron et al., 2000).

Radioligand-binding studies have shown that OX_1R has one order of magnitude greater affinity for OX-A (IC_{50}: 20 nM) than for OX-B (IC_{50}: 420 nM), indicating that OX_1R is highly selective for OX-A. In contrast, tracer binding to OX_2R shows that OX-A and OX-B bind with OX_2R with similar affinity indicating that OX_2R is a nonselective receptor for both OXs (Sakurai *et al.*, 1998; Smart *et al.*, 2000; Okumura *et al.*, 2001).

A

Orexin A
(human/rat/mouse/pig/dog/sheep)
Orexin B

Pyr-PLPDCCRQKTCSCRLYELLHGAGNHAAGILTL-NH_2

----RSGPPGLQGRLQRLLQASGNHAAGILTM-NH_2

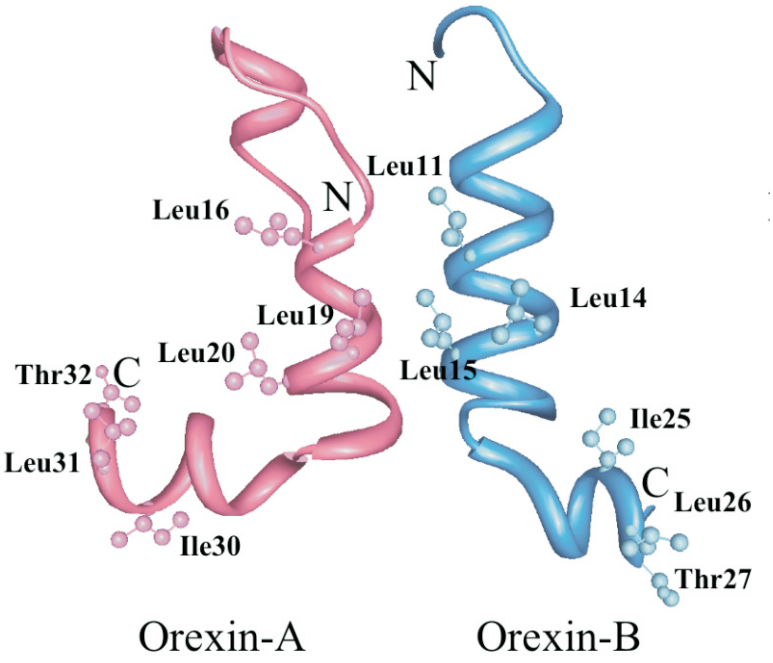

B

Human Orexin B	----RSGPPGLQGRLQRLLQASGNHAAGILTM-NH_2
Pig/dog Orexin B	----RPGPPGLQGRLQRLLQASGNHAAGILTM-NH_2
Mouse/rat Orexin B	----RPGPPGLQGRLQRLLQANGNHAAGILTM-NH_2

Figure 1.7. Structures of orexin A (OX-A) and orexin B and their sequences in different species.

A,B: Grey boxes indicate dissimilar amino acids (as compared with human variants). Cystine bridges in OX-A are shown in **A** with solid lines.

In recombinant systems, activation of either OX_1R or OX_2R, coupled to Gq G-protein, results in the elevation of intracellular Ca^{2+} concentrations (Smart *et al.*, 1999; Lund *et al.*, 2000). In chinese hamster ovary (CHO) cells, stimulation of OX_1R activates the receptor-operated influx of extracellular Ca^{2+} that occurs via opening of N-/L-type voltage-gated Ca^{2+} channels. This influx of Ca^{2+} enhances Gq-mediated stimulation of phosphatidylinositol-specific phospholipase C leading to inositol triphosphate (IP_3) production and Ca^{2+} release from intracellular stores (Figure 1.8) (Smart *et al.*, 1999; Lund *et al.*, 2000). In CHO cells, Smart et al, (1999) and Lund et al, (2000) have shown that Ca^{2+} elevation requires extracellular Ca^{2+} and removal of extracellular Ca^{2+} causes a significant drop in the potency of OX-A for the OX_1R. The exact identity of the Ca^{2+} influx pathway, its activation mechanism by OX receptors, and the relation between Ca^{2+} influx and Gq mediated intracellular Ca^{2+} release remains unresolved. However it can be suggested that in both neuronal and nonneuronal cells, OX receptors activate both Ca^{2+} influx and the phosphatidylinositol-specific phospholipase C pathway (Figure 1.8). Other studies have shown that OX causes protein kinase C-mediated Ca^{2+} influx in hypothalamic cultures (van den Pol et al., 1998); inhibits K^+ channels in rat LC and in guinea pig ileal submucosal ganglia (Horvath *et al.*, 1999; Kirchgessner & Liu, 1999); and activates Ca^{2+} sensitive K^+ channels in immune cells (Figure 1.8) (Ichinose et al., 1998).

1.6.2 Distribution of OXs and its receptors

1.6.2.1 Distribution in the CNS

OXs and their precursor, prepro-orexin, have been identified in the CNS of mammals including human (Sakurai et al, 1998), rat (Chen et al., 1999; Mondal et al., 1999; Nambu et al., 1999), mouse, pig (Dyer et al., 1999) and cows (Sakurai et al., 1999) as well as in the CNS of amphibians (Shibahara *et al.*, 1999; Galas *et al.*, 2001). Within the CNS, orexinergic cell bodies are localized solely in the hypothalamus, particularly in the perifornical nucleus, lateral hypothalamic area (LHA) and posterior hypothalamic area (Broberger *et al.*, 1998; de Lecea *et al.*, 1998; Peyron *et al.*, 1998; Sakurai *et al.*, 1998; Chen *et al.*, 1999; Cutler *et al.*, 1999; Date *et al.*, 1999; Nambu *et al.*, 1999). Occasionally isolated orexinergic cell bodies have also been found in median eminence, dorsal and dorsomedial hypothalamus (DMH) and arcuate nucleus (Arc) and sub-incertal nucleus (Peyron *et al.*, 1998; Chen *et al.*, 1999; Cutler *et al.*, 1999). OX neurons are variable in area (diameter of cell body: 15-40 µm) and

shape (spherical, fusiform, multipolar) (Chen et al., 1999; Cutler et al., 1999; Date et al., 1999; Nambu et al., 1999) and are believed to number 1100-3400, ~20000 and 50000-83000 in the rat, dog and human brain, respectively (Peyron *et al.*, 1998; Harrison *et al.*, 1999; Thannickal *et al.*, 2000; Ripley *et al.*, 2001). While orexinergic cell bodies are restricted to the hypothalamus, OX fibres project widely throughout the CNS (Figure 1.9). The most important areas receiving orexinergic projections include the hypothalamus, cerebral cortex, thalamic nuclei, circumventricular organs, brainstem and along the whole length of the spinal cord (Table 1.1).

As with the OX peptides, the distribution of OX receptors in the CNS has been investigated in detail with molecular biological and immunological methods; mostly in rats. OX receptors are expressed in regions that have a high density of OX projections, as described above. OX_1R and OX_2R mRNAs show partially overlapping and partially distinct distribution patterns suggesting that they may play diverse physiological roles. Both OX_1R and OX_2R are expressed in many brain regions including the amygdala, hippocampus, thalamus, anterior hypothalamus, hypothalamic preoptic nucleus, Arc, PVN, ventromedial hypothalamus (VMH), supraoptic nucleus, dorsal tegmental nucleus, ventral tegmental area (VTA), dorsal raphé (DR), NTS, RVMM, nucleus ambiguus, preBötC, and spinal cord (Trivedi *et al.*, 1998; Bingham *et al.*, 2001; Hervieu *et al.*, 2001; Marcus *et al.*, 2001; Cluderay *et al.*, 2002; Ciriello & de Oliveira, 2003). On the other hand, OX_1R is prominent in the prefrontal cortex, CA2 region of the hippocampus and LC while OX_2R is predominantly expressed in the CA3 region of the hippocampus, DMH, PVN of hypothalamus, tuberomammillary nucleus (TMN) and spinal trigeminal nucleus (Trivedi *et al.*, 1998; Marcus *et al.*, 2001). This differential distribution of the OX receptors suggests that each may have a physiologically distinct role.

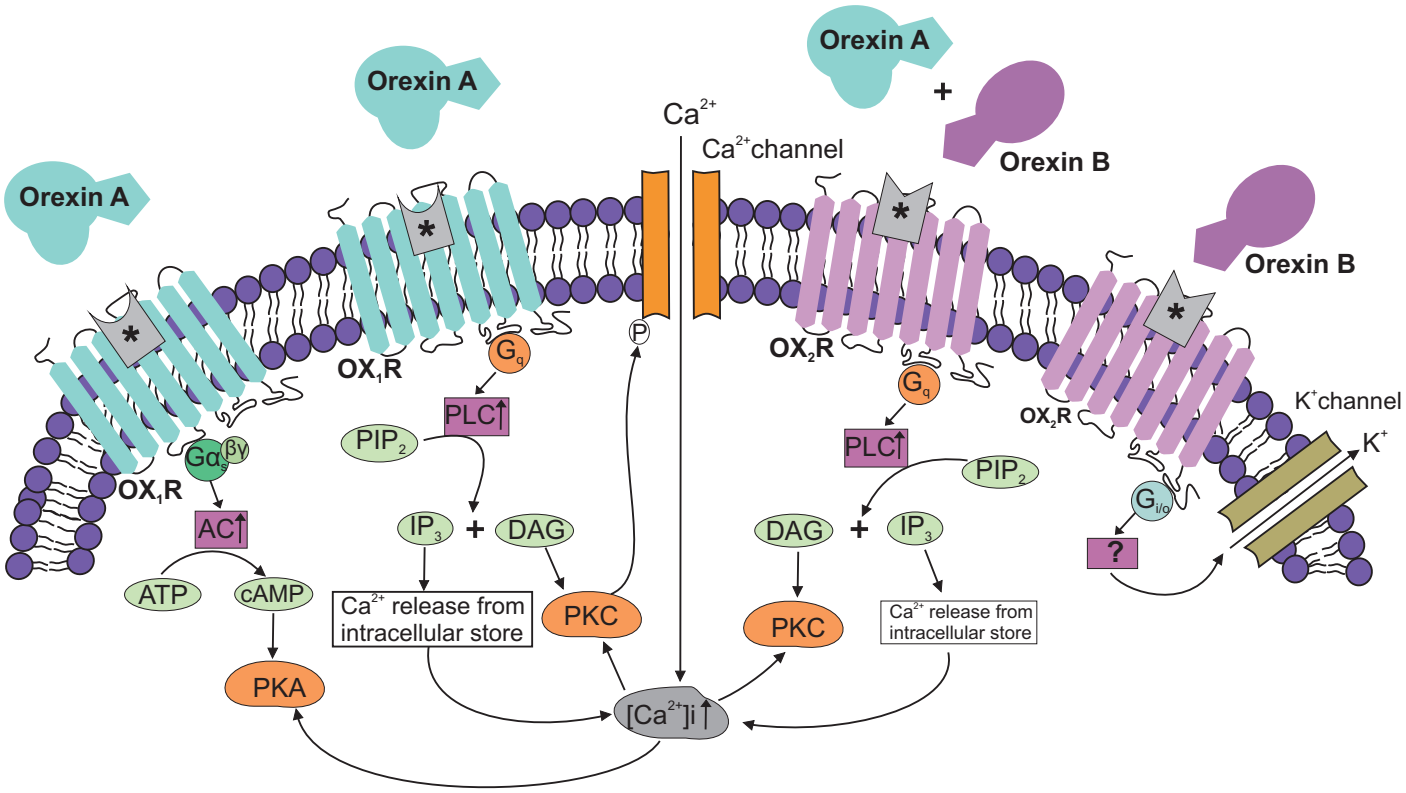

Figure 1.8. Schematic of the main signalling pathways of OX_1R and OX_2R upon activation by orexin A, and orexin A or orexin B, respectively.

AC, adenylate cyclase; cAMP, cyclic adenosine monophosphate; DAG, diacylglycerol; G, G protein; IP_3, inositol triphosphate; P, phosphorylation site; PIP_2, phosphatidylinositol biphosphate; PKA, protein kinase A; PKC, protein kinase C; PLC, phospholipase C. Asterisks mark the orexin recognizing sites of OX_1R and OX_2R.

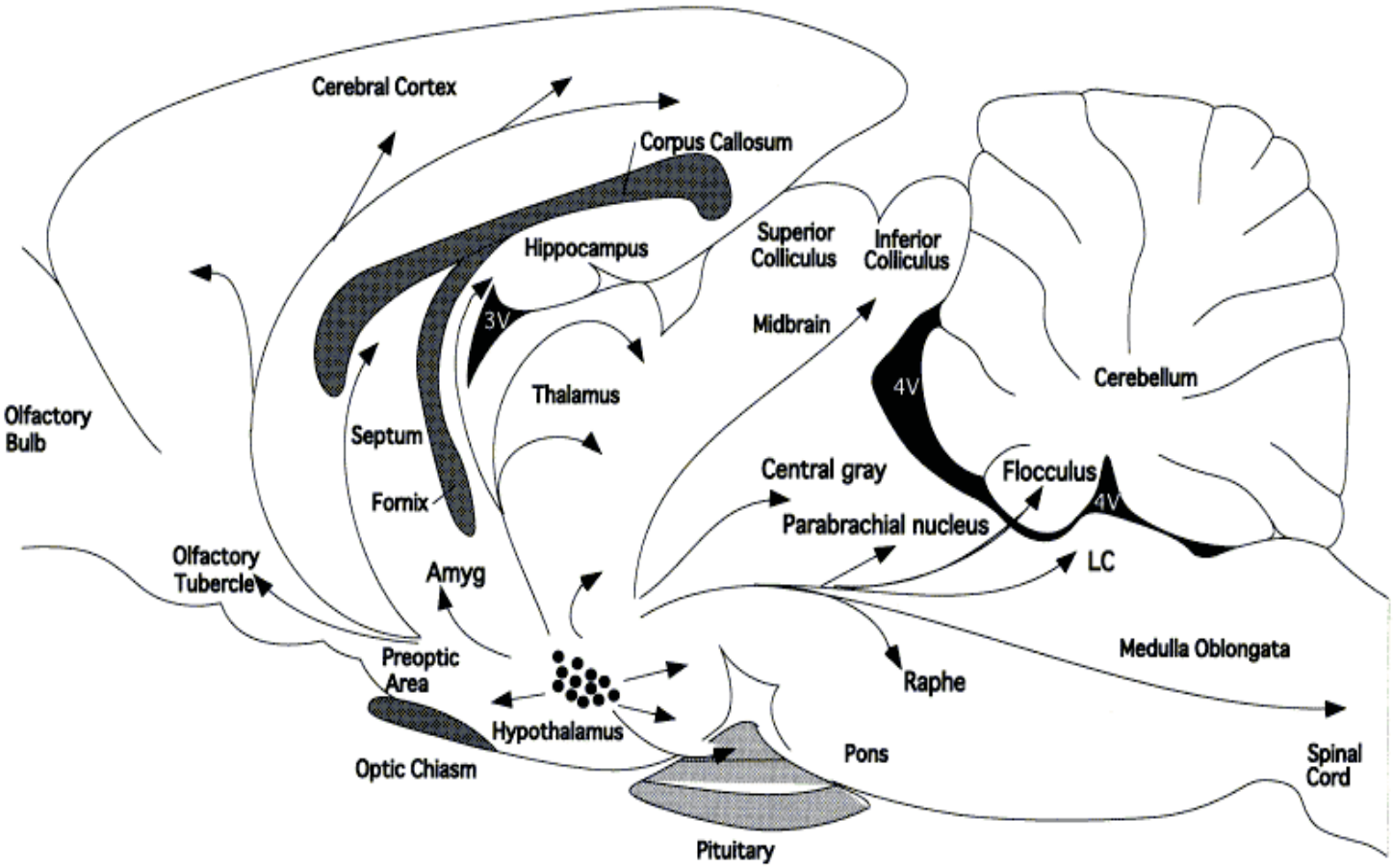

Figure 1.9. Schematic drawing of sagittal section through the rat brain to summarize the organization of orexin neuronal system.

Dots indicate the relative location of orexin-immunoreactive neurons, and arrows show some of the more prominent terminal fields. Adapted from Nambu *et al.,* 1999.

Table 1.1. Orexin distribution in rat central nervous system

Brain Division	Orexin Levels in Subdivision
Forebrain	Olfactory nucleus, cerebral cortex, hippocampus, septal nucleus, BST, subfornical organ, amygdala, substantia nigra, subthalamic nucleus, PVN, preoptic area, supraoptic nucleus, zona incerta, VMH, DMH, Arc, posterior part of the paraventricular hypothalamic nucleus, TMN.
Brainstem	dorsal raphé, median raphé, locus coeruleus, parabrachial nucleus, A1 noradrenergic cells, area postrema, NTS, RVMM, RVLM, NA, pre-Bötzinger complex, RTN, dorsal motor nucleus of the vagus, trigeminal motor nucleus, facial motor nucleus, hypoglossal nucleus, Spinal trigeminal nucleus.
Spinal cord	Whole length of the spinal cord from cervical to lumbar segments.

Data are from Ciriello *et al.*, 2003; Date *et al.*, 1999; de Lecea *et al.*, 1998; Machado *et al.*, 2002; Nambu *et al.*, 1999; Peyron *et al.*, 1998; Young *et al.*, 2005.

1.6.2.2 Distribution in the periphery

OX immunoreactivity or prepro-orexin mRNA has been found in a variety of peripheral organs, including both neurons and endocrine cells. OX immunoreactivity has been detected in the neurons (submucosal and myenteric plexi) and endocrine (enterochromaffin) cells of the gastrointestinal tract (rat, mouse, guinea pig and human), extrinsic neurons in pancreatic ganglia and endocrine B cells of the pancreas (rat, guinea pig), endocrine cells (anterior and intermediate lobe) of rat pituitary, rat testis and endocrine cells of the rat pineal gland (Kirchgessner & Liu, 1999; Arihara *et al.*, 2000; Date *et al.*, 2000; Jöhren *et al.*, 2001; Nanmoku *et al.*, 2002; Näslund *et al.*, 2002). OX-A has also been detected in human adult adrenal glands (Randeva et al., 2001) and at very low levels in the rat heart (Jöhren et al., 2001). However, it still needs to be determined whether OX-A is released into plasma from the CNS and if so to what extent peripheral and central OX production sites contribute to plasma levels of OX.

As with OXs, OX receptors are also expressed in the periphery; and are mostly colocated with the same organs as the peptide proteins. The receptors might be expressed in endocrine, muscle and nerve cells and the expression of receptor subtypes varies in different tissues. Immunoreactivity for both OX_1R and OX_2R have been found in the gastrointestinal tract, pancreas, pituitary, adrenals, medulla (including chromaffin cells) and cortex of mammals (human and rat) (Kirchgessner & Liu, 1999; Lopez *et al.*, 1999; Blanco *et al.*, 2001; Jöhren *et al.*, 2001; Malendowicz *et al.*, 2001a; Malendowicz *et al.*, 2001b; Blanco *et al.*, 2002; Näslund *et al.*, 2002). Only OX_1R has been found in the kidney, thyroid and testis (Jöhren et al., 2001) while only OX_2R in the lung and pineal gland (Jöhren et al., 2001; Mikkelsen et al., 2001). Distribution of OX and OX receptors in the peripheral tissues suggest that OXs are involved in the regulation of many peripheral functions.

1.6.3 Connections of OXs with other transmitters

OX neurons in the hypothalamus are innervated by a variety of upstream neuronal populations including those involved in feeding, reward system, sleep-wakefulness, memory and emotional state regulation. Some of the important brain regions innervating OX neurons include the basal forebrain cholinergic neurons, GABA-containing neurons in the ventrolateral preoptic area (VLPO), neurons in the dorsomedial/posterior hypothalamus, VTA neurons, and serotonergic neurons in the raphé nuclei. OX neurons also receive inputs from regions associated with energy homeostasis including NPY, agouti-related peptide, and α-melanin-stimulating hormone-immunoreactive fibres presumably coming from the Arc. Brain regions associated with emotion including the amygdala, infralimbic cortex, shell region of nucleus accumbens (NAc), lateral septum (LS) and the bed nucleus of stria terminalis (BST) also innervate OX neurons (Sakurai et al., 2005; Yoshida et al., 2006). Orexinergic neurons even make contact with other orexinergic neurons within the hypothalamus (Horvath *et al.*, 1999; Bäckberg *et al.*, 2002).

From the regions mentioned above, neurons provide an input to OX neurons and regulate OX neuronal activity by secretion of neurotransmitters or neuromodulators. OX neurons are activated by glutamate, ghrelin, cholecystokinin, CRF, neurotensin, vasopressin, oxytocins and glucagon-like peptide (Li *et al.*, 2002; Yamanaka *et al.*, 2003a; Yamanaka *et al.*, 2003b; Acuna-Goycolea & van den Pol, 2004; Winsky

Sommerer *et al.*, 2004; Tsujino *et al.*, 2005). On the other hand, GABA, NA, serotonin, dopamine, NPY, leptin and adenosine inhibit the activity of OX neurons (Li *et al.*, 2002; Yamanaka *et al.*, 2003a; Yamanaka *et al.*, 2003b; Fu *et al.*, 2004; Muraki *et al.*, 2004; Xie *et al.*, 2006; Yamanaka *et al.*, 2006; Liu & Gao, 2007). The cholinergic agonist, carbachol, activates 27% and inhibits 6% of OX neurons (Yamanaka *et al.*, 2003b; Sakurai *et al.*, 2005). Metabolic signals also contribute to the regulation of OX neuron acivity; hypoglycaemia stimulates OX neurons whereas hyperglycaemia has an inhibitory effect (Yamanaka et al., 2003a). OX neurons are also affected by physiological fluctuations in pH and CO_2 levels. Increased H^+ concentration or CO_2 level increases OX neuronal excitability, whereas reduced levels have the opposite effect (Williams et al., 2007).

Orexinergic nerves from the lateral hypothalamus also innervate, and regulate the activity of, various neuronal circuits that utilize many different neurotransmitters or neuromodulators, for instance, NA, glutamate, GABA, dopamine, serotonin, histamine, acetylcholine, vasopressin, vasoactive intestinal peptide (VIP), somatostatin, CRF, NPYand melanin concentrating hormone (MCH) (Peyron *et al.*, 1998; Cutler *et al.*, 1999; Date *et al.*, 1999; Nambu *et al.*, 1999; Bäckberg *et al.*, 2002).

1.6.4 Systemic effects of OX

1.6.4.1 In feeding behaviour and energy homeostasis

There is a considerable body of evidence for a role of OX in the regulation of feeding and energy homeostasis. Orexinergic cell bodies are located in the LHA which is a known feeding centre. OX and OX receptor immunoreactivity have also been found in brain regions involved in food intake and energy homeostasis including the Arc, VMH, DMH and PVN (Elias *et al.*, 1998; Peyron *et al.*, 1998; Sakurai *et al.*, 1998; Trivedi *et al.*, 1998; Cutler *et al.*, 1999; Nambu *et al.*, 1999; Marcus *et al.*, 2001). Intracerebroventricular (icv), and microinjection of OX-A into several hypothalamic nuclei, including the PVN, DMH, LHA and perifornical area, increases food intake (Sakurai *et al.*, 1998; Dube *et al.*, 1999; Sutcliffe & De Lecea, 2000; Willie *et al.*, 2001). Both prepro-orexin and OX receptors are up-regulated in fasted animals (Sakurai *et al.*, 1998; Cai *et al.*, 1999; Lu *et al.*, 2000). In addition, central administration of anti-OX antibody or an OX_1R selective antagonist caused a

profound inhibition of feeding in fasted rats as well as OX-A induced feeding (Haynes *et al.*, 2000; Yamada *et al.*, 2000; Rodgers *et al.*, 2001). Moreover, prepro-orexin knockout mice and transgenic mice lacking OX neurons have a lower food intake compared to control wild-type mice (Hara et al., 2001; Willie et al., 2001). Taken together, these data provide strong pharmacological evidence for a physiological role of the endogenous OX in the modulation of feeding behaviours.

Additional evidence for a role of OX in feeding has been provided by data from a wide range of studies. OX neurons in the LHA send dense projections to the Arc and are innervated by POMC and NPY neurons in the Arc (Elias *et al.*, 1998; Peyron *et al.*, 1998; Date *et al.*, 1999; Yamanaka *et al.*, 2000). Icv injection of OX increases *Fos* expression in NPY neurons of the Arc (Yamanaka et al., 2000), and electrophysiological data revealed that OX directly or indirectly activated NPY neurons but inhibited POMC neurons (Muroya *et al.*, 2004; van den Top *et al.*, 2004; Li & van den Pol, 2006; Ma *et al.*, 2007). Furthermore, prior administration of NPY-Y1 receptor antagonist has been found to reduce OX induced food intake (Yamanaka et al., 2000). These experiments suggest that activation of NPY neurons are, at least in part, involved in OX-stimulated food intake.

Recent studies have demonstrated that feeding behaviour is increased following infusion of OX-A into the shell of NAc, an area involved in the regulation of the limbic system (Thorpe & Kotz, 2005). Moreover, administration of the $GABA_A$ receptor agonist, muscimol, into the NAc shell causes a profound increase in food intake, and increases *Fos* expression, particularly in OX neurons (Baldo et al., 2004). These findings indicate that interaction between OX neurons and the limbic systems also have a role in the regulation of feeding.

OX neurons also participate in the regulation of feeding and energy homeostasis via responding to several metabolic signals that reflect the state of energy resources. Increased extracellular glucose concentration, as well as leptin, inhibits the firing of OX neurons. Conversely, decreased glucose concentration activates and causes depolarization of the same neurons (Yamanaka *et al.*, 2003a; Burdakov *et al.*, 2005). In addition, prepro-orexin mRNA levels are increased after 48 hr of fasting and by acute insulin induced hypoglycaemia, suggesting activation of these neurons in

hunger (Sakurai *et al.*, 1998; Cai *et al.*, 1999; Mondal *et al.*, 1999). However, hypothalamic prepro-orexin mRNA levels are not increased in rats with increased appetite due to insulin-deficient diabetes, or access to palatable foods, indicating that OX neurons are not activated under all conditions of hunger (Cai *et al.*, 1999; Cai *et al.*, 2000). Taken together, the findings suggest that low plasma glucose levels and/or absence of food from gut stimulates OX neurons, and that OXs are involved in short-term regulation of feeding behaviour.

1.6.4.2 In sleep-wakefulness

Regulation of sleep/wakefulness is the most well demonstrated systemic effect of the orexinergic system. Anatomically, OX neurons are placed between sleep-promoting neurons in the VLPO and wake-promoting neurons in the brainstem including neurons in the TMN, LC and DR. VLPO neurons play a crucial role in initiation of non-rapid-eye-movement (NREM) sleep and maintenance of NREM and rapid-eye-movement (REM) sleep (Sherin et al., 1998). These neurons fire rapidly during sleep, with attenuation of firing during waking periods. Sleep-active neurons in the VLPO mostly contain GABA and/or galanin and inhibit wake active monoaminergic and cholinergic neurons in the arousal regions including noradrenergic neurons of the LC, serotonergic neurons of the DR and histaminergic neurons of the TMN during sleep (Sherin *et al.*, 1998; Lu *et al.*, 2002). On the other hand, monoaminergic neurons in the TMN, LC and DR play crucial roles for the maintenance of arousal. These neurons fire tonically during the awake state, less during NREM sleep and are virtually silent during REM sleep (Vanni-Mercier et al., 1984). These monoaminergic and cholinergic wake-promoting neurotransmitters inhibit sleep-active neurons in the VLPO during waking periods (Gallopin et al., 2000). These reciprocal interactions of inhibition between sleep-active and wake-active neurons are crucial for switching between the sleep/awake states.

In addition to the reciprocal connection between VLPO and sleep-active brainstem neurons, OX neurons act as a link between these neurons and stabilize behavioural states by activating arousal regions during wakefulness, preventing undesirable transitions between wakefulness and sleep.

It is now well established that OX neurons fire during active waking and virtually cease firing during sleep, including the NREM and REM periods (Lee et al., 2005). Furthermore, monoaminergic neurons in the TMN, LC and DR express both OX receptors and are densely innervated by OX neurons suggesting that these neurons might be activated during wakeful periods, and that they exert excitatory influence on these wake-active neurons to sustain their activity. In fact, in vitro studies revealed that noradrenergic neurons of the LC, dopaminergic cells of the VTA, serotonergic neurons of the DR and histaminergic neurons of the TMN are all activated by OXs (Hagan *et al.*, 1999; Nakamura *et al.*, 2000; Brown *et al.*, 2002; Liu *et al.*, 2002; Yamanaka *et al.*, 2002). On the other hand, noradrenergic and serotonergic neurons send inhibitory projections to OX neurons (Muraki et al., 2004; Sakurai, 2005; Yamanaka et al., 2006). These connections between OX neurons and wake-active neurons, as well as *in vitro* results, suggest that OX neurons activate monoaminergic neurons, which in turn inhibit OX neurons during active waking. This small decrease in the activity of monoaminergic neurons results in a decreased inhibitory influence on OX neurons. Subsequently, OX neurons are disinhibited and their excitatory influence on monoaminergic neurons to maintain their activity. OX neurons also receive dense projection from GABAergic neurons in the VLPO, and are inhibited by them during sleep (Yamanaka *et al.*, 2003a; Sakurai *et al.*, 2005; Xie *et al.*, 2006; Yoshida *et al.*, 2006). Moreover, selective deletion of the $GABA_B$ receptor gene in OX neurons causes highly unstable sleep/wake architecture in mice (Matsuki et al., 2009). This pathway might be important to turn off OX neurons during sleep. OX neurons are also reciprocally connected with cholinergic neurons of the BF, which also play an important role in regulating arousal. Cholinergic neurons in the BF are activated by OXs, and in turn activate some populations of these neurons, thereby playing a role in stabilization of wakefulness (Eggermann et al., 2001; Sakurai et al., 2005).

Electrophysiological and knock-out studies provide further evidence of the physiological role of OXs and/or OX receptors in sleep-wakefulness. Icv injection of OX during light periods potently increases the awake period in rats. This effect is markedly attenuated by H_1 antagonists and is completely absent in histamine H_1-receptor-deficient mice suggesting that TMN-histaminergic pathway is an important effector site of OX for sleep/wake regulation (Huang et al., 2001; Yamanaka et al.,

2002). Prepro-orexin knockout mice and OX_1R/OX_2R-double knockout mice are severely affected by behaviourally abnormal attacks of NREM sleep and show a similar degree of disrupted wakefulness (Willie et al., 2003). These findings suggest that the profound dysregulation of wakefulness in narcolepsy syndrome is due to a loss of signalling through OX and/or OX receptor dependent pathways.

1.6.5 Other responses

1.6.5.1 OX and reward system

There is considerable evidence that OXs are involved in the modulation of reward function. OX neurons receive projections from regions involved in the reward system including the VTA, NAc and LS (Yoshida et al., 2006). In the LHA/PFA, dopamine has an inhibitory influence on reward pathways, and inhibits OX neurons (Yang *et al.*, 1997; Yamanaka *et al.*, 2003b). On the other hand, OX neurons project to, and directly activate dopaminergic neurons of the VTA (Peyron *et al.*, 1998; Nakamura *et al.*, 2000; Fadel & Deutch, 2002; Korotkova *et al.*, 2003). These reciprocal interactions may constitute regulatory mechanisms of a reward system. Injection of OX_1R antagonist into the VTA blocks the development of heroin-conditioned place preferences (Narita et al., 2006). In addition, *in vivo* administration of OX_1R antagonist blocks locomotor sensitization to cocaine (Borgland et al., 2006). Taken together these findings suggest a role for OX in the mechanism of reward system and drug addiction.

1.6.5.2 Neuroendocrine effects of OX

The anatomical distribution of OX as well as its receptors in the Arc and PVN suggest that OX systems are involved in the control of neuroendocrine function. Icv administration of OXs increases plasma levels of corticosterone in rats (Hagan et al., 1999; Malendowicz et al., 1999a). OXs also stimulate the release of CRF, VIP, neurotensin and luteinizing hormone-releasing hormone from hypothalamic explants (Russell et al., 2000). OX-A also inhibits plasma levels of prolactin via both dopamine -dependent and -independent mechanisms. OX-A also inhibits the secretion of growth hormone by stimulating the release of somatostatin from the hypothalamus via a direct action on the pituitary (Hagan et al., 1999; Russell et al., 2000).

1.6.5.3 OX and pain

Several studies suggest that OXs play a role in the transmission of nociceptive information. OX-A immunoreactive fibres and OX receptors, OX_1R in particular, are abundantly expressed throughout the spinal cord including lamina I, an area associated with nociception. OX_1R are also expressed in dorsal root ganglia. In addition, intravenous injection of OX-A has an analgesic effect in both the mouse and rat models of nociception and hyperalgesia. This effect is mediated solely by OX_1R since the analgesic effect of OX-A was blocked by a selective OX_1R antagonist, SB 334867, but not by the opioid antagonist, naloxone. Furthermore, SB 334867 enhances hyperalgesia under certain inflammatory conditions suggesting a tonic inhibitory OX input in these circumstances (Bingham et al., 2001).

1.6.5.4 Peripheral effects of OX

The presence of OX, and OX receptors, in different peripheral tissues suggests that OXs play an important role in the periphery along with their central function. OX-A activates secretomotor neurons in the guinea pig submucosal plexus and regulates gut motility by increasing the velocity of propulsion in isolated guinea pig colon. OXs have also been reported to inhibit fasting motility in the rat duodenum (Yamanaka et al., 2000). OXs may affect glucose homeostasis by regulating the secretion of pancreatic hormones including insulin and glucagon. Both *in vivo* (subcutaneous injection of OX-A) and *in vitro* studies have revealed that OX-A stimulates insulin and glucagon secretion (Nowak et al., 1999). OXs may also activate adrenals independently of central mechanisms (via endocrine, paracrine or neurocrine mechanisms) by binding with OX receptors. OXs stimulate corticosteroid secretion from rat and human adrenocortical cells (Malendowicz et al., 1999b; Mazzocchi et al., 2001). In addition, OX-A stimulates the release of adrenaline and NA from cultured porcine adrenal medullary cells and of aldosterone from cultured porcine adrenal cortex cells (Fujiki et al., 2001)

1.6.6 Central cardiovascular effects of OX

The distribution of OXs and OX receptors in the cardiovascular regulatory centres, as well as functional studies, indicate a crucial role of OX in the regulation of autonomic function. OX neurons in the hypothalamus project to the PVN and to different brainstem nuclei involved in the control of sympathetic and parasympathetic outflow

including the NTS, RVMM, RVLM and NA, and to the final relay centre of sympathetic tone - SPN of the spinal cord (de Lecea *et al.*, 1998; Peyron *et al.*, 1998; Cutler *et al.*, 1999; Date *et al.*, 1999; Nambu *et al.*, 1999; van den Pol, 1999; Machado *et al.*, 2002; Ciriello *et al.*, 2003). OX receptors are also expressed in most of these areas (Trivedi *et al.*, 1998; Marcus *et al.*, 2001; Sunter *et al.*, 2001; Cluderay *et al.*, 2002; Ciriello & de Oliveira, 2003; van den Top *et al.*, 2003). However, the expression of OX_1R and OX_2R in the RVLM neurons including TH-immunoreactive (TH-ir) neurons is unknown.

In OX knockout mice, basal BP is lower than their wild-type littermates (Kayaba et al., 2003), suggesting that OXs physiologically stimulate sympathetic outflow. It has been demonstrated that icv injection of OXs increases BP, HR, rSNA and plasma catecholamine in the rat and the rabbit (Samson *et al.*, 1999; Shirasaka *et al.*, 1999; Matsumura *et al.*, 2001). On the other hand, intravenous injection of OX produces no cardiovascular effect (Matsumura et al., 2001) suggesting that OX mediated cardiovascular function operates solely via central mechanisms. Furthermore, intrathecal (i.t.) injection of OX-A at the level of thoracic 1-2 (T1-T2), a site that principally innervates the heart, increases MAP and HR in urethane anaesthetized rats and the effects are markedly attenuated by iv injection of α-or β-adrenoceptor antagonist (Antunes et al., 2001).

Direct microinjection of OX-A into the NA, an area involved in the parasympathetic control of HR, elicits a dose-related decrease in HR with little or no direct change in MAP (Ciriello & De Oliveira, 2003). Whereas the effect of OX-A microinjection into the NTS is controversial and appears to depend on the doses administered. Low doses of OX-A (10 pM – 10 nM) injected into the NTS increased MAP and HR in a dose-dependent manner (Smith et al, 2002). However, at high doses (25 µM - 250 µM), microinjection of OX-A into the NTS was shown to decrease MAP and HR in a dose-dependent manner (De Oliveira et al., 2003). As well, Shih and Chuang (2007) found that at a dose of 100 µM, OX-A injection into the NTS elicited slight decrease in MAP and HR while at higher doses of 4 mM, MAP and HR were decreased. NO is suggested to be a neuromodulator responsible for the bidirectional activity of OXs. Low concentrations of NO, synthesized by low dose of OX, stimulate NOS potentiating glutamatergic excitatory postsynaptic potentials, thereby decreasing BP.

On the other hand a high dose of OX-A stimulates the production of more NO which increases BP through potentiation of GABA-ergic inhibitory pathways (Shih & Chuang, 2007). Microinjection of OX-A into the RVMM has also been shown to increase HR dose-dependently with a little or no change in MAP (Ciriello et al., 2003).

OX-A has also been microinjected into the RVLM in both anaesthetized and conscious rats. In both conditions, OX-A injection into the RVLM increased MAP and HR (Chen et al., 2000; Machado et al., 2002). In addition, *in vitro* recordings of RVLM neuronal activity showed that OX dose-dependently depolarizes RVLM neurons and this depolarization is mediated predominantly via OX_2R (Huang et al., 2010).

Several studies also indicate a role of OX-A on HR baroreflex. OX-A potentiates reflex bradycardia induced by activation of the arterial baroreflex when injected into nucleus ambiguus (Ciriello & De Oliveira, 2003) or into the NTS (De Oliveira *et al.*, 2003) while it has been shown to attenuate the reflex response after microinjection into RVMM (Ciriello et al, 2003).

Differential effects of OXs in various regions of the brain, along with evidence of orexinergic projections in most of these areas, strongly suggest its involvement in regulation of the cardiovascular system. Activation or inhibition of reflex bradycardia, evoked by the activation of arterial baroreceptor after administration of OXs to the NTS and nucleus ambiguus or RVMM, also support the sensitivity of the baroreflex to OXs. Effects of an endogenous level of OXs in different central cardioregulatory areas as well as in the baroreflex arc may reveal a new aspect in cardiovascular regulation.

1.6.7 Respiratory effects of OX

The role of hypothalamic OX system in the regulation of breathing is well recognised from both anatomical and functional evidence. Axons of OX neurons project to respiratory-related nuclei including RVLM sympathoexcitatory neurons, pre-BötC (part of respiratory rhythm generator), the NTS (area containing inspiratory cells responsive to sensory afferents), retrotrapezoid nucleus (RTN) (central chemoreceptor), raphé nuclei (an area regulating respiratory long term facilitation),

and hypoglossal and phrenic nuclei (areas that control swallowing and diaphragm movements (Fung *et al.*, 2001; Machado *et al.*, 2002; Volgin *et al.*, 2002; Krout *et al.*, 2003; Young *et al.*, 2005; Rosin *et al.*, 2006). OX receptors are also expressed in most of these neurons (Trivedi *et al.*, 1998; Marcus *et al.*, 2001; Sunter *et al.*, 2001; Cluderay *et al.*, 2002; Young *et al.*, 2005; Dias *et al.*, 2009).

Physiological evidence indicates that OXs affect ventilation. Icv administration of OX increases breathing frequency and tidal volume (Zhang et al., 2005). In addition, microinjection of OX-A into the preBötC and microperfusion into phrenic motoneurons, results in the increase of diaphragm electromyographic activity (Young et al., 2005). In addition, Toyama *et al.,* (2009) showed that phrenic long-term facilitation (LTF) is attenuated in OX neuron-ablated mice. These results suggest that OX plays an important role in respiration as well as in the development of respiratory LTF.

Further evidence linking OX and breathing comes from studies on the response of OX to changes in pH or extracellular CO_2 levels. OX neurons themselves are chemosensitive both *in vivo* and *in vitro* (Williams *et al.*, 2007; Sunanaga *et al.*, 2009). A physiological level of acidosis (low pH, high CO_2) depolarizes OX neurons and increases their firing, while alkalosis (high pH, low CO_2) causes hyperpolarization and an inhibition of firing (Williams et al., 2007). Prepro-orexin deficient mice have a 50% decrease in the ventilatory CO_2 (hypercapnia) response during wakefulness but not sleep. OX knockout mice also display a markedly higher frequency of spontaneous apnoeic episodes during sleep (Nakamura et al., 2007). Furthermore, icv administration of SB334867 decreases the respiratory chemoreflex in wild-type mice (Deng et al., 2007) suggesting a role for OX in modulation of the chemoreflex. Moreover, antagonism of OX_1R in the RTN, which is a key chemosensory nucleus (Stornetta *et al.*, 2009; Guyenet *et al.*, 2010), or in medullary slices containing preBötC and hypoglossal motornuclei, blunts the response to hypercapnia (Dias *et al.*, 2009; Corcoran *et al.*, 2010). These findings suggest that OX may modulate chemoreflex responses directly through the activation of OX neurons or indirectly via an action in the RTN, preBötC, or hypoglossal motornuclei.

No previous studies have demonstrated the effects of OX-A on sympathetic outflow, PNA and sympathetic reflexes by injection into the spinal cord (chapter 3) and the RVLM (chapter 4) of normotensive rats as well as into the RVLM of a hypertensive animal model (chapter 5).

1.7 Aims

OX-A, a hypothalamic peptide, has several known functions in the body, but its role in central cardiorespiratory regulation remains poorly understood. The overall aim of this thesis is to investigate the role played by OX-A in the central control of cardiorespiratory function and sympathetic reflexes and also in the pathogenesis of hypertension.

This overall aim will be addressed with several specific-aims:

1. Chapter 3

i. To determine if OX-A modulates sympathetic vasomotor output and breathing at the spinal level

ii. To evaluate the effects of i.t. OX-A on the somatosympathetic, baroreceptor and peripheral chemoreceptor reflexes

iii. To determine if the responses following i.t. OX-A are due to an action in the spinal cord, or if supraspinal regions are required to elaborate the responses

(**Appendix 2**, Shahid *et al.,* 2011).

2. Chapter 4

i. To determine whether OX_1 and OX_2 receptors are expressed within neurons in the RVLM, and to determine if they are co-localized with putative sympatho-excitatory catecholamine-containing neurons of the rostral C1 cell group

ii. To determine the cardiovascular and respiratory effects elicited by microinjection of OX-A into the RVLM

iii. To determine which type of OX receptor mediates the central effects of OX-A

iv. To evaluate the effects of OX-A on somatosympathetic, baro- and chemoreflexes in the RVLM

(**Appendix 2**, Shahid *et al.,* 2012a)

3. Chapter 5

i. To determine the effects of bilateral microinjection of OX-A on baseline cardiorespiratory variables in hypertensive and normotensive rat models

ii. To investigate the role of OX-A in the regulation of adaptive reflexes when microinjected into the RVLM in hypertensive and normotensive rat models.

Chapter 2.

General Methods

General Methods

Methods commonly used during studies are discussed here. Please refer to the individual methods sections of each results Chapter for specific methods used in the individual studies. Complete details of the equipment, chemicals/reagents, drugs, and analysis software used to conduct the experiments in this thesis are listed in **Appendix 1**.

2.1 Ethical approval

All procedures were approved by the Macquarie University Animal Ethics Committee (ARA 2009/016; see **Appendix 3**) in accordance with the guidelines of the Australian Code of Practice for the Care and Use of Animals for Scientific Purposes (http://www.nhmrc.gov.au/guidelines/publications/ea16)

2.2 Animals

Most of the experiments were conducted using adult male Sprague-Dawley (SD), rats weighing between 350g and 500g (chapters 3-4). Wistar Kyoto rats (WKY) and Spontaneously Hypertensive rats (SHR) weighing between 315g and 380g were used in chapter 5 only. SHR and WKY rats were age-matched and only used (including phenotyping) after 18 weeks of age. All animals were supplied by the Animal Resources Centre (Perth, WA, Australia) and housed at the Macquarie University Animal House in a 12-hour light/dark cycle. Rats had access to food and water *ad libitum* and were provided with environmental enrichment items.

2.3 Anaesthesia and maintenance of animal

Individual rats were collected from the Macquarie University Animal House on the day of the experiment and transported to the laboratory. Animals were handled carefully to minimise stress prior to anaesthesia and surgery.

2.3.1 Anaesthesia

All experiments were performed under surgical anaesthesia. The choice of anaesthetic agent differed according to the aims of the study. Surgical anaesthesia

was ascertained in the unparalysed condition by the absence of reflex responses to nociceptive stimuli (e.g. paw/tail pinches), or alternatively, by the absence of corneal blink reflex to corneal touch. In paralysed condition, it was confirmed by <10 mmHg change in mean arterial pressure (MAP) in response to noxious paw/tail pinch.

In electrophysiological studies, anaesthesia was induced via intraperitoneal (i.p.) injection of urethane (Ethyl Carbamate) (1.2-1.4 g kg^{-1}; 10% w/v in 0.9% physiological saline) using a 26.5G needle. Urethane provides long periods of stable surgical anaesthesia with a large therapeutic window, minimal cardiorespiratory depression and enables for stable nerve recordings (Field et al., 1993). The injection was given in 3 bolus doses separated by 10 minutes, to minimise the risk of anaesthetic overdose. This injection was supplemented with atropine sulfate (50µg i.p.) to reduce bronchial secretions. When adequate anaesthesia was achieved, bodily regions of the rat were shaved to expose skin sites for surgical incisions. Throughout the experiment, the withdrawal reflex and/or arterial pressure changes (>10 mmHg) in response to a strong hind paw pinch were used to assess the depth of anaesthesia at every 30 min. Intravenous (i.v.) doses of sodium pentobarbital (10 mg in 20% solution w/v) or urethane (0.2 g kg^{-1} i.v.) were administered as required to suppress reflexes and maintain anaesthesia.

2.3.2 Temperature monitoring

Core body temperature was monitored by using a rectal probe thermometer, and was maintained between 36.5°C and 37.5°C by placing rats on a feedback-controlled heating blanket with the aid of an infrared heating lamp as necessary.

2.4 General surgical procedures for electrophysiological experiments

2.4.1 Arterial and venous cannulation

The right carotid artery and left jugular vein were cannulated for measurement of BP and regular injections of drugs and fluids, respectively. In addition, the right femoral artery was cannulated to enable withdrawal of arterial blood for blood gas measurements while continuously monitoring BP. In some experiments, both femoral veins were cannulated to enable administration of sodium nitroprusside (SNP) or phenylephrine hydrochloride (PE). A midline incision on the ventral surface of the

neck was made to access the right carotid artery and left jugular vein. The femoral veins and artery were approached via a ventral superficial skin incision. Each blood vessel was carefully isolated from surrounding tissues and a silk suture (5/0) was tied proximally to occlude distal blood flow temporarily (occlusion of blood flow in the artery was assisted with the use of an artery clip). A small incision was then made in the vessel wall and a cannula was inserted and advanced 1-2 cm, and secured with silk suture (5/0). Cannulas were made from plastic (polyvinyl chloride) tubing (OD: 0.96 mm x ID: 0.58 mm) attached to a 3-way tap via a 18G needle and silastic tubing. The venous catheter contained 0.9% saline and the arterial catheter was filled with heparinised (~ 10 IU heparin mL^{-1}) 0.9% saline to prevent blood clotting in the line. The arterial catheter was attached to a pressure transducer.

2.4.2 Tracheal intubation

A tracheotomy was performed to allow mechanical ventilation. The trachea was exposed using the same midline incision used for venous and arterial cannulations (section 2.4.1). A gap was blunt dissected between the bilateral sternohyoid muscles to reveal the trachea. A small incision was made in the trachea. A 14-guage i.v. catheter was inserted into the trachea and secured with braided silk suture (2/0). Rats continued to breathe freely up until such time that a bilateral vagotomy (section 2.4.3) was performed, after which, mechanical ventilation (section 2.4.4) was commenced.

2.4.3 Vagotomy

A bilateral vagotomy was performed to prevent entrainment of the phrenic nerve discharge to the ventilator and also to remove parasympathetic activity, creating a ‘purely’ sympathetic system. The right vagus nerve was separated from the carotid sheath and transected at the time of carotid artery cannulation. The left vagus nerve was later cut during the phrenic nerve dissection, using a dorsal approach (section 2.4.5.2).

2.4.4 Ventilation

Immediately following vagotomy, the tracheal cannula was connected to a rodent ventilator, and rats were mechanically ventilated with oxygen-enriched room air at a ventilation rate of 60-80 rpm with a tidal volume of 1.0 mL per 100 g. End tidal CO_2 was monitored with a CO_2 analyser connected to the expiratory ventilator line, close

to the rat and maintained between 3.5-5.0% by altering the ventilation rate and/or stroke volume accordingly.

Adequacy of ventilation was verified by measuring arterial blood gas and electrolyte concentrations 30 min following the start of mechanical ventilation. The normal ranges for measured variables in an arterial blood gas analysis were; pH (7.35 – 7.45), PaO_2 (>200 mmHg as ventilated with hyperoxic/room air mixture), $PaCO_2$ (35 – 45 mmHg) and HCO_3- (22 – 28 mM). If respiratory acidosis/alkalosis was observed, ventilation parameters (rate and/or volume) were adjusted accordingly to keep blood gas and electrolyte concentrations within the optimum range. If necessary, a bolus injection of 5% w/v sodium bicarbonate in saline was given when metabolic acidosis (HCO_3- <20 mM) was apparent.

Animals were paralysed with pancuronium bromide (0.8 mg i.v. initially, followed by 0.4 mg h^{-1} i.v.), an agent that acts at the neuromuscular junction. Neuromuscular blockade was maintained with continuous infusion of 10% pancuronium bromide in a 5% w/v glucose in water, infused with an automated infuser at a rate of 1.0-2.0 mL hr^{-1}. Continuous infusion with fluids helped support hydration, energy production and electrolyte balance, along with maintaining paralysis.

2.4.5 Nerve dissection for recording

Sympathetic nerve discharge was recorded from the left greater splanchnic nerve. The splanchnic nerve innervates the abdominal vasculature and viscera, and splanchnic sympathetic nerve activity (sSNA) was used as a measure of sympathetic outflow. Respiratory activity was quantified by recording phrenic nerve activity (PNA). More specifically, phrenic nerve amplitude (PNamp) and phrenic nerve frequency (PNf) were used as a measure of inspiratory drive and to calculate carediorespiratory coupling.

2.4.5.1 Splanchnic sympathetic nerves

The splanchnic nerve was isolated using a retroperitoneal approach. A midline incision was made from the lower thoracic level to the pelvis to expose the nerve. The underlying muscle layers were cauterised and the fascia was separated by blunt dissection to expose the retroperitoneal cavity. The muscles and skin were retracted by ties to expose the left kidney and adrenal gland. The adipose tissue covering the

adrenal gland and celiac ganglion were removed by blunt dissection. The adrenal was then carefully tied with a silk suture and retracted to expose the celiac ganglion. The left greater splanchnic was isolated and tied off proximal to celiac ganglion with 5/0 silk sutures and cut distal to the tie. Saline-soaked cotton wool was placed in the cavity surrounding the splanchnic nerve to keep the nerve moist until the rat was placed on the stereotaxic frame.

2.4.5.2 Phrenic nerve

A longitudinal dorso-caudal incision from the base of the skull to the mid thoracic level was made to access the phrenic nerve. The parascapular muscles and scapula were retracted to expose the brachial plexus and a superomedially directed blunt dissection distal to the plexus exposed the phrenic nerve. The nerve was identified as the medium-sized, striated nerve deep to the communication of the origin of the supra- and sub-scapular nerves. The phrenic nerve was then carefully separated from surrounding fascia, tied distally with 5/0 silk sutures and cut distal to the tie. The nerve was covered with saline-soaked cotton wool to keep moist until recording.

2.4.6 Nerve dissection for stimulation

In some animals, the sciatic nerve was isolated for electrical stimulation to test the somatosympathetic reflex.

2.4.6.1 Sciatic nerve

To isolate the sciatic nerve, an incision was made at the upper-thigh level and blunt dissection through the hip extensor muscle, including gluteal and hamstring muscles. The overlaying muscles and surrounding tissue were dissected away from the nerve. The distal end of the sciatic nerve was tied with silk suture (5/0) and cut distal to the tie and covered with cotton wool soaked in saline. Once the nerve was prepared for stimulation, it was used for testing the somatosympathetic reflex (section 2.8.2).

2.4.7 Temporary spinal blockade by microinjection of bupivacaine anaesthetic at the C8 spinal level

In some cases (chapter 3), the spinal cord was anaesthetized at the C8 level by microinjection of a local anaesthetic, bupivacaine (500 nL) into the middle of each hemi-spinal cord. These injections were always adequate to cause BP and sSNA to

fall to levels equivalent to that seen following spinal transection at the C8 level (Goodchild *et al.*, 2008) .

2.4.8 Exposure of atlanto-occipital junction and the dorsal medulla

Following nerve dissections, rats were secured in a stereotaxic frame. A skin incision was made from the top of the skull to the level of T2. The occipital musculature and tissue were removed to expose the occipital bone and the atlanto-occipital membrane, which consists of dura mater and the underlying arachnoid. The atlanto-occipital junction (chapter 3) was exposed, and a slit was made through the dura mater. The intrathecal catheter was inserted into the intrathecal space through this slit, and advanced caudally to the level of T6-T8. Intrathecal injections were made using a 25 µl Hamilton syringe; the time course for each injection was approximately 20 seconds.

For dorsal medulla exposure (chapters 4 and 5), an occipital craniotomy was performed using bone rongeurs, and the dura was cut and removed exposing the dorsal surface of the medulla oblongata at the level of the obex and fourth ventricle.

2.4.9 Euthanasia

At the end of each experiment, rat was euthanized with a bolus i.v. injection of 0.5mL of 3M potassium chloride. This dose was sufficient to instantly stop the heart. Death was confirmed by zero blood pressure and lack of respiratory activity. Recordings of all parameters were continued for at least 10 minutes after death to obtain the background level of noise (death level) from the nerve recordings.

2.5 Electrophysiological recordings

All signals were digitised (A/D Converter 1401) and recorded in real time on a computer using Spike2 (7.07) acquisition and analysis software.

2.5.1 Arterial blood pressure (BP) and heart rate (HR) recordings

The arterial catheter was attached to a pressure transducer. This signal was amplified 1000 fold by a bridge amplifier, digitalised and recorded on computer using Spike2 software at a sampling rate of 250 Hz. A smoothing function (1 s) was applied to the BP recording to measure mean arterial pressure (MAP). The pressure

transducer was periodically, manually calibrated with a sphygmomanometer to ensure accuracy.

A custom made three lead needle electrodes was used to record electrocardiogram (ECG). The positive and negative leads were inserted into the front-paws of the rat and the ground lead was placed in into exposed muscle as close as possible to nerve recording sites. HR was then derived from either BP or ECG waveforms with an event channel triggered systole (BP) or triggered the major voltage deflection (QRS complex) of the ECG.

2.5.2 Nerve recordings

Before starting nerve record, a pool filled with paraffin oil or silgel was created for each nerve by securing the surrounding tissues and skin to the stereotaxic frame. The paraffin oil or silgel maintains a hydrophobic medium that electrically isolates the nerve. Bipolar silver wire recording hook electrodes were fabricated and used to record the nerves. The electrodes were carefully placed in the pools and the isolated nerves (section 2.4.5) were laid/suspended across the two poles of the electrodes. To ensure good quality nerve recording by minimising electrical noise, several measures were taken including: (i) earthing of all electrical equipment and metal objects (ii) pre-amplification close to the signal (iii) passing signals via a noise cancelling ‘Humbug’ (50/60-Hz line frequency filter).

Nerve signals were pre-amplified 10 times by a preamplifier, band pass filtered (0.1 – 2 kHz) and then amplified a further 1000 times by a scaling amplifier (Bioamplifier), 50/60-Hz line frequency filtered, digitalised, sampled at a rate of 2kHz and recorded and displayed on computer using Spike2 software as a waveform (in arbitrary units or in µV). The recording system for nerve activity was calibrated by introducing a known voltage at the amplifier headstage.

2.5.3 Nerve stimulation

The sciatic nerve was stimulated with custom built bipolar silver wire electrodes connected to a stimulator that was operated by a ‘pulser’ script (Lidierth, 2005) using Spike 2 software. The stimulus intensity was 50 sweeps at 1 Hz; 0.2 ms pulse width; 5-30 volts (chapters 3-5).

2.6 Intrathecal (i.t.) drug administration

I.t. drug administration was performed as described previously (Rahman *et al.*, 2011; Rahman *et al.*, 2012a). The i.t. catheter (PVC; OD: 0.8 mm x ID: 0.4 mm) of appropriate size was taken by measuring the length between the atlanto-occipital junction and T5-T7 (identified by counting the spinous processes). To enable of Hamilton syringe attachment, a small piece of silastic tubing was attached to the external end of the catheter. The catheter was then inserted into the intrathecal space through the slit in the atlanto-occipital membrane (section 2.4.8) and advanced caudally to the level of T5-T7.

Drawing cerebrospinal fluid up the catheter with a glass Hamilton syringe ensures the positioning of the catheter within the intrathecal space. The location of the catheter tip was confirmed by injecting L-glutamate (100 mM, 10 µL). Sharp increases in BP (~20 mmHg), HR (~30 bpm) and SNA (~30%) indicated a successful catheterization (Hong & Henry, 1992).

2.6.1 I.t. drug administration procedure

Intrathecal injections were performed using a 25 µl Hamilton syringe; the time course for each injection was approximately 20 seconds. Volume of all injections is 10µl flushed by catheter volume (dead space: range 6–7 µL) of 10 mM phosphate buffered 0.9% saline (PBS). All animals received control injections of the vehicle, PBS (10µl of PBS flushed by catheter volume of PBS), 30 min prior to their drug treatments. Drugs were dissolved in 10mM PBS, aliquoted and immediately frozen at -20°C until needed. In 11 animals, a selective OX_1 antagonist, N-(2-methyl-6-benzoxazolyl)-N-1,5-naphthyridin-4-yl-urea 200 nmol (SB 334867; Tocris Bioscience, Bristol, UK), was injected i.t. 20 min prior to the i.t. injection of OX-A (20 nmol): six with OX-A and five without. Drugs injected into the intrathecal space in this study include those listed in **Table 2.1**.

Table 2.1 : Drugs used in intrathecal injection studies

Drug	Concentration	Injection Volume	Vehicle
L-glutamic acid	100 mM	10 µL	10 mM PBS (0.9%), pH 7.4
OX-A	100 µM, 500 µM, 1mM, 2mM	10 µL	10 mM PBS (0.9%), pH 7.4
SB 334867	20 mM	10 µL	10 mM PBS (0.9%), pH 7.4

Refer to **Appendix 1** for company/supplier information.

Specific drug treatments used in experiments varied depending on the study and its aims, please refer to chapter 3 for the specifics of the treatments used in each study.

2.6.2 Injection site validation

The location of the injection site was marked by an injection of 10 µl of India ink flushed with PBS at the end of each experiment. Following euthanasia (section 2.4.9) a laminectomy was performed to assess the location of the catheter tip. The spinal segment level of the catheter was recorded as the level where the tip of the catheter was found or where the blue/black spot appeared most intensely on the spinal cord. Data which failed to meet the T5-T7 anatomical criteria were excluded from analysis.

2.7 RVLM microinjection

Single or multi-barrelled glass micropipettes were used for microinjection of vehicle and drug into the RVLM (Goodchild *et al.*, 1982; Rahman *et al.*, 2012b). Single barrel glass pipettes were made using borosilicate glass capillary tubes (OD 1.0 mm, ID 0.25 mm) and a laser pipette puller. Same glass capillaries bound by heat-shrink tubing were used to prepare triple barreled micropipettes with a programmable multi-pipette puller.

Each micropipette was filled using suction applied by a syringe and tubing attached to the pipette. Pressure microinjections were carried out using an air-filled syringe

and attached tubing. The injection volume was ascertained by direct observation of the fluid meniscus against an attached calibrated grid (each square = 50 nL) using the operating microscope.

The RVLM was identified functionally by an increase of >30 mmHg in the MAP following microinjection of L-glutamic acid (100 mM, 50 nL). The preliminary coordinates used to locate the RVLM were 1.8 mm rostral, 1.8 mm lateral, and 3.5 mm ventral to calamus scriptorius. All variables were allowed to return to baseline (>30 min) before microinjection of vehicle solutions, PBS. PBS contained 2% rhodamine beads were used to aid in subsequent histological verification of the injection site. After a further 30 min, OX-A was microinjected into the same site and observation was continued for a further 60 min. Microinjections of vehicle (PBS) and drug were bilateral and performed over 5 s. During the course of the experiment, the pipette was not exchanged or removed from the electrode holder. For single barrel microinjections, the pipette was rinsed with vehicle after microinjection of glutamate to find the appropriate RVLM site.

Table 2.2 : Drugs used in micoinjection studies

Drug	**Concentration**	**Injection Volume**	**Vehicle**
L-glutamic acid	100 mM	50 nL	10 mM PBS (0.9%), pH 7.4
OX-A	250 µM, 500 µM, 1 mM, 2 mM	50 nL	10 mM PBS (0.9%), pH 7.4
SB 334867	20 mM	50 nL	10 mM PBS (0.9%), pH 7.4
[Ala11,D-Leu 15]orexin B	15 µM	50 nL	10 mM PBS (0.9%), pH 7.4

Refer to **Appendix 2** for company/supplier information.

Specific drug treatments given in experiments varied depending on the study and its aims, please refer to chapters 4 and 5 for the specifics of the treatments used in each study.

2.7.1 Verification of microinjection site

Brainstem microinjection sites were marked with a 50 nL injection of 10 mM PBS (0.9%), contained 2% rhodamine beads, pH 7.4 (chapters 4 and 5). Following euthanasia (section 2.4.9), the brain was removed and post-fixed in 4% paraformaldehyde solution overnight.

After removal of meningeal layers, the separated brainstem was cut into serial 100 µm sections on a vibrating microtome. Then the sections were mounted on gelatinized glass slides, air-dried and coverslipped. The microinjection sites were visualized using an epifluorescence microscope. The RVLM was defined as a triangular area ventral to the nucleus ambiguus, medial to the spinal trigeminal tract, and lateral to the pyramidal tract or the inferior olive (Goodchild & Moon, 2009). Only rats with microinjection sites within the defined boundaries of the RVLM were used for data analysis.

2.8 Activation of sympathetic reflexes

2.8.1 Baroreceptor reflex

Stimulation of the sympathetic baroreceptor is used to measure the ability of an animal to respond to instantaneous changes in BP, and it is also used as an indicator of cardiovascular health (see section 1.3.1). The sympathetic baroreflex sensitivity was assessed by sequential i.v. injections of PE (0.1 mg kg^{-1}), and SNP (10µg kg^{-1}) to create baroreflex function curves. PE is an α1-adrenergic receptor agonist that induces a rapid increase in BP due to vasoconstriction, causing a reflex decrease in SNA. SNP is a NO- donor that induces a rapid decrease in BP due to vasodilatation, causing a reflex increase in SNA. BP and SNA return to baseline shortly (within 2-3 minutes).

2.8.2 Somatosympathetic reflex

The somatosympathetic reflex was induced by stimulating the sciatic nerve, and was used to reveal any changes in the sympathetic response to noxious stimuli (see section 1.3.2). Threshold for the SSR was measured by reducing the stimulus voltage until the classic two-peak averaged SNA response was no longer detected.

The nerve was stimulated at three times threshold (3xT; 5-30 V, 0.2 ms pulse width, 50 sweeps at 1Hz). Peri-stimulus waveform averaging of SNA following sciatic nerve stimulation was used to analyze the somatosympathetic reflex.

2.8.3 Peripheral (hypoxic) chemoreflex

The hypoxic chemoreflex is an indication of alterations in cardiovascular responsiveness to changes in arterial partial O_2 (see section 1.3.3.1). Peripheral chemoreceptors were stimulated by ventilating rat with 100% N_2 for 12-14 s.

2.8.4 Central (hypercapnic) chemoreflex

The hypercapnic chemoreflex is a measure of alterations in cardiovascular responsiveness to the acidification of brain extracellular fluid or an increase in the CO_2 level in the CNS (see section 1.3.3.2). Central chemoreceptors were stimulated by ventilating the animals with 10% CO_2:90%O_2 for 1 min.

2.9 Data analysis

Data were analysed off-line using Spike2 (v 7) software and either entered into a Microsoft Excel spreadsheet for further calculations or exported directly into GraphPad Prism software (5.04). Data analysis varied depending on the experiment; please refer to chapters 3 - 5for the specifics of the data analysis used in each study.

2.9.1 Mean arterial pressure (MAP) and heart rate (HR)

All raw traces used in chapters 3 – 5 presents BP (grey) and MAP (black line). HR is expressed as beats per minute (bpm). Baseline values for MAP and HR were obtained by averaging 60 s of data 5 min prior to PBS or drug injection and maximum responses were expressed as absolute (MAP and HR) changes from baseline values.

2.9.2 Sympathetic nerve activity (SNA)

SNA neurograms were rectified and smoothed/averaged to 1 s time constant. Zero SNA value was taken from the minimum background activity after death and was subtracted from SNA. Baseline values were obtained by averaging 60 s of data 5 min prior to PBS or drug injection and the maximum responses were expressed as percentage (%) changes from the baseline values.

2.9.3 Phrenic nerve activity (PNA)

All raw PNA data were rectified and smoothed/averaged to 0.05 s time constant. Waveform averages of PNA were generated by averaging 60 s of data triggered from the onset of the phrenic burst. Baseline values were obtained by averaging 60 s of data 5 min prior to PBS or OX-A injection. Phrenic variables measured were: duration of inspiratory burst (T_I); duration of expiratory period (T_E); PNf and PNamp. Maximum responses were expressed as absolute (T_I, T_E and PNf), or percentage (PNamp) changes from baseline values.

Cardio-respiratory coupling was determined as previously (Rahman *et al.*, 2012b). Phrenic-triggered ensemble averages of SNA were created from 60 s portions of data before and after OX-A injection to determine cardiorespiratory coupling. The area under the curve (AUC), less baseline, of SNA activity during the inspiratory (I) and post-inspiratory (PI) phases were evaluated.

2.9.4 Sympathetic reflexes

SNA was rectified and smoothed at 1 s and 5 ms time constants to analyze the baroreceptor reflex and somatosympathetic reflex, respectively. To analyze reflexes, SNA was normalized between the activity of SNA before PBS injection (100%) and the SNA after death (0%). The SNA response to the sciatic nerve stimulation was analyzed using peristimulus waveform averaging. The area under the curve (AUC) of the sympathoexcitatory peaks was analyzed. The responses to hypoxia (100% N_2 inhalation for 12-14 s) and hypercapnia (10% CO_2 in 90% O_2 for 1 min) were measured by comparing the average maximum SNA during hypoxia or hypercapnia with a baseline period during normal hyperoxic ventilation. To normalize the difference in baseline values, efficiency of the somatosympathetic and chemoreceptor reflexes were determined by calculating percent change from the control. The percentage changes for the somatosymapthetic, peripheral chemo- and central chemo- reflexes were measured according to Eq 1.

(Response to drug or vehicle or control/control response) x 100% Eq 1

To analyse the data from the baroreflex function tests, the mean MAP was divided into 1 s consecutive bins and the average SNA during each bin was determined;

successive values were tabulated and graphed as XY plots, taking MAP as the abscissa and SNA as the ordinate. Each data set was then analysed to determine the sigmoidal curve of best fit (Kent *et al.*, 1972), which is described by Eq 2.

$$y = A1 / [1 + \exp \{A2(x - A3)\}] + A4 \qquad \text{Eq 2}$$

where y is SNA, x is MAP, $A1$ is the y range (y at the top plateau – y at the bottom plateau), $A2$ is the gain coefficient, $A3$ is the value of x at the midpoint (which is also the point of maximum gain), and $A4$ is y at the bottom plateau. The computed baroreflex function curves were differentiated to determine the gain of SNA of the baroreflex across the full range of MAP and the peak gain of each curve was determined. The range of SNA was calculated as the difference between the values at the upper and lower plateaus of the curve. The threshold and saturation values for MAP were defined (McDowall & Dampney, 2006) as the values of MAP at which y was 5% (of the y range) below and above the upper and lower plateaus, respectively.

2.9.5 Statistical analysis

All statistical analysis and graphical representations were performed using GraphPad Prism (v 5.0), graphs were aesthetically altered in CorelDraw software for presentation in figures. Statistical analysis varied depending on the experiment and included paired Student's t-tests, one and two way ANOVAs. All data were expressed as mean ± standard error (SE), results were presented as either vehicle control versus drug treatment, or as a treatment pre-stimulus versus post-stimulus. In all cases, responses and differences were considered statistically significant if $P<0.05$. Please refer to chapters 3 - 5 for the specifics of the statistical analysis used in each study.

2.10 General methods for molecular biology studies

2.10.1 Anaesthesia

Rats perfused for immunohistochemistry (IHC) studies were anesthetized (overdose) with i.p. injections of sodium pentobarbital (70 mg/kg i.p.).

2.10.2 Transcardial perfusion

A midline ventral incision was made from the neck to the abdomen and the peritoneum opened. The diaphragm was cut and bilateral cuts were made into the thoracic cage, which was then reflected rostrally to expose the heart. In a rapid manner, the cannula tip attached to a 3-way tap of the perfusion line was inserted into the left ventricle and advanced towards the aorta. 1 mL mixture containing 0.9 mL heparin (900 IU) and 0.1 mL 5% sodium nitrate (in 0.1 M PBS) was injected to prevent blood coagulation during perfusion. A small cut into the right atrium was made to open the circulatory system on the venous side and allow fluid drainage. The animal was exsanguinated by pumping 350mL of saline (0.9% w/v, pH 7.4) through the animal using a perfusion pump until the outflow of fluid ran clear. Thereafter, 350 mL of fixative, 4% paraformaldehyde in 0.1 M phosphate buffer (pH 7.4), was pumped through the animal. Once completed, the brainstem was removed and post-fixed overnight in 4% paraformaldehyde at 4°C on an orbital shaker.

Once fixed, the brainstem was rinsed with Tris-phosphate buffered saline (TPBS; Tris–HCl 10 mM, PBS 10 mM, 0.9% saline, pH 7.4) and the dura and arachnoid layers removed. The brainstem was then mounted on the stage of a vibrating microtome and serial 40 µm coronal sections were cut into TPBS. The brain slices were used in fluorescence IHC protocols.

2.10.3 Fluorescence IHC protocol

Free floating 40 µm brainstem sections were washed in TPBS for 15 minutes at room temperature on an orbital shaker. Sections were incubated in 5x sodium citrate (SSC) + 0.1% Tween at 58^0 C overnight. Sections were then washed in cold TPBS 3x30 minutes at room temperature on an orbital shaker. Primary antibodies were added to 10% normal horse serum (NHS) + TPBSm (TPBS, pH 7.4, containing 0.05% merthiolate) solution: anti-OX-A (rabbit, 1:2000), anti-tyrosine hydroxylase (TH) (mouse, 1:2500), OX_1 receptors (rabbit, 1:50) and OX_2 receptors (goat, 1:50). Sections were incubated at room temperature for one hour on the orbital shaker, then at 4^0 C for 48 hours. Sections were then washed in cold TPBS 3x30 minutes at room temperature. Thereafter, fluorophore-conjugated secondary antibodies were added to 2% NHS+ TPBSm solution. Mouse anti-TH was visualized by incubation overnight with Alexa Fluor 488 donkey anti-mouse IgG (1:500). Rabbit anti-OX-A was

visualized by incubation overnight with a Cy3-conjugated donkey anti-rabbit IgG secondary (1:500). Rabbit OX_1 receptors and goat OX_2 receptors were visualized by incubation overnight with a Cy3-conjugated donkey anti-rabbit IgG (1:500) and Cy3-conjugated donkey anti-sheep IgG (1:500) respectively. Brainstem sections were washed in cold TPBS 3x30 minutes at room temperature on the orbital shaker, and then sequentially mounted on slides and coverslipped with Vectashield to prevent photobleaching and sealed with nail polish.

2.10.4 Cell counts and data analysis

Brainstem slices were viewed using an epifluorescence microscope. Cy3-stained OX_1, OX_2 receptors expressing neurons were visualized using a Cy3–4040B filter set, and Alexa Fluor 488 -stained TH-immunoreactive (ir) neurons were visualized using a FITC-3540B filter set. Images were captured in greyscale with an Axiocam MR3 digital camera. Pseudo-coloring was applied to the images (Cy3, red; Alexa Fluor 488, green) for better visualization of distribution and colocalization. The images were adjusted individually for brightness and contrast with Axiovision 4.5 software to best reflect the original images.

Cell counts within the RVLM of each replicate were performed bilaterally on six to seven serial sections at 200 µm increments. The sections extended from Bregma -1.6 mm caudally to Bregma -12.6 mm. The RVLM was defined as a triangular region ventral to the nucleus ambiguus pars compacta, medial to the spinal trigeminal tract (Sp5), and lateral to the inferior olive or the pyramidal tracts. Data were plotted as the means ± SEM at 200-µm intervals. Counts were made for OX_1, OX_2 receptors expressing neurons and TH-ir neurons, as well as all double-labelling (TH-ir/OX_1 receptor and TH-ir/OX_2 receptor) combinations. OX-ir fibres and terminals were also observed in the RVLM.

Chapter 3.

Intrathecal orexin A increases sympathetic outflow and respiratory drive, enhances baroreflex sensitivity and blocks the somato-sympathetic reflex

Intrathecal orexin A increases sympathetic outflow and respiratory drive, enhances baroreflex sensitivity and blocks the somato-sympathetic reflex

3.1 Abstract

Intrathecal (i.t.) injection of orexin A (OX-A) increases blood pressure and heart rate (HR), but the effects of OX-A on sympathetic and phrenic, nerve activity, and the baro-, somatosympathetic and hypoxic chemo-, reflexes are unknown. Urethane-anesthetized, vagotomised and artificially ventilated male Sprague-Dawley rats (n = 38) were examined in this study. The effects of i.t. OX-A (20 nmol/10µL) on cardiorespiratory parameters, and responses to stimulation of the sciatic nerve (electrical), arterial baroreceptors (phenylephrine hydrochloride, 0.01 mg kg^{-1} i.v.) and peripheral (hypoxia) chemoreceptors were also investigated. Intrathecal OX-A caused a prolonged dose-dependent sympathoexcitation, pressor response and tachycardia. The peak effect was observed at 20 nmol with increases in mean arterial pressure (MAP), HR and splanchnic sympathetic nerve activity (sSNA) of 32 mmHg, 52 bpm and 100 % from baseline, respectively. OX-A also dose-dependently increased respiratory drive as indicated by a rise in phrenic nerve amplitude (PNamp) and a fall in phrenic nerve frequency (PNf), an increase in neural minute ventilation, a lengthening of the expiratory period (T_E), and a shortening of the inspiratory period (T_I). All effects of OX-A (20 nmol) were attenuated by the OX1R antagonist SB 334867. OX-A significantly reduced both sympathoexcitatory peaks of somato-sympathetic reflex while increasing baroreflex sensitivity. OX-A increased the amplitude of the pressor response and markedly amplified the effect of hypoxia on sSNA. Thus, activation of OX receptors in rat spinal cord alters cardiorespiratory function and differentially modulates sympathetic reflexes.

The results of this chapter has been published in *British Journal of Pharmacology* (see **Appendix 2**)

Israt Z. Shahid, Ahmed A. Rahman, Paul M. Pilowsky. (2011). Intrathecal orexin A increases sympathetic outflow and respiratory drive, enhances baroreflex sensitivity and blocks the somatosympathetic reflex. *Br J Pharmacol* **162**, 961–973.

3.2 Introduction

Orexin A (OX-A) and orexin B (OX-B), also referred to as hypocretin-1 and -2, are neuropeptides that are cleaved from a common precursor, prepro-orexin. The amino acid sequences of the 33-residue peptide OX-A and the 28-residue peptide OX-B are encoded by a single gene localized on human chromosome 17q21 and share 46% homology (de Lecea *et al.*, 1998; Sakurai *et al.*, 1998). The actions of these peptides are mediated by two G-protein coupled receptors, orexin receptor-1 (OX1R) and orexin receptor-2 (OX2R). OX1R is selective for orexin-A and OX2R interacts with both orexin-A and -B (Sakurai *et al.*, 1998). Activation of OX1R results in the activation of $G\alpha_{q/11}$, which results in the elevation of intracellular Ca^{+2} and the OX2R couples to both $G\alpha_{q/11}$ and inhibitory $G\alpha_{i}$ G proteins (Zhu *et al.*, 2003).

Immunohistochemical and *in situ* hybridisation studies have revealed that OX containing cell bodies are restricted to the lateral hypothalamus, perifornical area and dorsomedial hypothalamus. OX containing nerve terminals and receptors, on the other hand, are widely distributed in the hypothalamus, thalamus, cerebral cortex, circumventricular organs, brainstem and spinal cord (Elias *et al.*, 1998; Llewellyn-Smith *et al.*, 2003; Nambu *et al.*, 1999). This distribution of OX-nerve terminals establishes a basis for the contributions by OX to the control of multiple physiological functions, including control of energy homeostasis, feeding behaviour, sleep–wake state, stress response, reward and nociception (Kukkonen *et al.*, 2002; Sakurai, 2007; Tsujino and Sakurai, 2009).

There is a growing body of evidence to suggest that OX is involved in central cardiovascular and respiratory control. Intracerebroventricular (ICV; 3rd ventricle) or intracisternomagnal (ICM) application of OX-A or OX-B augments sympathetic outflow and catecholamine release and a dose-dependent increase in systemic arterial pressure (SAP) and heart rate (HR) (Matsumura *et al.*, 2001; Shirasaka *et al.*, 1999; Zhang *et al.*, 2005). On the other hand, prepro-orexin knockout mice with a complete lack of both OX-A and OX-B manifest lower baseline arterial pressure than the wild-type controls (Kayaba *et al.*, 2003). However, the effects of intrathecal OX-A on *in vivo* splanchnic sympathetic nerve activity (sSNA), phrenic nerve activity (PNA) as well as on sympathetic reflexes are unknown.

Sympathetic preganglionic neurons (SPN), located in the intermediolateral cell column (IML) of the spinal cord, receive inputs from different brain regions and regulate the cardiovascular responses through their projections to the adrenal medulla and sympathetic autonomic ganglia in periphery (Guyenet, 2006; Pilowsky and Goodchild, 2002). Orexinergic fibers and receptors are distributed throughout the spinal cord including IML. OX fibers have also been found in the dorsal and ventral horn neurons of spinal cord (Cluderay *et al.*, 2002; Date *et al.*, 2000; van den Pol, 1999). The dense innervation of all spinal cord regions by OX fibers, expression of OX receptors on SPN and the depolarizing action of OX on spinal neurons (van den Top *et al.*, 2003) also suggest that OX is a neuropeptide in the spinal cord. Therefore, it is likely that OX not only regulates cardiovascular function acting as a neurotransmitter in the spinal cord but also modulates sympathetic reflexes.

Since OX-A has a greater selectivity for the OX1R we first evaluated the hypothesis that OX-A, by acting on SPN, might influence spinal sympathetic outflow, as assessed by a change in mean arterial pressure (MAP), HR, sSNA when delivered intrathecally. Additionally, the effects of i.t. OX-A on phrenic nerve activity and cardiovascular responses to stimulation of somato-sympathetic, arterial baroreceptor and peripheral chemoreceptor reflexes were examined. Our principal findings are that intrathecal OX-A causes a dose-dependent increase in MAP, HR and sSNA, and an increase in phrenic nerve discharge. Adaptive reflexes are differentially affected: barosensitivity is enhanced, the somato-sympathetic reflex is attenuated, and the hypoxic chemoreflex is enhanced for MAP and sSNA. The data reveal that OX-A has pleiotropic effects on cardiorespiratory functions and reflexes that warrant further investigation. Part of this work was presented to the Australian Neuroscience Society (Shahid and Pilowsky, 2010).

3.3 Methods

All animal experiments in this study complied with the guidelines of the Australian Code of Practice for the Care and Use of Animals for Scientific Purposes (NSW – Animal Research Act 1985) and were approved by the Animal Ethics Committee of Macquarie University, Sydney, Australia.

3.3.1 Surgical preparation

Surgical preparation was performed as described previously (Burke *et al.*, 2008; Farnham *et al.*, 2008; Gaede *et al.*, 2009). Briefly, male Sprague-Dawley rats (*n* = 38, 350–600 g) were anesthetized with urethane (1.2-1.4 g kg^{-1}, i.p.). The depth of anaesthesia was assessed approximately every 30 min by monitoring changes in arterial pressure in response to pinching a hind paw; supplemental doses of urethane 20-30 mg, i.v. were given if blood pressure rose more than 10mmHg. Animals were placed on a feedback-controlled heating blanket for the duration of the experiment to maintain body temperature between 36^0C and 37^0C (Harvard Apparatus).

The right jugular vein and carotid artery were cannulated with polyethylene tubing (I.D.= 0.58 mm; O.D.= 0.96 mm) for administration of drugs and fluids, and for measurement of arterial blood pressure (AP), respectively. In some experiments, both femoral veins were cannulated to enable administration of sodium nitroprusside (SNP) or phenylephrine hydrochloride (PE). HR was derived from AP. A tracheal cannula permitted artificial ventilation. Ventilation was adjusted so that phrenic nerve discharge was just above the apnoeic threshold. Nerve recordings were made of PNA and sSNA. The left phrenic nerve was approached dorsally and the left greater splanchnic nerve was dissected using a retro-peritoneal approach. The distal end of the respective nerves were tied with silk thread and cut to permit recording of efferent nerve activity. In an additional subset of animals, sciatic nerve was isolated, tied and cut. Once the nerves were isolated, they were covered with saline-soaked cotton wool for the duration of the remainder of surgical preparation to prevent desiccation. The neurograms were amplified (x10,000, CWE Inc., Ardmore, PA, USA), band-pass filtered (0.1-2 kHz), sampled at 3 kHz (1401 plus, CED Ltd, Cambridge, UK) and recorded on computer using Spike2 software (v7, CED Ltd., Cambridge, UK).

Rats were secured in a stereotaxic frame, paralysed (pancuronium bromide; 0.8 mg i.v. initially, then 0.4 mg/h i.v.) and artificially ventilated with oxygen enriched room air. End-tidal CO_2 was monitored and maintained between 4.0% and 4.5%. Arterial blood gas was monitored and the rate and depth of ventilation adjusted to maintain pH at an optimum range (7.35-7.45, pH 7.4 ± 0.01, P_aCO_2 40.9 ± 0.8). Animals were infused with 5% glucose in saline (1.0-2.0 ml/h) to ensure hydration. Three needle electrodes were placed under the skin at the right and left arm and the right hind limb

to record an electrocardiogram (ECG). Nerve recordings were made with bipolar silver wire electrodes. The recording electrodes were immersed in a pool of liquid paraffin oil to prevent dehydration and for electrical insulation. After being placed on the recording electrodes, the rat was allowed to stabilize for 30-60 min.

3.3.2 Activation of sympathetic reflexes

Reflexes were evoked as described previously (Makeham *et al.*, 2004; Miyawaki *et al.*, 2002a). Activation of somato-sympathetic reflex was achieved by electrical stimulation (10-25 V, 100, 0.2 ms pulses at 1 Hz) of the sciatic nerve with bipolar electrodes. Sympathetic baroreflex function curves were generated by sequential intravenous injection of SNP (0.01 mg kg^{-1}) and PE (0.01 mg kg^{-1}) via two different vein lines. Peripheral chemoreceptors were stimulated with a brief period of hypoxia induced by ventilating the animals with 100% N_2 for 12-14 s.

3.3.3 Intrathecal drug administration

The occipital crest of the skull was exposed, and the atlanto-occipital membrane was incised. A polyethylene catheter (I.D.= 0.4 mm; O.D.= 0.8 mm) was inserted through this slit into the intrathecal space and advanced caudally to the levels of T6-T8. The slit was left open to prevent increases in intrathecal pressure caused by the injection of agents or by flushing. The volume of each catheter was measured before insertion (range 6-7 µl) and this volume was then used to flush the catheter. A 25- µl Hamilton syringe was used to inject drugs (OX-A; 100 µM, 500 µM, 1 mM and 2 mM equivalent to 1, 5, 10 and 20 nmol) or vehicle (10 mM phosphate-buffered saline (PBS); pH 7.4) in a total volume of 10 µl. Injections were made over a 15- to 20-s period. In 11 animals, a selective OX1R antagonist, SB 334867, (N-(2-methyl-6-benzoxazolyl)-N´-1,5-naphthyridin-4-yl-urea, Tocris Bioscience, Bristol, UK) 200 nmol) was injected i.t., 20 min prior to the i.t. injection of OX-A (20 nmol): 6 with OX-A, and 5 without. Successful catheterization into the intrathecal space was confirmed by administering L-glutamate (100 mM, 10 µl) and observing sharp increases in BP (~20 mmHg), HR (~30 bpm) and sSNA (~30%) (e.g. Hong and Henry, 1992).

To reveal the physiological role of any neuropeptide (e.g. OX-A) is based on its pharmacological properties. The well-established way to choose dose for any *in vivo* experiment is to use the ten times of the effective dose used in *in vitro* experiments.

The minimum dose of OX-A administered into the spinal cord was based on the *in vitro* studies published with OX-A. The dose was then increased until a near plateau level of response was obtained.The following reflexes were activated before and 40 or 15 min after intrathecal injection of OX-A (20 nmol) or PBS, respectively: (a) somatosympathetic reflex, (b) baroreflex (c) peripheral chemoreceptor reflex. The spread of injectate was determined by observing the distribution of a 10 µL injection of India ink. Following euthanasia (3 M KCl, 0.5 ml, i.v.) a laminectomy was performed to verify the location of the catheter tip. To avoid possible confounding effects of drug interactions, each animal received only one treatment of OX-A.

3.3.4 Temporary spinal blockade by microinjection of bupivacaine anaesthetic at the C8 spinal level

The spinal cord was anaesthetised at the C8 level by microinjection of a local anaesthetic, bupivacaine (500 nl, AstraZeneca, Australia) into the middle of each hemi-spinal cord in four animals. These injections were always adequate to cause blood pressure and sympathetic nerve activity to fall to levels equivalent to that seen following spinal transection at the C8 level (Goodchild *et al*., 2008). Following local anaesthetic injection at C8, OX-A (20 nmol) or PBS was injected intrathecally.

3.3.5 Data acquisition and analysis

Neurograms were rectified and smoothed (sSNA, 1 s time constant; PNA, 50 ms). Minimum background activity after death was taken as zero sSNA, and this value was subtracted from sSNA before analysis with off-line software (Spike 2 version 6.01). To analyze blood pressure, HR, sSNA, PNamp, PNf, neural minute ventilation (=PNamp x PNf), duration of inspiratory burst (T_I) and duration of expiratory period (T_E), baseline values were obtained by averaging 60 s of data 5 min prior to drug or PBS injection. Maximum responses were expressed as absolute changes in MAP, HR and PNf, and percent changes in sSNA, PNamp and neural minute ventilation from baseline values. Time course analysis averaged 60 s of data every 5 min from 0 min to 60 or 70 min post injection for OX-A. To evaluate cardio-respiratory coupling, phrenic-triggered ensemble averages of sSNA were generated from 60 s portions of data. The area under the curve (AUC), less baseline, of sSNA activity during the inspiratory and post-inspiratory phases was determined. sSNA was rectified and smoothed at 1 s and 5 ms time constants to analyse baroreceptor reflex and somato-sympathetic reflex, respectively. To analyse reflexes, sSNA was

normalized between the activity of sSNA before PBS injection (100%) and the sSNA after death (0%). The sSNA response to sciatic nerve stimulation was analysed using peristimulus waveform averaging. The AUC of the sympathoexcitatory peaks was analysed. The maximum response to stimulation was then expressed as a percentage change from the baseline (control). The response to hypoxia (100% N_2 inhalation for 12-14s) was quantified by comparing the average maximum sSNA during hypoxia compared with a control period during normal hyperoxic ventilation. The percentage changes were calculated according to the formulae below.

$$\frac{OXAHR - CHR}{CHR} * 100$$

$$\frac{PBSHR - CHR}{CHR} * 100$$

Where OXAHR is the response to hypoxia following OX-A, PBSHR is the response to hypoxia following PBS injection. CHR is the response to hypoxia in the absence of any intrathecal injection.

Analysis was conducted with GraphPad Prism (version 5.0). All values are expressed as mean ± SE. Results are presented as control versus OX-A. Paired t-test was used to analyse peak effects and reflexes. A one-way repeated-measures ANOVA with Dunnett's *post hoc* multiple comparison test was used to compare values after OX-A (20 nmol) administration with the baseline value. $P < 0.05$ was considered significant.

3.3.6 Drugs

OX-A (MW = 3561.2) was obtained from, Bachem AG, Bubendorf, Switzerland), SB 334867 from Tocris Bioscience. Urethane, L-glutamate, PE and SNP were purchased from Sigma-Aldrich (St. Louis, MO, USA), pancuronium bromide and bupivacaine from AstraZeneca Pty Ltd (NSW, Australia) and PBS (10 mM in 0.9% NaCl) tablets from AMRESCO (USA). OX-A was dissolved and further diluted in PBS (10 mM; pH 7.4). SB 334867 was dissolved and further diluted in 10% dimethyl sulfoxide (DMSO). PBS, PE and SNP were prepared in de-ionised water. Urethane was dissolved in 0.9% NaCl and L-glutamate in PBS.

3.4 Results

3.4.1 Effects of intrathecal OX-A on resting cardio-respiratory parameters

To test the hypothesis that exogenous application of OX-A to the spinal cord modulates cardio-respiratory responses, OX-A (1, 5, 10 and 20 nmol) was administered intrathecally and the effects on MAP, HR, sSNA, PNf, PNamp, neural minute ventilation,T_E and T_I were evaluated (n=34). OX-A evoked a dose-dependent and significant increase in MAP, HR and sSNA (Figures 3.1A, 3.2). The maximum elevation occurred after injection of 20 nmol OX-A and the highest levels attained were 32 ± 5 mmHg (MAP, n= 6, *P*<0.01), 52 ± 6 bpm (HR, n= 6, *P* <0.001) and 100 ± 9 % (sSNA, n= 6, *P* <0.001) from the baseline (Figure 3.2). Following administration of OX-A (20 nmol, i.t.), the peak pressor effect was reached after approximately 20 min (Figure 3.1A, B). Blood pressure was monitored for about 70 min, and remained elevated (Figure 3.1B). Both HR and sSNA increased progressively after 20 nmol OX-A injection reaching a maximum change of 35 bpm and 97%, respectively, at the end of the recording period (Figure 3.1A, B). Injection of PBS (vehicle) into the spinal cord was without effect on MAP (5 ± 1 mmHg, n= 6), HR (5 ± 1 bpm, n= 6) or sSNA (8 ± 1 %, n= 6) above basal values (Figure 3.2).

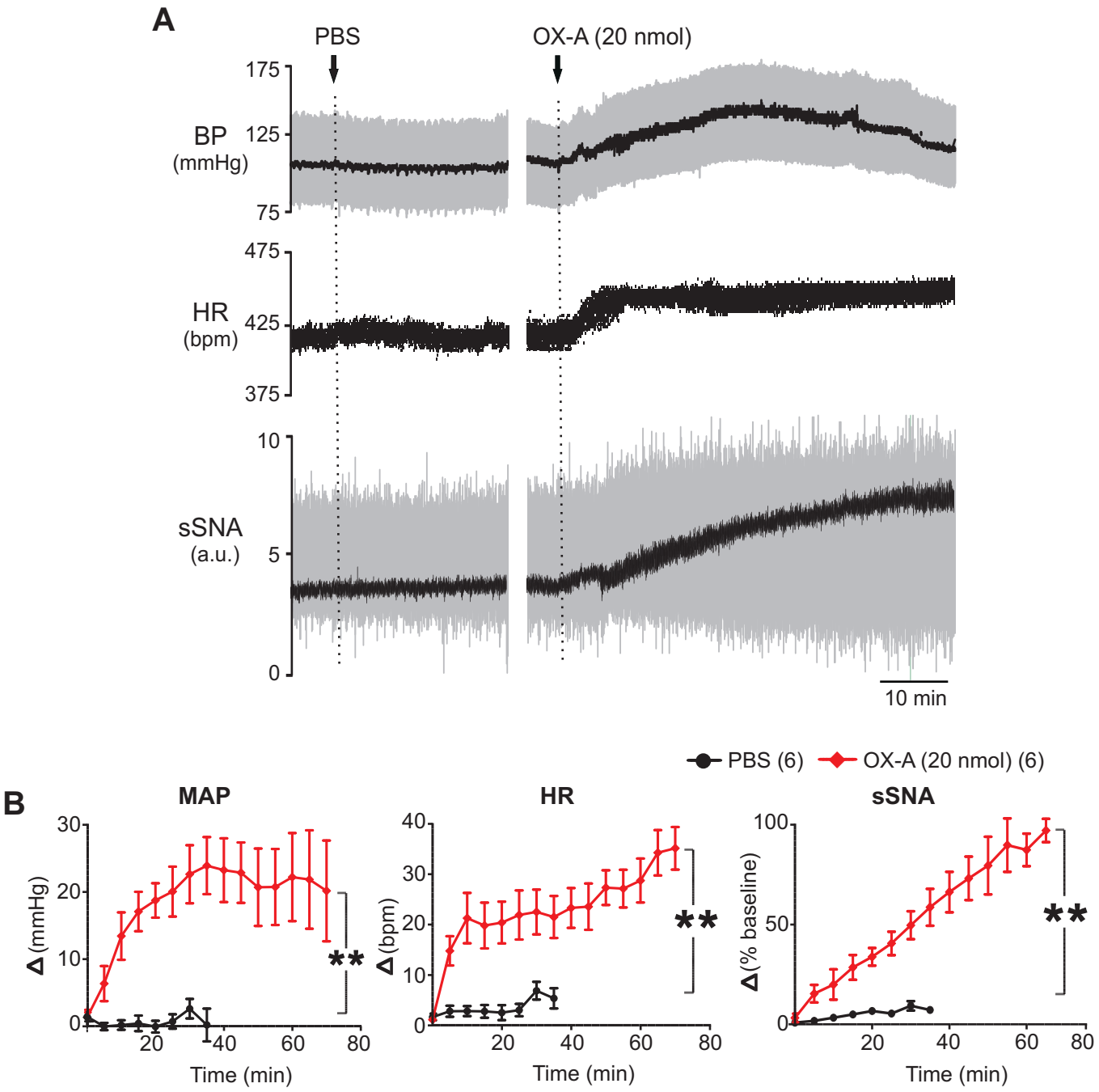

Figure 3.1. Effect of intrathecal injection of OX-A on mean arterial pressure (MAP), heart rate (HR) and splanchnic sympathetic nerve activity (sSNA).

A: Representative trace data from a recording of blood pressure (BP), HR and sSNA [arbitrary unit (a.u.)] before and after injection of PBS or OX-A (20 nmol). Rectified and integrated sSNA (black) is superimposed over rectified sSNA (grey). MAP (black) is superimposed on BP (grey). **B**: Grouped time course effects of PBS or OX-A (20 nmol) on MAP, HR and sSNA . Values are expressed as mean ± SE. Number of animals are shown in parentheses. ns, non-significant; ** $P < 0.01$ compared with PBS . bpm, beats per minute.

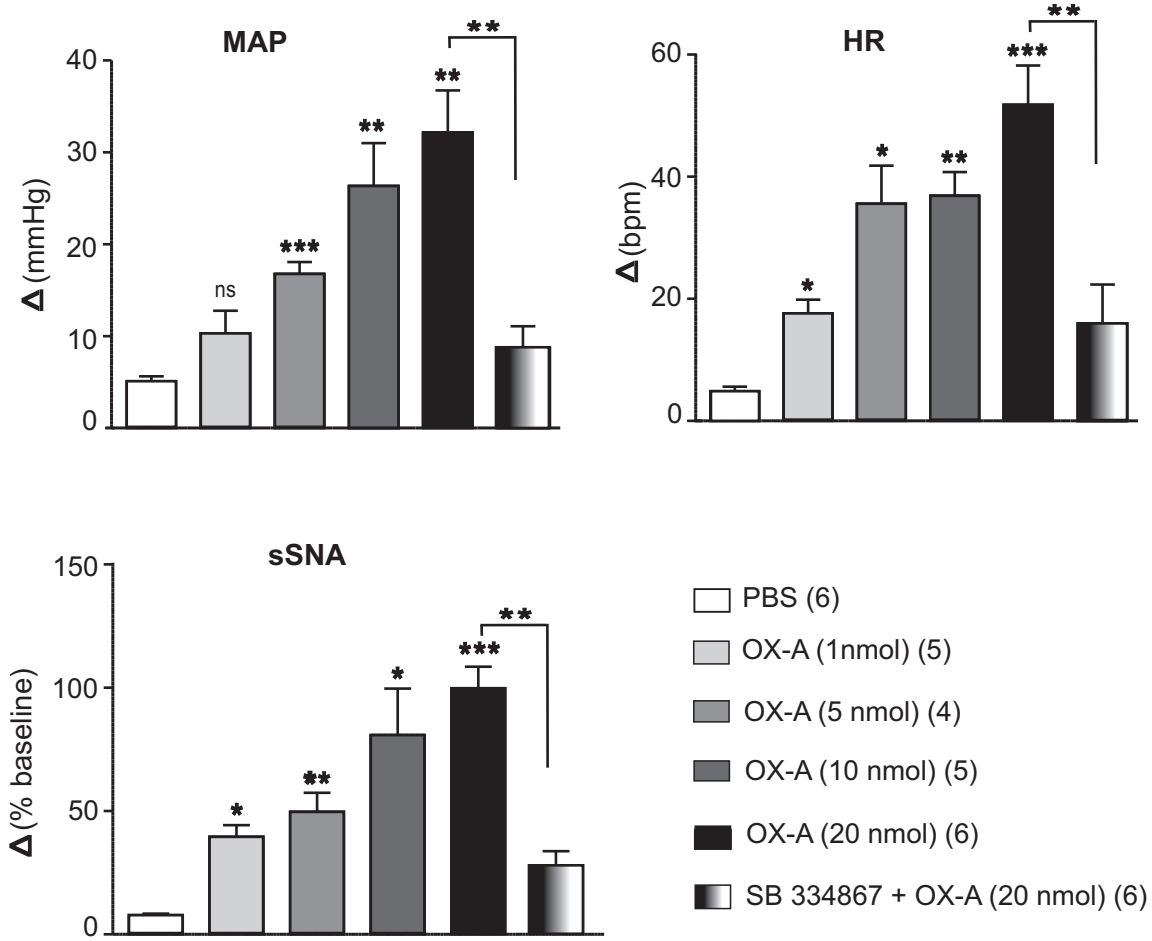

Figure. 3.2. Effect of intrathecal injection of OX-A on mean arterial pressure (MAP), heart rate (HR) and splanchnic sympathetic nerve activity (sSNA).

Comparison of peak cardiovascular effects produced by PBS, OX-A (1, 5, 10 and 20 nmol) or SB 334867 (200 nmol). Peak effects are shown as absolute (BP, HR) or percentage (sSNA) change from respective basal values. Values are expressed as mean ± SE. Number of animals are shown in parentheses. ns, non-significant; *** $P < 0.001$, ** $P < 0.01$, * $P < 0.05$ compared with PBS (except SB 334867 (200 nmol) + OX-A (20 nmol) that was compared with OX-A (20 nmol)). bpm, beats per minute.

Injection of OX-A (1, 5, 10 and 20 nmol) evoked a dose-dependent increase in PNamp, and neural minute ventilation and a decrease in PNf (Figures 3.3A, B; 3.4A). The maximum decrease in PNf of 18 ± 2 bpm (n=6, *P* <0.01) was elicited by OX-A (20 nmol). OX-A (20 nmol) also caused a peak increase in PNamp of 62 ± 9% (n=6, *P*<0.01) and neural minute ventilation of 53.47 ± 12% (n= 6, *P* <0.05) from the baseline (Figure 3.4A). Following OX-A (20 nmol) administration, PNf decreased, PNamp and neural minute ventilation increased gradually reaching peak levels after about 30 min (Figure 3.3A, B). There is a clear dose response relationship between the concentration of OX-A, and increasing PNamp (Figure 3.4A). A dose-response relationship is also seen between the concentration of OX-A and the fall in PNf (Figure 3.4A). However, the maximum effect on phrenic nerve amplitude is seen at 20 nmol, whilst the effect on phrenic nerve frequency is maximal at 5 nmol; this means that beyond 5 nmol, there is an increasing effect on phrenic neural minute ventilation. OX-A (20 nmol) caused a lengthening of T_E and a shortening of T_I reaching a peak level of 0.75 ± 0.1 s (n=5, *P* <0.05) and -0.122 ± 0.03 s (n=3, *P* <0.05), respectively (Figures 3.3A, B; 3.4B). No significant changes in PNf, PNamp, neural minute ventilation, T_E or T_I were observed after injection of PBS (vehicle) (Figures 3.3A, B; 3.4A, B).

In the absence of OX-A, SB 334867 (200 nmol) did not affect MAP, HR, sSNA, PNamp, PNf or neural minute ventilation (n=5) (data not shown). On the other hand, the cardio-respiratory effects of OX-A (20 nmol) were significantly reduced by prior i.t. injection of SB 334867 (MAP: 9 ± 2 vs. 32 ± 5 mmHg, *P* <0.01; HR: 16 ± 6 vs. 52 ± 6 bpm, *P* <0.01; sSNA: 28 ± 6 vs. 100 ± 9%, *P* <0.01; PNamp: 34 ± 3 vs. 62 ± 8%, ns; PNf: -8 ± 1 vs. -18 ± 2 bpm, *P* <0.05; neural minute ventilation: 23 ± 6 vs. 53 ± 12%, ns, of baseline; n= 6, Figures 3.2; 3.4 A).

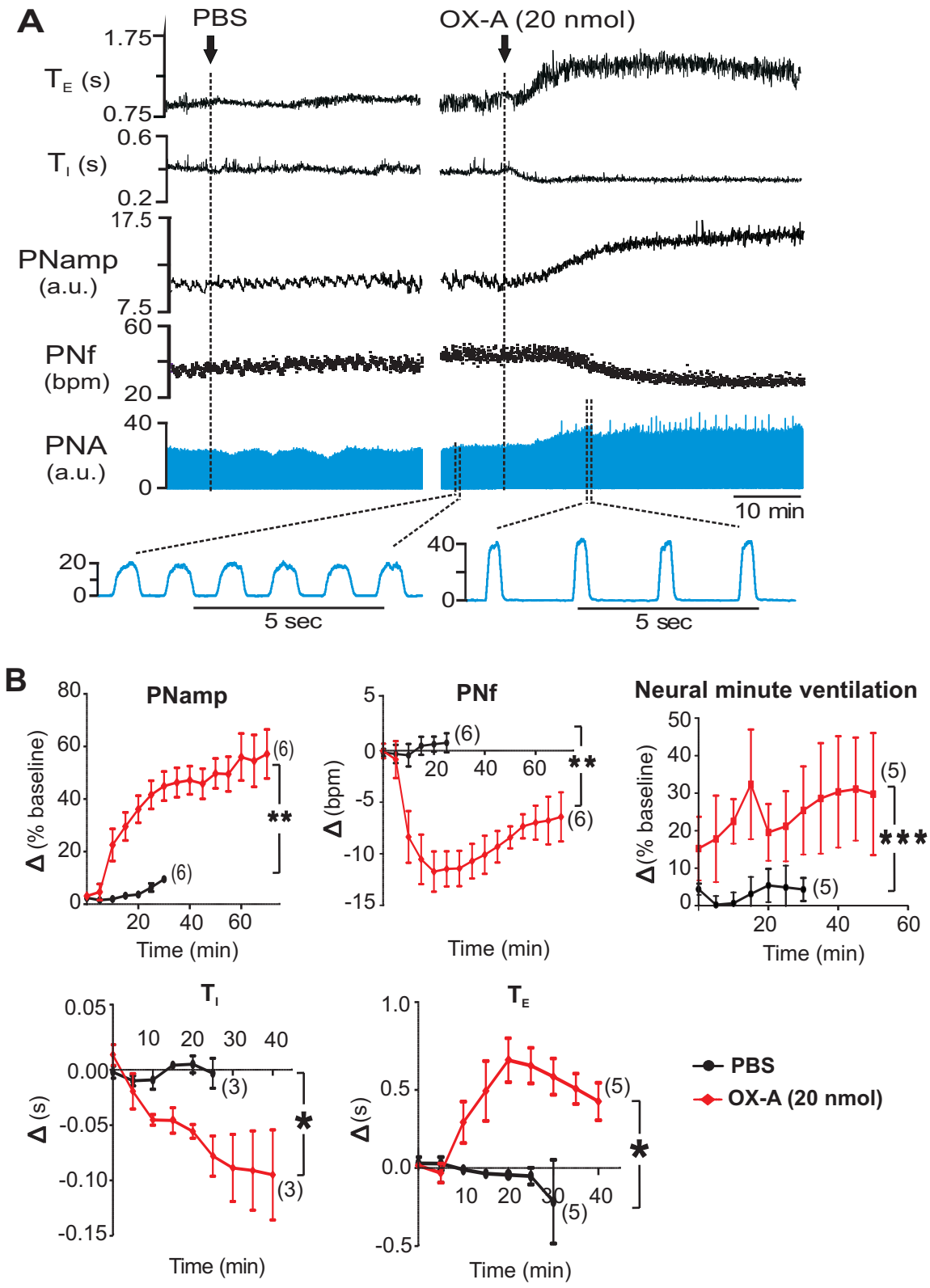

Figure 3.3. Effect of intrathecal injection of OX-A on phrenic nerve activity (PNA).

A: Representative trace of data from a recording of rectified PNA [arbitrary unit (a.u.)],phrenic nerve frequency (PNf), phrenic nerve amplitude (PNamp), inspiratory period (T_I) and expiratory period (T_E) before and after injection of PBS or OX-A. **B**: Grouped time course effects of PBS or OX-A (20 nmol) on PNamp, PNf, neural minute ventilation, T_I and T_E. Values are expressed as mean ± SE. Number of animals are shown in parentheses. ns, non-significant; *** $P < 0.001$, ** $P < 0.01$, * $P < 0.05$ compared with PBS. bpm, bursts per minute.

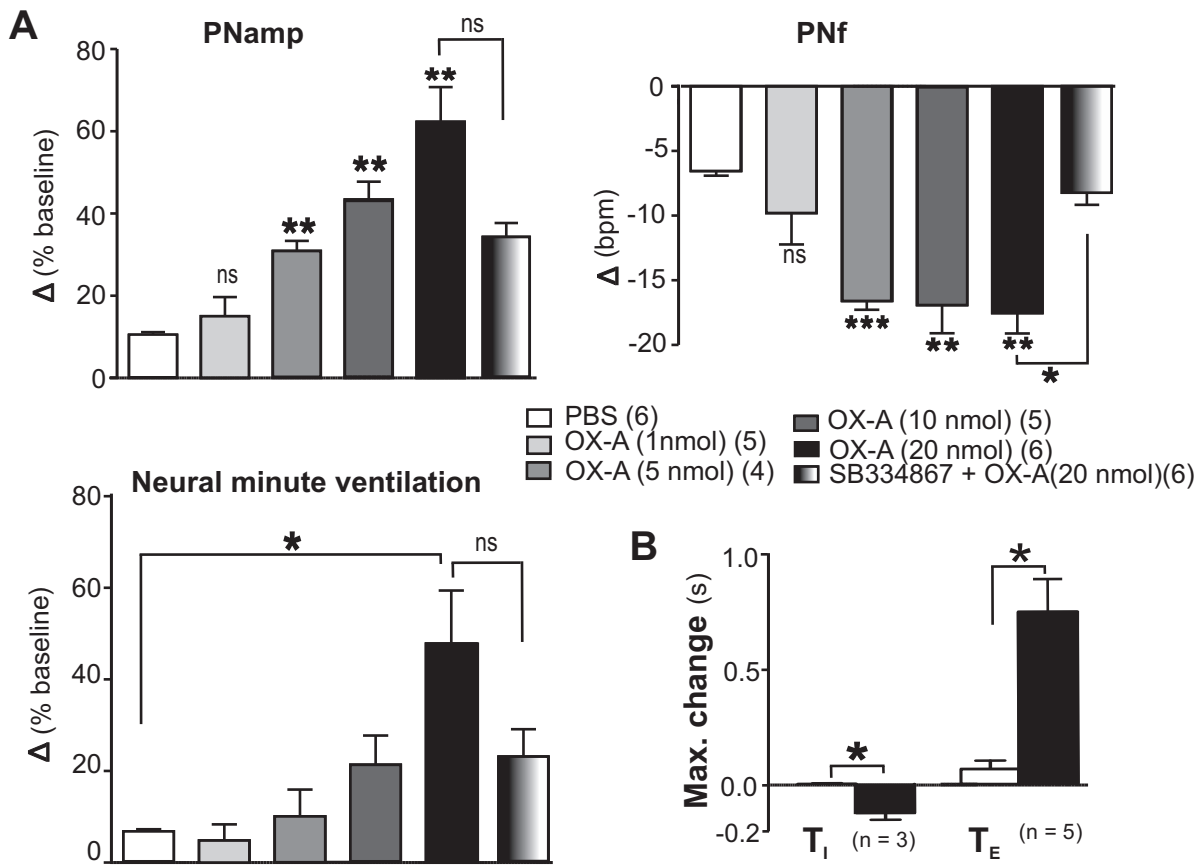

Figure 3.4. Effect of intrathecal injection of OX-A on phrenic nerve activity (PNA).

A: Comparison of peak effects produced by PBS, OX-A (1, 5, 10 and 20 nmol) or SB 334867 (200 nmol) + OX-A (20 nmol) on PNamp, PNf and neural minute ventilation. Peak effects are shown as absolute or percentage change from respective basal values. **B**: Grouped data illustrating the effects of PBS and OX-A (20 nmol) on T_I and T_E. Values are expressed as mean ± SE. Number of animals are shown in parentheses. ns, non-significant; *** $P < 0.001$, ** $P < 0.01$, * $P < 0.05$ compared with PBS (except SB 334867 (200 nmol) + OX-A (20 nmol) that was compared with OX-A (20 nmol)). bpm, bursts per minute.

Peri-phrenic averaging of the sympathetic nerve activity reveals an inspiratory (I) and post-inspiratory (P-I) peak of sSNA (Figure 3.5A). The amplitude of P-I peak of sSNA was significantly increased by i.t. injection of 20 nmol OX-A (153 ± 41% vs 13 ± 7% of PBS; *P* <0.05; n=5) (Figure 3.5A, C) over baseline (control). OX-A showed a gradual increase in P-I peak over time (Figure 3.5B). In contrast, no significant change in the amplitude of I-peak was observed (43 ± 9% vs 27 ± 3% of PBS; *ns*; n=5, Figure 3.5A, C).

3.4.2 Effects of bupivacaine anaesthesia at the C8 spinal level on OX-A activity

C8 anaesthesia caused a fall in MAP (from 95 ± 7 to 59 ± 3 mmHg), HR (from 459 ± 8 to 408 ± 19 bpm) and sSNA (-45 ± 12 %) without any change in PNA (n= 3, Figure 3.6B). Following C8 transection, i.t. OX-A (20 nmol) caused a greater increase in MAP, HR and sSNA, but for a shorter period when compared to intact animals (MAP: 74 ± 7 vs. 32 ± 5 mmHg, *P* <0.05; HR: 51 ± 10 vs. 52 ± 6 bpm, ns; sSNA: 292 ± 26 vs. 100 ± 9%, *P* <0.05, of the baseline, Figure 3.6A-C). Conversely, the effects of OX-A on PNA were abolished when compared to the response prior to C8 anaesthesia (PNamp: 10 ± 4 vs. 62 ± 8%, *P* <0.05; PNf: 0.7 ± 1 vs. -18 ± 2 bpm, *P* <0.05, of the baseline; Figure 3.6A-C). PBS injection after C8 anaesthesia showed no change on MAP, HR, sSNA or PNA (n= 1) (data not shown).

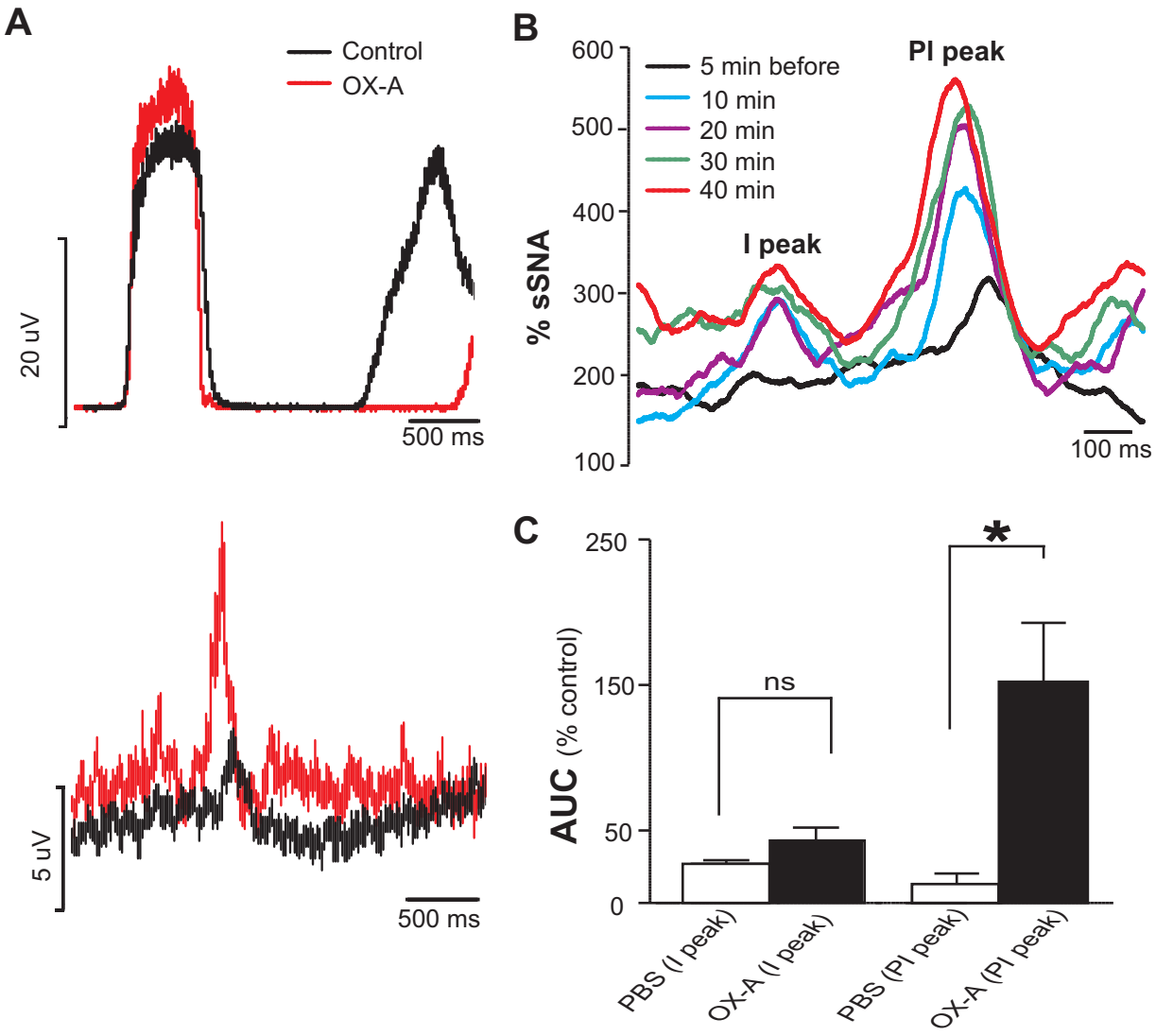

Figure 3.5. Effect of OX-A on phrenic nerve discharge-related rhythmicity of sSNA.

A: Phrenic-triggered average of sSNA before (black) and after (red) intrathecal injection of OX-A (20 nmol). **B**: Time course effect of OX-A (20 nmol) on inspiratory (I) and post-inspiratory (PI) related activity of sSNA. **C**: Grouped data illustrating the effects of OX-A (20 nmol, n=5) on the area under the curve (AUC) of inspiratory and post-inspiratory peaks of sSNA. Values are expressed as mean ± SE. ns, non-significant; * $P < 0.05$ compared with PBS. Both PBS and OX-A values were normalised to the control period prior to injections.

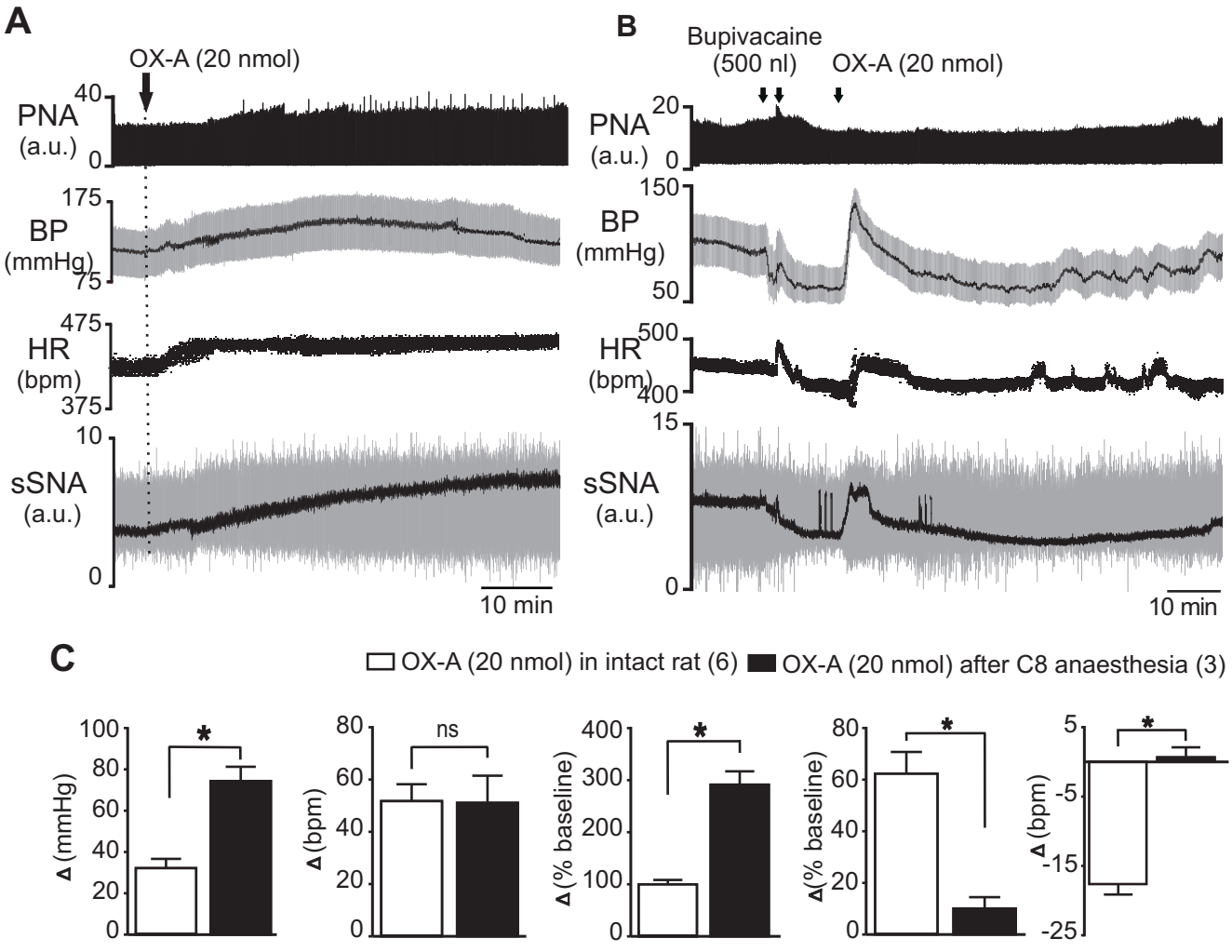

Figure 3.6. Effect of intrathecal OX-A (20 nmol) on mean arterial pressure (MAP), heart rate (HR), splanchnic sympathetic nerve activity (sSNA) and phrenic nerve activity (PNA) in intact rat (A) and C8 anaesthetized rat (B).

A: Representative trace of data from a recording of PNA, blood pressure (BP), HR and sSNA [arbitrary unit (a.u.)] in intact rat. Integrated sSNA (black) is superimposed over raw sSNA (grey). MAP (black) is superimposed over blood pressure (BP)(grey). **B**: Representative trace of data from a recording of PNA, BP, HR and sSNA [arbitrary unit (a.u.)] in a C8 anaesthetized rat. **C**: Comparison of peak cardio-respiratory effects produced by OX-A (20 nmol) in intact (n= 6) and C8 anaesthetized rat (n= 3). Peak effects are shown as absolute or percentage change from respective basal values. Values are expressed as mean ± SE. Number of animals are shown in parentheses. ns, non-significant; * $P < 0.05$ compared with OX-A response in intact animal. bpm, beats per minute, bursts per minute.

3.4.3 Effects of OX-A on somatosympathetic reflex

The average sSNA response to intermittent stimulation of the sciatic nerve was evaluated (somato-sympathetic reflex) before and after i.t. injection of PBS (vehicle) or OX-A (20 nmol). In five animals, intermittent stimulation of the sciatic nerve resulted in two characteristic excitatory peaks in sSNA with latencies of 93 ± 3 ms and 188 ± 2 ms (n=5, Figure 3.7A). The latencies were not significantly altered by PBS (91 ± 3 ms and 186 ± 1 ms, n=5, ns) or by OX-A (89 ± 2 ms and 191 ± 4 ms, n=5, ns) injection. OX-A significantly increased the basal sSNA to 221 ± 22% (n=5, *P*<0.05) as compared to PBS (100 ± 7%). OX-A markedly attenuated the amplitude of both excitatory peaks. The first and second sympatho-excitatory peaks were attenuated by 25 ± 10% and 72 ± 13% of the baseline (n=5, *P* <0.05, Figure 3.7A) as compared to the effect seen following PBS injection (Figure 3.7A).

3.4.4 Effects of OX-A on baroreflex

In five animals, the changes in sSNA were plotted against the changes in MAP evoked by intravenous injection of SNP and PE. The changes in arterial blood pressure following PE injection were of nearly equal magnitude (71 ± 7 mmHg following PBS injection, and 65 ± 8 mmHg following OX-A injection). In fact, the blood pressure increase following PE after OX-A injection was, if anything, slightly smaller than the increase that followed PBS injection. OX-A (20 nmol, i.t.) significantly enhanced the reflex sympathoexcitatory and inhibitory responses evoked by these equipotent doses of SNP and PE (Figure 3.7B). OX-A significantly increased the upper plateau, range of sSNA and maximum gain of the sSNA without significantly altering lower plateau, the threshold level, midpoint, the saturation levels of MAP and the operating range as compared to PBS (Table 3.1).

3.4.5 Effects of OX-A on peripheral chemoreflex

Activation of peripheral chemoreceptors with brief hypoxia evoked an increase in MAP, sSNA and HR (Figure 3.7C). Peak effects occurred near the end of stimulus and recovered rapidly to baseline. Injection of OX-A (20 nmol) into spinal cord significantly increased the pressor response which was 25 ± 4% greater than control, compared with the PBS response which was only 1 ± 1% greater than control (n= 5, *P*<0.01, Figure 3.7C). The sympathoexcitatory effect was also markedly increased by OX-A compared with the response following PBS (94 ± 7% vs 6 ± 7%, n=5, *P*<0.001,

Figure 3.7C). The effect on heart rate was unchanged by OX-A (-25 ± 10 vs -10 ± 11%, n=5, ns, Figure 3.7C). OX-A increased peak PNf, but had no effect on the peak amplitude of PNamp and neural minute ventilation during hypoxia (PNf: 21 ± 5 vs. 1 ± 2%, $P<0.05$; peak PNamp: -35 ± 11 vs. -21 ± 12%, ns; neural minute ventilation: 7 ± 5 vs. -4 ± 7%, ns, of control baseline (n=5).

Table 3.1. Parameters describing baroreflex control of sSNA after intrathecal injection of PBS or OX-A (20 nmol)

	Lower Plateau (%)	Upper Plateau (%)	Mid Point (mmHg)	Max. Gain (%/mmHg)	Range of SNA (%)	Threshold Level (mmHg)	Saturation Level (mmHg)	Operating Range (mmHg)
PBS	29.7±8.7	111.2±2.3	157.9±7.0	-1.8±0.4	81.6±9.4	118.0±6.6	197.8±12.9	79.7±14.9
OX-A (20 nmol)	24.6±16.9 (ns)	279.1±38.0 (p<0.01)	175.2±6.2 (ns)	-3.6±0.6 (p<0.05)	254.6±48 (p<0.01)	121.4±10.4 (ns)	228.9±12.1 (ns)	107.5±18.8 (ns)

Values are means ± SE (n = 5). Maximum (Max.) gain is the slope of the sigmoid curve of best fit at the MAP corresponding to steepest part of the curve. ns, non-significant.

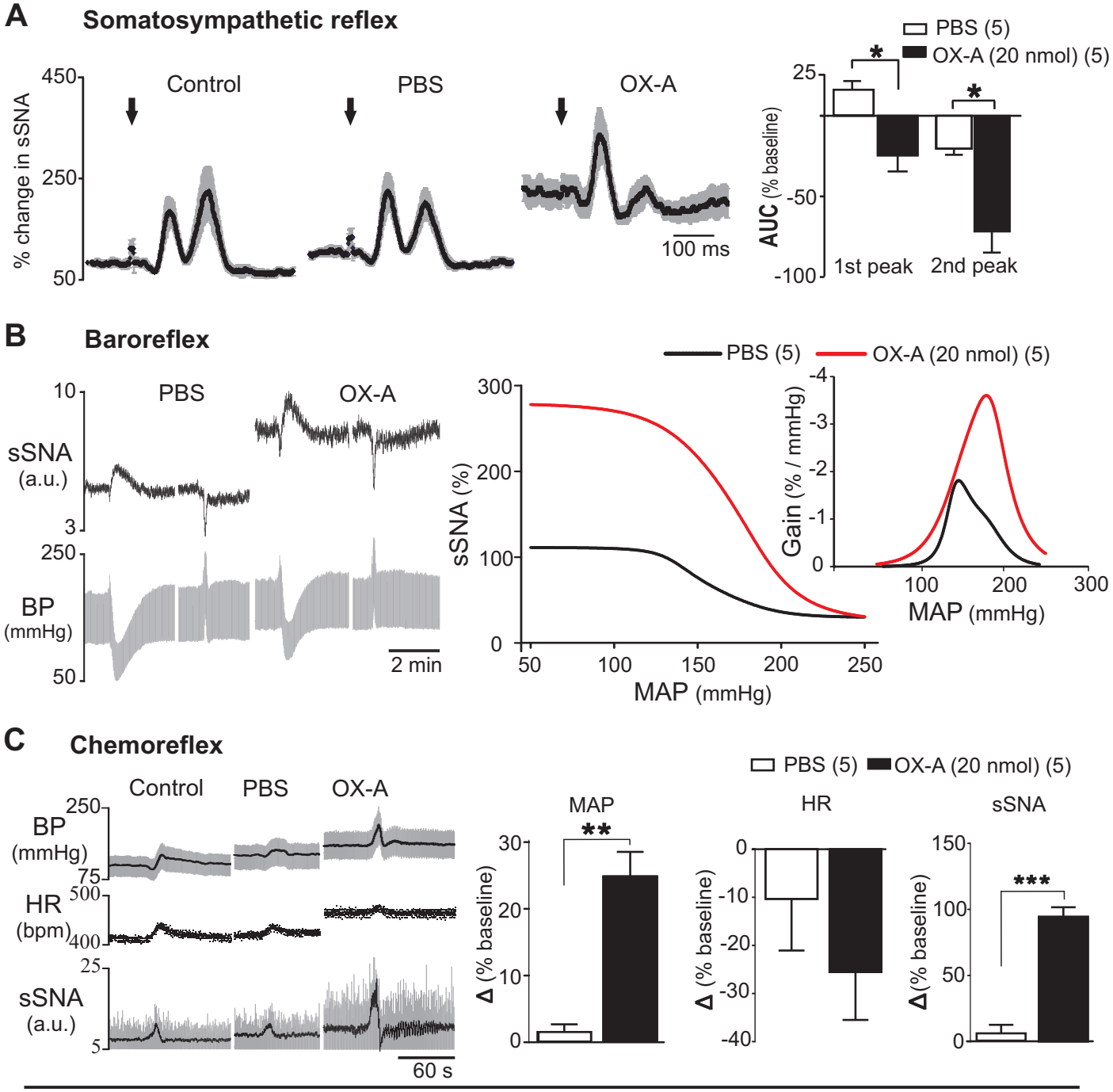

Figure 3.7. Effect of intrathecal injection of OX-A on somatosympathetic, baroreceptor and peripheral chemoreceptor reflex.

A: Effect on somatosympathetic reflex evoked by sciatic nerve (SN) stimulation. *Left 3 traces* represent grouped effect of SN-evoked stimulation of sSNA at control period and after injection of PBS and OX-A. Data are mean (black) ± SE (grey). Arrows indicate the time of stimulation. *Trace at right* represents group data illustrating the area under the curve (AUC) of 1st and 2nd sympathoexcitatory peaks. **B**: Effect on baroreceptor reflex evoked by intravenous injection of SNP and PE. *Left trace* represents experimental recording of the effect of changes in BP on sSNA due to SNP or PE after PBS and OX-A injection. Middle trace shows average sympathetic baroreflex functional curves generated for data after PBS (black) or OX-A (red) injection. Trace at right represents baroreflex gain for sSNA (error bars are omitted for clarity). **C**: Effect of peripheral chemoreceptor reflex activated by brief hypoxia with 100% N_2 for 12-14 s. Left trace shows experimental recording of hypoxic episodes at control period and after PBS or OX-A injection. Three histograms at right represent comparison of peak effects on MAP, HR and sSNA after intrathecal injection of PBS and OX-A in response to brief hypoxia. Values are expressed as mean ± SE. Number of

3.5 Discussion

This study is the first to investigate the *in vivo* effects of intrathecal OX-A on sympathetic outflow, phrenic burst discharge, and sympathetic physiological reflexes. The major findings are that i.t. injection of OX-A in the 1 - 20 nmol range *1*) elicits sympathetically mediated hypertension and tachycardia, confirming an earlier report (Antunes *et al.*, 2001), *2*) modulates respiratory drive by increasing phrenic nerve amplitude and decreasing phrenic nerve frequency, *3*) reduces both sympathoexcitatory peaks in response to sciatic nerve stimulation, *4*) increases sympathetic baroreflex sensitivity and *5*) potentiates the pressor responses and sympathoexcitation to hypoxia.

SPN integrate the central nervous system output to vasomotor pathways and chromaffin cells (Gilbey, 1997). L-Glutamate, or a related amino acid, is likely to be the major excitatory neurotransmitter to these neurons (Pilowsky and Goodchild, 2002; Pilowsky *et al.*, 2009). Extensive evidence supports the view that the excitatory cardiovascular effects in the spinal cord are modulated by a number of neuropeptides (Pilowsky *et al.*, 2009) including vasopressin (Riphagen and Pittman, 1989), angiotensin (Yashpal *et al.*, 1989), substance P (Yashpal *et al.*, 1987), PACAP (Farnham *et al.*, 2008).

OX-A fibers and nerve terminals are widely distributed throughout the spinal cord in rat, mouse and human (Cutler *et al.*, 1999; Date *et al.*, 2000; van den Pol, 1999). OX-A directly, and reversibly, depolarises SPN by activation of pertussis toxin-sensitive G-proteins and closure of a K^+ conductance via a protein kinase-A dependent pathway (Antunes *et al.*, 2001; van den Top *et al.*, 2003). Pre-treatment with α_1 and β-adrenoceptor antagonists attenuates the pressor and tachycardiac response to intrathecal OX-A. Intravenous OX-A does not affect blood pressure or heart rate (Antunes *et al.*, 2001; Chen *et al.*, 2000). These reports support the idea that the pressor and tachycardiac effects induced by i.t. OX-A are mediated centrally. In addition, mRNA for OX1R and OX2R are expressed on the majority of SPN and neurons in the dorsal and ventral horns of the spinal cord (Cluderay *et al.*, 2002; Guan *et al.*, 2004; van den Top *et al.*, 2003). OX1R is selective for orexin-A and OX2R interacts with both orexin-A and -B (Sakurai *et al.*, 1998). As a selective OX1R

antagonist was unable to abolish entirely, it seems likely that the excitatory effects of OX-A observed in our study may be due to both OX1R and OX2R.

An unanticipated finding of this study is that phrenic nerve activity increased after OX-A injection at T6-T8 spinal levels. The respiratory effects of intrathecal OX-A do not appear to be due to either retrograde diffusion of the peptide into supra-spinal structures or diffusion to C3-C5 level, because 1) C8 anaesthesia abolishes the effects of OX-A on PNA and 2) India ink injected i.t. at the end of the experiments only spread as far rostral as T2. Moreover, in our previous study we reported that transection at the C1 level leaves the effects of i.t. bicuculline infusion unaltered (Goodchild *et al.*, 2000; Goodchild *et al.*, 2008) and i.t. administration of drugs appear not to spread more than a few segments away from the site of administration (Yaksh and Rudy, 1976) and are able to penetrate around 2mm (Yamada *et al.*, 1984). Furthermore, it is known that in adult cat, SPN have dendrites that reach the dorsal pial surface of the spinal cord (Pilowsky *et al.*, 1994); in the neonatal rat, dendrites of SPN are reported to project towards the dorsolateral funiculus (Shen and Dun, 1990), but it is not yet known if they reach the sub-pial area in the adult. Paralysis, vagotomy and artificial ventilation of the animals rule out the possibility that OX-A acts directly on intercostal and abdominal motor neurons thereby limiting lung inflation leading to an increase in phrenic nerve output. The mechanisms underlying the increase in PNamp, decrease in PNf and increase in neural minute ventilation following i.t. OX-A injection are currently unknown. Conceivably, activation of spinal OX receptors might affect sensory and intraspinal pathways thereby modulating spinal pattern generators. On the other hand, the decrease in PNf is likely to be mediated by spino-bulbar connections modulating the respiratory rhythm generator.

The very long-lasting increase in PNA and SNA following i.t. OX-A seen here mimics the long term facilitation (LTF) of PNA and SNA induced by acute intermittent hypoxia (AIH) (Xing and Pilowsky, 2010). A possible role for OX-A in AIH/LTF is supported by the finding that OX neuron ablated mice have reduced capacity for the development of AIH/LTF (Toyama *et al.*, 2009).

SNA activity displays a rhythmic fluctuation in relation to PNA (Adrian *et al*., 1932; Miyawaki *et al.*, 2002b) that is dependent on the level of arterial CO_2. The significant increase in post-inspiratory peak as well as change in baseline activity of sSNA by i.t.

OX-A may be due to the depolarization and increase in sensitivity of SPN (Antunes *et al.*, 2001; Date *et al.*, 2000; van den Top *et al.*, 2003). A large part of the enhancement of SNA seen here was clearly related to a marked increase in phrenic discharge-related activity in SNA.

Lamina I of spinal cord receives inputs from myelinated and unmyelinated nociceptors and transfers the information to brainstem including RVLM and higher regions of the brain (McMullan *et al.*, 2008; Sato and Schmidt, 1973). The somato-sympathetic response, integrated in the RVLM, is relayed to SPN (Makeham *et al.*, 2005; Miyawaki *et al.*, 2002a; Stornetta *et al.*, 1989). The present study demonstrates that the activation of OX receptors in the spinal cord inhibited both the first and second sympatho-excitatory peaks of the somato-sympathetic reflex induced by sciatic nerve stimulation. This reflex inhibition was unrelated to OX-A induced sympathoexcitation. The distribution of orexin fibers as well as receptors in dorsal horn including superficial lamina (Date *et al.*, 2000; Grudt *et al.*, 2002; van den Pol, 1999) and in dorsal root ganglionic cells (Bingham *et al.*, 2001) suggest that OX-A might modulate somato-sympahetic reflex at spinal level. Activation of spinal $GABA_A$ receptors is hypothesized to decrease nociceptive traffic in the spinothalamic tract. OX receptors have been found to increase pre-synaptic release of GABA in lateral hypothalamus (van den Pol *et al.*, 1998). If this is also the case in spinal cord, intrathecal OX-A induced inhibition of somato-sympathetic reflex might be due to the modulation of sensory information from primary afferents by increasing the release of GABA. However, the precise mechanism is yet to be established.

RVLM neurons that are inhibited by baroreceptors project to SPN and provide the major descending excitatory input responsible for baroreflex activity (Pilowsky and Goodchild, 2002; Pilowsky *et al.*, 2009). Two pathways may mediate baroreceptor induced sympathoinhibition, i) inhibition of tonically active descending excitatory pathway which is believed to be the principal mode of action (Pilowsky and Goodchild, 2002) and ii) a direct spinal inhibitory mechanism (Wang *et al.*, 2008). The present study reveals an increase in the upper plateau, range and maximum gain of the baroreflex function curves obtained from sSNA, indicating that intrathecal OX-A significantly increases baroreflex sensitivity. OX-A may modulate either the disfacilitation or the direct inhibition at the spinal level to enhance the baroreflex sensitivity.

Hypoxia causes a rapid and reversible excitation of reticulospinal sympathoexcitatory RVLM neurons that monosynaptically excite SPN. Intrathecal kynurenate blocks the sympathetic excitation elicited by hypoxia revealing the involvement of glutamatergic transmission (Sun and Reis, 1994). Intrathecal OX-A increases the amplitude of the pressor response and markedly amplifies the chemoreflex effect on sSNA. PNf was increased, but PNamp was not affected, and neural minute ventilation was unchanged following OX-A.

In conclusion, the present study reveals a direct excitatory effect of OX-A on SPN, that is presumably mediated by the activation of OX1R and OX2R in the rat spinal cord and a potent modulation of respiratory drive to SPN. Our results also show that OX-A differentially modulates behavioural reflexes. Collectively, these data help to elucidate the role of OX-A system in the regulation of autonomic nervous system and physiological reflexes.

Perspective

RVLM, the key nucleus maintaining SNA and adaptive reflexes, sends a direct input to the spinal cord and regulates its activity. RVLM receive input from orexin neurons in the hypothalamus and injection of OX-A into the RVLM increases BP and HR (Chen *et al*., 2000; Machado *et al*., 2002). However the expression of OX receptors and the effects of OX-A on SNA, PNA and sympathetic reflexes are as yet unexplored.

Thus, our next aim is to determine the expression of OX receptors in the RVLM and to evaluate the effect of bilateral microinjection of OX-A into the RVLM on cardiorespiratory parameters and sympathetic reflexes.

Chapter 4.

Orexin A in rat rostral ventrolateral medulla is pressor, sympathoexcitatory, increases barosensitivity and attenuates the somatosympathetic reflex

Orexin A in rat rostral ventrolateral medulla is pressor, sympathoexcitatory, increases barosensitivity and attenuates the somatosympathetic reflex

4.1 Abstract

The rostral ventrolateral medulla (RVLM) maintains sympathetic nerve activity (SNA), and integrates adaptive reflexes. Orexin A (OX-A)-immunoreactive (-ir) neurons in the lateral hypothalamus project to the RVLM. Microinjection of OX-A into RVLM increases blood pressure and heart rate (HR). The expression of orexin receptors, and effect of OX-A in the RVLM on splanchnic SNA (sSNA), respiration and adaptive reflexes is unknown. The effect of OX-A on baseline cardiorespiratory variables as well as the somatosympathetic, baroreceptor and chemoreceptor reflexes in RVLM were investigated in urethane-anaesthetized, vagotomized and artificially ventilated male Sprague-Dawley rats (n = 49). OX-A and its receptors were detected with fluorescence immunohistochemistry. RVLM tyrosine hydroxylase-ir (TH-ir) neurons were frequently colocalised with orexin receptor 1 (OX_1) and orexin receptor 2 (OX_2), and closely apposed by OX-A-ir terminals. RVLM injection of OX-A is pressor and sympathoexcitatory. The peak effect was observed at 50 pmol with increase in mean arterial pressure (MAP) and SNA of 42 mmHg and 45 % from baseline, respectively. The responses to OX-A (50 pmol) were attenuated by the OX_1 antagonist, SB334867, and reproduced by the OX_2 agonist, [Ala_{11}, D-Leu_{15}]orexin B. OX-A attenuated the somatosympathetic reflex but increased baroreflex sensitivity. OX-A increased or reduced the sympathoexcitation following hypoxia or hypercapnia respectively. The results demonstrate that while the central cardiorespiratory control mechanisms at rest do not rely on orexin, responses to adaptive stimuli are dramatically affected by the functional state of orexin receptors.

The results of this chapter has been published in *British Journal of Pharmacology* (see **Appendix 2**)

Israt Z. Shahid, Ahmed A. Rahman, Paul M. Pilowsky. (2012). Orexin A in rat rostral ventrolateral medulla is pressor, sympathoexcitatory, increases barosensitivity and attenuates the somatosympathetic reflex. *Br J Pharmacol* **165,** 2292–2303.

4.2 Introduction

Tonically active sympathetic premotor neurons in the rostral ventrolateral medulla (RVLM) project to the intermediolateral cell column of the spinal cord and provide an excitatory input to sympathetic preganglionic neurons so as to maintain the resting level of sympathetic vasomotor tone (Pilowsky and Goodchild, 2002; Pilowsky *et al.*, 2009). The RVLM is the key site for cardiovascular homoeostasis. Neurons in the RVLM integrate information from the centre and periphery, including: respiration, and baro-, chemo- and somatosympathetic reflex afferent neurons. Although synaptic input modulates the excitability of RVLM neurons (Pilowsky *et al*., 2009), the sources of this input and the transmitters involved are not thoroughly characterized. Glutamate and gamma amino butyric acid (GABA) are the key contributors for the short-term control of RVLM neurons. Regulation of RVLM neurons by metabotropic transmitters, including neuropeptides that have long-term effects on cell function, may affect adaptive reflexes, and encode distinct patterns of autonomic output (Pilowsky *et al*., 2009).

Orexin A (OX-A) and orexin B (OX-B) (also known as hypocretin 1 and hypocretin 2) have well-established roles in feeding and sleep-wakefulness. Recent evidence suggests a role for orexin as neuromodulators in central cardiorespiratory regulation. OX-A increases blood pressure (BP) and heart rate (HR) following intracisternal injection, or microinjection into the RVLM, to awake or anaesthetized rats (Chen *et al*., 2000; Machado *et al*., 2002). However, the effects of RVLM orexin (OX) receptors activation on sympathetic nerve activity, or autonomic reflexes is unknown.

Although OX-containing cell bodies are restricted to the lateral hypothalamus, perifornical area and dorsomedial hypothalamus, OX-immunoreactive (-ir) fibers are widely distributed in the brain, including many brainstem areas that influence cardiorespiratory function, including the nucleus tractus solitarius (NTS), RVLM, rostral ventromedial medulla (RVMM), pre-Bötzinger complex, retrotrapezoid nucleus (RTN), dorsal motor nucleus of the vagus, and the raphe (Ciriello *et al.*, 2003b; Date *et al.*, 1999; de Lecea *et al.*, 1998; Machado *et al.*, 2002; Nambu *et al.*, 1999; Peyron *et al.*, 1998; Young *et al.*, 2005). OX binds to two G protein coupled ($G\alpha_{q/11}$ and/or $G\alpha_i$) receptors: OX receptor 1 (OX_1) and OX receptor 2 (OX_2). OX_1 has preferential affinity for OX-A, whereas OX_2 exhibits similar affinities for OX-A and OX-B *in vitro*

(Sakurai *et al*., 1998). OX receptors also showed wide spread distribution throughout the brain including thalamus, hypothalamus, brainstem areas like nucleus ambiguus (NA), RVMM, pre-Bötzinger complex, NTS and spinal cord (Trivedi *et al.*, 1998; Marcus *et al.*, 2001; Sunter *et al.*, 2001; Cluderay *et al.*, 2002; Ciriello and de Oliveira, 2003a). The distribution of OX_1 and OX_2 in relation to putative sympathoexcitatory neurons in the RVLM is unknown.

The aims of this study were 1) to determine whether OX_1 and OX_2 are expressed within neurons in the RVLM, and to determine if they are co-localised with putative sympathoexcitatory catecholamine-containing neurons of the rostral C1 cell group; 2) to evaluate the actions of OX-A in the RVLM on splanchnic sympathetic (sSNA) and phrenic nerve activity (PNA), and on the baro-, chemo-, and somatosympathetic reflexes; 3) to determine which type of OX-receptor mediates the central effects of orexin.

Our principal findings are that OX_1 and OX_2 are expressed abundantly in the RVLM neurons. Bilateral injection of OX-A in the RVLM increases mean arterial pressure (MAP), HR, sSNA and phrenic nerve amplitude (PNamp). OX-A in the RVLM attenuates the somatosympathetic reflex but increases barosensitivity. Following OX-A injection into the RVLM, sympathoexcitatory responses to hypoxia or hypercapnia were increased or reduced, respectively,. The findings demonstrate a role for OX-A in the RVLM in both the tonic and reflex regulation of central cardiorespiratory control.

4.3 Methods

Experiments were conducted on male Sprague-Dawley rats (n = 49, 350–500 g). Rats were housed under controlled conditions with a standard 12-h light/dark cycle. Standard laboratory rat chow and tap water were available ad libitum. They were allowed to acclimatize for at least 7 days before experimental manipulations. Food and water were withdrawn 30 min before anaesthesia. All experiments were carried out following the guidelines of the Australian Code of Practice for the Care and Use of Animals for Scientific Purposes (http://www.nhmrc.gov.au/publications/

synopses/eal6syn.htm) and with the approval of the Animal Ethics Committee of Macquarie University, Sydney, Australia.

4.3.1 Immunohistochemical experiments

Rats (n = 3) were anaesthetized (pentobarbitone sodium, 70 mg kg^{-1}, ip), transcardially perfused and brainstems were processed for fluorescence immunohistochemistry (IHC) as described previously (Li *et al*., 2005; Padley *et al*., 2007). In brief, 40 µm sections were incubated with species-specific primary antibodies to detect tyrosine hydroxylase (TH) (mouse, 1:2500), OX-A (rabbit, 1:2000), OX_1 (rabbit, 1:50) and OX_2 (goat, 1:50). Sections were then washed (3 x 30 min) in TPBS buffer (10 mM Tris HCl, 10 mM sodium phosphate buffer, 0.9% NaCl, pH 7.4) and incubated with fluorophore-conjugated secondary antibodies (Alexa Fluor 488 donkey anti-mouse IgG, and Cy3 donkey anti-rabbit IgG or Cy3 donkey anti-sheep IgG; 1:500) to reveal TH, OX-A, OX_1 and OX_2, respectively. Finally, sections were mounted on glass slides, coverslipped with Vectashield, and sealed with nail polish.

Brainstem sections, including RVLM region, extending from 11.6 to 12.8 mm caudal to Bregma were examined using an epifluorescence microscope (Axio- Imager Z1; Zeiss, Germany). The RVLM was defined as a triangular area ventral to the NA, medial to the spinal trigeminal tract and lateral to the pyramidal tract or the inferior olive. Labelled neurons in the RVLM were counted from 6-7 sections, 200 µm apart. Counts were made for OX_1, OX_2 and TH-ir neurons, as well as all double- labeling combinations. Results were plotted as the mean ± standard error (SE) at 200 µm intervals. Images were captured in grey scale with an Axiocam MR3 digital camera and pseudocolouring was applied. Staining for all antigens was observed throughout the depth of the section indicating adequate antibody penetration.

4.3.2 Electrophysiological experiments

4.3.2.1 Experimental design

Electrophysiological experiments were conducted as described previously (Shahid *et al*., 2011). Briefly, rats (n = 47) were anaesthetized with urethane (1.2-1.4 g kg^{-1}, i.p.). Supplemental doses of urethane (30-40 mg, i.v.) were given when necessary if

nociceptive stimuli (tested every half an hour) caused a change in MAP of more than 10 mmHg. Rectal temperature was maintained at ~36.5^{0}C with a thermostatically controlled heating pad (Harvard Apparatus, Holliston, MA, USA) and infrared heat lamp.

The left jugular vein and right carotid artery were cannulated with polyethylene tubing (internal diameter = 0.58 mm; outer diameter = 0.96 mm) for administration of drugs and fluids and for measurement of BP, respectively. In some experiments, both femoral veins were cannulated to enable administration of sodium nitroprusside (SNP) or phenylephrine hydrochloride (PE). The trachea was cannulated to enable artificial ventilation and a 3 lead electrocardiogram was recorded. HR was derived from the BP. The left greater splanchnic nerve and phrenic nerve were isolated, tied with silk thread and cut distally to permit recording of efferent sSNA and PNA, respectively. In an additional subset of animals, the sciatic nerve was isolated, tied and cut distally for electrical stimulation to allow activation of somatosympathetic reflex. Rats were secured in a stereotaxic frame, vagotomized, paralyzed (pancuronium bromide; 0.8 mg initially, then 0.4 mg h^{-1}) and artificially ventilated with oxygen enriched room air. End-tidal CO_2 was monitored and maintained between 4.0% and 4.5% (Capstar 100, CWE Inc., Ardmore, PA, USA). Arterial blood gas was analyzed to maintain pH at 7.35-7.45 (pH 7.4 ± 0.03; $PaCO_2$ 40.4 ± 0.9) by electrolyte and blood gas analyzer (IDEXX Vetstat, West brook, Maine, USA). Animals were infused with 5% glucose in water (1.0-2.0 ml h^{-1}) to ensure hydration. Nerve recordings were made with bipolar silver wire electrodes. The neurograms were amplified (x10 000, CWE Inc., Ardmore, PA, USA), bandpass filtered (0.1–2 kHz), sampled at 3 kHz (1401 plus, CED Ltd, Cambridge, UK) and recorded on computer using Spike2 software (v7, CED Ltd, Cambridge, UK).

The dorsal medulla was exposed after an occipital craniotomy. Bilateral microinjections of L-glutamate (100mM, 5nmol in 50nl), OX-A (250 µM, 500 µM, 1 mM, 2 mM equivalent to 12.5, 25, 50 and 100 pmol; 50 nl per side) and vehicle (phosphate buffered saline (PBS)) into the RVLM were made, using single- or multi-barrel glass pipettes and, as described previously (Miyawaki *et al*., 2001; Rahman *et al*., 2011a). The RVLM was functionally identified by an increase of >30 mmHg in MAP following microinjection of L-glutamate. All variables were allowed to return to

baseline (>30 min) before microinjection of PBS. After a further 30 min, OX-A was microinjected into the same site and observation continued for a further 60 min. For all experiments, microinjections (50 nl) were performed over 5 seconds. Injection sites were marked with 2% rhodamine beads added to the PBS (50nl) which was also microinjected as a volume, and vehicle, control.

Cardiorespiratory reflexes were evoked as described previously (Abbott and Pilowsky, 2009; Rahman *et al.*, 2011b; Shahid *et al.*, 2011), with sequential iv injection of SNP and PE (0.01 mg kg^{-1}) or electrical stimulation (10-25 V, 50, 0.2 ms pulses at 1 Hz) of the sciatic nerve. Chemoreceptors were activated by ventilating animals with 100% N_2 (12-14 s, brief hypoxia; peripheral; BOC gas and gear, NSW, Australia) or 5% CO_2:95%O_2 (3 min, hypercapnia; central; BOC gas and gear, NSW, Australia), respectively. Reflexes were activated before and after bilateral microinjection of PBS or OX-A (50 pmol, per side, 50 nl), respectively. Following euthanasia (3 M KCl, 0.5 ml, i.v.) brainstems were removed and injection sites were verified. Preliminary experiments revealed that tachyphylaxis occurs following OX-A injection, therefore, each animal received only one injection of OX-A. Different reflexes and antagonist studies were conducted on different sets of animals. Cardio-respiratory coupling was analyzed from the same group used to determine the cardio-respiratory responses.

4.3.2.2 Data acquisition and analysis

Neurograms were rectified and smoothed (sSNA, 1 s time constant; PNA, 50 ms). Minimum background activity after death was taken as zero sSNA, and this value was subtracted from sSNA before analysis with off-line software (Spike 2 version 7). Baseline values were obtained by averaging 60 s of data 5 min prior to OX-A or PBS injection and maximum changes were expressed as absolute or percentage changes from baseline values. Phrenic-triggered ensemble averages of sSNA were generated from 60-s portions of data to evaluate cardiorespiratory coupling. The area under the curve (AUC), less baseline, of sSNA activity during the inspiratory and post-inspiratory phases was determined. sSNA was rectified and smoothed at 1 s and 5 ms time constants to analyse baroreceptor reflex and somatosympathetic reflex, respectively. To analyse reflexes, sSNA was normalized between the activity of sSNA before PBS injection (100%) and the sSNA after death (0%). The sSNA

response to sciatic nerve stimulation was analyzed using peristimulus waveform averaging. The AUC of the sympathoexcitatory peaks was analyzed. The response to hypoxia (100% N_2 inhalation for 12–14 s) was quantified by comparing the average maximum sSNA during hypoxia compared with a control period during normal hyperoxic ventilation. The maximum response to stimulation was then expressed as a percentage change from the baseline (control) considering maximum reflex response in control as 100%.

Statistical analysis was conducted with GraphPad Prism (version 5.0) (GraphPad, La Jolla, CA, USA). Grouped data are expressed as mean ± SE. A two way repeated measures ANOVA with Bonferroni's correction was used to compare values after OX-A (50 pmol) administration on sSNA and PNA with the PBS value. Paired t-test was used to analyze peak effects and reflexes. $P < 0.05$ was considered significant.

4.3.3 Drugs

OX-A (MW = 3561.16; Cat. No: H-4172; Lot No: 1013059) was obtained from, Bachem AG (Bubendorf, Switzerland) while OX_1 antagonist, SB334867 (*N*-(2-Methyl-6-benzoxazolyl)-*N*′-1,5-naphthyridin-4-yl urea) (Cat. No: 1960; Batch No: 5), and OX_2 agonist, [Ala11, D-Leu15]OX-B (Cat. No: 2142; Batch No: 10), were from Tocris Bioscience (Missouri, USA). Urethane, L-glutamate, glucose, PE and SNP were purchased from Sigma-Aldrich (Sydney, Australia), pancuronium bromide from AstraZeneca Pty Ltd (Sydney, Australia), pentobarbitone sodium from Merial Australia Pty Ltd (NSW, Australia), rhodamine microbeads from Molecular Probes (Sydney, Australia) and PBS (10 mM in 0.9% NaCl) tablets from AMRESCO Inc. (Solon, OH, USA). Primary antibodies for OX-A (Cat No: PC362), OX_1 (Cat. No: AB3092; Lot No: LV1387169), OX_2 (Cat. No: sc-8074) and TH were from Merck (Darmstadt, Germany), Millipore (Billerica, MA, USA), Santa Cruz Biotechnology, Inc. (Santa Cruz, CA, USA) and Sigma-Aldrich, respectively. Fluorophore-conjugated secondary antibodies such as Alexa Fluor 488 donkey anti-mouse IgG (Cat. No: A21202; Lot No: 811493), Cy3 donkey anti-rabbit IgG (Cat. No: 711-166-152; Lot No: 92082) or Cy3 donkey anti-sheep IgG (Cat. No: 713-166-147; Lot No: 89763) were from Invitrogen (Victoria, Australia) and Jackson ImmunoResearch Laboratories (West Grove, PA, USA), and vectashield from Vector Laboratories (QLD, Australia). OX-A, [Ala11, D-Leu15]OX-B, and rhodamine (2% v/v) were dissolved and further

diluted in PBS (10 mM; pH 7.4). SB334867 was dissolved and further diluted in 10% dimethyl sulfoxide (DMSO). PBS, PE and SNP were prepared in de-ionised water. Urethane was dissolved in 0.9% NaCl and L-glutamate in PBS.

All drug and receptor nomenclature conforms to the BJP's guide to receptors and channels (Alexander *et al*., 2009).

4.4 Results

4.4.1 Expression of OX-A terminals and its receptors in the RVLM

The expression of OX-A, OX_1 and OX_2 in the RVLM was examined using fluorescence immunohistochemistry. OX-A-ir fibers and terminals were found commonly throughout the RVLM (Figure 4.1A). OX-A-ir terminals were also closely apposed to TH-ir cell bodies as well as dendrites (n = 3, Figure 4.1A).

Both OX_1 and OX_2 were expressed in the RVLM. Intense immunoreactivity for both receptors was observed on cell bodies as well as on dendrites, fibers and terminals throughout the RVLM (Figure 4.1B, C). OX_1-ir and TH-ir were frequently colocalized in the RVLM neurons (Figure 4.1B). OX_1-ir was found in 78 ± 2% (561 of 727 neurons across the region counted from -11.6 to -12.8; n = 3) of TH-ir neurons in the RVLM (Figure 4.1B); OX_2-ir was found in 77 ± 3% (475 of 611 neurons) of TH-ir neurons in the RVLM (Figure 4.1C). Within the RVLM about 51% of OX_1 (590 of 1151 neurons across the entire region counted from -11.6 to -12.8, n = 3) and 56% of OX_2 (615 of 1090 neurons across the entire region counted from -11.6 to -12.6, n = 3) were expressed in non-TH-ir or non-C1 neurons, suggesting that both C1 and non-C1 neurons in the RVLM contain both OX receptors (Figure 4.1B, C). OX_1-ir, OX_2-ir and TH-ir showed similar distribution pattern in the RVLM being expressed most frequently in the rostral pole (Figure 4.1B, C).

4.4.2 Effects of OX-A in the RVLM on cardiorespiratory parameters

Bilateral microinjection of OX-A at four different doses (12.5, 25, 50 and 100 pmol, per side) evoked a pressor response, tachycardia and sympathoexcitation in a dose-dependent manner (Figure 4.2A, B). The maximum effects occurred following injection of 50 pmol OX-A and the highest levels attained were 42 ± 2 mmHg (MAP,

n= 6, *P*<0.001), 16 ± 1 bpm (HR, n= 6, *P* <0.01) and 45 ± 4 % (sSNA, n= 6, *P* <0.001) from the baseline (Figure 4.2B). Bilateral injection of PBS (vehicle) in the RVLM was without effect on MAP (4 ± 1 mmHg, n= 6), HR (3 ± 1 bpm, n= 6) or sSNA (2 ± 1 %, n= 6; Figure 4.2B).

OX-A injected bilaterally (12.5, 25, 50 and 100 pmol, per side) in the RVLM evoked a significant increase in PNamp without any effect on phrenic nerve frequency (PNf) (Figure 4.2A, B). The maximum increase in PNamp of 31 ± 2% (n= 6, *P* <0.001) was elicited by 50 pmol OX-A (Figure 4.2B). No significant change in PNamp or PNf was observed after injection of PBS (vehicle) (Figure 4.2A, B).

In some experiments (n = 5), bilateral injection of OX-A (50 or 100 pmol, per side) in the RVLM evoked a long-lasting increase in sSNA and PNA (Figure 4.2A, C) that mimics the pattern of long term facilitation (LTF) of sSNA and PNA induced by acute intermittent hypoxia (Baker-Herman and Mitchell, 2002; Dick *et al.*, 2007) or by intrathecal injection of OX-A (Shahid *et al*, 2011). All injection sites were centred in the RVLM (Figure 4.2D).

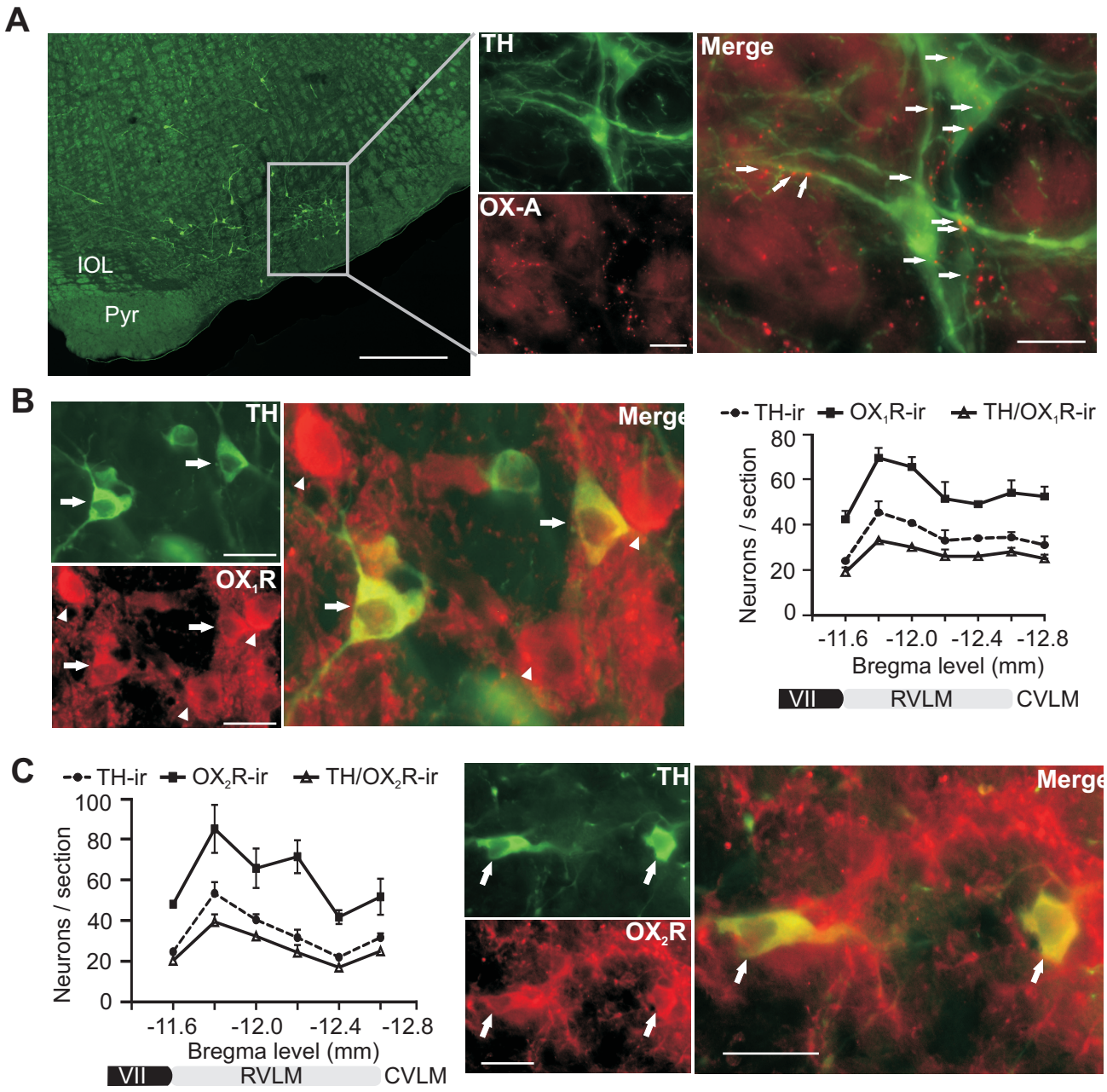

Figure 4.1. Orexin A (OX-A) terminals, orexin receptor 1 (OX_1) and orexin receptor 2 (OX_2) in the rostral ventrolateral medulla (RVLM).

A: Tyrosine hydroxylase (TH) positive C1 neurons (green) in the RVLM are surrounded by OX-A immunoreactive (ir) varicosities (red) that form close appositions with TH-positive cell bodies and dendrites (arrows). **B**: Expression of OX_1-ir in the RVLM. OX_1-ir (red) is expressed in TH-ir neurons (green) (arrows) as well as in some non-TH neurons (arrowheads). XY plot represents rostrocaudal distribution of TH-ir neurons, OX_1-ir neurons and TH-ir/OX_1-ir neurons. **C**: XY plot represents rostrocaudal distribution of TH-ir neurons, OX_2-ir neurons and TH-ir/OX_2-ir neurons. OX_2-ir (red) is colocalized with TH-ir neurons (green; arrows). VII, facial nucleus; CVLM, caudal ventrolateral medulla. Scale bars: 500 µm (A, left); 20 µm (A, right); 25 µm (B and C).

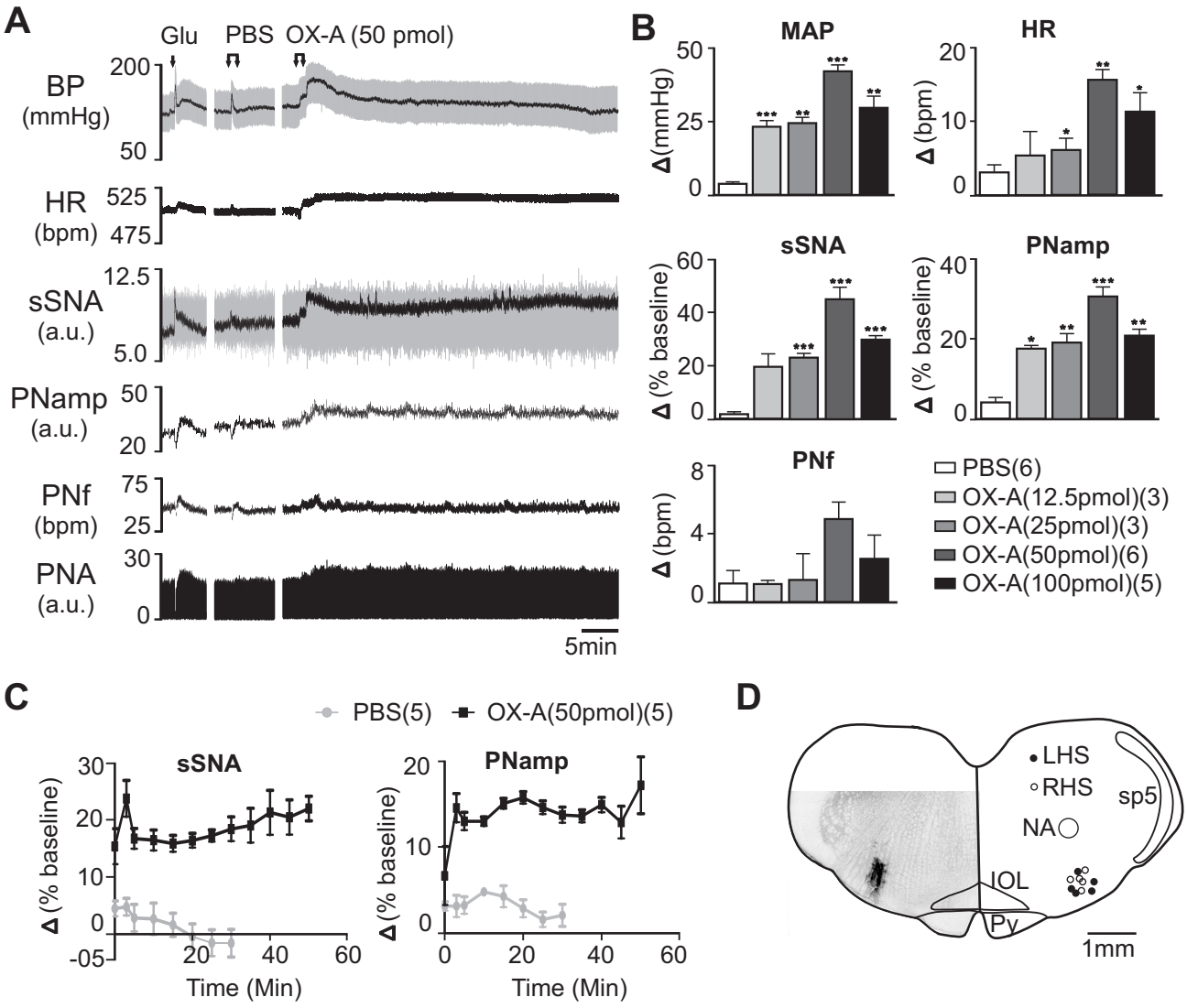

Figure 4.2. Effect of bilateral microinjection of orexin A (OX-A) in the rostral ventrolateral medulla.

A: Continuous recording of blood pressure (BP) (grey – pulsatile and black – mean), heart rate (HR), splanchnic sympathetic nerve activity (sSNA) (grey – raw and black - rectified and integrated) [arbitrary unit (a.u.)], rectified PNA (a.u.), phrenic nerve frequency (PNf) and phrenic nerve amplitude (PNamp) before and after injection of glutamate (Glu), phosphate buffered saline (PBS) or OX-A (50 pmol). **B**: Grouped data of maximum cardiovascular and respiratory effects following PBS or OX-A (12.5, 25, 50 and 100 pmol). Peak effects are shown as absolute (mean arterial pressure (MAP), HR, PNf) or percentage (sSNA, PNamp) change from respective basal values. **C**: Grouped time course effects of PBS (grey) or OX-A (50 pmol) (black) on sSNA and PNamp. **D**: Microinjection sites in the RVLM and a section showing an injection site stained following an injection of rhodamine microbeads . NA: nucleus ambiguus; sp5: spinal trigeminal tract; IOL: inferior olive; Py: pyramidal tract. Data are expressed as mean ± SE. Number of animals are shown in parentheses. *** $P < 0.001$, ** $P < 0.01$, * $P < 0.05$ compared with PBS. bpm, beats per minute for HR or bursts per minute for PNf.

4.4.3 Effects of OX receptor antagonism or agonism on OX-A mediated cardiorespiratory responses

In the absence of OX-A, SB334867 (1 nmol, per side) did not affect MAP, HR, sSNA, PNamp or PNf (n=5) (data not shown). On the other hand, the cardiorespiratory effects of OX-A (50 pmol per side) in the RVLM were significantly reduced by prior bilateral injection of SB334867 (MAP: 21 ± 7 vs. 42 ± 2 mmHg, *P* <0.05; HR: 08 ± 2 vs. 16 ± 1 bpm, *P* <0.05; sSNA: 22 ± 2 vs. 45 ± 4%, *P* <0.05; PNamp: 14 ± 2 vs. 31 ± 2%, *P* <0.01, of baseline; n= 5, Figure 4.3).

Bilateral microinjection of the OX_2 agonist, [Ala_{11}, D-Leu_{15}]OX-B (0.75 pmol, per side; n=6), into the RVLM significantly increased MAP, HR, sSNA and PNamp to an extent that was similar or slightly higher in magnitude with OX-A (50 pmol) response (Figure 4.3). The only exception was a decrease in PNf as compared to PBS (Figure 4.3).

4.4.4 Effects of OX-A in the RVLM on cardiorespiratory coupling

Peri-phrenic averaging of the sympathetic nerve activity reveals an inspiratory (I) and post-inspiratory (PI) peak of sSNA (Figure 4.4A). The AUC of both I and PI peaks of sSNA was significantly increased by bilateral injection of 50 pmol OX-A (I peak: 45 ± 9%, *P* <0.05; PI peak: 41 ± 9%; *P* <0.05; n=4, Figure 4.4B) compared with injection of PBS.

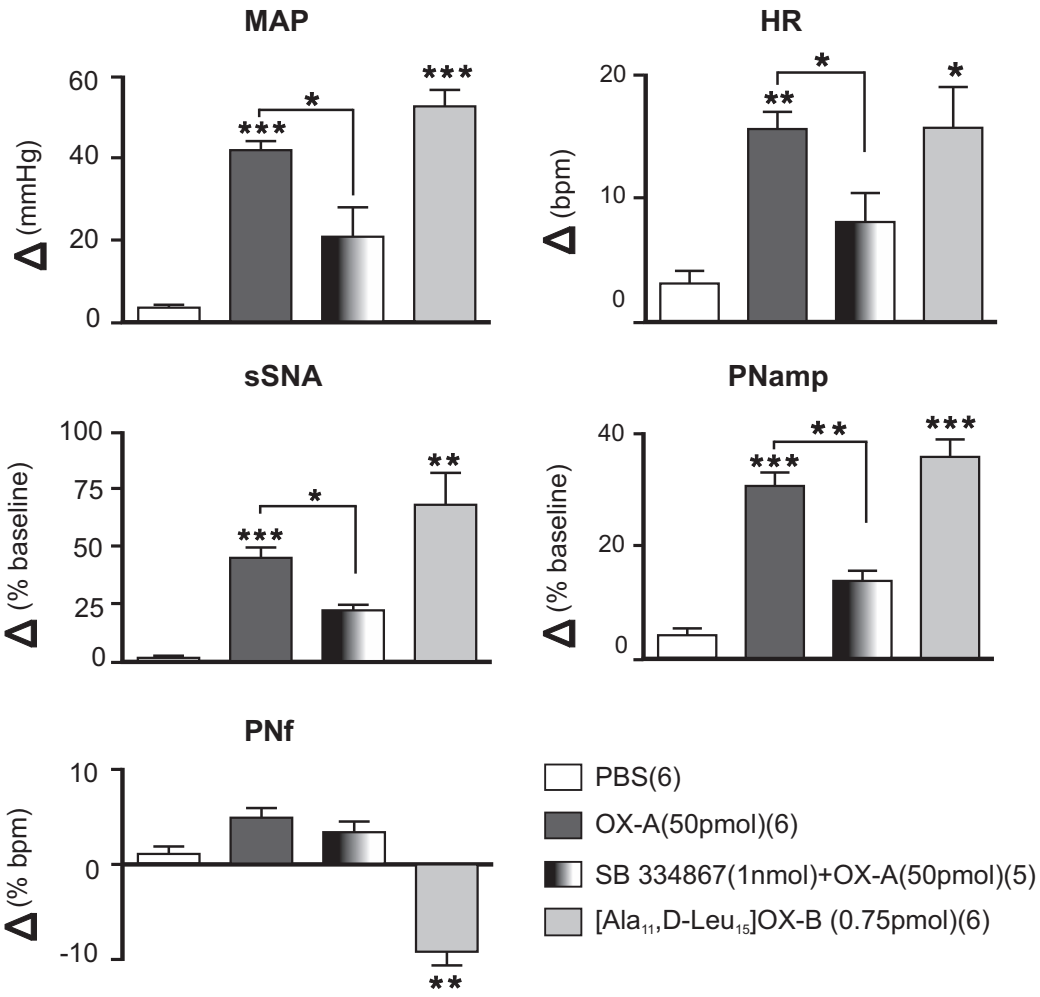

Figure 4.3. Effects of SB 334867 and [Ala11, D-Leu15]OX-B on orexin A (OX-A) induced cardiorespiratory effects in the RVLM.

Bar charts showing group data of maximum cardiovascular and respiratory effects following injection of PBS, OX-A (50 pmol), SB 334867 (1 nmol + OX-A (50 pmol)) or [Ala11, D-Leu15]OX-B (0.75 pmol). Peak effects are shown as absolute (mean arterial pressure (MAP), HR, PNf) or percentage (sSNA, PNamp) change from respective basal values. Data are expressed as mean ± SE. Number of animals are shown in parentheses. *** $P < 0.001$, ** $P < 0.01$, * $P < 0.05$ compared with PBS (except SB 334867 (1 nmol + OX-A (50 pmol)), which was compared with OX-A (50 pmol)). bpm, beats per minute for HR or bursts per minute for PNf.

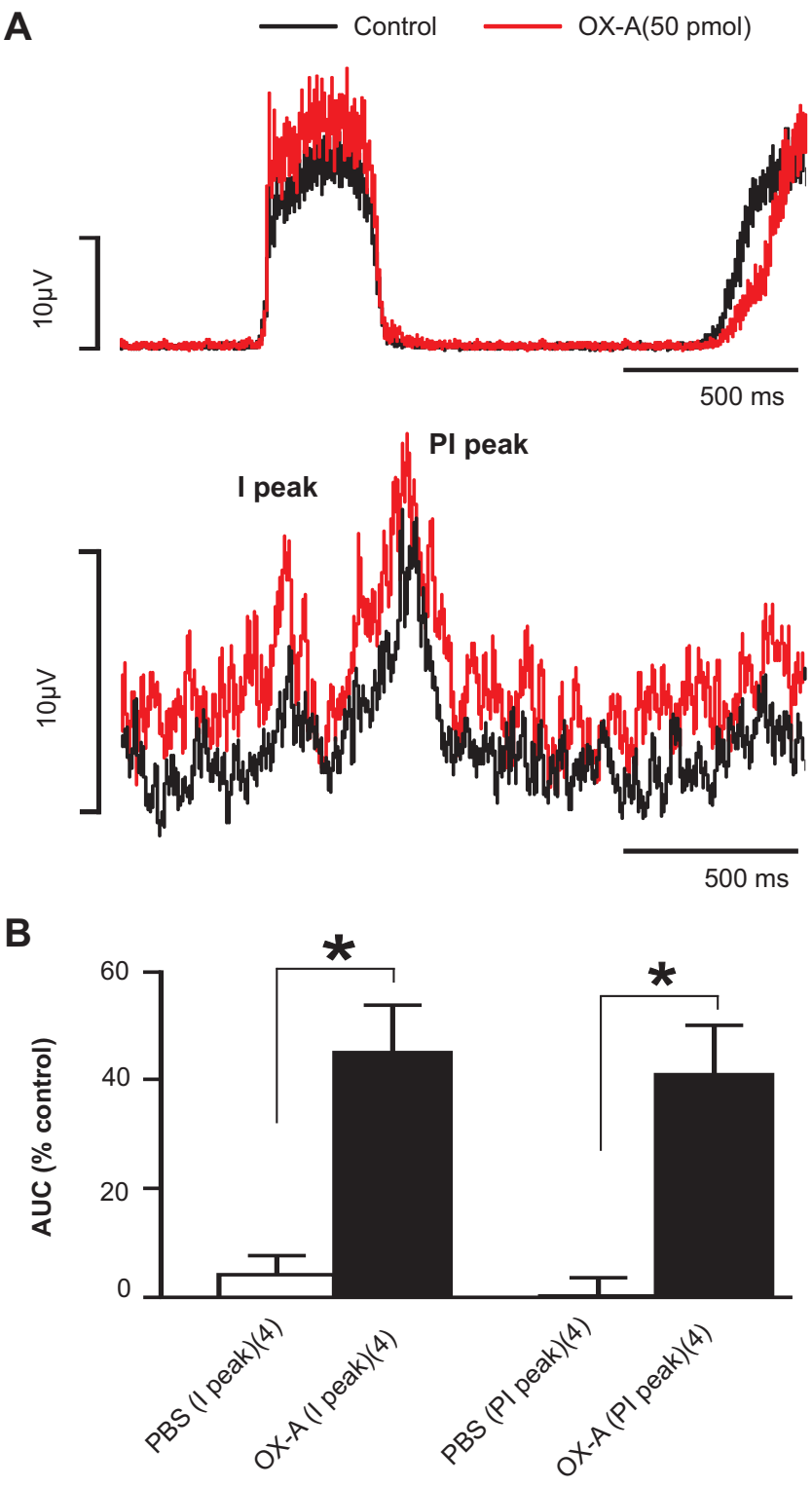

Figure 4.4. Effect of orexin A (OX-A) on phrenic nerve discharge-related rhythmicity of splanchnic sympathetic nerve activity (sSNA) in the rostral ventrolateral medulla.

A: Phrenic-triggered average of sSNA before (grey) and after (black) bilateral OX-A (50 pmol, each side) injection. **B**: Grouped data illustrating the effects of phosphate buffered saline (PBS) or OX-A (50 pmol, n=4) on inspiratory (I) and post-inspiratory (PI) peaks of sSNA. Values are expressed as mean ± SE. * $P < 0.05$ compared with PBS. Both PBS and OX-A values were normalised to the control period prior to injections.

4.4.5 Effects of OX-A in the RVLM on somatosympathetic reflex

Intermittent stimulation of the sciatic nerve resulted in two characteristic excitatory peaks in sSNA with latencies of 84 ± 6 ms and 186 ± 7 ms prior to microinjection (n = 5, Figure 4.5A). The latencies of the peaks were not significantly altered by PBS (89 ± 5 ms and 190 ± 7 ms, n = 5, ns), or by OX-A (88 ± 5 ms and 189 ± 8 ms, n = 5, ns), injection. Bilateral OX-A injection (50 pmol per side) in the RVLM markedly attenuated the AUC of both excitatory peaks by 32% (68 ± 6% and 68 ± 5%, respectively; *P* <0.01) of baseline (n = 5, Figure 4.5B).

4.4.6 Effects of OX-A in the RVLM on baroreflex

In five animals, the changes in sSNA were plotted against the changes in MAP evoked by intravenous injection of SNP and PE. Bilateral RVLM microinjection of OX-A (50 pmol per side) significantly enhanced the reflex sympathoinhibitory responses evoked by PE (Figure 4.6A). OX-A significantly increased the upper plateau, range of sSNA, operating range and maximum gain of the sSNA without significantly altering the lower plateau, the threshold level, midpoint and the saturation levels of MAP as compared to control (Figure 4.6B, Table 4.1).

Table 4.1. Parameters describing baroreflex control of sSNA after bilateral microinjection of OX-A (50 pmol)

	Lower Plateau (%)	Upper Plateau (%)	Mid Point (mmHg)	Max. Gain (%/mmHg)	Range of SNA (%)	Threshold Level (mmHg)	Saturation Level (mmHg)	Operating Range (mmHg)
Control	24.1± 6.9	93.2 ± 9.1	131.2 ± 3.2	-1.4 ± 0.2	57.3 ± 8.5	93.7 ± 6.5	168.8 ± 5.3	68.3 ± 10.2
OX-A (50 pmol)	26.5± 7.6 (ns)	131.0 ± 4.6 (**)	138.0 ± 3.1 (ns)	-2.1 ± 0.3 (**)	100.4 ± 5.2 (*)	99.3 ± 3.6 (ns)	176.6 ± 7.5 (ns)	104.7 ± 16.2 (ns)

Values are mean ± SE (n = 5). Maximum (Max.) gain is the slope of the sigmoid curve of best fit at the MAP corresponding to steepest part of the curve. ns, non-significant; ** $P < 0.01$, * $P < 0.05$ compared with control.

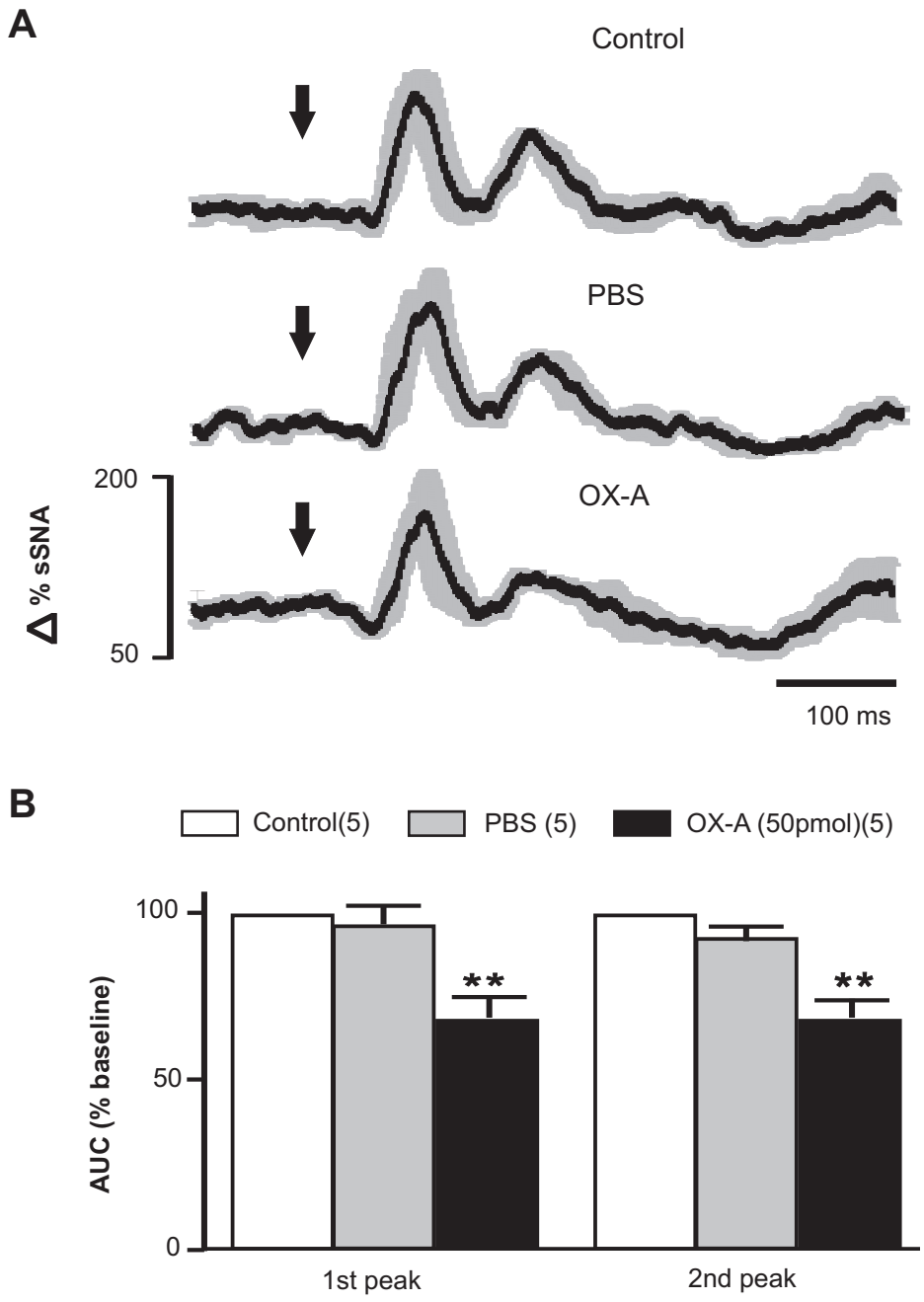

Figure 4.5. Effect of bilateral microinjection of orexin A (OX-A) on somatosympathetic reflex.

A: Grouped effect of sciatic nerve (SN)-evoked stimulation of splanchnic sympathetic nerve activity (sSNA) at control period and after injection of phosphate buffered saline (PBS) and OX-A. Data are mean (black) ± SE (grey). Arrows indicate the time of stimulation. **B**: Group data illustrating the effects of PBS or OX-A (50 pmol, n=5) on the AUC of 1st and 2nd sympathoexcitatory peaks. ** $P < 0.01$, compared with control.

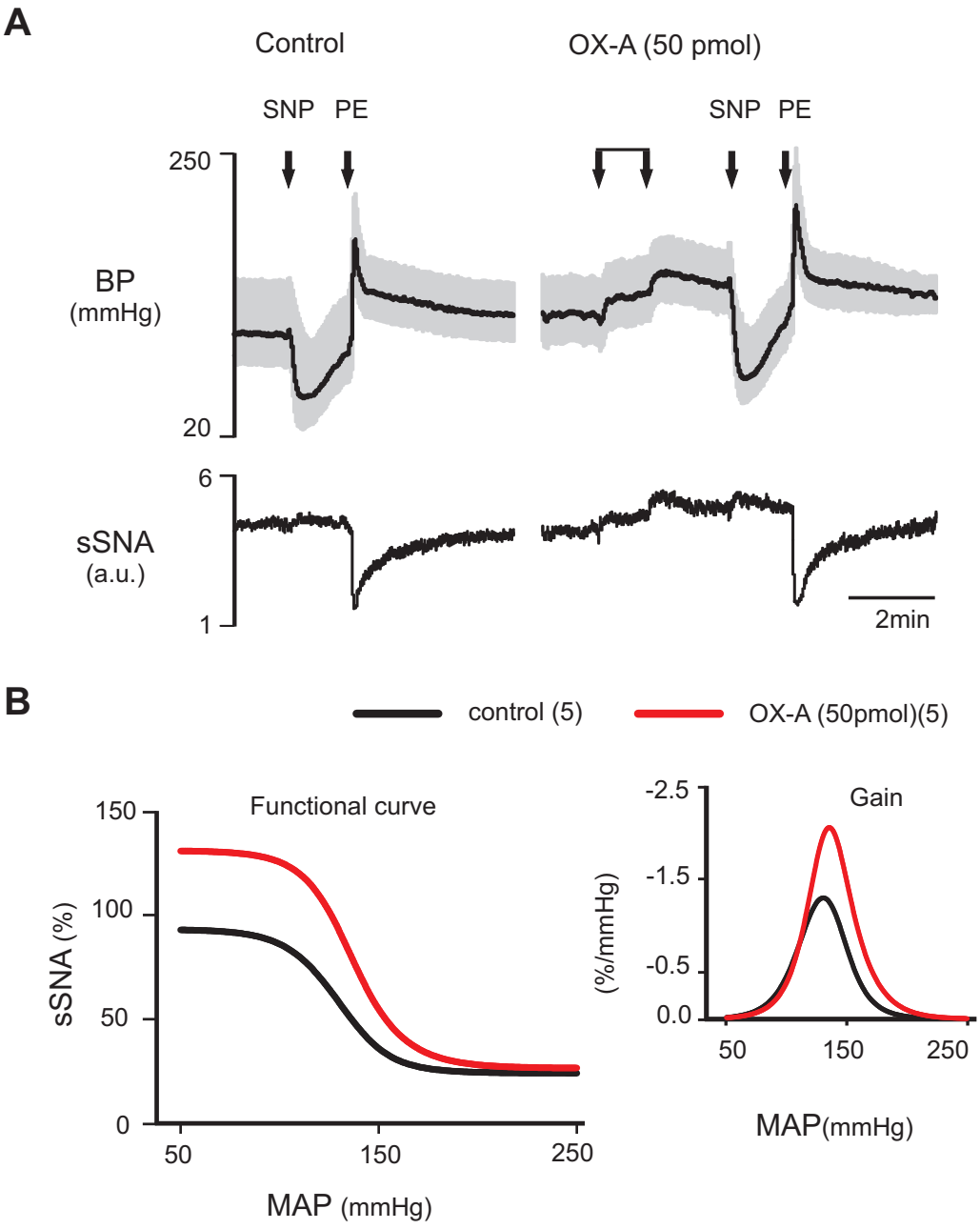

Figure 4.6. Effect of bilateral orexin A (OX-A) injection in the RVLM on the arterial baroreflex evoked by intravenous injection of sodium nitroprusside (SNP) and phenylephrine hydrochloride (PE).

A: Representative experimental recording of the effect of changes in blood pressure (BP) on splanchnic sympathetic nerve activity (sSNA) due to SNP or PE before (control) or after OX-A injection. **B**: Average sympathetic baroreflex function curves generated for data before (control, grey) or after OX-A (black) (50 pmol, n=5) injection. Trace at right represents baroreflex gain for sSNA (error bars are omitted for clarity - see Table 4.1). The range and gain of the reflex are significantly increased.

4.4.7 Effects of OX-A in the RVLM on chemoreflex

Activation of peripheral chemoreceptors with brief hypoxia evoked an increase in MAP, sSNA, HR, PNamp and PNf (Figure 4.7A). Peak effects occurred near the end of stimulus and recovered rapidly to baseline. Bilateral injection of OX-A (50 pmol per side) in the RVLM significantly increased the sympathoexcitatory response by 23% (123 ± 4% of baseline, *P* <0.01) while attenuated the tachycardia by 43% (57 ± 5% of baseline, *P* <0.01) without any significant alteration in the pressor response (n = 4, Figure 4.7B). OX-A caused significant attenuation of peak amplitude of PNamp and peak PNf during hypoxia by 33% and 24%, respectively (peak PNamp: 67 ± 9, *P* <0.05; PNf: 74 ± 2, *P*<0.001; of baseline; n = 4; Figure 4.7B).

Activation of central chemoreceptors with hypercapnia evoked an increase in MAP, sSNA, PNamp and a decrease in HR (Figure 4.7C). OX-A (50 pmol per side) markedly attenuated the effect of hypercapnia on MAP by 143% (-43 ± 12% of baseline, *P* <0.01) and sSNA by 82% (18 ± 11% of baseline, *P* <0.01) without any significant alteration in the bradycardia response (n = 5, Figure 4.7D). The effects of hypercapnia on peak PNamp was also reduced (65 ± 8, *P* <0.05; of baseline) following OX-A (50 pmol per side) injection in the RVLM (n = 5, Figure 4.7D).

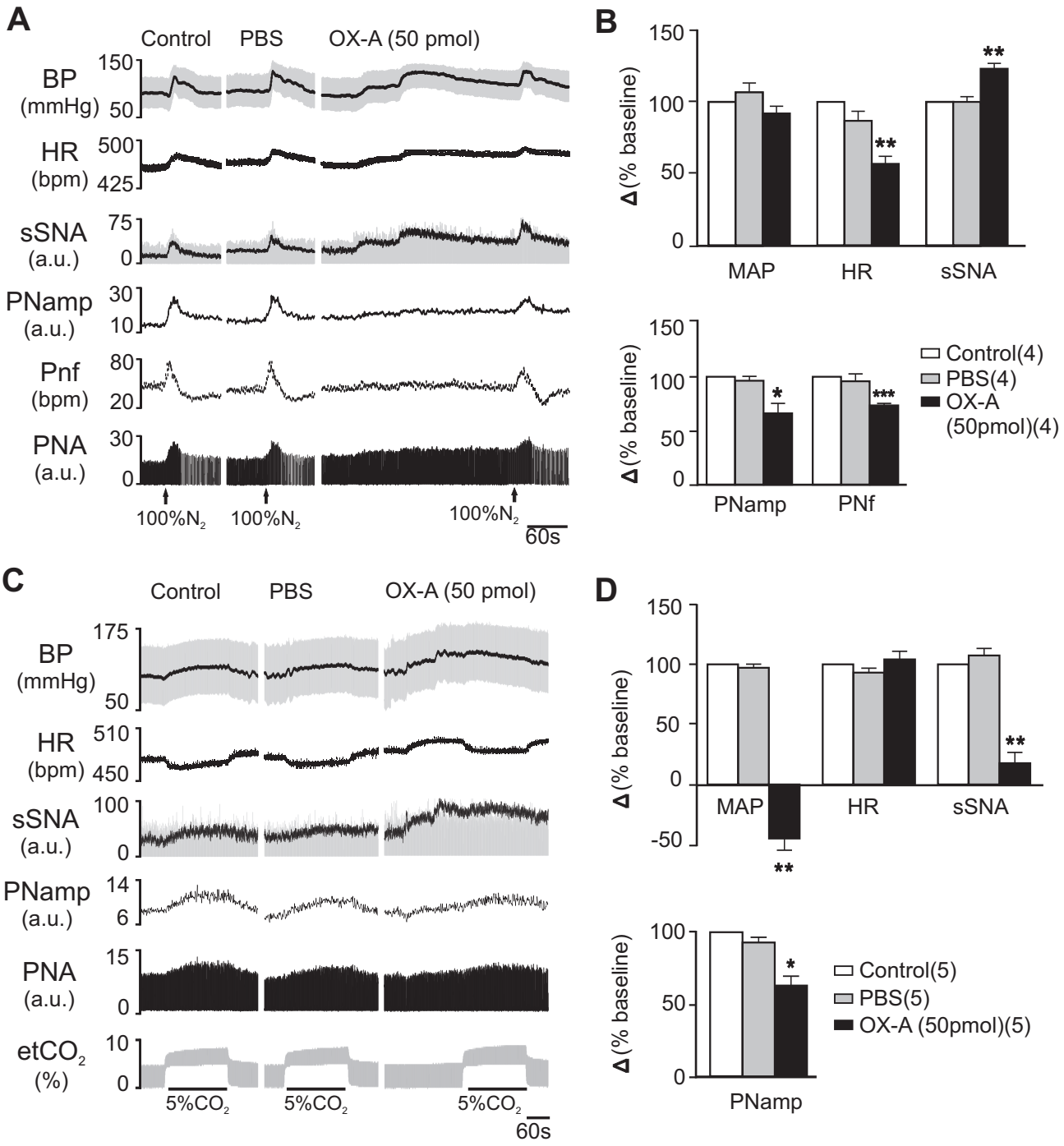

Figure 4.7. Effect of bilateral orexin A (OX-A) injection in RVLM on the cardiovascular and respiratory response to hypoxia and hypercapnia.

A: Effect on the peripheral chemoreceptor reflex activated by brief hypoxia with 100% N2 for 12-14s - experimental recording of hypoxic episodes at control period and after PBS or OX-A injection. **B**: Grouped data of peak effects on cardiovascular (MAP, HR and sSNA) (top bar chart) and respiratory function (PNamp and PNf) (bottom bar chart) after injection of PBS and OX-A (50 pmol, n=4) in response to brief hypoxia. **C**: Effect on central chemoreceptor reflex activated by hypercapnia with 5% CO2 in oxygen for 3min - experimental recording of hypercapnic episodes at control period and after PBS or OX-A injection. **D**: Comparison of peak effects on cardiovascular (MAP, HR and sSNA) and respiratory function (PNamp) after injection of PBS and OX-A (50 pmol, n=5) in response to hypercapnia. Values are expressed as mean ± SE. *** $P < 0.001$, ** $P < 0.01$, * $P < 0.05$ compared with control. bpm, beats per minute for HR or bursts per minute for PNf.

4.5 Discussion

The principal new findings of the present study are 1) OX_1 and OX_2 are expressed in both C1 and non-C1 neurons of the RVLM; 2) Microinjection of OX-A into the RVLM causes sympathoexcitation, hypertension and tachycardia; 3) OX-A microinjection significantly increases PNamp without affecting PNf. 4) The respiratory modulation of sSNA is dramatically increased after microinjection of OX-A; 5) Both OX_1 and OX_2 are involved in the cardiorespiratory responses to OX-A.; 6) Both peaks of somatosympathetic reflex are attenuated by OX-A; 7) Sympathetic baroreflex sensitivity is increased following OX-A microinjection; 8) The sympathoexcitatory response to hypoxia is potentiated, but there is a decrease in the HR, and PNA, response. 9) The cardiovascular and respiratory responses to hypercapnia are attenuated by OX-A.

Both C1 and non-C1 neurons in the RVLM play a role in the tonic and reflex control of sympathetic vasomotor tone (Lipski *et al.*, 1995b; Lipski *et al.*, 1996a; Pilowsky and Goodchild, 2002; Guyenet, 2006; Pilowsky *et al.*, 2009). The results of this study reveal that both OX_1 and OX_2 are expressed in a discrete population of C1 and non-C1 neurons throughout the rostro-caudal pole of the RVLM, some of which may be bulbospinal and barosensitive. This study also demonstrates that varicose OX-A-ir fibres are present in RVLM and are in close proximity to TH-ir neurons, consistent with the findings of Machado *et al*., (2002). The findings suggest $OX_1/_2$R's are activated under physiological or pathological conditions to modulate the activity of cardiorespiratory neurons in RVLM. OX_1 and OX_2 are found throughout the brainstem in regions involved in cardiorespiratory regulation, including: the NTS, RVMM, NA, pre-Bötzinger complex (Trivedi *et al.*, 1998; Marcus *et al.*, 2001; Sunter *et al.*, 2001; Cluderay *et al.*, 2002; Ciriello and de Oliveira, 2003a). The presence of OX_1/2R's within C1 neurons in the rostral 600 µm of the RVLM is consistent with the idea that these receptors are expressed by bulbospinal barosensitive sympathoexcitatory neurons (Brown and Guyenet, 1984; Lipski *et al.*, 1995b; Lipski *et al.*, 1996a; Schreihofer *et al.*, 1997), and that OX-A is involved in regulating sympathetic outflow.

Here we find that the hypertensive and tachycardiac effects of centrally administered OX-A, reported in previous studies (Chen *et al*., 2000; Machado *et al*., 2002), are

likely due to an increase in sympathetic vasomotor tone mediated by the RVLM. In previous studies OX-A microinjection into the RVLM resulted in hypertension and tachycardia for 25-30 min in anaesthetized rat (Chen *et al*., 2000) and for about 7 min in awake rat (Machado *et al*., 2002). We observed a significant sympathetically mediated hypertension and tachycardia after bilateral microinjection of OX-A into the RVLM that last for ~10 min. There were several differences between this study, and earlier work; first, the rats used in this study were vagotomized, second, the rats used here were significantly larger (~280 g vs ~425g) and third, the doses used in this study, based on an initial dose-response study, was higher (~250 µM vs 1 mM). The dose and weight used here was similar to that used in our earlier study of the effects of OX-A in the spinal cord (Shahid *et al*., 2011).

Presympathetic neurons in the RVLM region are close to, and intermingled with, neurons in the Bötzinger region and pre-Bötzinger complex (Kanjhan *et al.*, 1995; Pilowsky *et al.*, 1990; Sun *et al.*, 1994) and receive projections from the respiratory column (Sun *et al.*, 1994.). Here, we find that PNamp is increased following OX-A microinjection into RVLM while PNf remained unchanged. This result agrees with previous studies demonstrating that OX-A in the pre-Bötzinger complex increased amplitude without affecting breathing rate (Young *et al*., 2005). We also observed a LTF of sSNA and PNA in some of the experiments following OX-A microinjection into the RVLM that strengthens previous suggestions for a role for OX-A in LTF in the brain (Mileykovskiy *et al.*, 2002; Terada *et al.*, 2008; Toyama *et al.*, 2009; Walling *et al.*, 2004; Wayner *et al.*, 2004). One possible explanation is that OX-A triggers the release of excitatory neurotransmitters (glutamate or noradrenaline) in the spinal cord, and respiratory column, to cause LTF of SNA and PNA (Shi *et al*., 1988).

RVLM neurons are influenced by central respiratory activity (Guyenet *et al*., 1990; Miyawaki *et al*., 1996a; Pilowsky *et al*., 1996), and sympathetic nerve discharge shows a respiratory rhythmicity in relation to PNA (Adrian *et al*., 1932; Guyenet, 2000). The significant increase in the I- and PI-burst in sSNA, with an increase on baseline activity, following OX receptor activation suggests that they enhance the respiratory-related excitatory synaptic drive to RVLM neurons.

To determine if OX-A is involved in the tonic regulation of neurons in RVLM, and to find out which type of OX receptor mediates the central effects of OX-A, the selective OX_1 antagonist, SB334867 (pK_b OX_1=7.2), and the selective OX_2 (400 times compared with OX_1) agonist, [Ala_{11}, D-Leu_{15}]OX-B, were injected into RVLM. SB334867 itself did not affect baseline cardiorespiratory parameters, suggesting that OX_1 is not constitutively, or tonically, active. SB334867 reduced OX-A induced cardiorespiratory responses by about 50%. Furthermore, [Ala_{11}, D-Leu_{15}]OX-B induced sympathoexcitation, hypertension, tachycardia and increases respiratory drive, in a similar manner to OX-A. Taken together, the results suggest that both OX_1 and OX_2 mediate the central effects of OX-A, confirming previous *in vitro* study (Huang *et al*., 2010). Huang *et al*, (2010) suggested a minor role of OX_1 on OX-A induced depolarization of RVLM neurons in the brainstem slice preparation. This discrepancy may be due to the lower dose of SB334867 used compared to other studies (Deng *et al.*, 2007; Shih and Chuang, 2007), or developmental differences between the neonate and the adult. In this study we also found that activation of OX_2 increases phrenic nerve amplitude, but decreases phrenic nerve frequency. We speculate that activation of orexin receptors decreases the activity of inhibitory Bötzinger neurons, resulting in an increase in phrenic nerve amplitude. This increase in amplitude may be counteracted by a reflex decrease in frequency by the unaffected preBötzinger complex, which controls respiratory rhythm. Further studies will be required to clarify this issue.

In order to maintain cardiovascular homoeostasis, RVLM neurons integrate information from many peripheral afferent neurons, including: somatic receptors, baroreceptors and chemoreceptors (Dampney, 1994; Pilowsky *et al.*, 2009; Sun, 1995). Peptide neurotransmitters modulate the different reflex responses of RVLM neurons via pre- or post- synaptic pathways (Abbott and Pilowsky, 2009; Burke *et al.*, 2008; Kashihara *et al.*, 2008; Makeham *et al.*, 2005; Miyawaki *et al.*, 2002a). The somatosympathetic reflex evoked by sciatic nerve stimulation was significantly attenuated by OX-A microinjection into the RVLM. This result suggests that the attenuation of somatosympathetic reflex was not an indirect effect of raised sympathetic activity following OX-A injection into the RVLM. The mechanism by which OX-A exerts its effect on the somatosympathetic reflex is likely to be complicated, since OX_1 were found to be localised both pre- and post- synaptically.

The reflex responses of sSNA to baroreceptor loading and unloading induced by vasoactive drug administration were markedly enhanced by OX-A microinjection into RVLM. This response is not due to an increase in sSNA following OX-A injection, since PE injection was equally able to reduce sSNA to the same low levels seen in the control situation. Exogenous OX-A increased the upper plateau of the baroreflex curve as well as the maximum gain and operating range, suggesting that OX-A in RVLM regulates baroreflex control of sSNA by increasing disinhibition of RVLM neurons or by activation of barosensitive RVLM neurons.

Neurons in the ventral respiratory column and the RVLM are activated directly, and indirectly, by hypoxia. (De Paula and Branco, 2005; Alheid and McCrimmon, 2008; Sun and Reis, 1994). OX-A microinjection into RVLM enhanced the sympathoexcitatory response to hypoxia while reducing tachycardiac and phrenic responses. Enhanced sympathoexitatory, but reduced tachycardiac effects, suggest that OX-A activates different population of presympathetic RVLM neurons projecting to different levels of the spinal cord. On the other hand, attenuated respiratory responses to hypoxia following OX-A microinjection into RVLM suggest that OX-A may act on inhibitory Bötzinger neurons that project to other respiratory nuclei in the brainstem and spinal cord.

The reflex sympathetic response to hypercapnia is initiated by central chemoreceptors in the RTN, which then activate presympathetic neurons in RVLM (Guyenet, 2000; Guyenet *et al*., 2010). OX-A microinjection in RVLM markedly attenuated cardiorespiratory responses to hypercapnia. It is not known whether chemosensitive RTN neurons make monosynaptic or polysynaptic connection with bulbospinal RVLM neurons. The inhibition of cardiovascular response to hypercapnia suggest the possible activation of GABAergic interneurons in RVLM by OX-A.

Our findings show that OX_1 and OX_2 are present in both C1 and non-C1 neurons in RVLM and activation of OX receptors in RVLM causes sympathetically mediated hypertension, tachycardia and increase in respiratory drive. OX receptor activation in RVLM reduces the somatosympathetic reflex, but increases barosensitivity. Sympathoexcitatory responses to hypoxia and hypercapnia are enhanced and inhibited, respectively, by OX receptors activation in RVLM. OX-A and OX-B play a

key role in the stabilization of wakefulness, and are thought to be arousal-promoting peptides. OX ablated mice have disrupted sleep patterns (Sakurai, 2007). OX neurons are activated just before awakening, remain activated during wakefulness and cease firing during sleep (Kuwaki and Zhang, 2010). Active waking causes increase in HR, MAP, respiration and locomotor activity. However, the neural mechanisms and pathways that mediate the pressor and tachycardic responses to arousal are poorly understood. The presence of OX receptors in C1 bulbospinal sympathoexcitatory neurons of the rostral RVLM and the effects of OX-A in RVLM on basal cardiorespiratory parameters and adaptive reflexes suggests that OX receptor activation plays a key role in mediating the sympathoexcitatory responses to arousal. Finally, the results suggest that drugs affecting central orexinergic pathways may be a useful target for the pharmacological treatment of disorders such as hypertension.

Perspective

Based on the presence of OX receptors in the RVLM and its excitatory effect on cardiorespiratory function in normotensive rat as described in this chapter we hypothesize that OX-A effects in the RVLM are exaggerated in hypertensive rat model and participate in the pathogenesis of hypertension. Thus our next aim is to determine the cardiorespiratory effects of microinjection of OX-A into the RVLM of spontaneously hypertensive rats (SHR) and normotensive Wistar-Kyoto rats (WKY), and to evaluate the effects of OX-A on somatosympathetic, and baroreceptor reflexes in the RVLM.

Chapter 5.

Role of orexin A in rostral ventrolateral medulla in regulation of sympathetic nerve activity and reflexes in wistar-kyoto and spontaneously hypertensive rats

Role of orexin A in rostral ventrolateral medulla in regulation of sympathetic nerve activity and reflexes in wistar-kyoto and spontaneously hypertensive rats

5.1 Abstract

Orexin A (OX-A), located in the central nervous system, plays an important role in sleep-wakefulness, feeding, respiration and energy homeostasis. We demonstrated previously that OX receptor activation in the rostral ventrolateral medulla (RVLM) of normotensive rat increases blood pressure (BP), heart rate, sympathetic nerve activity (SNA) and phrenic nerve activity, and differentially modulates sympathetic reflexes. However, the functional role of OX-A signalling in cardiorespiratory regulation in hypertension, particularly in the RVLM, is unknown. Thus, we investigated whether OX-A signalling in the RVLM is involved in the modulation of cardiorespiratory function, and somatosympathetic and baroreceptor reflexes in urethane anaesthetized, vagotomised and artificially ventilated male spontaneously hypertensive rats (SHR) and Wistar-Kyoto rats (WKY). OX-A injected into the RVLM increased BP, SNA and phrenic nerve amplitude in both hypertensive and normotensive rat models. The pressor, sympathoexcitatory and respiratory responses of OX-A were exaggerated in SHR as compared to WKY. OX-A injection into the RVLM attenuated both the excitatory peaks of somatosympathetic reflex in both SHR and WKY. The extent of attenuation of sympathoexcitatory peaks is greater in SHR as compared to WKY. Baroreflex sensitivity was increased in both SHR and WKY as indicated by an increase in the maximum gain. However, the extent of increase in maximum gain is smaller in SHR as compared to WKY. Our findings indicate that increased OX-A signalling in the RVLM may contribute to the neural mechanisms of hypertension.

Co-contributors: Experiments were conducted by both the candidate and AA Rahman. The analysis was performed, and the manuscript was written by the candidate.

5.2 Introduction

Hypertension is the most common cardiovascular disorder, causing severe target organ damage at many sites including: arteries, brain, heart, and kidneys. (Hennersdorf & Strauer, 2001). Accumulating evidence suggests that over activity of sympathetic nerve activity (SNA) participates in the pathogenesis of hypertension (Judy & Farrell, 1979; Lundin *et al.*, 1984; Cabassi *et al.*, 1998; Guyenet, 2006). Altered SNA in hypertension is associated with an increased sensitivity of RVLM neurons (a key, integrative site within the medulla participating in the tonic and reflex control of blood pressure (BP) and SNA) to excitatory synaptic inputs, increased neuronal firing rates or changes in the regulation of the neurotransmitter noradrenaline (Adams *et al.*, 1989; Cabassi *et al.*, 1998). Moreover, sympathetic baroreflex function is impaired and reset to higher BP leading to change in sympathetic outflow in hypertension (Head, 1995; Esler *et al.*, 2001), and may also contribute to the development and maintenance of the disease. Alterations in the functional state of neuropeptide receptors, along with neurotransmitters, at the level of the RVLM may be involved in the change of afferent and efferent signalling, or integration of information in hypertension (Boone Jr & McMillen, 1994; Kishi *et al.*, 2010). However, the exact role of this altered peptidergic mechanism in the generation or maintenance of hypertension is poorly understood.

Orexin A (OX-A) and orexin B (also known as hypocretin 1 and hypocretin 2) are neuropeptides solely produced by a group of neurons in the hypothalamic region of the brain. From the hypothalamus, OX-A producing cells communicate with many different regions of the brain that are critical for regulating BP and breathing including paraventricular nucleus (PVN), the nucleus tractus solitarius (NTS), RVLM, rostral ventromedial medulla (RVMM), pre-Bötzinger complex, retrotrapezoid nucleus (RTN), dorsal motor nucleus of the vagus, the raphe and spinal cord (de Lecea *et al.*, 1998; Peyron *et al.*, 1998; Date *et al.*, 1999; Nambu *et al.*, 1999; Machado *et al.*, 2002; Ciriello *et al.*, 2003; Young *et al.*, 2005). OX-A is generally excitatory, acting through two G-protein coupled receptors (coupled to $G\alpha_{q/11}$ and/or $G\alpha_{i}$), orexin 1 (OX_1) and orexin 2 (OX_2) receptors (nomenclature follows Alexander *et al.*, 2011). Stimulation of OX receptors activates several intracellular signalling pathways including: adenylate cyclase and phospholipase C, to exert short- and long- term changes on neuronal activity (Smart *et al.*, 1999; Lund *et al.*, 2000; Shahid *et al.*, 2011; Shahid *et al.*,

2012a). Application of OX-A into the central nervous system is known to increase food intake (Sakurai *et al.*, 1998; Dube *et al.*, 1999; Sutcliffe & De Lecea, 2000; Willie *et al.*, 2001).

OX receptors are also widely expressed throughout the brain including thalamus, hypothalamus, and brainstem areas such as the nucleus ambiguus, RVMM, pre-Bötzinger complex, the raphe, NTS and spinal cord (Trivedi *et al.*, 1998; Marcus *et al.*, 2001; Sunter *et al.*, 2001; Cluderay *et al.*, 2002; Ciriello & de Oliveira, 2003). OX-A plays a critical role in the maintenance of sleep and wakefulness (Eggermann *et al.*, 2001; Sakurai *et al.*, 2005), feeding and energy homeostasis (Haynes *et al.*, 2000; Yamada *et al.*, 2000; Rodgers *et al.*, 2001). Recently we have shown that OX_1 and OX_2 receptors are abundantly expressed in the RVLM neurons and frequently colocalize with tyrosine hydroxylase immunoreactive neurons. We have also shown that OX-A, injected into the RVLM and spinal cord, causes persistent increase in BP, splanchnic SNA (sSNA) and breathing. Moreover, OX-A differentially modulates reflex cardiorespiratory responses to high or low BP, hypoxia, hypercapnia and stimulation of somatic nerve (Shahid *et al.*, 2011; Shahid *et al.*, 2012a). But whether the effects of OX-A in the RVLM are altered in hypertensive rat models are unknown.

Based on the anatomic location of OX-A and OX receptors, and on the effects of OX-A on cardiorespiratory parameters and sympathetic reflexes in normotensive animals we hypothesize that OX-A effects in the RVLM are exaggerated in hypertensive rat model and participate in the pathogenesis of hypertension. The objectives of the present study were 1) to determine whether OX-A in the RVLM contributes to the maintenance or elevation of BP in a rat model of hypertension through investigating the cardiorespiratory effects of microinjection of OX-A into the RVLM of spontaneously hypertensive rats (SHR) and normotensive Wistar-Kyoto rats (WKY), and 2) to evaluate the effects of OX-A on somatosympathetic, and baroreceptor reflexes in the RVLM. Our principal findings are that bilateral microinjection of OX-A into the RVLM causes pressor responses, tachycardia and sympathoexcitation in both SHR and WKY. The pressor and sympathoexcitatory effects in SHR are significantly higher than those in WKY. OX-A also increases respiratory drive in both strains and the extent is greater in SHR. OX-A in the RVLM of both SHR and WKY attenuates both the sympathoexcitatory peaks of the somatosympathetic reflex. Baroreflex sensitivity is enhanced following microinjection of OX-A into the RVLM in

SHR and WKY. The findings demonstrate a role for OX-A in the RVLM on the cardiovascular and reflex responses in hypertension.

5.3 Methods

All animal experiments in this study complied with the guidelines of the Australian Code of Practice for the Care and Use of Animals for Scientific Purposes (http: //www.nhmrc.gov.au/guidelines/publications/ea16) and were approved by the Animal Ethics Committee of Macquarie University, Sydney, Australia.

Experiments were performed in 18-20 weeks, age-matched adult male SHR (315-380 g) (n=10) and WKY (355-385 g) (n=10). Rats were anaesthetized with urethane (1.2-1.4 g kg^{-1}, i.p.; supplemental doses of 30-40 mg, i.v. were given when necessary). Animals were prepared as described in detail in chapter 2 (Sections 2.1-2.5).

5.3.1 RVLM microinjection of OX-A

The dorsal medulla was exposed as described in section 2.4.8. Single or multibarrel glass pipettes were used to microinject drugs to the RVLM. L-Glutamate (100 mM, 5 nmol in 50 nl per side) and OX-A (1 mM, 50 pmol in 50 nl per side) were dissolved in phosphate buffered saline (PBS) (10 mM, pH 7.4) and injected bilaterally into the RVLM in all rats. PBS (50 nl per side) was also microinjected as a volume and vehicle control. The RVLM was first functionally identified (section 2.7) on both side by an increase of >30 mmHg in WKY and of >60 mmHg in SHR in mean arterial pressure (MAP) following microinjection of L-glutamate (100 mM, 5 nmol in 50 nl), as determined in previous studies (Abbott & Pilowsky, 2009; Shahid *et al.*, 2012a). All variables were allowed to return to baseline (~30 min) before microinjection of PBS was performed. After a further 30 min, OX-A was microinjected into the same site and observation continued for a further 60 min. At the completion of each experiment, the injection site was marked with rhodamine beads (2% in PBS). Rats were then killed with 0.5 ml of 3 M KCl i.v., the brainstem was removed and placed in fixative (4% formaldehyde in 0.1 M PBS, pH 7.4). Histology was performed to identify injection sites (section 2.7.1).

5.3.2 Activation of sympathetic reflexes

Reflexes were evoked as described in chapter 2 (section 2.8). The cardiorespiratory reflexes that were activated before and after microinjection of OX-A include: (a) somatosympathetic reflex by SN stimulation, and (b) baroreflex by intravenous injection of PE.

5.3.3 Data acquisition and analysis

Data from the experiments was acquired and analysed as described in chapter 2 (section 2.9). All statistical analysis was conducted with GraphPad Prism (version 5.0). Paired t-test was used to analyse peak effects and reflexes. $P < 0.05$ was considered significant in all cases. All values are expressed as means ± SE.

5.4 Results

5.4.1 Cardiorespiratory effects of OX-A injection into the RVLM

Microinjection of OX-A (50 pmol, 50 nl per side) into the RVLM of both WKY and SHR elicited rapid increase in resting MAP, HR and sSNA (Figure 5.1). Although the time course for these cardiovascular changes appears to be similar between strains, OX receptor activation in RVLM of SHR produced a significantly greater increase in both MAP (51 ± 4.9 vs 30 ± 1.0 mmHg, $P < 0.01$) and sSNA (62 ± 10.5 vs 43 ± 6.6 %, $P < 0.05$), but similar increase in HR (21 ± 3.7 vs 20 ± 3.0 bpm) compared with WKY (Figure 5.1).

OX-A microinjected bilaterally into the RVLM also caused a significant increase in phrenic nerve amplitude (PNamp) and the increase was significantly greater in SHR than in WKY (57 ± 5.1 vs 27 ± 5.8 %, $P < 0.05$, Figure 5.2). No significant change in phrenic nerve frequency was observed in either strain (Figure 5.2).

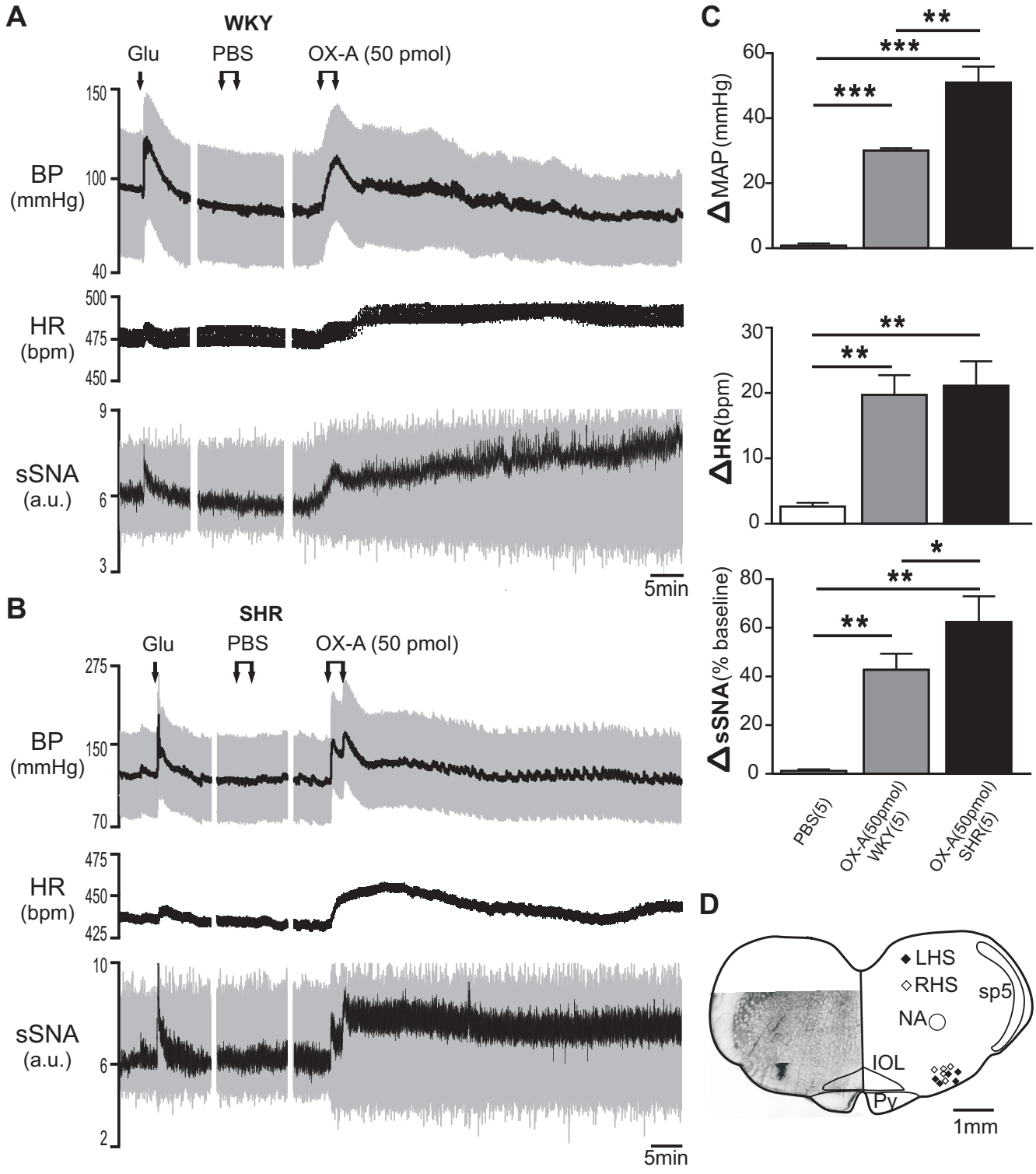

Figure 5.1. Effect of bilateral microinjection of orexin A (OX-A) into the RVLM on cardiovascular function of SHR and WKY.

A, B: Representative recording of blood pressure (BP) (grey – pulsatile and black – mean), heart rate (HR) and splanchnic sympathetic nerve activity (sSNA) (grey – unrectified and black - rectified and integrated) [arbitrary unit (a.u.)] before and after injection of L-glutamic acid (Glu), phosphate buffered saline (PBS) or OX-A (50 pmol) in WKY (A) and SHR (B). **C:** Grouped data of maximum cardiovascular effects following PBS or OX-A. Peak effects are shown as absolute (mean arterial pressure (MAP), HR) or percentage (sSNA) change from respective basal values. **D:** Microinjection sites in the RVLM and a section showing an injection site stained following an injection of rhodamine microbeads. NA: nucleus ambiguus; sp5: spinal trigeminal tract; IOL: inferior olive; Py: pyramidal tract; LHS: left hand side; RHS: right hand side. Data are expressed as mean ± SE. Number of animals are shown in parentheses. *** $P < 0.001$, ** $P < 0.01$, * $P < 0.05$. bpm, beats per minute.

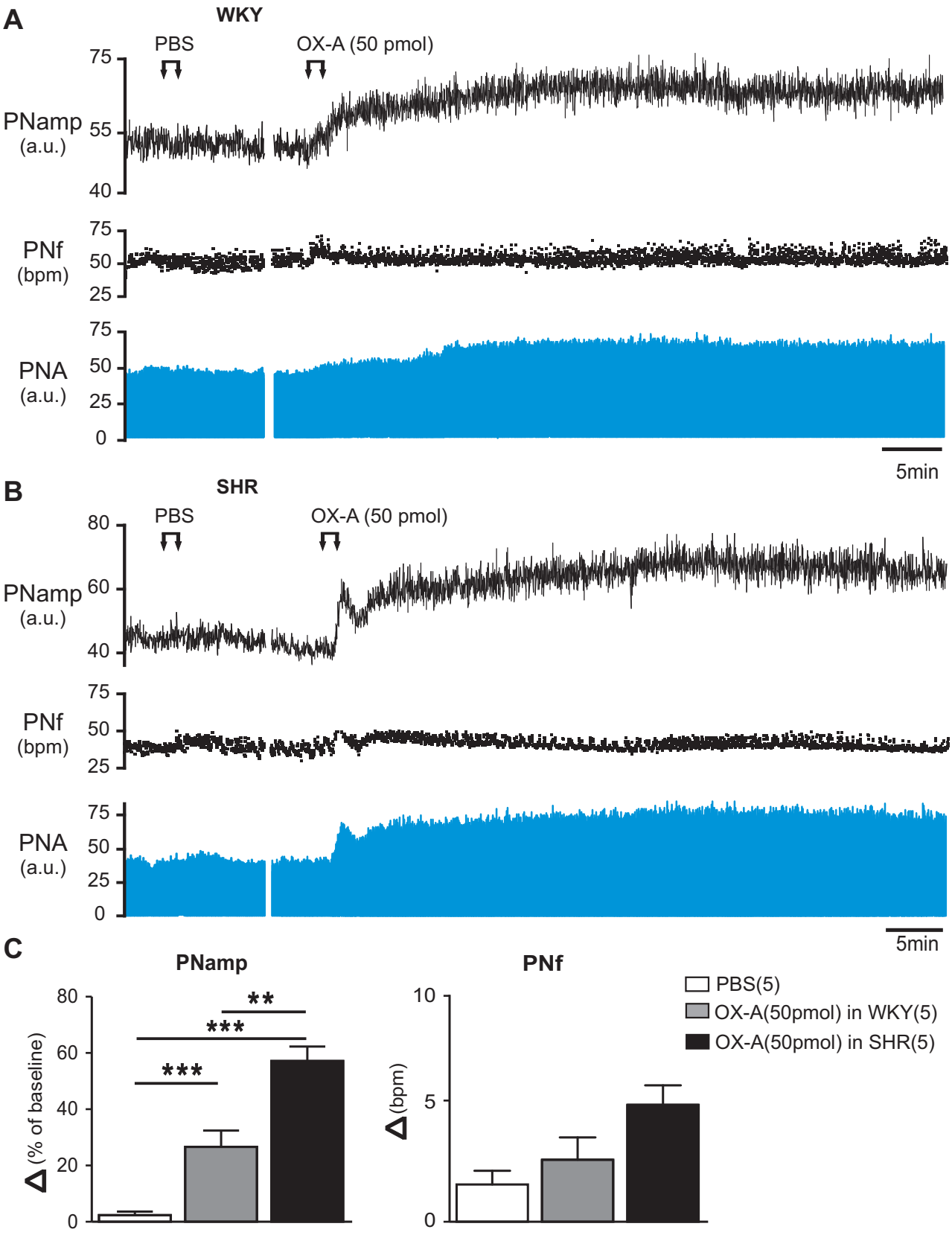

Figure 5.2. Effect of bilateral microinjection of orexin A (OX-A) into the RVLM on respiratory function of SHR and WKY.

A, B: Representative recording of rectified phrenic nerve activity (PNA) [arbitrary unit (a.u.)], phrenic nerve frequency (PNf) and phrenic nerve amplitude (PNamp) before and after injection of phosphate buffered saline (PBS) or OX-A (50 pmol) in WKY (A) and SHR (B). **C:** Grouped data of maximum respiratory effects following PBS or OX-A. Peak effects are shown as absolute (PNf) or percentage (PNamp) change from respective basal values. Data are expressed as mean ± SE. Number of animals are shown in parentheses. *** $P < 0.001$, ** $P < 0.01$. bpm, bursts per minute.

5.4.2 Effects of OX-A injection into the RVLM on splanchnic sympathetic responses to SN stimulation

The response to intermittent SN stimulation was recorded in the sSNA of SHR and WKY. In both strains SN stimulation evoked two distinct peaks in sSNA (latencies: 82 ± 1.2 ms and 160 ± 1.8 ms in WKY; 80 ± 2.6 ms and 153 ± 2.2 ms in SHR). In the control period (pre-injection level) in WKY the first excitatory peak of sSNA was greater than the second peak whereas in SHR both peaks were of almost equal amplitude (Figure 5.3A, B). The AUC of the first peak in SHR was significantly smaller than that in WKY (Figure 5.3B). Bilateral microinjection of OX-A into the RVLM significantly reduced the AUC of both the sympathoexcitatory peaks of sSNA in both SHR and WKY as compared with pre-injection level (Figure 5.3C-F). The extent of decline in the sympathoexcitatory peaks of sSNA in SHR was significantly greater than in WKY (1^{st} peak: 27 ± 5.3 vs 64 ± 3.9 %; 2^{nd} peak: 50 ± 3.4 vs 63 ± 1.5 %; $P < 0.05$; Figure 5.3C-F). No significant change in latency was observed after OX-A injection into the RVLM in either strain (WKY: 79 ± 6.2 ms and 155 ± 1.1 ms; SHR: 82 ± 2.8 ms and 152 ± 2.7 ms; Figure 5.3 A, C, E).

5.4.3 Effects of OX-A injection into the RVLM on sSNA barosensitivity

A partial sSNA baroreflex curve was generated in response to baroreceptor loading by PE in both SHR and WKY. At control period, baroreflex sensitivity is reduced in SHR as indicated by attenuation of maximum gain as compared to WKY. In both strains, bilateral microinjection of OX-A into the RVLM significantly increased maximum gain as compared to control, thereby suggesting an increase in barosensitivity (Figure 5.4, Tables 5.1, 5.2). The increase in maximum gain in SHR was significantly smaller than that in WKY (Figure 5.4E). OX-A also caused a significant increase in upper plateau, range of sSNA and the threshold level of MAP in SHR; whereas increased range of sSNA and the saturation level of MAP in WKY as compared to control (Tables 5.1, 5.2).

Table 5.1. Parameters describing baroreflex control of sSNA after bilateral microinjection of OX-A (50 pmol) in the RVLM of SHR

	Lower Plateau (%)	Upper Plateau (%)	Mid Point (mmHg)	Max. Gain (%/mmHg)	Range of SNA (%)	Threshold Level (mmHg)	Saturation Level (mmHg)	Operating Range (mmHg)
Control	14.5 ± 4.8	108.6 ± 6.4	160.1 ± 8.9	-1.1 ± 0.1	103.6 ± 9.1	87.7 ± 13.1	232.5 ± 11.6	144.8 ± 17.1
OX-A (50 pmol)	14.3 ± 4.2 (ns)	144.0 ± 13.6 (*)	169.5 ± 7.6 (ns)	-1.7 ± 0.2 (*)	150 ± 21.3 (*)	107.1 ± 10.7 (*)	231.9 ± 7.5 (ns)	124.8 ± 10.6 (ns)

Values are mean ± SE (n = 4). Maximum (Max.) gain is the slope of the sigmoid curve of best fit at the MAP corresponding to steepest part of the curve. ns, non-significant; * $P < 0.05$ compared with control.

Table 5.2. Parameters describing baroreflex control of sSNA after bilateral microinjection of OX-A (50 pmol) in the RVLM of WKY

	Lower Plateau (%)	Upper Plateau (%)	Mid Point (mmHg)	Max. Gain (%/mmHg)	Range of SNA (%)	Threshold Level (mmHg)	Saturation Level (mmHg)	Operating Range (mmHg)
Control	32.7 ± 5.2	100.2 ± 2.1	123.2 ± 5.9	-1.8 ± 0.1	68.1 ± 7.3	92.7 ± 6.6	156.7 ± 5.6	57.3 ± 4.8
OX-A (50 pmol)	31.1 ± 3.5 (ns)	107.1 ± 7.0 (ns)	130.9 ± 9.9 (ns)	-2.7 ± 0.2 (*)	87.2 ± 7.2 (*)	105.2 ± 11.8 (ns)	165.7 ± 4.4 (*)	62.5 ± 8.1 (ns)

Values are mean ± SE (n = 4). Maximum (Max.) gain is the slope of the sigmoid curve of best fit at the MAP corresponding to steepest part of the curve. ns, non-significant; * $P < 0.05$ compared with control.

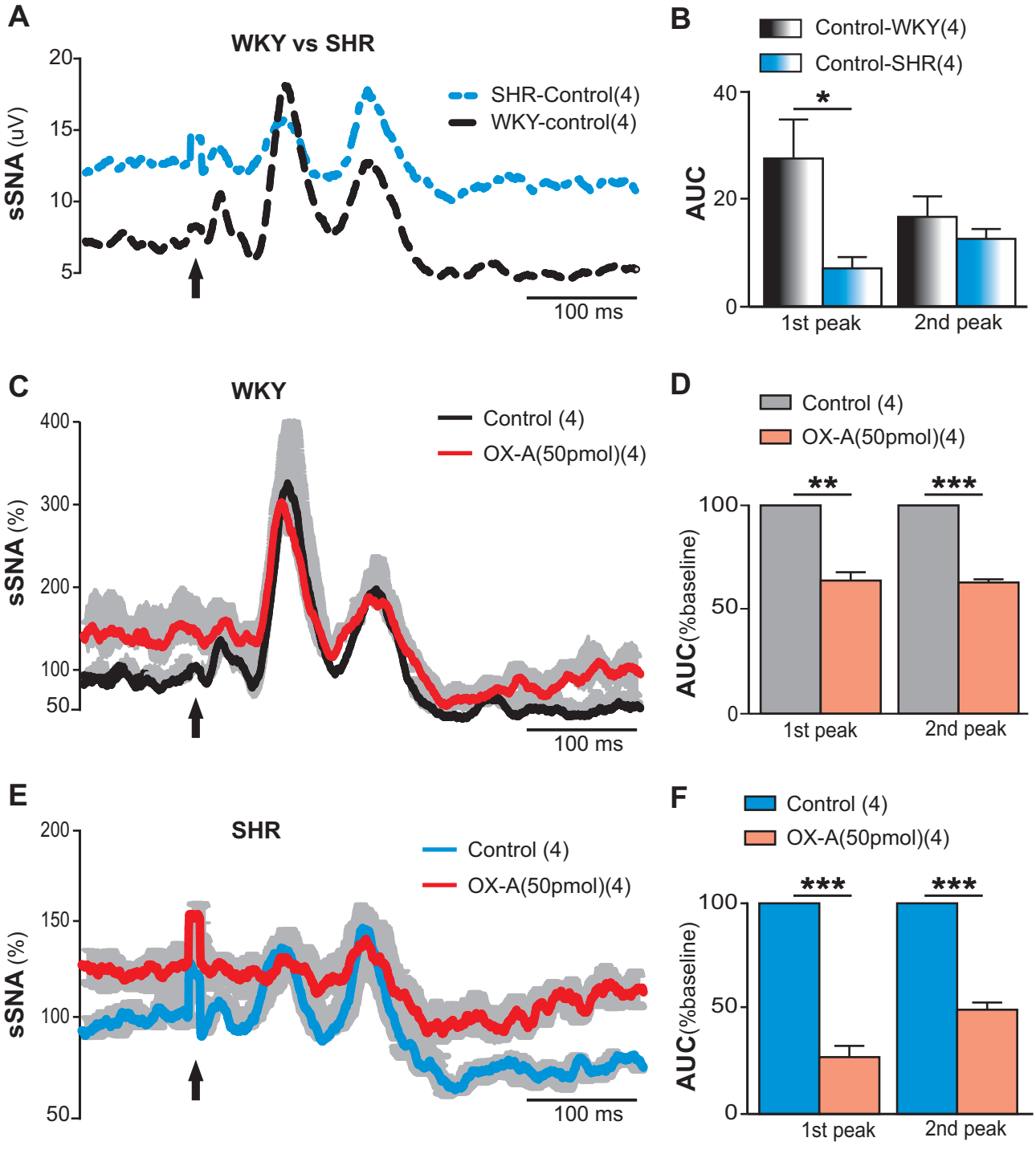

Figure 5.3. Effect of bilateral microinjection of orexin A (OX-A) on somatosympathetic reflex in SHR and WKY.

A: Grouped effect of sciatic nerve (SN)-evoked stimulation of splanchnic sympathetic nerve activity (sSNA) (μV) at control period in SHR and WKY. **C, E:** Grouped effect of SN-evoked stimulation of sSNA (%) at control period and after injection of OX-A in WKY (C) and SHR (E). Error bars are omitted for clarity. Arrows indicate the time of stimulation. **B:** Grouped data comparing the AUC of 1st and 2nd sympathoexcitatory peaks between WKY and SHR during control (pre-drug administration) period. **D, F:** Grouped data illustrating the effects of OX-A (50 pmol, n = 4 for each strain) on the AUC of 1st and 2nd sympathoexcitatory peaks in WKY (D) and SHR (F). ** $P < 0.001$, ** $P < 0.01$, * $P < 0.05$.

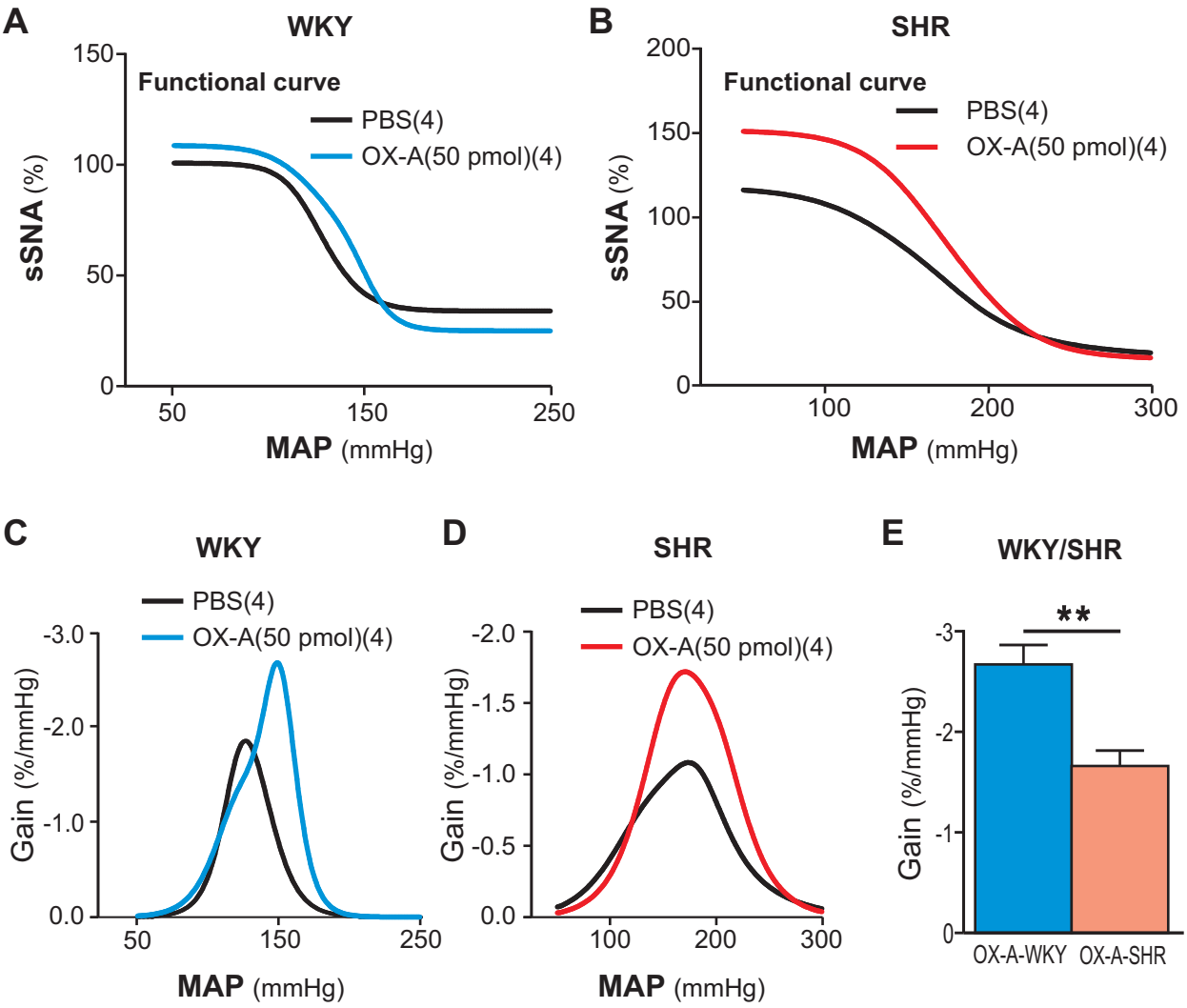

Figure 5.4. Effect of bilateral microinjection of orexin A (OX-A) in the RVLM on arterial baroreflex in SHR and WKY.

A, B: Average splanchnic sympathetic baroreflex function curves generated for data before (control) or after OX-A (50 pmol, n = 4 for each strain) injection in SHR (A) and WKY (B). **C, D**: Baroreflex gain for sSNA (error bars are omitted for clarity - see Table 5.1 for SHR and Table 5.2 for WKY). **E**: Comparison of the effect of OX-A on the baroreflex gain in WKY and SHR. Data are expressed as mean ± SE. Number of animals are shown in parentheses. ** $P < 0.01$.

5.5 Discussion

The findings of the present study demonstrate for the first time that, i) OX-A microinjected bilaterally into the RVLM evokes a pressor response, tachycardia and sympathoexcitation in both hypertensive and normotensive rats; ii) OX-A injection into the RVLM also increases respiratory drive; iii) Somatosympathetic reflex is attenuated after OX-A injection into the RVLM of both strains and the extent of attenuation is greater in SHR as compared with WKY; iv) OX-A injection into the RVLM causes a significant increase in the barosensitivity in both SHR and WKY, but the extent of the increase is smaller in SHR than in WKY.

It is now well established that altered RVLM function and elevated SNA are implicated in the pathogenesis of hypertension in several hypertensive animal models (Esler, 2000; Mancia *et al.*, 2000; Colombari *et al.*, 2001; de Wardener, 2001). OX-A fibres are distributed throughout the medulla oblongata including the RVLM (Machado *et al.*, 2002; Shahid *et al.*, 2012a). Recently we reported that OX_1 and OX_2 receptors are abundantly expressed in catecholaminergic as well as non-catecholaminergic neurons in the RVLM of Sprague-Dawley (SD) rats. We have also shown that OX-A injected bilaterally into the RVLM elicits pressor, tachycardiac and sympathoexcitatory responses, attenuates the somatosympathetic reflex, and increases sympathetic barosensitivity in SD rats (Shahid *et al.*, 2012a). Here we report for the first time that bilateral microinjection of OX-A into the RVLM significantly increases MAP, HR and sSNA in both SHR and WKY, and the pressor and sympathoexcitatory response in SHR is greater than that in WKY. Plausible explanations for the exaggerated effects in SHR are that; i) one or both OX receptors are over-expressed in the RVLM; or ii) the OX receptors become more sensitive; or iii) the 2^{nd} messenger system become more activated, in hypertensive rats. Thus additional experiments will be necessary to reveal the role of OX receptors as well as the signalling pathway(s) involved in the excitatory action of OX-A in hypertension. Considerable evidence indicates that increased SNA is a critical mechanism in hypertension, in the development of cardiac and vascular hypertrophy as well as in diabetes and obesity that may lead to cardiovascular diseases (Leenen, 1999; Palatini, 2001; Campese & Krol, 2002; Stas *et al.*, 2004; Rahmouni *et al.*, 2005). Thus, the excitatory effect of OX-A on sympathetic outflow suggest that OX systems

in the RVLM may play a critical role in cardiovascular diseases such as hypertension and heart failure.

As previously noted in SD rats (Shahid *et al.*, 2012a), in anesthetized and vagotomized SHR and WKY, discrete application of OX-A in the RVLM increases respiratory drive as indicated by an increase in PNamp. The respiratory changes start immediately after the microinjection of OX-A into the RVLM suggesting that these effects are not due to the drug diffusion to other respiratory (ventral respiratory column) regions of the brainstem. Cardiovascular and respiratory (Bötzinger and pre-Bötzinger) neurons are intermingled in the RVLM (Pilowsky *et al.*, 1990; Kanjhan *et al.*, 1995). RVLM neurons also receive synaptic input from respiratory neurons (Pilowsky *et al.*, 1994; Sun *et al.*, 1994) suggesting a possible interaction between the two systems (Haselton & Guyenet, 1989; Pilowsky, 1995) and a possible explanation for the effects of OX-A on respiration observed in this study. The respiratory changes observed in SD, SHR and WKY following OX-A injection into the RVLM clearly indicate a role of OX-A on respiration. Furthermore, the increase in PNamp in SHR is greater than in WKY that suggest a change in the interaction between the cardiovascular and respiratory neurons at the level of RVLM modulated by OX-A. However the exact mechanism for this exaggerated effect is yet to be revealed.

Afferent signal due to stimulation of somatic (sciatic) nerve is suggested to contribute in the formation of background (spontaneous) activity of sympathetic nerves (Shcherbin & Tsyrlin, 2004). Medulla oblongata, RVLM in particular, is a key site for the integration of afferent information with efferent sympathetic discharge (Sun, 1995). Stimulation of SN evokes two excitatory peaks in sSNA in both hypertensive and normotensive rat model. An interesting finding of this study is that the 1st sympathoexcitatory peak in the control period is significantly lower in SHR compared with WKY. We demonstrated for the first time that direct injection of OX-A into the RVLM causes a significant attenuation of the sympathoexcitatory peaks of the somatosympathetic reflex in both SHR and WKY; consistent with our previous observation in SD rats (Shahid *et al.*, 2012a). Furthermore, the extent of attenuation of both peaks is smaller in SHR than in WKY. The increased baseline value of sSNA in SHR compared with WKY, the further increase in sSNA after OX-A injection and the possibility of saturation of the excitability of sSNA cannot be excluded as the

reasons for this reduction in the sympathoexcitatory peaks in SHR. However, the exact mechanism for the effects observed here is not clear, and is yet to be resolved.

The sympathetic baroreflex plays a crucial role in the regulation of cardiovascular function by buffering BP changes through regulation of sympathetic and parasympathetic activity. Baroreflex sensitivity is reduced or impaired in hypertensive animal models and thus is involved in the development and maintenance of hypertension (Gonzalez *et al.*, 1983; Widdop *et al.*, 1990; Head & Adams, 1992). RVLM plays a key role in the integration of afferent and efferent signals of sympathetic reflexes including baroreceptor loading and unloading. Consistent with previous studies (Hayward *et al.*, 2002; Huang *et al.*, 2006), our findings here demonstrate that the resting MAP and sSNA are higher, but that barosensitivity is blunted in SHR before experimental intervention as compared to WKY. In SD rats, centrally administered OX-A (into the RVLM and spinal cord) increased sympathetic outflow and baroreflex sensitivity (Shahid *et al.*, 2011; Shahid *et al.*, 2012a). Here we show that OX-A injected bilaterally into the RVLM elicits a significant increase in sympathetic barosensitivity as indicated by an increase in the maximum gain in both hypertensive and normotensive rats compared with control. However, the magnitude of increase in maximum gain in SHR is smaller than in WKY after OX-A injection. The exact mechanism behind the role of OX-A in the attenuation of barosensitivity in SHR is not clear. The possible explanation is that OX-A participates in the alteration of afferent or efferent signalling, or of integrating baroreceptor information within the RVLM in hypertensive animal model.

In conclusion, our findings indicate that OX signalling in the RVLM exerts pressor response, tachycardia, sympathoexcitation, and increases respiratory drive in both hypertensive and normotensive rats. Furthermore, activation of OX receptors in the RVLM attenuates the somatosympathetic reflex but increases barosensitivity in both strains. The OX effects in SHR are higher or lower in magnitude as compared to WKY. OX system is crucial to maintain arousal (Sakurai, 2007), and increases feeding (Sakurai *et al.*, 1998; Dube *et al.*, 1999; Sutcliffe & De Lecea, 2000; Willie *et al.*, 2001) that may lead to obesity as well as obesity induced hypertension. Previous studies showed that OX-A injected into the RVLM, RVMM and NTS increases BP and HR (Chen *et al.*, 2000; Machado *et al.*, 2002; Smith *et al.*, 2002; Ciriello *et al.*, 2003; Shih & Chuang, 2007) while reducing them following injection into the nucleus

ambiguous and NTS (Ciriello & de Oliveira, 2003; De Oliveira *et al.*, 2003). OX-A also potentiates or attenuates reflex bradycardia evoked by activation of arterial baroreceptor when injected into the NTS (De Oliveira *et al.*, 2003) or RVMM (Ciriello *et al.*, 2003). All these area receive orexinergic projection from the hypothalamus and express OX receptors. The findings of this study, along with our observation in SD rat and other previous studies, provide strong evidence for the role of OX-A in the central regulation of cardiorespiratory system and sympathetic reflexes as well as in the pathogenesis of hypertension thereby making OX system a potential target for the pharmacological treatment of cardiovascular disorders.

Chapter 6.

General Discussion

OX-A and its receptors are widely distributed throughout the brain including areas associated with cardiorespiratory and reflex control, such as the RVLM, NTS and SPN of spinal cord (Trivedi *et al.*, 1998; Marcus *et al.*, 2001; Cluderay *et al.*, 2002; Peyron *et al.*, 1998; Date *et al.*, 1999; Nambu *et al.*, 1999; Machado *et al.*, 2002). However, very little is known about the functional role of OX-A in the regulation of cardiorespiratory system and sympathetic reflexes in the RVLM and spinal cord.

The aims of this thesis were:

1. To investigate the effects of OX-A in the spinal cord on vasomotor tone and adaptive reflexes (chapter 3).

OX-A containing neurons are restricted to the lateral hypothalamus and perifornical areas. However, orexinergic fibres travel throughout the brain and synapses with neurons expressing OX receptors located in key regions of the neuraxis including the SPN of the entire spinal cord, that are crucial for central regulation of the cardiorespiratory function. The pharmacological experiments described in chapter 3 (Shahid *et al.,* 2011) demonstrate for the first time that exogenous OX-A injected intrathecally causes long lasting increase of splanchnic and phrenic nerves along with previously reported pressor response and tachycardia (Antunes *et al.,* 2000). OX-A also increases post-inspiratory peak of sSNA. The cardiorespiratory responses to OX-A are not abolished but attenuated following pre-injection of SB 334867, a selective OX_1 receptor antagonist, indicating that both OX receptors participate in OX-A mediated response in the spinal cord. The phrenic response to i.t. OX-A precluded the idea of diffusing drug to phrenic motor neuron whereas the cardiovascular response was solely via spinal cord as C8 anaesthesia completely abolished the effects of OX-A on respiration but did not attenuate the effects on MAP and sSNA.

I.t. injection of OX-A at thoracic spinal cord increased barosensitivity and potentiated the pressor and sympathoexcitatory response to hypoxia, but attenuated the somatosympathetic reflex. The spinal cord receives and conveys afferent information of somatosympathetic reflex to higher centres and relays the integrated efferent signals of different reflexes including somatosympathetic, baroreceptor and chemoreceptor reflexes (Coote & Lewis, 1995; Lewis & Coote, 1996; Sun & Reis, 1994; Stornetta *et al*., 1989; Makeham *et al*., 2005) to effector organs. Neurons that are involved in the transmission of afferent or efferent signals of these reflexes, closely appose to OX-A fibres and also express OX receptors indicating that OX-A might be involved in the modulation of these reflexes in the spinal cord. The use of OX receptor antagonists is required to determine whether OX-A is released by neurons in response to the reflex challenges investigated here or whether it is released from neurons that modulate cardiovascular function at the level of the spinal cord but are not directly involved in the expression of these challenges.

In summary, OX-A acts as an excitatory neuropeptide in the spinal cord, consistent with the intracellular signalling cascades linked to its receptors. This work adds to the body of literature concerning the modulatory role of neuropeptides in the spinal cord in autonomic regulation.

2. To determine the expression of OX receptors, and to evaluate the effects of exogenous OX-A on sympathetic outflow and reflexes, in the RVLM (chapter 4).

The RVLM is a key site for cardiovascular homoeostasis that integrates information from the centre and periphery, including: respiration, and baro-, chemo- and somatosympathetic reflex afferent neurons. Neurons in the RVLM receive projection from orexinergic neurons in the hypothalamus (Machado *et al.,* 2002). The anatomical experiments in chapter 4 (Shahid *et al.,* 2012) described for the first time the expression of OX_1 and OX_2 receptors in the RVLM neurons with a focus on the TH-ir neurons. Abundant immunoreactivity for both OX receptors was evident in a discrete population of C1 and non-C1 neurons throughout the rostro-caudal pole of the RVLM. About 80% of TH-ir neurons express OX_1 and OX_2 receptors, whereas around 50% of the OX receptors were found in non-C1 neurons suggesting a role for

OX-A on a variety of actions mediated by both type of neurons in the RVLM. OX-A fibres and terminals were also found frequently in, and closely apposed to TH-ir cell bodies and dendrites, in the RVLM as consistent with previous findings (Machado *et al.,* 2002).

The electrophysiological experiments described in chapter 4 (Shahid *et al.,* 2012) show that bilateral microinjection of OX-A into the RVLM elicited splanchnic sympathoexcitation, pressor response and tachycardia. The cardiovascular effects were associated with an increase in respiratory drive. OX-A induced sympathoexcitation and an increase in PNamp that persists for more than one hour, mimicking the pattern of long term facilitation (LTF) of sSNA and PNA induced by acute intermittent hypoxia (Xing & Pilowsky, 2010) or by i.t. injection of OX-A (Shahid *et al.,* 2011). The evidence that phrenic LTF is reduced in OX neuron ablated mice (Toyama *et al.,* 2010) further strengthens the role of OX-A in LTF in the brain. Another novel finding of this study was an increase in the inspiratory and post-inspiratory burst in sSNA suggesting, at least pharmacologically, that OX-A participates in the coupling of respiratory rhythm and sympathetic nerve discharge.

The cardiorespiratory responses to OX-A in the RVLM were reduced by about 50% following pre-injection of SB 334867. In addition the responses were reproduced by bilateral microinjection of OX_2 receptor agonist, [Ala11, D-Leu15]orexin B. Taken together, the results suggest that OX-A activates both OX_1 and OX_2 receptors in the RVLM, confirming results from a previous *in vitro* study (Huang *et al*., 2010). However, Huang *et al*., (2010) suggested a minor role of OX_1 receptors on OX-A induced depolarization of RVLM neurons in the brainstem slice preparation. The lower dose of SB 334867 used compared with other studies (Deng *et al*., 2007; Shih & Chuang, 2007), or developmental differences between the neonate and the adult animal may explain the observed discrepancy.

The study of this chapter also demonstrates that OX-A attenuated both peaks of somatosympathetic reflex but increased sympathetic baroreflex sensitivity. The sympathoexcitatory response to hypoxia was potentiated, but that to hypercapnia was reduced by OX-A in the RVLM. The respiratory responses to hypoxia and hypercapnia were attenuated by orexin A. The baseline increase in sSNA following

microinjection of OX-A into the RVLM cannot be excluded as a reason for the attenuation of somatosympathetic reflex. Expression of both OX receptors on nerve terminals as well as cell bodies and dendrites suggest that OX-A contributes to the reflex responses by increasing presynaptic neurotransmitter release or by acting on the presympathetic neurons. Further investigation is needed to reveal the exact mechanism behind this effect. Moreover, experiments using OX receptor antagonist are required to determine if OX-A is involved in the regulation of sympathetic reflexes in the RVLM at normal physiology.

These results suggest that OX-A and its receptors play an integral role in the regulation of autonomic nervous system and adaptive reflexes in the RVLM.

3. To investigate whether OX-A signalling in the RVLM is involved in the modulation of cardiorespiratory function, and somatosympathetic and baroreceptor reflexes in hypertensive rat models (chapter 5).

Over-activity of SNA is suggested to contribute in the pathogenesis of hypertension (Judy & Farrell, 1979; Lundin *et al.*, 1984; Cabassi *et al.*, 1998; Guyenet, 2006), and this altered SNA is associated with an increased sensitivity of RVLM neurons to excitatory synaptic inputs, increased neuronal firing rates or changes in the regulation of the neurotransmitter noradrenaline (Adams *et al.*, 1989; Cabassi *et al.*, 1998). Sympathetic baroreflex function is also impaired and reset to higher BP leading to change in sympathetic outflow in hypertension (Head, 1995; Esler *et al.*, 2001), and may contribute to the development and maintenance of the disease. Functional state of neuropeptides and their receptors may also be altered at the level of the RVLM in hypertension (Boone Jr & McMillen, 1994; Kishi *et al.*, 2010).

The findings described in chapter 5, reveal for the first time that OX-A microinjection into the RVLM of both normotensive and hypertensive rats increased BP, sSNA and HR. Increase in phrenic nerve amplitude was also enhanced following OX-A in both SHR and WKY. The higher magnitude of pressor, sympathoexcitatory and respiratory responses of OX-A in SHR as compared to WKY clearly indicates a functional role of OX-A in hypertension.

An interesting finding of chapter 5 is that the first sympathoexcitatory peak of the somatosympathetic reflex in the control period was significantly lower in SHR as compared to WKY. Direct injection of OX-A into the RVLM significantly attenuated both the sympathoexcitatory peaks of the somatosympathetic reflex in both SHR and WKY, as consistent with previous observation in SD rats (chapter 4; Shahid *et al.*, 2012). The extent of attenuation of sympathoexcitatory peaks is smaller in SHR than in WKY. The reduction in the sympathoexcitatory peaks in SHR may be due to increased baseline value of sSNA in SHR compared with WKY with a further increase in sSNA after OX-A injection and the excitability of sSNA is saturated in SHR, although this is entirely speculative. Result of this study also shows that OX-A injected bilaterally into the RVLM caused a significant increase in sympathetic barosensitivity in both strains, but the magnitude of increase in maximum gain in SHR is smaller than in WKY after OX-A injection. The possible explanation behind the reduced barosensitivity in SHR is that OX-A participates in the alteration of afferent or efferent signalling, or of integrating baroreceptor information within the RVLM in hypertensive animal model. However, the exact mechanism for the effects observed here is not clear, and is yet to be resolved.

In summary, OX-A effects are exaggerated and/or attenuated in hypertensive model as compared to normotensive rats suggesting a clear role of OX-A in the central regulation of cardiorespiratory system and sympathetic reflexes in physiology and pathology.

Concluding remarks and future directions

Successful homeostatic regulation requires, *inter alia*, delicate interactions between neuroendocrine systems and central autonomic control pathways. Minor changes in one system will cause feedback changes in others. It is now well established that metabotropic neurotransmitters, including neuropeptides, that act on GPCRs are crucial in the modulation of the regulatory activity of classical neurotransmitters (e.g. glutamate, GABA and glycine) on the autonomic control of cardiorespiratory function and behavioural reflexes. After more than a decade of research, orexin neurons have emerged as a crucial neurophysiological link between energy balance, emotion, reward systems and arousal. An OX receptor antagonist is now used for the

treatment of insomnia. Taken together, the presence of orexinergic fibre and terminals as well as its receptors throughout the brain and spinal cord, and the physiological and pharmacological role played suggest that OX-A can be a key modulator in the central control of cardiorespiratory system (Figure 6.1).

This thesis provides several novel insights into orexinergic system that increases cardiorespiratory outflow and modulates sympathetic reflexes in normotensive as well as hypertensive animal models. Future studies will aim to determine; i) the physiological significance of OX-A in the autonomic control of cardiorespiratory regulation, ii) the circumstances in which OX-A in released onto the neurons in the RVLM and spinal cord, iii) any alteration in the expression of OX receptors or in OX signalling in cardiovascular disorders including hypertension, and iv) pharmacological and physiological importance of OX-A in other brainstem areas crucial for cardiorespiratory regulation. The more precise physiological role of OX in the central cardiorespiratory regulation may further be investigated by using OX or OX receptor knockout animals. Furthermore the long lasting increases observed in sSNA and PNA following administration of OX-A into both the spinal cord and RVLM require further investigation to elucidate the precise mechanism and its role in diseases caused by long term elevation of sympathetic and phrenic nerve such as sleep apnoea, and hypertension.

Obesity and hypertension, two of the most common health problems in the world including Australia, are both associated with elevated SNA. These abnormal states also accompany other cardiorespiratory disorders including sleep apnoea. Orexin neurons are activated, and remain so, in wakefulness. Central administration of OX-A increases feeding that may lead to obesity. BP, HR and breathing are increased during active waking. Previous studies showed functional role of OX-A on BP and HR in different brainstem regions (for review, see Shahid *et al.,* 2012b). This thesis provides a unique insight into the role of OX-A in the regulation of sympathetic outflow, respiratory function and sympathetic reflexes that are altered in hypertensive models. Together, the evidence suggests that OX-A may be one of the important factors linking active waking to elevated BP and respiration as well as in the pathogenesis of hypertension or other respiratory disorder thereby making OX and its receptors a potential target for the pharmacological treatment of cardiorespiratory diseases.

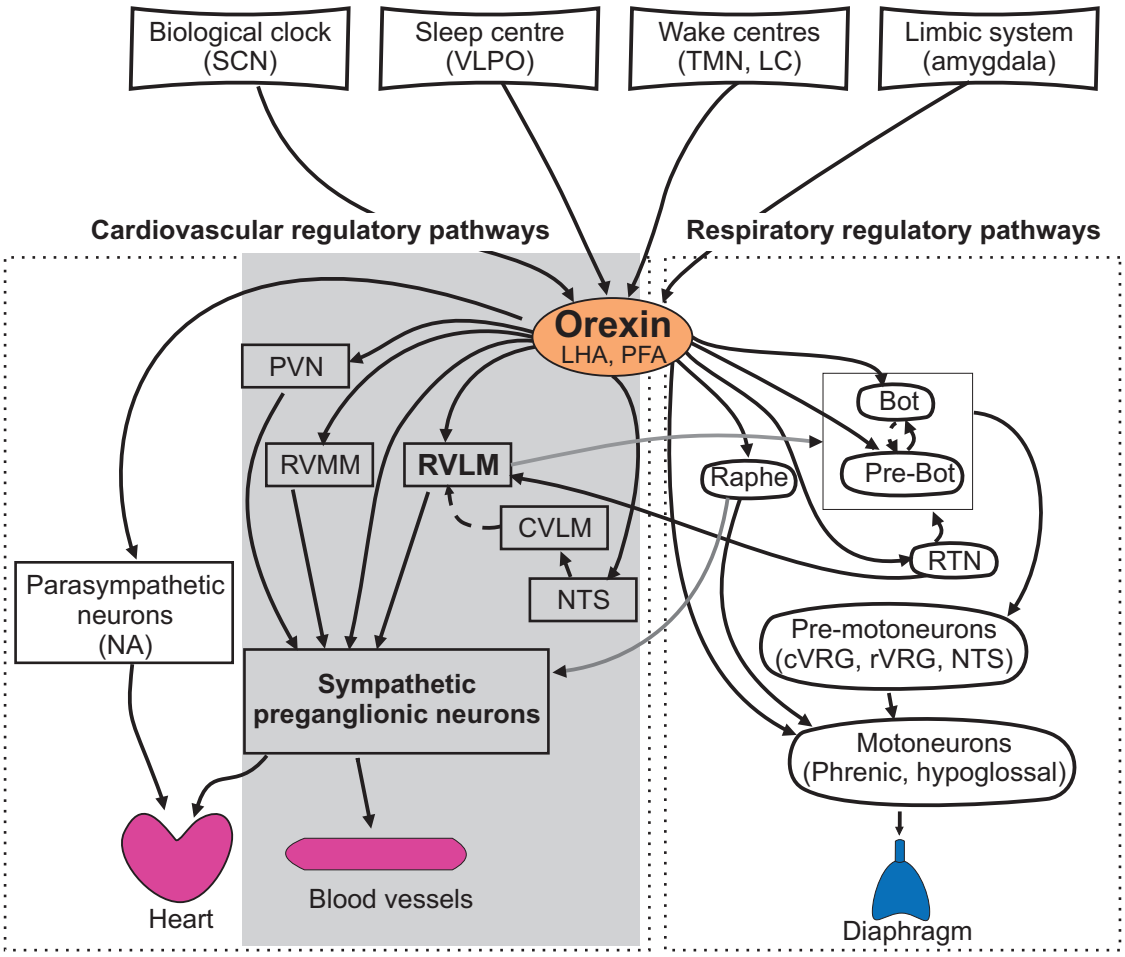

Figure 6.1. Schematic showing role of orexin in the central regulation of cardiovascular and respiratory function.

Orexin neurons receive projections from higher centres (thick lines). Orexin neurons play a complex role in the regulation of the cardiovascular system (left half) via projections to both sympathetic (shaded part) and parasympathetic neurons. Simultaneously orexin neurons project to respiratory regulatory centres (right half). Thus orexin can modulate the cardiorespiratory system in a state-dependent manner. Arows, excitatory projections; broken arrows, inhibitory projections. Bot, Bötzinger region; CVLM, caudal ventrolateral medulla; LC, locus coeruleus; NA, nucleus ambiguus, NTS, nucleus tractus solitarius; Pre-Bot, pre-Bötzinger region; PVN, paraventricular nucleus; RVLM, rostral ventrolateral medulla; RVMM, rostral ventromedial medulla; RTN, retrotrapizoid nucleus; SCN, suprachiasmatic nucleus; TMN, tuberomammillary nucleus; VLPO, ventrolateral preoptic area.

References

Abbott SB & Pilowsky PM. (2009). Galanin microinjection into rostral ventrolateral medulla of the rat is hypotensive and attenuates sympathetic chemoreflex. *Am J Physiol Regul Integr Comp Physiol* **296,** R1019-1026.

Abbott SB, Stornetta RL, Socolovsky CS, West GH & Guyenet PG. (2009a). Photostimulation of channelrhodopsin-2 expressing ventrolateral medullary neurons increases sympathetic nerve activity and blood pressure in rats. *J Physiol* **587,** 5613-5631.

Abbott SBG, Stornetta RL, Fortuna MG, Depuy SD, West GH, Harris TE & Guyenet PG. (2009b). Photostimulation of retrotrapezoid nucleus Phox2b-expressing neurons *in vivo* produces long-lasting activation of breathing in rats. *J Neurosci* **29,** 5806-5819.

Acuna-Goycolea C & van den Pol A. (2004). Glucagon-Like Peptide 1 Excites Hypocretin/Orexin Neurons by Direct and Indirect Mechanisms: Implications for Viscera-Mediated Arousal. *J Neurosci* **24,** 8141-8152.

Adair JR, Hamilton BL & Scappaticci KA. (1977). Cardiovascular responses to electrical stimulation of the medullary raphe area of the cat. *Brain Res* **128,** 141-145.

Adams M, Bobik A & Korner P. (1989). Differential development of vascular and cardiac hypertrophy in genetic hypertension. Relation to sympathetic function. *Hypertension* **14,** 191-202.

Adrian ED, Bronk DW & Phillips G. (1932). Discharges in mammalian sympathetic nerves. *J Physiol* **74,** 115-133.

Ahmad Z, Milligan CJ, Paton JF & Deuchars J. (2003). Angiotensin type 1 receptor immunoreactivity in the thoracic spinal cord. *Brain Res* **985,** 21-31.

Aicher SA, Saravay RH, Cravo S, Jeske I, Morrison SF, Reis DJ & *et al*. (1996). Monosynaptic projections from the nucleus tractus solitarii to C1 adrenergic neurons in the rostral ventrolateral medulla: comparison with input from the caudal ventrolateral medulla. *J Comp Neurol* **373,** 62-75.

Alexander RS. (1946). Tonic and reflex functions of medullary sympathetic cardiovascular centers. *J Neurophysiol* **9,** 205-217.

Alexander SP, Mathie A & Peters JA. (2011). Guide to Receptors and Channels (GRAC), 5th edition. *Br J Pharmacol* **164 Suppl 1,** S1-324.

Alheid GF & McCrimmon DR. (2008). The chemical neuroanatomy of breathing. *Respir Physiol Neurobiol* **164,** 3-11.

Alheid GF, Milsom WK & McCrimmon DR. (2004). Pontine influences on breathing: an overview. *Respir Physiol Neurobiol* **143,** 105-114.

Allen AM. (2002). Inhibition of the hypothalamic paraventricular nucleus in spontaneously hypertensive rats dramatically reduces sympathetic vasomotor tone. *Hypertension* **39,** 275-280.

Allen AM. (2011). Role of angiotensin in the rostral ventrolateral medulla in the development and maintenance of hypertension. *Curr Opin Pharmacol* **11,** 117-123.

Amano M & Kubo T. (1993). Involvement of both GABAA and GABAB receptors in tonic inhibitory control of blood pressure at the rostral ventrolateral medulla of the rat. *Naunyn-Schmiedeberg's Arch pharmacol* **348,** 146-153.

Amendt K, Czachurski J, Dembowsky K & Seller H. (1979). Bulbospinal projections to the intermediolateral cell column; a neuroanatomical study. *J Auton Nerv Syst* **1,** 103-117.

Andersen MB, Krauhs JM & Brown AM. (1978). Relationship of aortic wall and baroreceptor properties during development in normotensive and spontaneously hypertensive rats. *Circ Res* **43,** 728-737.

Anderson CR. (1992). NADPH diaphorase-positive neurons in the rat spinal cord include a subpopulation of autonomic preganglionic neurons. *Neurosci Lett* **139,** 280-284.

Anderson CR. (1998). Identification of cardiovascular pathways in the sympathetic nervous system. *Clin Exp Pharmacol Physiol* **25,** 449-452.

Anderson CR, Edwards SL, Furness JB, Bredt DS & Snyder SH. (1993). The distribution of nitric oxide synthase-containing autonomic preganglionic terminals in the rat. *Brain Res* **614,** 78-85.

Andrade R & Aghajanian GK. (1982). Single cell activity in the noradrenergic A-5 region: Responses to drugs and peripheral manipulations of blood pressure. *Brain Res* **242,** 125-135.

Andresen MC & Yang M. (1989). Arterial baroreceptor resetting: Contributions of chronic and acute processes. *Clin Exp Pharmacol Physiol Suppl* **16,** 19-30.

Andrew D, Krout KE & Craig AD. (2003). Differentiation of lamina I spinomedullary and spinothalamic neurons in the cat. *J Comp Neurol* **458,** 257-271.

Antunes VR, Cristina Brailoiu G, Kwok EH, Scruggs P & Dun ANJ. (2001). Orexins/hypocretins excite rat sympathetic preganglionic neurons in vivo and in vitro. *Am J Physiol* **281,** R1801-1807.

Arihara Z, Takahashi K, Murakami O, Totsune K, Sone M, Satoh F, Ito S, Hayashi Y, Sasano H & Mouri T. (2000). Orexin-A in the human brain and tumor tissues of ganglioneuroblastoma and neuroblastoma. *Peptides* **21,** 565-570.

Arribas SM, Alonso MJ, Marin J, Fernandes F, Llergo JL, Sanchez-Ferrer CF & Salaices M. (1996). Noradrenergic transmission in the tail artery of hypertensive rats transgenic for the mouse renin gene Ren-2. *J Auton Pharmacol* **16,** 69-77.

Bäckberg M, Hervieu G, Wilson S & Meister B. (2002). Orexin receptor-1 (OX-R1) immunoreactivity in chemically identified neurons of the hypothalamus: focus on orexin targets involved in control of food and water intake. *Eur J Neurosci* **15,** 315-328.

Bacon SJ & Smith AD. (1988). Preganglionic sympathetic neurones innervating the rat adrenal medulla: Immunocytochemical evidence of synaptic input from nerve terminals containing substance P, GABA or 5-hydroxytryptamine. *J Auton Nerv Syst* **24,** 97-122.

Bacon SJ, Zagon A & Smith AD. (1990). Electron microscopic evidence of a monosynaptic pathway between cells in the caudal raphé nuclei and sympathetic preganglionic neurons in the rat spinal cord. *Exp Brain Res* **79,** 589-602.

Baekey DM, Dick TE & Paton JF. (2008). Pontomedullary transection attenuates central respiratory modulation of sympathetic discharge, heart rate and the baroreceptor reflex in the in situ rat preparation. *Exp Physiol* **93,** 803-816.

Bago M, Marson L & Dean C. (2002). Serotonergic projections to the rostroventrolateral medulla from midbrain and raphe nuclei. *Brain Res* **945,** 249-258.

Baker-Herman TL & Mitchell GS. (2002). Phrenic long-term facilitation requires spinal serotonin receptor activation and protein synthesis. *J Neurosci* **22,** 6239-6246.

Baldo BA, Gual-Bonilla L, Sijapati K, Daniel RA, Landry CF & Kelley AE. (2004). Activation of a subpopulation of orexin/hypocretin-containing hypothalamic neurons by $GABA_A$ receptor-mediated inhibition of the nucleus accumbens shell, but not by exposure to a novel environment. *Eur J Neurosci* **19,** 376-386.

Barman SM & Gebber GL. (1985). Axonal projection patterns of ventrolateral medullospinal sympathoexcitatory neurons. *J Neurophysiol* **53,** 1551-1566.

Barman SM & Gebber GL. (1989). Lateral tegmental field neurons of cat medulla: A source of basal activity of raphespinal sympathoinhibiory neurons. *J Neurophysiol* **61,** 1011-1024.

Baron R, Janig W & McLachlan EM. (1985). On the anatomical organization of the lumbosacral sympathetic chain and the lumbar splanchnic nerves of the cat--Langley revisited. *J auton nerv syst* **12,** 289-300.

Bazil MK & Gordon FJ. (1993). Sympathoexcitation from the rostral ventrolateral medulla is mediated by spinal NMDA receptors. *Brain Res Bull* **31,** 273-278.

Benarroch EE. (2005). Paraventricular nucleus, stress response, and cardiovascular disease. *Clin Auton Res* **15,** 254-263.

Benarroch EE, Granata AR, Giuliano R & Reis DJ. (1986). Neurons of the C1 area of rostral ventrolateral medulla mediate nucleus tractus solitarii hypertension. *Hypertension* **8,** I-56-60.

Benoliel R, Tanaka M, Caudle RM & Iadarola MJ. (2000). Co-localization of N-methyl-D-aspartate receptors and substance P (neurokinin-1) receptors in rat spinal cord. *Neurosci Lett* **291,** 61-64.

Bernstein-Goral H & Bohn MC. (1989). Phenylethanolamine N-methyltransferase-immunoreactive terminals synapse on adrenal preganglionic neurons in the rat spinal cord. *Neuroscience* **32,** 521-537.

Bessou P, Burgess PR, Perl ER & Taylor CB. (1971). Dynamic properties of mechanoreceptors with unmyelinated (C) fibers. *J Neurophysiol* **34,** 116-131.

Bianchi AL, Denavit-Saubie M & Champagnat J. (1995). Central control of breathing in mammals: neuronal circuitry, membrane properties, and neurotransmitters. *Physiol Rev* **75,** 1-45.

Bingham S, Davey PT, Babbs AJ, Irving EA, Sammons MJ, Wyles M & *al.et*. (2001). Orexin-A, an hypothalamic peptide with analgesic properties. *Pain* **92,** 81-90.

Blanco M, García-Caballero T, Fraga M, Gallego R, Cuevas J, Forteza J, Beiras A & Diéguez C. (2002). Cellular localization of orexin receptors in human adrenal gland, adrenocortical adenomas and pheochromocytomas. *Regul Pept* **104,** 161-165.

Blanco M, López M, García-Caballero T, Gallego R, Vázquez-Boquete A, Morel G, Señarís R, Casanueva F, Diéguez C & Beiras A. (2001). Cellular Localization of Orexin Receptors in Human Pituitary. *J Clin Endocrinol Metab* **86,** 3444-3447.

Blessing WW, Goodchild AK, Dampney RA & Chalmers JP. (1981). Cell groups in the lower brain stem of the rabbit projecting to the spinal cord, with special reference to catecholamine-containing neurons. *Brain Res* **221,** 35-55.

Bogan N, Mennone A & Cabot JB. (1989). Light microscopic and ultrastructural localization of GABA-like immunoreactive input to retrogradely labeled sympathetic preganglionic neurons. *Brain Res* **505,** 257-270.

Boone Jr JB & McMillen D. (1994). Proenkephalin gene expression is altered in the brain of spontaneously hypertensive rats during the development of hypertension. *Brain Res Mol Brain Res* **24,** 320-326.

Borgland SL, Taha SA, Sarti F, Fields HL & Bonci A. (2006). Orexin A in the VTA Is Critical for the Induction of Synaptic Plasticity and Behavioral Sensitization to Cocaine. *Neuron* **49,** 589-601.

Briganti EM, Shaw JE, Chadban SJ, Zimmet PZ, Welborn TA, McNeil JJ & Atkins RC. (2003). Untreated hypertension among Australian adults: The 1999-2000 Australian Diabetes, Obesity and Lifestyle Study (AusDiab). *Med J Aust* **179,** 135-139.

Broberger C, De Lecea L, Sutcliffe JG & Hökfelt T. (1998). Hypocretin/Orexin- and melanin-concentrating hormone-expressing cells form distinct populations in the rodent lateral hypothalamus: Relationship to the neuropeptide Y and agouti gene-related protein systems. *J Comp Neurol* **402,** 460-474.

Brooke RE, Pyner S, McLeish P, Buchan S, Deuchars J & Deuchars SA. (2002). Spinal cord interneurones labelled transneuronally from the adrenal gland by a GFP-herpes virus construct contain the potassium channel subunit Kv3.1b. *Auton Neurosci* **98,** 45-50.

Brown AM. (1980). Receptors under pressure. An update on baroreceptors. *Circulation research* **46,** 1-10.

Brown DL & Guyenet PG. (1984). Cardiovascular neurons of brain stem with projections to spinal cord. *Am J Physiol* **247,** R1009-R1016.

Brown DL & Guyenet PG. (1985). Electrophysiological study of cardiovascular neurons in the rostral ventrolateral medulla in rats. *Circ Res* **56,** 359-369.

Brown RE, Sergeeva OA, Eriksson KS & Haas HL. (2002). Convergent excitation of dorsal raphe serotonin neurons by multiple arousal systems (orexin/hypocretin, histamine and noradrenaline). *J Neurosci* **22,** 8850-8859.

Burdakov D, Gerasimenko O & Verkhratsky A. (2005). Physiological changes in glucose differentially modulate the excitability of hypothalamic melanin-concentrating hormone and orexin neurons in situ. *J Neurosci* **25,** 2429-2433.

Burke PG, Li Q, Costin ML, McMullan S, Pilowsky PM & Goodchild AK. (2008). Somatostatin 2A receptor-expressing presympathetic neurons in the rostral ventrolateral medulla maintain blood pressure. *Hypertension* **52,** 1127-1133.

Burke PGR, Neale J, Korim WS, McMullan S & Goodchild AK. (2011). Patterning of somatosympathetic reflexes reveals nonuniform organization of presympathetic drive from C1 and non-C1 RVLM neurons. *Am J Physiol* **301,** R1112-1122.

Burman KJ, Sartor DM, Verberne AJM & Llewellyn-Smith IJ. (2004). Cocaine- and amphetamine-regulated transcript in catecholamine and noncatecholamine presympathetic vasomotor neurons of rat rostral ventrolateral medulla. *J Comp Neurol* **476,** 19-31.

Byrum CE & Guyenet PG. (1987). Afferent and efferent connections of the A5 noradrenergic cell group in the rat. *J Comp Neurol* **261,** 529-542.

Byrum CE, Stornetta R & Guyenet PG. (1984). Electrophysiological properties of spinally-projecting A5 noradrenergic neurons. *Brain Res* **303,** 15-29.

Cabassi A, Vinci S, Calzolari M, Bruschi G & Borghetti A. (1998). Regional sympathetic activity in pre-hypertensive phase of spontaneously hypertensive rats. *Life Sci* **62,** 1111-1118.

Cabassi A, Vinci S, Cantoni AM, Quartieri F, Moschini L, Cavazzini S, Cavatorta A & Borghetti A. (2002). Sympathetic activation in adipose tissue and skeletal muscle of hypertensive rats. *Hypertension* **39,** 656-661.

Cabot JB, Alessi V & Bushnell A. (1992). Glycine-like immunoreactive input to sympathetic preganglionic neurons. *Brain Res* **571,** 1-18.

Cai XJ, Lister CA, Buckingham RE, Pickavance L, Wilding J, Arch JRS, Wilson S & Williams G. (2000). Down-regulation of orexin gene expression by severe obesity in the rats: studies in Zucker fatty and Zucker diabetic fatty rats and effects of rosiglitazone. *Mol Brain Res* **77,** 131-137.

Cai XJ, Widdowson PS, Harrold J, Wilson S, Buckingham RE, Arch JR, Tadayyon M, Clapham JC, Wilding J & Williams G. (1999). Hypothalamic orexin expression: modulation by blood glucose and feeding. *Diabetes* **48,** 2132-2137.

Campese VM & Krol E. (2002). Neurogenic factors in renal hypertension. *Curr Hypertens Rep* **4,** 256-260.

Cao WH & Morrison SF. (2003). Disinhibition of rostral raphe pallidus neurons increases cardiac sympathetic nerve activity and heart rate. *Brain Res* **980,** 1-10.

Card JP, Rinaman L, Schwaber JS, Miselis RR, Whealy ME, Robbins AK & Enquist LW. (1990). Neurotropic properties of pseudorabies virus: uptake and transneuronal passage in the rat central nervous system. *J Neurosci* **10,** 1974-1994.

Card JP, Sved JC, Craig B, Raizada M, Vazquez J & Sved AF. (2006). Efferent projections of rat rostroventrolateral medulla C1 catecholamine neurons: Implications for the central control of cardiovascular regulation. *J Comp Neurol* **499,** 840-859.

Carretero OA & Oparil S. (2000). Essential hypertension. Part I: Definition and etiology. *Circulation* **101,** 329-335.

Cechetto DF & Saper CB. (1988). Neurochemical organization of the hypothalamic projection to the spinal cord in the rat. *J Comp Neurol* **272,** 579-604.

Chalmers J, Arnolda L, Llewellyn-Smith I, Minson J, Pilowsky P & Suzuki S. (1994). Central neurons and neurotransmitters in the control of blood pressure. *Clin Exp Pharmacol Physiol* **21,** 819-829.

Chamberlin NL. (2004). Functional organization of the parabrachial complex and intertrigeminal region in the control of breathing. *Respir Physiol Neurobiol* **143,** 115-125.

Chan RK, Chan YS & Wong TM. (1991). Electrophysiological properties of neurons in the rostral ventrolateral medulla of normotensive and spontaneously hypertensive rats. *Brain Res* **549,** 118-126.

Chapleau MW, Cunningham JT, Sullivan MJ, Wachtel RE & Abboud FM. (1995). Structural versus functional modulation of the arterial baroreflex. *Hypertension* **26,** 341-347.

Chapleau MW, Li Z, Meyrelles SS, Ma X & Abboud FM. (2001). Mechanisms determining sensitivity of baroreceptor afferents in health and disease. *Ann N Y Acad Sci* **940,** 1-19.

Chen CT, Dun SL, Kwok EH, Dun NJ & Chang JK. (1999). Orexin A-like immunoreactivity in the rat brain. *Neurosci Lett* **260,** 161-164.

Chen CT, Hwang LL, Chang JK & Dun NJ. (2000). Pressor effects of orexins injected intracisternally and to rostral ventrolateral medulla of anesthetized rats. *Am J Physiol* **278,** R692-697.

Chiba T. (1989). Direct synaptic contacts of 5-hydroxytryptamine-, neuropeptide Y-, and somatostatin-immunoreactive nerve terminals on the preganglionic sympathetic neurons of the guinea pig. *Neurosci Lett* **105,** 281-286.

Chiba T & Masuko S. (1986). Direct synaptic contacts of catecholamine axons on the preganglionic sympathetic neurons in the rat thoracic spinal cord. *Brain Res* **380,** 405-408.

Chiba T & Masuko S. (1987). Synaptic structure of the monoamine and peptide nerve terminals in the intermediolateral nucleus of the guinea pig thoracic spinal cord. *J Comp Neurol* **262,** 242-255.

Chiba T & Semba R. (1991). Immuno-electronmicroscopic studies on the gamma-aminobutyric acid and glycine receptor in the intermediolateral nucleus of the thoracic spinal cord of rats and guinea pigs. *J Auton Nerv Syst* **36,** 173-182.

Chiba T, Tanaka K, Tatsuoka H, Dun SL & Dun NJ. (1996). The synaptic structure of PACAP immunoreactive axons in the intermediolateral nucleus of the rat. *Neurosci Lett* **214,** 65-68.

Chitravanshi VC & Sapru HN. (1999). Phrenic nerve responses to chemical stimulation of the subregions of ventral medullary respiratory neuronal group in the rat. *Brain Res* **821,** 443-460.

Chizh BA, Headley PM & Paton JF. (1998). Coupling of sympathetic and somatic motor outflows from the spinal cord in a perfused preparation of adult mouse in vitro. *J Physiol* **508,** 907-918.

Christensen BN & Perl ER. (1970). Spinal neurons specifically excited by noxious or thermal stimuli: marginal zone of the dorsal horn. *Journal of Neurophysiology* **33,** 293-307.

Ciriello J. (1983). Brainstem projections of aortic baroreceptor afferent fibers in the rat. *Neurosci Lett* **36,** 37-42.

Ciriello J & Caverson MM. (1986). Bidirectional cardiovascular connections between ventrolateral medulla and nucleus of the solitary tract. *Brain Res* **367,** 273-281.

Ciriello J, Caverson MM & Calaresu FR. (1985). Lateral hypothalamic and peripheral cardiovascular afferent inputs to ventrolateral medullary neurons. *Brain Res* **347,** 173-176.

Ciriello J & de Oliveira CV. (2003). Cardiac effects of hypocretin-1 in nucleus ambiguus. *Am J Physiol* **284,** R1611-1620.

Ciriello J, Kline RL, Zhang TX & Caverson MM. (1984). Lesions of the paraventricular nucleus alter the development of spontaneous hypertension in the rat. *Brain Res* **310,** 355-359.

Ciriello J, Li Z & De Oliveira CVR. (2003). Cardioacceleratory responses to hypocretin-1 injections into rostral ventromedial medulla. *Brain Res* **991,** 84-95.

Cluderay JE, Harrison DC & Hervieu GJ. (2002). Protein distribution of the orexin-2 receptor in the rat central nervous system. *Regul Pept* **104,** 131-144.

Coles SK & Dick TE. (1996). Neurones in the ventrolateral pons are required for post-hypoxic frequency decline in rats. *J Physiol* **497,** 79-94.

Colombari E, Sato MA, Cravo SL, Bergamaschi CT, Campos Jr RR & Lopes OU. (2001). Role of the medulla oblongata in hypertension. *Hypertension* **38,** 549-554.

Coote JH. (1988). The organisation of cardiovascular neurons in the spinal cord. *Rev Physiol Biochem Pharmacol* **110,** 147-285.

Coote JH. (2005). A role for the paraventricular nucleus of the hypothalamus in the autonomic control of heart and kidney. *Exp Physiol* **90,** 169-173.

Coote JH & Lewis DI. (1995). The spinal organisation of the baroreceptor reflex. *Clin Exp Hypertens* **17,** 295-311.

Coote JH, Yang Z, Pyner S & Deering J. (1998). Control of sympathetic outflows by the hypothalamic paraventricular nucleus. *Clin Exp Pharmacol Physiol* **25,** 461-463.

Corcoran A, Richerson G, Harris M, Homma I, Fukuchi Y & Onimaru H. (2010). Modulation of Respiratory Activity by Hypocretin-1 (Orexin A) In Situ and In Vitro. In *Adv Exp Med Biol* pp. 109-113. Springer New York.

Cowley AW, Jr., Liard JF & Guyton AC. (1973). Role of baroreceptor reflex in daily control of arterial blood pressure and other variables in dogs. *Circ Res* **32,** 564-576.

Craig AD. (2003). Interoception: the sense of the physiological condition of the body. *Current Opinion in Neurobiology* **13,** 500-505.

Cravo SL & Morrison SF. (1993). The caudal ventrolateral medulla is a source of tonic sympathoinhibition. *Brain Res* **621,** 133-136.

Cravo SL, Morrison SF & Reis DJ. (1991). Differentiation of two cardiovascular regions within caudal ventrolateral medulla. *Am J Physiol* **261,** R985-R994.

Cruz JC, Bonagamba LGH, Machado BH, Biancardi VC & Stern JE. (2008). Intermittent activation of peripheral chemoreceptors in awake rats induces Fos expression in rostral ventrolateral medulla-projecting neurons in the paraventricular nucleus of the hypothalamus. *Neuroscience* **157,** 463-472.

Cutler DJ, Morris R, Sheridhar V, Wattam TAK, Holmes S, Patel S, Arch JRS, Wilson S, Buckingham RE, Evans ML, Leslie RA & Williams G. (1999). Differential distribution of orexin-A and orexin-B immunoreactivity in the rat brain and spinal cord. *Peptides* **20,** 1455-1470.

Dampney RA, Goodchild AK & Tan E. (1984). Identification of cardiovascular cell groups in the brain stem. *Clinical and experimental hypertension Part A, Theory and practice* **6,** 205-220.

Dampney RA & Moon EA. (1980). Role of ventrolateral medulla in vasomotor response to cerebral ischemia. *Am J Physiol* **239,** H349-358.

Dampney RAL. (1994). Functional organization of central pathways regulating the cardiovascular system. *Physiol Rev* **74,** 323-364.

Dampney RAL, Czachurski J, Dembowsky K, Goodchild AK & Seller H. (1987). Afferent connections and spinal projections of the pressor region in the rostral ventrolateral medulla of the cat. *J Auton Nerv Syst* **20,** 73-86.

Dampney RAL, Tagawa T, Horiuchi J, Fontes M & Polson JW. (2000). What Drives The Tonic Activity Of Presympathetic Neurons In The Rostral Ventrolateral Medulla? *Clin Exp Pharmacol Physiol* **27,** 1049-1053.

Darlington DN, Shinsako J & Dallman MF. (1988). Paraventricular lesions: Hormonal and cardiovascular responses to hemorrhage. *Brain Res* **439,** 289-301.

Das M, Vihlen CS & Legradi G. (2007). Hypothalamic and brainstem sources of pituitary adenylate cyclase-activating polypeptide nerve fibers innervating the hypothalamic paraventricular nucleus in the rat. *J Comp Neurol* **500,** 761-776.

Date Y, Mondal MS, Matsukura S & Nakazato M. (2000). Distribution of orexin-A and orexin-B (hypocretins) in the rat spinal cord. *Neurosci Lett* **288,** 87-90.

Date Y, Ueta Y, Yamashita H, Yamaguchi H, Matsukura S, Kangawa K, Sakurai T, Yanagisawa M & Nakazato M. (1999). Orexins, orexigenic hypothalamic peptides, interact with autonomic, neuroendocrine and neuroregulatory systems. *Proc Natl Acad Sci US A* **96,** 748-753.

de Lecea L, Kilduff TS, Peyron C, Gao X-B, Foye PE, Danielson PE, Fukuhara C, Battenberg ELF, Gautvik VT, Bartlett FS, Frankel WN, van den Pol AN, Bloom FE, Gautvik KM & Sutcliffe JG. (1998). The

hypocretins: Hypothalamus-specific peptides with neuroexcitatory activity. *Proc Natl Acad Sci USA* **95,** 322-327.

De Oliveira CVR, Rosas-Arellano MP, Solano-Flores LP & Ciriello J. (2003). Cardiovascular effects of hypocretin-1 in nucleus of the solitary tract. *Am J Physiol* **284,** H1369-1377.

De Paula PM & Branco LGS. (2005). Glutamatergic receptors of the rostral ventrolateral medulla are involved in the ventilatory response to hypoxia. *Respir Physiol Neurobiol* **146,** 125-134.

de Wardener HE. (2001). The hypothalamus and hypertension. *Physiol Rev* **81,** 1599-1658.

Dean C & Coote JH. (1986). A ventromedullary relay involved in the hypothalamic and chemoreceptor activation of sympathetic postganglionic neurones to skeletal muscle, kidney and splanchnic area. *Brain Res* **377,** 279-285.

Dembowsky K, Czachurski J & Seller H. (1985). An intracellular study of the synaptic input to sympathetic preganglionic neurones of the third thoracic segment of the cat. *J Auton Nerv Syst* **13,** 201-244.

Deng BS, Nakamura A, Zhang W, Yanagisawa M, Fukuda Y & Kuwaki T. (2007). Contribution of orexin in hypercapnic chemoreflex: Evidence from genetic and pharmacological disruption and supplementation studies in mice. *J Appl Physiol* **103,** 1772-1779.

Deuchars SA. (2007). Multi-tasking in the spinal cord--do 'sympathetic' interneurones work harder than we give them credit for? *J Physiol* **580,** 723-729.

Deuchars SA, Brooke RE, Frater B & Deuchars J. (2001). Properties of interneurones in the intermediolateral cell column of the rat spinal cord: Role of the potassium channel subunit Kv3.1. *Neuroscience* **106,** 433-446.

Deuchars SA, Milligan CJ, Stornetta RL & Deuchars J. (2005). GABAergic neurons in the central region of the spinal cord: A novel substrate for sympathetic inhibition. *J Neurosci* **25,** 1063-1070.

Deuchars SA, Morrison SF & Gilbey MP. (1995). Medullary-evoked EPSPs in neonatal rat sympathetic preganglionic neurones in vitro. *J Physiol* **487** 453-463.

Dias MB, Li A & Nattie E. (2008). Focal CO2 dialysis in raphe obscurus does not stimulate ventilation but enhances the response to focal CO2 dialysis in the retrotrapezoid nucleus. *J Appl Physiol* **105,** 83-90.

Dias MB, Li A & Nattie EE. (2009). Antagonism of orexin receptor-1 in the retrotrapezoid nucleus inhibits the ventilatory response to hypercapnia predominantly in wakefulness. *J Physiol* **587,** 2059-2067.

Dick TE, Baekey DM, Paton JF, Lindsey BG & Morris KF. (2009). Cardio-respiratory coupling depends on the pons. *Respir Physiol Neurobiol*.

Dick TE & Coles SK. (2000). Ventrolateral pons mediates short-term depression of respiratory frequency after brief hypoxia. *Respir Physiol* **121,** 87-100.

Dick TE, Hsieh YH, Morrison S, Coles SK & Prabhakar N. (2004). Entrainment pattern between sympathetic and phrenic nerve activities in the Sprague-Dawley rat: hypoxia-evoked sympathetic activity during expiration. *Am J Physiol* **286,** R1121-1128.

Dick TE, Hsieh YH, Wang N & Prabhakar N. (2007). Acute intermittent hypoxia increases both phrenic and sympathetic nerve activities in the rat. *Exp Physiol* **92,** 87-97.

Dobbins EG & Feldman JL. (1994). Brainstem network controlling descending drive to phrenic motoneurons in rat. *J Comp Neurol* **347,** 64-86.

Donoghue S, Felder RB, Jordan D & Spyer KM. (1984). The central projections of carotid baroreceptors and chemoreceptors in the cat: A neurophysiological study. *J Physiol* **347,** 397-409.

Dreteler GH, Wouters W, Saxena PR & G. RA. (1991). Pressor effects following microinjection of 5-HT1A receptor agonists into the raphe obscurus of the anaesthetized rat. *Br J Pharmacol* **102,** 317-322.

Drye RG, Baisden RH, Whittington DL & Woodruff ML. (1990). The effects of stimulation of the A5 region on blood pressure and heart rate in rabbits. *Brain Res Bull* **24,** 33-39.

Dube MG, Kalra SP & Kalra PS. (1999). Food intake elicited by central administration of orexins/hypocretins: identification of hypothalamic sites of action. *Brain Res* **842,** 473-477.

Dun SL, Ng YK, Brailoiu GC, Ling EA & Dun NJ. (2002). Cocaine- and amphetamine-regulated transcript peptide-immunoreactivity in adrenergic C1 neurons projecting to the intermediolateral cell column of the rat. *J Chem Neuroanat* **23,** 123-132.

Dyer CJ, Touchette KJ, Carroll JA, Allee GL & Matteri RL. (1999). Cloning of Porcine Prepro-Orexin cDNA and Effects of an Intramuscular Injection of Synthetic Porcine Orexin-B on Feed Intake in Young Pigs. *Domest Anim Endocrinol* **16,** 145-148.

Edwards SL, Anderson CR, Southwell BR & McAllen RM. (1996). Distinct preganglionic neurons innervate noradrenaline and adrenaline cells in the cat adrenal medulla. *Neuroscience* **70,** 825-832.

Eggermann E, Serafin M, Bayer L, Machard D, Saint-Mleux B, Jones BE & Muhlethaler M. (2001). Orexins/hypocretins excite basal forebrain cholinergic neurones. *Neuroscience* **108,** 177-181.

Elias CF, Saper CB, Maratos-Flier E, Tritos NA, Lee C, Kelly J, Tatro JB, Hoffman GE, Ollmann MM, Barsh GS, Sakurai T, Yanagisawa M & Elmquist JK. (1998). Chemically defined projections linking the mediobasal hypothalamus and the lateral hypothalamic area. *J Comp Neurol* **402,** 442-459.

Ellenberger HH & Feldman JL. (1988). Monosynaptic transmission of respiratory drive to phrenic motoneurons from brainstem bulbospinal neurons in rats. *J Comp Neurol* **269,** 47-57.

Ellenberger HH & Feldman JL. (1990). Brainstem connections of the rostral ventral respiratory group of the rat. *Brain Res* **513,** 35-42.

Esler M. (2000). The sympathetic system and hypertension. *Am J Hypertens* **13,** 99S-105S.

Esler M, Jennings G, Korner P, Willett I, Dudley F, Hasking G, Anderson W & Lambert G. (1988). Assessment of human sympathetic nervous system activity from measurements of norepinephrine turnover. *Hypertension* **11,** 3-20.

Esler M, Jennings G, Lambert G, Meredith I, Horne M & Eisenhofer G. (1990). Overflow of catecholamine neurotransmitters to the circulation: Source, fate, and functions. *Physiol Rev* **70,** 963-985.

Esler M, Rumantir M, Kaye D, Jennings G, Hastings J, Socratous F & Lambert G. (2001). Sympathetic nerve biology in essential hypertension. *Clin Exp Pharmacol Physiol* **28,** 986-989.

Ezure K. (1990). Synaptic connections between medullary respiratory neurons and considerations on the genesis of respiratory rhythm. *Prog Neurobiol* **35,** 429-450.

Ezure K & Tanaka I. (2000). Identification of deflation-sensitive inspiratory neurons in the dorsal respiratory group of the rat. *Brain Res* **883,** 22-30.

Ezure K, Tanaka I & Kondo M. (2003). Glycine is used as a transmitter by decrementing expiratory neurons of the ventrolateral medulla in the rat. *J Neurosci* **23,** 8941-8948.

Fadel J & Deutch AY. (2002). Anatomical substrates of orexin-dopamine interactions: lateral hypothalamic projections to the ventral tegmental area. *Neuroscience* **111,** 379-387.

Farkas E, Jansen ASP & Loewy AD. (1998). Periaqueductal gray matter input to cardiac-related sympathetic premotor neurons. *Brain Res* **792,** 179-192.

Farnham MM, Li Q, Goodchild AK & Pilowsky PM. (2008). PACAP is expressed in sympathoexcitatory bulbospinal C1 neurons of the brain stem and increases sympathetic nerve activity in vivo. *Am J Physiol* **294,** R1304-1311.

Fedorko L, Merrill EG & Lipski J. (1983). Two descending medullary inspiratory pathways to phrenic motoneurones. *Neurosci Lett* **43,** 285-291.

Feldberg W & Guertzenstein PG. (1972). A vasodepressor effect of pentobarbitone sodium. *J Physiol* **224,** 83-103.

Feldman JL & Del Negro CA. (2006). Looking for inspiration: New perspectives on respiratory rhythm. *Nat Rev Neurosci* **7,** 232-242.

Feldman JL, Loewy AD & Speck DF. (1985). Projections from the Ventral Respiratory Group to Phrenic and Intercostal Motoneurons in Cat - an Autoradiographic Study. *J Neurosci* **5,** 1993-2000.

Feldman JL, Smith JC, Ellenberger HH, Connelly CA, Liu GS, Greer JJ, Lindsay AD & Otto MR. (1990). Neurogenesis of respiratory rhythm and pattern: emerging concepts. *Am J Physiol* **259,** R879-886.

Fenwick NM, Martin CL & Llewellyn-Smith IJ. (2006). Immunoreactivity for cocaine- and amphetamine-regulated transcript in rat sympathetic preganglionic neurons projecting to sympathetic ganglia and the adrenal medulla. *J Comp Neurol* **495,** 422-433.

Field KJ, White WJ & Lang CM. (1993). Anaesthetic effects of chloral hydrate pentobarbitone and urethane in adult male rats. *Lab Anim* **27,** 258-269.

Finley JC & Katz DM. (1992). The central organization of carotid body afferent projections to the brainstem of the rat. *Brain Res* **572,** 108-116.

Fisher JP & Fadel PJ. (2010). Therapeutic strategies for targeting excessive central sympathetic activation in human hypertension *Exp Physiol* **95,** 572–580.

Fortuna MG, West GH, Stornetta RL & Guyenet PG. (2008). Botzinger expiratory-augmenting neurons and the parafacial respiratory group. *J Neurosci* **28,** 2506-2515.

Fu L-Y, Acuna-Goycolea C & van den Pol AN. (2004). Neuropeptide Y Inhibits Hypocretin/Orexin Neurons by Multiple Presynaptic and Postsynaptic Mechanisms: Tonic Depression of the Hypothalamic Arousal System. *J Neurosci* **24,** 8741-8751.

Fujiki N, Yoshida Y, Ripley B, Honda K, Mignot E & Nishino S. (2001). Changes in CSF hypocretin-1 (orexin A) levels in rats across 24 hours and in response to food deprivation. *NeuroReport* **12,** 993-997.

Fulop T, Radabaugh S & Smith C. (2005). Activity-dependent differential transmitter release in mouse adrenal chromaffin cells. *J Neurosci* **25,** 7324-7332.

Funakoshi K, Abe T & Kishida R. (1996). Direct projections from the spinal cord to the trigeminal sympathetic ganglion of the puffer fish, Takifugu niphobles. *Neurosci Lett* **213,** 115-118.

Fung SJ, Yamuy J, Sampogna S, Morales FR & Chase MH. (2001). Hypocretin (orexin) input to trigeminal and hypoglossal motoneurons in the cat: a double-labeling immunohistochemical study. *Brain Res* **903,** 257-262.

Futuro-Neto HA & Coote JH. (1982). Desynchronized sleep-like pattern of sympathetic activity elicited by electrical stimulation of sites in the brainstem. *Brain Res* **252,** 269-276.

Gaede AH, Lung MS & Pilowsky PM. (2009). Catestatin attenuates the effects of intrathecal nicotine and isoproterenol. *Brain Res* **1305,** 86-95.

Galabov PG. (1992). Ultrastructural localization of angiotensin II-like immunoreactivity (A II-LI) in the vegetative networks of the spinal cord of the guinea pig. *J Auton Nerv Syst* **40,** 215-222.

Galas L, Vaudry H, Braun B, Van Den Pol AN, De Lecea L, Sutcliffe JG & Chartrel N. (2001). Immunohistochemical localization and biochemical characterization of hypocretin/orexin-related peptides in the central nervous system of the frog Rana ridibunda. *J Comp Neurol* **429,** 242-252.

Gallopin T, Fort P, Eggermann E, Cauli B, Luppi P-H, Rossier J, Audinat E, Muhlethaler M & Serafin M. (2000). Identification of sleep-promoting neurons in vitro. *Nature* **404,** 992-995.

Gaytan SP, Calero F, NunezAbades PA, Morillo AM & Pasaro R. (1997). Pontomedullary efferent projections of the ventral respiratory neuronal subsets of the rat. *Brain Res Bull* **42,** 323-334.

Geerling JC, Mettenleiter TC & Loewy AD. (2003). Orexin neurons project to diverse sympathetic outflow systems. *Neuroscience* **122,** 541-550.

Gilbey MP. (1997). Fundamental aspects of the control of sympathetic preganglionic neuronal discharge. In: Jordan D (ed). In *Central nervous control of autonomic function*, pp. 1-28. Harwood Academic Publishers, Singapore.

Gilbey MP, Coote JH, Fleetwood-Walker S & Peterson DF. (1982). The influence of the paraventriculo-spinal pathway, and oxytocin and vasopressin on sympathetic preganglionic neurones. *Brain Res* **251,** 283-290.

Gillis RA, Quest JA, Pagani FD, Souza JD, Da Silva AM, Jensen RT, Garvey TQ, 3rd & Hamosh P. (1983). Activation of central nervous system cholecystokinin receptors stimulates respiration in the cat. *J Pharmacol Exp Ther* **224,** 408-414.

Giuliano R, Ruggiero DA, Morrison S, Ernsberger P & Reis DJ. (1989). Cholinergic regulation of arterial pressure by the C1 area of the rostral ventrolateral medulla. *J Neurosci* **9,** 923-942.

Goldblatt H. (1964). Hypertension of renal origin. Historical and experimental background. *Am J Surg* **107,** 21-25.

Gonzalez E, Krieger A & Sapru H. (1983). Central resetting of baroreflex in the spontaneously hypertensive rat. *Hypertension* **5,** 346-352.

Goodchild AK, Dampney RA & Bandler R. (1982). A method for evoking physiological responses by stimulation of cell bodies, but not axons of passage, within localized regions of the central nervous system. *J Neurosci Methods* **6,** 351-363.

Goodchild AK & Moon EA. (2009). Maps of cardiovascular and respiratory regions of rat ventral medulla: focus on the caudal medulla. *J Chem Neuroanat* **38,** 209-221.

Goodchild AK, Moon EA, Dampney RA & Howe PR. (1984). Evidence that adrenaline neurons in the rostral ventrolateral medulla have a vasopressor function. *Neurosci Lett* **45,** 267-272.

Goodchild AK, Van Deurzen BTM, Hildreth CM & Pilowsky PM. (2008). Control of sympathetic, respiratory and somatomotor outflow by an intraspinal pattern generator. *Clin Exp Pharmacol Physiol* **35,** 447-453.

Goodchild AK, Van Deurzen BTM, Sun Q-J, Chalmers J & Pilowsky PM. (2000). Spinal GABA(A) receptors do not mediate the sympathetic baroreceptor reflex in the rat. *Am J Physiol* **279,** R320-331.

Grassi G. (2010). Sympathetic neural activity in hypertension and related diseases. *Am J Hypertens* **23,** 1052–1060.

Grassi G, Cattaneo BM, Seravalle G, Lanfranchi A & Mancia G. (1998). Baroreflex control of sympathetic nerve activity in essential and secondary hypertension. *Hypertension* **31,** 68-72.

Gray PA, Janczewski WA, Mellen N, McCrimmon DR & Feldman JL. (2001). Normal breathing requires preBotzinger complex neurokinin-1 receptor-expressing neurons. *Nat Neurosci* **4,** 927-930.

Green JH & Heffron PF. (1966). The origin of the right aortic nerve in the rabbit. *Q J Exp Physiol Cogn Med Sci* **51,** 276-283.

Grkovic I & Anderson CR. (1996). Distribution of immunoreactivity for the NK1 receptor on different subpopulations of sympathetic preganglionic neurons in the rat. *J Comp Neurol* **374,** 376-386.

Grudt TJ, van den Pol AN & Perl ER. (2002). Hypocretin-2 (orexin-B) modulation of superficial dorsal horn activity in rat. *J Physiol* **538,** 517-525.

Guan JL, Wang QP, Hori T, Takenoya F, Kageyama H & Shioda S. (2004). Ultrastructure of orexin-1 receptor immunoreactivities in the spinal cord dorsal horn. *Peptides* **25,** 1307-1311.

Guertzenstein PG & Silver A. (1974). Fall in blood pressure produced from discrete regions of the ventral surface of the medulla by glycine and lesions. *J Physiol* **242,** 489-503.

Guyenet PG. (1984). Baroreceptor-mediated inhibition of A5 noradrenergic neurons. *Brain Res* **303,** 31-40.

Guyenet PG. (2000). Neural structures that mediate sympathoexcitation during hypoxia. *Respir Physiol* **121,** 147-162.

Guyenet PG. (2006). The sympathetic control of blood pressure. *Nat Rev Neurosci* **7,** 335-346.

Guyenet PG, Bayliss DA, Stornetta RL, Fortuna MG, Abbott SBG & Depuy SD. (2009). Retrotrapezoid nucleus, respiratory chemosensitivity and breathing automaticity. *Respir Physiol Neurobiol* **168,** 59-68.

Guyenet PG, Darnall RA & Riley TA. (1990). Rostral ventrolateral medulla and sympathorespiratory integration in rats. *Am J Physiol* **259,** 1063-1074.

Guyenet PG, Filtz TM & Donaldson SR. (1987). Role of excitatory amino acids in rat vagal and sympathetic baroreflexes. *Brain Res* **407,** 272-284.

Guyenet PG, Koshiya N, Huangfu D, Verberne AJ & Riley TA. (1993). Central respiratory control of A5 and A6 pontine noradrenergic neurons. *Am J Physiol* **264,** R1035-1044.

Guyenet PG & Mulkey DK. (2010). Retrotrapezoid nucleus and parafacial respiratory group. *Resp Physiol Neurobiol* **173,** 244-255.

Guyenet PG, Mulkey DK, Stornetta RL & Bayliss DA. (2005a). Regulation of ventral surface chemoreceptors by the central respiratory pattern generator. *J Neurosci* **25,** 8938-8947.

Guyenet PG, Schreihofer AM & Stornetta RL. (2001). Regulation of sympathetic tone and arterial pressure by the rostral ventrolateral medulla after depletion of C1 cells in rats. *Ann N Y Acad Sci* **940,** 259-269.

Guyenet PG, Sevigny CP, Weston MC & Stornetta RL. (2002). Neurokinin-1 receptor-expressing cells of the ventral respiratory group are functionally heterogeneous and predominantly glutamatergic. *J Neurosci* **22,** 3806-3816.

Guyenet PG, Stornetta RL, Abbott SBG, Depuy SD, Fortuna MG & Kanbar R. (2010). Central CO2 chemoreception and integrated neural mechanisms of cardiovascular and respiratory control. *J Appl Physiol* **108,** 995-1002.

Guyenet PG, Stornetta RL, Bayliss DA & Mulkey DK. (2005b). Retrotrapezoid nucleus: A litmus test for the identification of central chemoreceptors. *Exp Physiol* **90,** 247-253.

Hagan JJ, Leslie RA, Patel S, Evans ML, Wattam TA, Holmes S, Benham CD, Taylor SG, Routledge C, Hemmati P, Munton RP, Ashmeade TE, Shah AS, Hatcher JP, Hatcher PD, Jones DNC, Smith MI, Piper DC, Hunter AJ, Porter RA & Upton N. (1999). Orexin A activates locus coeruleus cell firing and increases arousal in the rat. *Proc Natl Acad Sci U S A* **96,** 10911-10916.

Haibara AS, Tamashiro E, Olivan MV, Bonagamba LGH & Machado BH. (2002). Involvement of the parabrachial nucleus in the pressor response to chemoreflex activation in awake rats. *Auton Neurosci* **101,** 60-67.

Hara J, Beuckmann CT, Nambu T, Willie JT, Chemelli RM, Sinton CM, Sugiyama F, Yagami K-i, Goto K, Yanagisawa M & Sakurai T. (2001). Genetic ablation of orexin neurons in mice results in narcolepsy, hypophagia, and obesity. *Neuron* **30,** 345-354.

Harrison TA, Chen CT, Dun NJ & Chang JK. (1999). Hypothalamic orexin A-immunoreactive neurons project to the rat dorsal medulla. *Neurosci Lett* **273,** 17-20.

Haselton JR & Guyenet PG. (1989). Central respiratory modulation of medullary sympathoexcitatory neurons in rat. *Am J Physiol* **256,** R739-750.

Haselton JR, Winters RW, Liskowsky DR, Haselton CL, McCabe PM & Schneiderman N. (1988). Cardiovascular responses elicited by electrical and chemical stimulation of the rostral medullary raphe of the rabbit. *Brain Res* **453,** 167-175.

Hayashi J, Takeda K, Kuwabara T, Takesako T, Itoh H, Hirata M, Tanabe S, Nakata T, Sasaki S & Nakagawa M. (1993). Clonidine improves central attenuation of the baroreflex in spontaneously hypertensive rats. *Jpn Heart J* **34,** 333-339.

Haynes AC, Jackson B, Chapman H, Tadayyon M, Johns A, Porter RA & Arch JRS. (2000). A selective orexin-1 receptor antagonist reduces food consumption in male and female rats. *Regul Pept* **96,** 45-51.

Hayward LF, Riley AP & Felder RB. (2002). Alpha2-adrenergic receptors in NTS facilitate baroreflex function in adult spontaneously hypertensive rats. *Am J Physiol* **282,** H2336-H2345.

Head GA. (1995). Baroreflexes and cardiovascular regulation in hypertension. *J Cardiovasc Pharmacol* **26,** S7-16.

Head GA & Adams MA. (1992). Characterization of the baroreceptor heart rate reflex during development in spontaneously hypertensive rats. *Clin Exp Pharmacol Physiol* **19,** 587-597.

Head GA & Mayorov DN. (2001). Central angiotensin and baroreceptor control of circulation. *Ann N Y Acad Sci* **940,** 361-379.

Heinricher MM, Tavares I, Leith JL & Lumb BM. (2009). Descending control of nociception: Specificity, recruitment and plasticity. *Brain Res Rev* **60,** 214-225.

Helke CJ, Capuano S, Tran N & Zhuo H. (1997). Immunocytochemical studies of the 5-HT1A receptor in ventral medullary neurons that project to the intermediolateral cell column and contain serotonin or tyrosine hydroxylase immunoreactivity. *J Comp Neurol* **379,** 261-270.

Helke CJ, Sayson SC, Keeler JR & Charlton CG. (1986). Thyrotropin-releasing hormone-immunoreactive neurons project from the ventral medulla to the intermediolateral cell column: Partial coexistence with serotonin. *Brain Res* **381,** 1-7.

Helke CJ, Shults CW, Chase TN & O'Donohue TL. (1984). Autoradiographic localization of substance P receptors in rat medulla: Effect of vagotomy and nodose ganglionectomy. *Neuroscience* **12,** 215-223.

Hennersdorf MG & Strauer BE. (2001). Arterial hypertension and cardiac arrhythmias. *J Hypertens* **19,** 167-177.

Herbert H, Moga MM & Saper CB. (1990). Connections of the parabrachial nucleus with the nucleus of the solitary tract and the medullary reticular formation in the rat. *J Comp Neurol* **293,** 540-580.

Herbert H & Saper CB. (1992). Organization of medullary adrenergic and noradrenergic projections to the periaqueductal gray matter in the rat. *J Comp Neurol* **315,** 34-52.

Hervieu GJ, Cluderay JE, Harrison DC, Roberts JC & Leslie RA. (2001). Gene expression and protein distribution of the orexin-1 receptor in the rat brain and spinal cord. *Neuroscience* **103,** 777-797.

Heslop DJ, Bandler R & Keay KA. (2004). Haemorrhage-evoked decompensation and recompensation mediated by distinct projections from rostral and caudal midline medulla in the rat. *Eur J Neurosci* **20,** 2096-2110.

Hilton SM, Marshall JM & Timms RJ. (1983). Ventral medullary relay neurones in the pathway from the defence areas of the cat and their effect on blood pressure. *J Physiol* **345,** 149-166.

Hirooka Y, Polson JW, Potts PD & Dampney RAL. (1997). Hypoxia-induced fos expression in neurons projecting to the pressor region in the rostral ventrolateral medulla. *Neuroscience* **80,** 1209-1224.

Hirooka Y, Sagara Y, Kishi T & Sunagawa K. (2010). Oxidative stress and central cardiovascular regulation - Pathogenesis of hypertension and therapeutic aspects. *Circ J* **74,** 827-835.

Hirsch MD & Helke CJ. (1988). Bulbospinal thyrotropin-releasing hormone projections to the intermediolateral cell column: a double fluorescence immunohistochemical-retrograde tracing study in the rat. *Neuroscience* **25,** 625-637.

Hokfelt T, Broberger C, Xu ZQ, Sergeyev V, Ubink R & Diez M. (2000). Neuropeptides--an overview. *Neuropharmacology* **39,** 1337-1356.

Hokfelt T, Fuxe K, Goldstein M & Johansson O. (1973). Evidence for adrenaline neurons in the rat brain. *Acta Physiol Scand* **89,** 286-288.

Hong Y & Henry JL. (1992). Glutamate, NMDA and NMDA receptor antagonists: Cardiovascular effects of intrathecal administration in the rat. *Brain Res* **569,** 38-45.

Horiuchi J & Dampney RAL. (2002). Evidence for tonic disinhibition of RVLM sympathoexcitatory neurons from the caudal pressor area. *Auton Neurosci* **99,** 102-110.

Horvath TL, Diano S & van den Pol AN. (1999). Synaptic Interaction between Hypocretin (Orexin) and Neuropeptide Y Cells in the Rodent and Primate Hypothalamus: A Novel Circuit Implicated in Metabolic and Endocrine Regulations. *J Neurosci* **19,** 1072-1087.

Hosoya Y. (1985). Hypothalamic projections to the ventral medulla oblongata in the rat, with special reference to the nucleus raphe pallidus: A study using autoradiographic and HRP techniques. *Brain Res* **344,** 338-350.

Housley GD, Martin-Body RL, Dawson NJ & Sinclair JD. (1987). Brain stem projections of the glossopharyngeal nerve and its carotid sinus branch in the rat. *Neuroscience* **22,** 237-250.

Huang C, Yoshimoto M, Miki K & Johns EJ. (2006). The contribution of brain angiotensin II to the baroreflex regulation of renal sympathetic nerve activity in conscious normotensive and hypertensive rats. *J Physiol* **574,** 597-604.

Huang S-C, Dai Y-WE, Lee Y-H, Chiou L-C & Hwang L-L. (2010). Orexins depolarize rostral ventrolateral medulla neurons and increase arterial pressure and heart rate in rats mainly via orexin 2 receptors. *J Pharmacol Exp Ther* **334,** 522-529.

Huang Z-L, Qu W-M, Li W-D, Mochizuki T, Eguchi N, Watanabe T, Urade Y & Hayaishi O. (2001). Arousal effect of orexin A depends on activation of the histaminergic system. *Proc Natl Acad Sci U S A* **98,** 9965-9970.

Huangfu D, Hwang LJ, Riley TA & Guyenet PG. (1992). Splanchnic nerve response to A5 area stimulation in rats. *Am J Physiol* **263,** R437-446.

Huangfu D, Koshiya N & Guyenet PG. (1991). A5 noradrenergic unit activity and sympathetic nerve discharge in rats. *Am J Physiol* **261,** R393-402.

Huckstepp RT, Id Bihi R, Eason R, Spyer KM, Dicke N, Willecke K & et al. (2010). Connexin hemichannel-mediated CO2-dependent release of ATP in the medulla oblongata contributes to central respiratory chemosensitivity. *J Physiol* **588,** 3901-3920.

Hungs M, Fan J, Lin L, Lin X, Maki RA & Mignot E. (2001). Identification and Functional Analysis of Mutations in the Hypocretin (Orexin) Genes of Narcoleptic Canines. *Genome Res* **11,** 531-539.

Iadecola C, Faris PL, Hartman BK & Xu X. (1993). Localization of NADPH diaphorase in neurons of the rostral ventral medulla: Possible role of nitric oxide in central autonomic regulation and oxygen chemoreception. *Brain Res* **603,** 173-179.

Ichinose M, Asai M, Sawada M, Sasaki K & Oomura Y. (1998). Induction of outward current by orexin-B in mouse peritoneal macrophages. *FEBS Lett* **440,** 51-54.

Ito S, Hiratsuka M, Komatsu K, Tsukamoto K, Kanmatsuse K & Sved AF. (2003). Ventrolateral medulla AT1 receptors support arterial pressure in Dahl salt-sensitive rats. *Hypertension* **41,** 744-750.

Izawa H, Yamada Y, Okada T, Tanaka M, Hirayama H & Yokota M. (2003). Prediction of genetic risk for hypertension. *Hypertension* **41,** 1035-1040.

Janig W & Habler HJ. (2003). Neurophysiological analysis of target-related sympathetic pathways - from animal to human: similarities and differences. *Acta Physiol Scand* **177,** 255-274.

Jansen AS & Loewy AD. (1997). Neurons lying in the white matter of the upper cervical spinal cord project to the intermediolateral cell column. *Neuroscience* **77,** 889-898.

Jansen AS, Wessendorf MW & Loewy AD. (1995). Transneuronal labeling of CNS neuropeptide and monoamine neurons after pseudorabies virus injections into the stellate ganglion. *Brain Res* **683,** 1-24.

Jeske I & McKenna KE. (1992). Quantitative analysis of bulbospinal projections from the rostral ventrolateral medulla: Contribution of C1-adrenergic and nonadrenergic neurons. *J Comp Neurol* **324,** 1-13.

Jiang M, Alheid GF, Calandriello T & McCrimmon DR. (2004). Parabrachial-lateral pontine neurons link nociception and breathing. *Respir Physiol Neurobiol* **143,** 215-233.

Jiang M, Zhang C, Wang J, Chen J, Xia C, Du D, Zhao N, Cao Y, Shen L & Zhu D. (2011). Adenosine A2AR modulates cardiovascular function by activating ERK1/2 signal in the rostral ventrolateral medulla of acute myocardial ischemic rats. *Life Sci* **89,** 182-187.

Jöhren O, Neidert SJ, Kummer M, Dendorfer A & Dominiak P. (2001). Prepro-Orexin and Orexin Receptor mRNAs Are Differentially Expressed in Peripheral Tissues of Male and Female Rats. *Endocrinology* **142,** 3324-3331.

Judy WV & Farrell SK. (1979). Arterial baroreceptor reflex control of sympathetic nerve activity in the spontaneously hypertensive rat. *Hypertension* **1,** 605-614.

Kangrga IM & Loewy AD. (1995). Whole-cell recordings from visualized C1 adrenergic bulbospinal neurons: ionic mechanisms underlying vasomotor tone. *Brain Res* **670,** 215-232.

Kanjhan R, Lipski J, Kruszewska B & Rong W. (1995). A comparative study of pre-sympathetic and Botzinger neurons in the rostral ventrolateral medulla (RVLM) of the rat. *Brain Res* **699,** 19-32.

Kannan H, Hayashida Y & Yamashita H. (1989). Increase in sympathetic outflow by paraventricular nucleus stimulation in awake rats. *Am J Physiol* **256,** R1325-1330.

Kapoor V, Minson J & Chalmers J. (1992). Ventral medulla stimulation increases blood pressure and spinal cord amino acid release. *NeuroReport* **3,** 55-58.

Kasamatsu K & Sapru HN. (2005). Attenuation of aortic baroreflex responses by microinjections of endomorphin-2 into the rostral ventrolateral medullary pressor area of the rat. *Am J Physiol* **289,** R59-67.

Kashihara K, McMullan S, Lonergan T, Goodchild AK & Pilowsky PM. (2008). Neuropeptide Y in the rostral ventrolateral medulla blocks somatosympathetic reflexes in anesthetized rats. *Auton Neurosci* **142,** 64-70.

Kastin AJ & Akerstrom V. (1999). Orexin A but Not Orexin B Rapidly Enters Brain from Blood by Simple Diffusion. *J Pharmacol Exp Ther* **289,** 219-223.

Katafuchi T, Oomura Y & Kurosawa M. (1988). Effects of chemical stimulation of paraventricular nucleus on adrenal and renal nerve activity in rats. *Neurosci Lett* **86,** 195-200.

Kayaba Y, Nakamura A, Kasuya Y, Ohuchi T, Yanagisawa M, Komuro I, Fukuda Y & Kuwaki T. (2003). Attenuated defense response and low basal blood pressure in orexin knockout mice. *Am J Physiol* **285,** R581-593.

Kent BB, Drane JW, Blumenstein B & Manning JW. (1972). A mathematical model to assess changes in the baroreceptor reflex. *Cardiology* **57,** 295-310.

Kirchgessner AL & Liu M-t. (1999). Orexin Synthesis and Response in the Gut. *Neuron* **24,** 941-951.

Kishi T. (2012). Heart failure as an autonomic nervous system dysfunction. *J Cardiol ,* **59,** 117—122.

Kishi T, Hirooka Y, Konno S, Ogawa K & Sunagawa K. (2010). Angiotensin II type 1 receptor-activated caspase-3 through ras/mitogen-activated protein kinase/extracellular signal-regulated kinase in the rostral ventrolateral medulla is involved in sympathoexcitation in stroke-prone spontaneously hypertensive rats. *Hypertension* **55,** 291-297.

Korotkova TM, Sergeeva OA, Eriksson KS, Haas HL & Brown RE. (2003). Excitation of Ventral Tegmental Area Dopaminergic and Nondopaminergic Neurons by Orexins/Hypocretins. *J Neurosci* **23,** 7-11.

Koshiya N & Guyenet PG. (1996a). NTS neurons with carotid chemoreceptor inputs arborize in the rostral ventrolateral medulla. *Am J Physiol* **270,** R1273-1278.

Koshiya N & Guyenet PG. (1996b). Tonic sympathetic chemoreflex after blockade of respiratory rhythmogenesis in the rat. *J Physiol London* **491,** 859-869.

Koshiya N, Huangfu D & Guyenet PG. (1993). Ventrolateral medulla and sympathetic chemoreflex in the rat. *Brain Res* **609,** 174-184.

Krout KE, Mettenleiter TC & Loewy AD. (2003). Single CNS neurons link both central motor and cardiosympathetic systems: A double-virus tracing study. *Neuroscience* **118,** 853-866.

Kukkonen JP, Holmqvist T, Ammoun S & Akerman KE. (2002). Functions of the orexinergic/hypocretinergic system. *Am J Physiol* **283,** C1567-1591.

Kumada M, Terui N & Kuwaki T. (1990). Arterial baroreceptor reflex: its central and peripheral neural mechanisms. *Prog Neurobiol* **35,** 331-361.

Kumai T, Tanaka M, Watanabe M, Nakura H, Tateishi T & Kobayashi S. (1996). Elevated tyrosine hydroxylase mRNA levels in medulla oblongata of spontaneously hypertensive rats. *Mol Brain Res* **36,** 197-199.

Kumar NN, Ferguson J, Padley JR, Pilowsky PM & Goodchild AK. (2009). Differential muscarinic receptor gene expression levels in the ventral medulla of spontaneously hypertensive and Wistar-Kyoto rats: role in sympathetic baroreflex function. *J Hypertens* **27,** 1001-1008.

Kumazawa T & Perl ER. (1977). Primate cutaneous sensory units with unmyelinated (C) afferent fibers. *J Neurophysiol* **40,** 1325-1338.

Kuwaki T & Zhang W. (2010). Orexin neurons as arousal-associated modulators of central cardiorespiratory regulation. *Respir Physiol Neurobiol* **174,** 43-54.

Kuwaki T, Zhang W, Nakamura A & Deng B. (2008). Emotional and state-dependent modification of cardiorespiratory function: Role of orexinergic neurons. *Auto Neurosci* **142,** 11–16.

La Rovere MT, Bersano C, Gnemmi M, Specchia G & Schwartz PJ. (2002). Exercise-induced increase in baroreflex sensitivity predicts improved prognosis after myocardial infarction. *Circulation* **106,** 945–949.

Lambert E, Straznicky N, Schlaich M, Esler M, Dawood T, Hotchkin E & Lambert G. (2007). Differing pattern of sympathoexcitation in normal-weight and obesity-related hypertension. *Hypertension* **50,** 862-868.

Langley JN. (1916). Sketch of the progress of discovery in the eighteenth century as regards the autonomic nervous system. *J Physiol* **50,** 225-258.

Lazarenko RM, Milner TA, Depuy SD, Stornetta RL, West GH, Kievits JA, Bayliss DA & Guyenet PG. (2009). Acid sensitivity and ultrastructure of the retrotrapezoid nucleus in Phox2b-EGFP transgenic mice. *J Comp Neurol* **517,** 69-86.

Lee MG, Hassani OK & Jones BE. (2005). Discharge of Identified Orexin/Hypocretin Neurons across the Sleep-Waking Cycle. *J Neurosci* **25,** 6716-6720.

Leenen FH, Ruzicka M & Huang BS. (2002). The brain and salt-sensitive hypertension. *Curr Hypertens Rep* **4,** 129-135.

Leenen FHH. (1999). Cardiovascular consequences of sympathetic hyperactivity. *Can J Cardiol* **15,** 2A-7A.

Leone C & Gordon FJ. (1989). Is L-glutamate a neurotransmitter of baroreceptor information in the nucleus of the tractus solitarius? *J Pharmacol Exp Ther* **250,** 953-962.

Lewis DI & Coote JH. (1990). Excitation and inhibition of rat sympathetic preganglionic neurones by catecholamines. *Brain Res* **530,** 229-234.

Lewis DI & Coote JH. (1996). Baroreceptor-induced inhibition of sympathetic neurons by GABA acting at a spinal site. *Am J Physiol* **270,** H1885-1892.

Li A, Randall M & Nattie EE. (1999). CO(2) microdialysis in retrotrapezoid nucleus of the rat increases breathing in wakefulness but not in sleep. *J Appl Physiol* **87,** 910-919.

Li Q, Goodchild AK, Seyedabadi M & Pilowsky PM. (2005). Pre-protachykinin A mRNA is colocalized with tyrosine hydroxylase-immunoreactivity in bulbospinal neurons. *Neuroscience* **136,** 205-216.

Li Y, Gao XB, Sakurai T & Van den Pol AN. (2002). Hypocretin/orexin excites hypocretin neurons via a local glutamate neuron - A potential mechanism for orchestrating the hypothalamic arousal system. *Neuron* **36,** 1169-1181.

Li Y & van den Pol AN. (2006). Differential target-dependent actions of coexpressed inhibitory dynorphin and excitatory hypocretin/orexin neuropeptides. *J Neurosci* **26,** 13037-13047.

Li YW, Bayliss DA & Guyenet PG. (1995). C1 neurons of neonatal rats: intrinsic beating properties and alpha 2-adrenergic receptors. *Am J Physiol* **269,** R1356-1369.

Li YW, Gieroba ZJ, McAllen RM & Blessing WW. (1991). Neurons in rabbit caudal ventrolateral medulla inhibit bulbospinal barosensitive neurons in rostral medulla. *Am J Physiol* **261,** R44-51.

Li YW & Guyenet PG. (1996). Activation of GABAB receptors increases a potassium conductance in rat bulbospinal neurons of the C1 area. *Am J Physiol* **271,** R1304-R1310.

Li YW, Wesselingh SL & Blessing WW. (1992). Projections from rabbit caudal medulla to C1 and A5 sympathetic premotor neurons, demonstrated with phaseolus leucoagglutinin and herpes simplex virus. *J Comp Neurol* **317,** 379-395.

Lichtman JW, Purves D & Yip JW. (1979). On the purpose of selective innervation of guinea-pig superior cervical ganglion cells. *J Physiol* **292,** 69-84.

Lidierth M. (2005). Pulser: User-friendly, graphical user-interface based software for controlling stimuli during data acquisition with Spike2 for Windows. *J Neurosci Methods* **141,** 243-250.

Light AR & Perl ER. (1979). Spinal termination of functionally identified primary afferent neurons with slowly conducting myelinated fibers. *J Comp Neurol* **186,** 133-150.

Lind RW, Swanson LW & Ganten D. (1985). Organization of angiotensin II immunoreactive cells and fibers in the rat central nervous system. An immunohistochemical study. *Neuroendocrinology* **40,** 2-24.

Lipski J. (1981). Antidromic Activation of Neurons as an Analytic Tool in the Study of the Central Nervous-System. *J Neurosci Methods* **4,** 1-32.

Lipski J, Kanjhan R, Kruszewska B & Rong W. (1996a). Properties of presympathetic neurones in the rostral ventrolateral medulla in the rat: an intracellular study "in vivo'. *J Physiol* **490,** 729-744.

Lipski J, Kanjhan R, Kruszewska B & Rong WF. (1995a). Criteria for intracellular identification of pre-sympathetic neurons in the rostral ventrolateral medulla in the rat. *Clin Exp Hypertens* **17,** 51-65.

Lipski J, Kanjhan R, Kruszewska B, Rong WF & Smith M. (1996b). Pre-sympathetic neurones in the rostral ventrolateral medulla of the rat: electrophysiology, morphology and relationship to adjacent neuronal groups. *Acta Neurobiol Exp (Wars)* **56,** 373-384.

Lipski J, Kanjhan R, Kruszewska B & Smith M. (1995b). Barosensitive neurons in the rostral ventrolateral medulla of the rat in vivo: morphological properties and relationship to C1 adrenergic neurons. *Neuroscience* **69,** 601-618.

Lipski J, Lin J, Teo MY & van Wyk M. (2002). The network vs. pacemaker theory of the activity of RVL presympathetic neurons--a comparison with another putative pacemaker system. *Auton Neurosci* **98,** 85-89.

Lipski J, McAllen RM & Spyer KM. (1975). The sinus nerve and baroreceptor input to the medulla of the cat. *J Physiol* **251,** 61-78.

Lipski J, McAllen RM & Spyer KM. (1977). The carotid chemoreceptor input to the respiratory neurones of the nucleus of tractus solitarus. *J Physiol* **269,** 797-810.

Lipski J, Zhang X, Kruszewska B & Kanjhan R. (1994). Morphological study of long axonal projections of ventral medullary inspiratory neurons in the rat. *Brain Res* **640,** 171-184.

Liu Q & Wong-Riley MTT. (2002). Postnatal expression of neurotransmitters, receptors, and cytochrome oxidase in the rat pre-Botzinger complex. *J Appl Physiol* **92,** 923-934.

Liu R-J, van den Pol AN & Aghajanian GK. (2002). Hypocretins (Orexins) Regulate Serotonin Neurons in the Dorsal Raphe Nucleus by Excitatory Direct and Inhibitory Indirect Actions. *J Neurosci* **22,** 9453-9464.

Liu YY, Ju G & Wong-Riley MTT. (2001). Distribution and colocalization of neurotransmitters and receptors in the pre-Botzinger complex of rats. *J Appl Physiol* **91,** 1387-1395.

Liu Z-W & Gao X-B. (2007). Adenosine Inhibits Activity of Hypocretin/Orexin Neurons by the A1 Receptor in the Lateral Hypothalamus: A Possible Sleep-Promoting Effect. *J Neurophysiol* **97,** 837-848.

Llewellyn-Smith IJ, Arnolda LF, Pilowsky PM, Chalmers JP & Minson JB. (1998). GABA- and glutamate-immunoreactive synapses on sympathetic preganglionic neurons projecting to the superior cervical ganglion. *J Auton Nerv Syst* **71,** 96-110.

Llewellyn-Smith IJ, Dicarlo SE, Collins HL & Keast JR. (2005). Enkephalin-immunoreactive interneurons extensively innervate sympathetic preganglionic neurons regulating the pelvic viscera. *J Comp Neurol* **488,** 278-289.

Llewellyn-Smith IJ, Martin CL, Marcus JN, Yanagisawa M, Minson JB & Scammell TE. (2003). Orexin-immunoreactive inputs to rat sympathetic preganglionic neurons. *Neurosci Lett* **351,** 115-119.

Llewellyn-Smith IJ, Phend KD, Minson JB, Pilowsky PM & Chalmers JP. (1992). Glutamate-immunoreactive synapses on retrogradely-labelled sympathetic preganglionic neurons in rat thoracic spinal cord. *Brain Res* **581,** 67-80.

Loewy AD. (1981). Raphe pallidus and raphe obscurus projections to the intermediolateral cell column in the rat. *Brain Res* **222,** 129-133.

Loewy AD & Burton H. (1978). Nuclei of the solitary tract: Efferent projections to the lower brain stem and spinal cord of the cat. *J Comp Neurol* **181,** 421-450.

Loewy AD, Marson L & Parkinson D. (1986). Descending noradrenergic pathways involved in the A5 depressor response. *Brain Res* **386,** 313-324.

Lopez M, Senaris R, Gallego R, Garcia-Caballero T, Lago F, Seoane L, Casanueva F & Dieguez C. (1999). Orexin Receptors Are Expressed in the Adrenal Medulla of the Rat. *Endocrinology* **140,** 5991-5994.

Lovick TA & Coote JH. (1988). Electrophysiological properties of paraventriculo-spinal neurones in the rat. *Brain Res* **454,** 123-130.

Lu J, Bjorkum AA, Xu M, Gaus SE, Shiromani PJ & Saper CB. (2002). Selective activation of the extended ventrolateral preoptic nucleus during rapid eye movement sleep. *J Neurosci* **22,** 4568-4576.

Lu X-Y, Bagnol D, Burke S, Akil H & Watson SJ. (2000). Differential distribution and regulation of OX1 and OX2 orexin/hypocretin receptor messenger RNA in the brain upon fasting. *Horm Behav* **37,** 335-344.

Luiten PGM, Ter Horst GJ, Karst H & Steffens AB. (1985). The course of paraventricular hypothalamic efferents to autonomic structures in medulla and spinal cord. *Brain Res* **329,** 374-378.

Lumsden T. (1923). Observations on the respiratory centres in the cat. *J Physiol* **57,** 153-160.

Lund P-E, Shariatmadari R, Uustare A, Detheux M, Parmentier M, Kukkonen JP & Akerman KEO. (2000). The Orexin OX1 Receptor Activates a Novel Ca2+ Influx Pathway Necessary for Coupling to Phospholipase C. *J Biol Chem* **275,** 30806-30812.

Lundin S, Ricksten SE & Thoren P. (1984). Renal sympathetic activity in spontaneously hypertensive rats and normotensive controls, as studied by three different methods. *Acta Physiol Scand* **120,** 265-272.

Luppi PH, Fort P, Kitahama K, Denoroy L & Jouvet M. (1989). Adrenergic input from medullary ventrolateral C1 cells to the nucleus raphe pallidus of the cat, as demonstrated by a double immunostaining technique. *Neurosci Lett* **106,** 29-35.

Ma X, Zubcevic L, Bruning JC, Ashcroft FM & Burdakov D. (2007). Electrical inhibition of identified anorexigenic POMC neurons by orexin/hypocretin. *J Neurosci* **27,** 1529-1533.

Machado BH, Bonagamba LGH, Dun SL, Kwok EH & Dun NJ. (2002). Pressor response to microinjection of orexin/hypocretin into rostral ventrolateral medulla of awake rats. *Regul Pept* **104,** 75-81.

Madden CJ, Ito S, Rinaman L, Wiley RG & Sved AF. (1999). Lesions of the C1 catecholaminergic neurons of the ventrolateral medulla in rats using anti-DbetaH-saporin. *Am J Physiol* **277,** R1063-1075.

Madden CJ & Sved AF. (2003). Cardiovascular regulation after destruction of the C1 cell group of the rostral ventrolateral medulla in rats. *Am J Physiol* **285,** H2734-2748.

Makeham JM, Goodchild AK, Costin NS & Pilowsky PM. (2004). Hypercapnia selectively attenuates the somato-sympathetic reflex. *Respir Physiol Neurobiol* **140,** 133-143.

Makeham JM, Goodchild AK & Pilowsky PM. (2001). NK1 receptor and the ventral medulla of the rat: Bulbospinal and catecholaminergic neurons. *NeuroReport* **12,** 3663-3667.

Makeham JM, Goodchild AK & Pilowsky PM. (2005). NK1 receptor activation in rat rostral ventrolateral medulla selectively attenuates somato-sympathetic reflex while antagonism attenuates sympathetic chemoreflex. *Am J Physiol* **288,** R1707-1715.

Malendowicz LK, Hochol A, Ziolkowska A, Nowak M, Gottardo L & Nussdorfer GG. (2001a). Prolonged orexin administration stimulates steroid-hormone secretion, acting directly on the rat adrenal gland. *Int J Mol Med* **7,** 401-404.

Malendowicz LK, Jedrzejczak N, Belloni AS, Trejter M, Hochol A & Nussdorfer GG. (2001b). Effects of orexins A and B on the secretory and proliferative activity of immature and regenerating rat adrenal glands. *Histol Histopathol* **16,** 713-717.

Malendowicz LK, Tortorella C & Nussdorfer GG. (1999a). Acute effects of orexins A and B on the rat pituitary-adrenocortical axis. *Biomed Res* **20,** 301-304.

Malendowicz LK, Tortorella C & Nussdorfer GG. (1999b). Orexins stimulate corticosterone secretion of rat adrenocortical cells, through the activation of the adenylate cyclase-dependent signaling cascade. *J Steroid Biochem Mol Biol* **70,** 185-188.

Malpas SC. (2010). Sympathetic nervous system overactivity and its role in the development of cardiovascular disease. *Physiol Rev* **90,** 513-557.

Mancia G, Grassi G, Parati G & Zanchetti A. (2000). The sympathetic nervous system in human hypertension. *Rev Port Cardiol* **19** II15-19.

Mann JF, Phillips MI, Dietz R, Haebara H & Ganten D. (1978). Effects of central and peripheral angiotensin blockade in hypertensive rats. *Am J Physiol* **234,** H629–637.

Mansvelder HD & Kits KS. (2000). Calcium channels and the release of large dense core vesicles from neuroendocrine cells: spatial organization and functional coupling. *Prog Neurobiol* **62,** 427-441.

Marcus JN, Aschkenasi CJ, Lee CE, Chemelli RM, Saper CB, Yanagisawa M & Elmquist JK. (2001). Differential expression of Orexin receptors 1 and 2 in the rat brain. *J Comp Neurol* **435,** 6-25.

Marina N, Abdala APL, Korsak A, Simms AE, Allen AM, Paton JFR & Gourine AV. (2011). Control of sympathetic vasomotor tone by catecholaminergic C1 neurones of the rostral ventrolateral medulla oblongata. *Cardiovasc Res* **91,** 703-710.

Masuda N, Terui N, Koshiya N & Kumada M. (1991). Neurons in the caudal ventrolateral medulla mediate the arterial baroreceptor reflex by inhibiting barosensitive reticulospinal neurons in the rostral ventrolateral medulla in rabbits. *J Auton Nerv Syst* **34,** 103-117.

Matsuki T, Nomiyama M, Takahira H, Hirashima N, Kunita S, Takahashi S, Yagami KI, Kilduff TS, Bettler B, Yanagisawa M & Sakurai T. (2009). Selective loss of GABAB receptors in orexin-producing neurons results in disrupted sleep/wakefulness architecture. *Proc Natl Acad Sci U S A* **106,** 4459-4464.

Matsumura K, Tsuchihashi T & Abe I. (2001). Central Orexin-A Augments Sympathoadrenal Outflow in Conscious Rabbits. *Hypertension* **37,** 1382-1387.

Matsuura T, Kumagai H, Kawai A, Onimaru H, Imai M, Oshima N, Sakata K & Saruta T. (2002). Rostral ventrolateral medulla neurons of neonatal Wistar-Kyoto and spontaneously hypertensive rats. *Hypertension* **40,** 560-565.

Mazzocchi G, Malendowicz LK, Gottardo L, Aragona F & Nussdorfer GG. (2001). Orexin A Stimulates Cortisol Secretion from Human Adrenocortical Cells through Activation of the Adenylate Cyclase-Dependent Signaling Cascade. *J Clin Endocrinol Metab* **86,** 778-782.

McAllen RM. (1985). Mediation of the fastigial pressor response and a somatosympathetic reflex by ventral medullary neurones in the cat. *J Physiol* **368,** 423-433.

McAllen RM. (1986). Action and specificity of ventral medullary vasopressor neurones in the cat. *Neuroscience* **18,** 51-59.

McAllen RM. (1987). Central respiratory modulation of subretrofacial bulbospinal neurones in the cat. *J Physiol* **388,** 533-545.

McAllen RM. (1992). Actions of carotid chemoreceptors on subretrofacial bulbospinal neurons in the cat. *J Auton Nerv Syst* **40,** 181-188.

McAllen RM & Spyer KM. (1976). The location of cardiac vagal preganglionic motoneurones in the medulla of the cat. *J Physiol* **258,** 187-204.

McAllen RM & Spyer KM. (1978). Two types of vagal preganglionic motoneurones projecting to the heart and lungs. *J Physiol* **282,** 353-364.

McCall RB. (1988). Effects of putative neurotransmitters on sympathetic preganglionic neurons. *Annu Rev Physiol* **50,** 553-564.

McCall RB & Harris LT. (1987). Sympathetic alterations after midline medullary raphe lesions. *Am J Physiol* **253,** R91-R100.

McCall RB & Humphrey SJ. (1985). Evidence for GABA mediation of sympathetic inhibition evoked from midline medullary depressor sites. *Brain Res* **339,** 356-360.

McCorry LK. (2007). Physiology of the autonomic nervous system. *Am J Pharm Educ* **71,** 78.

McDowall LM & Dampney RAL. (2006). Calculation of threshold and saturation points of sigmoidal baroreflex function curves. *Am J Physiol* **291,** H2003-H2007.

McLachlan EM & Oldfield BJ. (1981). Some observations on the catecholaminergic innervation of the intermediate zone of the thoracolumbar spinal cord of the cat. *J Comp Neurol* **200,** 529-544.

McMullan S, Pathmanandavel K, Pilowsky PM & Goodchild AK. (2008). Somatic nerve stimulation evokes qualitatively different somatosympathetic responses in the cervical and splanchnic sympathetic nerves in the rat. *Brain Res* **1217,** 139-147.

Mifflin SW. (1992). Arterial chemoreceptor input to nucleus tractus solitarius. *Am J Physiol* **263,** R368-375.

Mikkelsen JD, Hauser F, DeLecea L, Sutcliffe JG, Kilduff TS, Calgari C, Pévet P & Simonneaux V. (2001). Hypocretin (orexin) in the rat pineal gland: a central transmitter with effects on noradrenaline-induced release of melatonin. *Eur J Neurosci* **14,** 419-425.

Mileykovskiy BY, Kiyashchenko LI & Siegel JM. (2002). Muscle tone facilitation and inhibition after orexin-A (Hypocretin-1) microinjections into the medial medulla. *J Neurophysiol* **87,** 2480-2489.

Millhorn DE & Eldridge FL. (1986). Role of ventrolateral medulla in regulation of respiratory and cardiovascular systems. *J Appl Physiol* **61,** 1249-1263.

Mills E, Minson J, Drolet G & Chalmers J. (1990). Effect of intrathecal amino acid receptor antagonists on basal blood pressure and pressor responses to brainstem stimulation in normotensive and hypertensive rats. *J Cardiovasc Pharmacol* **15,** 877-883.

Milner TA, Morrison SF, Abate C & Reis DJ. (1988a). Phenylethanolamine N-methyltransferase-containing terminals synapse directly on sympathetic preganglionic neurons in the rat. *Brain Res* **448,** 205-222.

Milner TA, Pickel VM, Abate C, Joh TH & Reis DJ. (1988b). Ultrastructural characterization of substance P-like immunoreactive neurons in the rostral ventrolateral medulla in relation to neurons containing catecholamine-synthesizing enzymes. *J Comp Neurol* **270,** 427-445, 402-425.

Milner TA, Pickel VM & Chan J. (1987). Phenylethanolamine N-methyltransferase-containing neurons in the rostral ventrolateral medulla. II. Synaptic relationships with GABAergic terminals. *Brain Res* **411,** 46-57.

Milner TA, Pickel VM, Morrison SF & Reis DJ. (1989). Adrenergic neurons in the rostral ventrolateral medulla: Ultrastructure and synaptic relations with other transmitter-identified neurons. *Prog Brain Res* **81,** 29-47.

Milner TA, Reis DJ & Giuliano R. (1996). Afferent sources of substance P in the C1 area of the rat rostral ventrolateral medulla. *Neurosci Lett* **205,** 37-40.

Minson J, Arnolda L, Llewellyn-Smith I, Pilowsky P & Chalmers J. (1996). Altered c-*fos* in rostral medulla and spinal cord of spontaneously hypertensive rats. *Hypertension* **27,** 433-441.

Minson J, Llewellyn-Smith I, Neville A, Somogyi P & Chalmers J. (1990). Quantitative analysis of spinally projecting adrenaline-synthesising neurons of C1, C2 and C3 groups in rat medulla oblongata. *J Auton Nerv Syst* **30,** 209-220.

Minson J, Pilowsky P, Llewellyn-Smith I, Kaneko T, Kapoor V & Chalmers J. (1991). Glutamate in spinally projecting neurons of the rostral ventral medulla. *Brain Res* **555,** 326-331.

Minson JB, Chalmers JP, Caon AC & Renaud B. (1987). Separate areas of rat medulla oblongata with populations of serotonin- and adrenaline-containing neurons alter blood pressure after L-glutamate stimulation. *J Auton Nerv Syst* **19,** 39-50.

Minson JB, Llewellyn-Smith IJ, Chalmers JP, Pilowsky PM & Arnolda LF. (1997). c-fos identifies GABA-synthesizing barosensitive neurons in caudal ventrolateral medulla. *Neuroreport* **8,** 3015-3021.

Miura M, Okada J, Takayama K & Jingu H. (1996). Barosensitive and chemosensitive neurons in the rat medulla: a double labeling study with c-Fos/glutamate, GAD, PNMT and calbindin. *J Auton Nerv Syst* **61,** 17-25.

Miura M, Onai T & Takayama K. (1983). Projections of upper structure to the spinal cardioacceleratory center in cats: An HRP study using a new microinjection method. *J Auton Nerv Syst* **7,** 119-139.

Miyagawa M, Chida K, Kawamura H & Takasu T. (1991). Effects of chemical stimulation and lesion of the rostral ventrolateral medulla in spontaneously hypertensive rats. *Neurosci Lett* **132,** 1-4.

Miyawaki T, Goodchild AK & Pilowsky PM. (2001). Rostral ventral medulla 5-HT1A receptors selectively inhibit the somatosympathetic reflex. *Am J Physiol* **280,** R1261-1268.

Miyawaki T, Goodchild AK & Pilowsky PM. (2002a). Activation of mu-opioid receptors in rat ventrolateral medulla selectively blocks baroreceptor reflexes while activation of delta opioid receptors blocks somato-sympathetic reflexes. *Neuroscience* **109,** 133-144.

Miyawaki T, Goodchild AK & Pilowsky PM. (2002b). Evidence for a tonic GABA-ergic inhibition of excitatory respiratory-related afferents to presympathetic neurons in the rostral ventrolateral medulla. *Brain Res* **924,** 56-62.

Miyawaki T, Minson J, Arnolda L, Chalmers J, Llewellyn-Smith I & Pilowsky P. (1996a). Role of excitatory amino acid receptors in cardiorespiratory coupling in ventrolateral medulla. *Am J Physiol* **271,** R1221-1230.

Miyawaki T, Minson J, Arnolda L, Llewellyn-Smith I, Chalmers J & Pilowsky P. (1996b). AMPA/kainate receptors mediate sympathetic chemoreceptor reflex in the rostral ventrolateral medulla. *Brain Res* **726,** 64-68.

Miyawaki T, Pilowsky P, Sun QJ, Minson J, Suzuki S, Arnolda L, Llewellyn-Smith I & Chalmers J. (1995). Central inspiration increases barosensitivity of neurons in rat rostral ventrolateral medulla. *Am J Physiol* **268,** R909-918.

Miyawaki T, Suzuki S, Minson J, Arnolda L, Chalmers J, Llewellyn-Smith I & Pilowsky P. (1997). Role of AMPA/kainate receptors in transmission of the sympathetic baroreflex in rat CVLM. *Am J Physiol* **272,** R800-R812.

Mizusawa A, Ogawa H, Kikuchi Y, Hida W, Kurosawa H, Okabe S, Takishima T & Shirato K. (1994). In vivo release of glutamate in nucleus tractus solitarii of the rat during hypoxia. *J Physiol* **478** 55-66.

Mondal MS, Nakazato M, Date Y, Murakami N, Yanagisawa M & Matsukura S. (1999). Widespread distribution of orexin in rat brain and its regulation upon fasting. *Biochem Biophys Res Commun* **256,** 495-499.

Monteau R & Hilaire G. (1991). Spinal Respiratory Motoneurons. *Prog Neurobiol* **37,** 83-144.

Moon EA, Goodchild AK & Pilowsky PM. (2002). Lateralisation of projections from the rostral ventrolateral medulla to sympathetic preganglionic neurons in the rat. *Brain Res* **929,** 181-190.

Moraes DJA, Bonagamba LGH, Zoccal DB & Machado BH. (2011). Modulation of respiratory responses to chemoreflex activation by L-glutamate and ATP in the rostral ventrolateral medulla of awake rats. *Am J Physiol* **300,** R1476-R1486.

Moreira TS, Takakura AC, Colombari E & Guyenet PG. (2006). Central chemoreceptors and sympathetic vasomotor outflow. *J Physiol* **577,** 369-386.

Moreira TS, Takakura AC, Damasceno RS, Falquetto B, Totola LT, Sobrinho CR, Ragioto DT & Zolezi FP. (2011). Central chemoreceptors and neural mechanisms of cardiorespiratory control. *Braz J Med Biol Res* **44,** 883-889.

Morgado-Valle C, Baca SM & Feldman JL. (2010). Glycinergic pacemaker neurons in preBotzinger complex of neonatal mouse. *J Neurosci* **30,** 3634-3639.

Morilak DA, Drolet G & Chalmers J. (1990a). Cardiovascular effects of opioid antagonist naloxone in rostral ventrolateral medulla of rabbits. *Am J Physiol* **258,** R325-331.

Morilak DA, Drolet G & Chalmers J. (1990b). Tonic opioid inhibition of the pressor region of the rostral ventrolateral medulla of rabbits is mediated by delta receptors. *J Pharmacol Exp Ther* **254,** 671-676.

Morris JL. (1999). Cotransmission from sympathetic vasoconstrictor neurons to small cutaneous arteries in vivo. *Am J Physiol* **277,** H58-64.

Morris KF, Arata A, Shannon R & Lindsey BG. (1996). Long-term facilitation of phrenic nerve activity in cats: responses and short time scale correlations of medullary neurones. *J Physiol* **490,** 463-480.

Morrison SF. (1993). Raphe pallidus excites a unique class of sympathetic preganglionic neurons. *Am J Physiol* **265,** R82-R89.

Morrison SF. (1999). RVLM and raphe differentially regulate sympathetic outflows to splanchnic and brown adipose tissue. *Am J Physiol* **276,** R962-973.

Morrison SF. (2001). Differential control of sympathetic outflow. *Am J Physiol* **281,** R683-698.

Morrison SF. (2003). Glutamate transmission in the rostral ventrolateral medullary sympathetic premotor pathway. *Cell Mol Neurobiol* **23,** 761-772.

Morrison SF, Callaway J, Milner TA & Reis DJ. (1989a). Glutamate in the spinal sympathetic intermediolateral nucleus: Localization by light and electron microscopy. *Brain Res* **503,** 5-15.

Morrison SF & Cao WH. (2000). Different adrenal sympathetic preganglionic neurons regulate epinephrine and norepinephrine secretion. *Am J Physiol* **279,** R1763-1775.

Morrison SF, Ernsberger P, Milner TA, Callaway J, Gong A & Reis DJ. (1989b). A glutamate mechanism in the intermediolateral nucleus mediates sympathoexcitatory responses to stimulation of the rostral ventrolateral medulla. *Prog Brain Res* **81,** 159-169.

Morrison SF & Gebber GL. (1982). Classification of raphe neurons with cardiac-related activity. *Am J Physiol* **12,** R49-R59.

Morrison SF & Gebber GL. (1985). Axonal branching patterns and funicular trajectories of raphespinal sympathoinhibitory neurons. *J Neurophysiol* **53,** 759-772.

Morrison SF, Milner TA & Reis DJ. (1988). Reticulospinal vasomotor neurons of the rat rostral ventrolateral medulla: relationship to sympathetic nerve activity and the C1 adrenergic cell group. *J Neurosci* **8,** 1286-1301.

Morrison SF, Nakamura K & Madden CJ. (2008). Central control of thermogenesis in mammals. *Exp Physiol* **93,** 773-797.

Morrison SF & Reis DJ. (1989). Reticulospinal vasomotor neurons in the RVL mediate the somatosympathetic reflex. *Am J Physiol* **256,** R1084-1097.

Mulkey DK, Stornetta RL, Weston MC, Simmons JR, Parker A, Bayliss DA & Guyenet PG. (2004). Respiratory control by ventral surface chemoreceptor neurons in rats. *Nat Neurosci* **7,** 1360-1369.

Muraki Y, Yamanaka A, Tsujino N, Kilduff TS, Goto K & Sakurai T. (2004). Serotonergic Regulation of the Orexin/Hypocretin Neurons through the 5-HT1A Receptor. *J Neurosci* **24,** 7159-7166.

Muroya S, Funahashi H, Yamanaka A, Kohno D, Uramura K, Nambu T, Shibahara M, Kuramochi M, Takigawa M, Yanagisawa M, Sakurai T, Shioda S & Yada T. (2004). Orexins (hypocretins) directly interact with neuropeptide Y, POMC and glucose-responsive neurons to regulate Ca^{2+} signaling in a reciprocal manner to leptin: orexigenic neuronal pathways in the mediobasal hypothalamus. *Eur J Neurosci* **19,** 1524-1534.

Nakamura A, Zhang W, Yanagisawa M, Fukuda Y & Kuwaki T. (2007). Vigilance state-dependent attenuation of hypercapnic chemoreflex and exaggerated sleep apnea in orexin knockout mice. *J Appl Physiol* **102,** 241-248.

Nakamura K, Wu SX, Fujiyama F, Okamoto K, Hioki H & Kaneko T. (2004). Independent inputs by VGLUT2- and VGLUT3-positive glutamatergic terminals onto rat sympathetic preganglionic neurons. *Neuroreport* **15,** 431-436.

Nakamura T, Uramura K, Nambu T, Yada T, Goto K, Yanagisawa M & Sakurai T. (2000). Orexin-induced hyperlocomotion and stereotypy are mediated by the dopaminergic system. *Brain Res* **873,** 181-187.

Nakaya Y, Kaneko T, Shigemoto R, Nakanishi S & Mizuno N. (1994). Immunohistochemical localization of substance P receptor in the central nervous system of the adult rat. *J Comp Neurol* **347,** 249-274.

Nambu T, Sakurai T, Mizukami K, Hosoya Y, Yanagisawa M & Goto K. (1999). Distribution of orexin neurons in the adult rat brain. *Brain Res* **827,** 243-260.

Nanmoku T, Isobe K, Sakurai T, Yamanaka A, Takekoshi K, Kawakami Y, Goto K & Nakai T. (2002). Effects of orexin on cultured porcine adrenal medullary and cortex cells. *Regul Pept* **104,** 125-130.

Narita M, Nagumo Y, Hashimoto S, Narita M, Khotib J, Miyatake M, Sakurai T, Yanagisawa M, Nakamachi T, Shioda S & Suzuki T. (2006). Direct Involvement of Orexinergic Systems in the Activation of the Mesolimbic Dopamine Pathway and Related Behaviors Induced by Morphine. *J Neurosci* **26,** 398-405.

Näslund E, Ehrström M, Ma J, Hellström PM & Kirchgessner AL. (2002). Localization and effects of orexin on fasting motility in the rat duodenum. *Am J Physiol* **282,** G470-G479.

Nattie E & Li A. (2000). Muscimol dialysis in the retrotrapezoid nucleus region inhibits breathing in the awake rat. *J Appl Physiol* **89,** 153-162.

Nattie E & Li A. (2006a). Central chemoreception 2005: a brief review. *Auton Neurosci* **126-127,** 332-338.

Nattie E & Li A. (2006b). Neurokinin-1 receptor-expressing neurons in the ventral medulla are essential for normal central and peripheral chemoreception in the conscious rat. *J Appl Physiol* **101,** 1596-1606.

Nattie E, Shi J & Li A. (2001). Bicuculline dialysis in the retrotrapezoid nucleus (RTN) region stimulates breathing in the awake rat. *Respir Physiol* **124,** 179-193.

Nattie EE & Li A. (1994). Retrotrapezoid nucleus glutamate injections: long-term stimulation of phrenic activity. *J Appl Physiol* **76,** 760-772.

Nattie EE & Li A. (2001). CO2 dialysis in the medullary raphe of the rat increases ventilation in sleep. *J Appl Physiol* **90,** 1247-1257.

Nattie EE & Li A. (2002a). CO_2 dialysis in nucleus tractus solitarius region of rat increases ventilation in sleep and wakefulness. *J Appl Physiol* **92,** 2119-2130.

Nattie EE & Li A. (2002b). Substance P-saporin lesion of neurons with NK1 receptors in one chemoreceptor site in rats decreases ventilation and chemosensitivity. *J Physiol* **544,** 603-616.

Nowak KW, MaÄ‡kowiak P, ÅšwitoÅ„ska MgM, FabiÅ› M & Malendowicz LK. (1999). Acute orexin effects on insulin secretion in the rat: in vivo and in vitro studies. *Life Sci* **66,** 449-454.

Nunez-Abades PA, Pasaro R & Bianchi AL. (1991). Localization of Respiratory Bulbospinal and Propriobulbar Neurons in the Region of the Nucleus Ambiguus of the Rat. *Brain Res* **568,** 165-172.

O'Sullivan RJ, Brown IG & Pender MP. (2008). Apneusis responding to buspirone in multiple sclerosis. *Mult Scler* **14,** 705-707.

Oikawa S, Hirakawa H, Kusakabe T, Nakashima Y & Hayashida Y. (2005). Autonomic cardiovascular responses to hypercapnia in conscious rats: the roles of the chemo- and baroreceptors. *Auton Neurosci* **117,** 105-114.

Okamoto K & Aoki K. (1963). Development of a strain of spontaneously hypertensive rats. *Jpn Circ J* **27,** 282-293.

Okumura T, Takeuchi S, Motomura W, Yamada H, Egashira S-i, Asahi S, Kanatani A, Ihara M & Kohgo Y. (2001). Requirement of Intact Disulfide Bonds in Orexin-A-Induced Stimulation of Gastric Acid Secretion That Is Mediated by OX1 Receptor Activation. *Biochem Biophys Res Commun* **280,** 976-981.

Oldfield BJ, Davern PJ, Giles ME, Allen AM, Badoer E & McKinley MJ. (2001). Efferent neural projections of angiotensin receptor (AT1) expressing neurones in the hypothalamic paraventricular nucleus of the rat. *J Neuroendocrinol* **13,** 139-146.

Oldfield BJ & McLachlan EM. (1981). An analysis of the sympathetic preganglionic neurons projecting from the upper thoracic spinal roots of the cat. *J Comp Neurol* **196,** 329-345.

Olivan MV, Bonagamba LGH & Machado BH. (2001). Involvement of the paraventricular nucleus of the hypothalamus in the pressor response to chemoreflex activation in awake rats. *Brain Res* **895,** 167-172.

Oshima N, Kumagai H, Onimaru H, Kawai A, Pilowsky PM, Iigaya K, Takimoto C, Hayashi K, Saruta T & Itoh H. (2008). Monosynaptic excitatory connection from the rostral ventrolateral medulla to sympathetic preganglionic neurons revealed by simultaneous recordings. *Hypertens Res* **31,** 1445-1454.

Oshima N, McMullan S, Goodchild AK & Pilowsky PM. (2006). A monosynaptic connection between baroinhibited neurons in the RVLM and IML in Sprague-Dawley rats. *Brain Res* **1089,** 153-161.

Oudit GY, Crackower MA, Backx PH & Penninger JM. (2003). The role of ACE2 in cardiovascular physiology. *Trends Cardiovasc Med* **13,** 93-101.

Padley JR, Kumar NN, Li Q, Nguyen TB, Pilowsky PM & Goodchild AK. (2007). Central command regulation of circulatory function mediated by descending pontine cholinergic inputs to sympathoexcitatory rostral ventrolateral medulla neurons. *Circ Res* **100,** 284-291.

Padley JR, Li Q, Pilowsky PM & Goodchild AK. (2003). Cannabinoid receptor activation in the rostral ventrolateral medulla oblongata evokes cardiorespiratory effects in anaesthetised rats. *Br J Pharmacol* **140,** 384-394.

Pagani FD, Taveira da Silva AM, Hamosh P, Garvey TQ, 3rd & Gillis RA. (1982). Respiratory and cardiovascular effects of intraventricular cholecystokinin. *Eur J Pharmacol* **78,** 129-132.

Palatini P. (2001). Sympathetic overactivity in hypertension: a risk factor for cardiovascular disease. *Curr Hypertens Rep* **3,** S3-9.

Pardal R & Lopez-Barneo J. (2002). Low glucose-sensing cells in the carotid body. *Nat Neurosci* **5,** 197-198.

Patel KP & Schmid PG. (1988). Role of paraventricular nucleus (PVH) in baroreflex-mediated changes in lumbar sympathetic nerve activity and heart rate. *J Auton Nerv Syst* **22,** 211-219.

Petras JM & Cummings JF. (1972). Autonomic neurons in the spinal cord of the Rhesus monkey: a correlation of the findings of cytoarchitectonics and sympathectomy with fiber degeneration following dorsal rhizotomy. *J Comp Neurol* **146,** 189-218.

Petrov T, Krukoff TL & Jhamandas JH. (1993). Branching projections of catecholaminergic brainstem neurons to the paraventricular hypothalamic nucleus and the central nucleus of the amygdala in the rat. *Brain Res* **609,** 81-92.

Peyron C, Faraco J, Rogers W, Ripley B, Overeem S, Charnay Y, Nevsimalova S, Aldrich M, Reynolds D, Albin R, Li R, Hungs M, Pedrazzoli M, Padigaru M, Kucherlapati M, Fan J, Maki R, Lammers GJ,

Bouras C, Kucherlapati R, Nishino S & Mignot E. (2000). A mutation in a case of early onset narcolepsy and a generalized absence of hypocretin peptides in human narcoleptic brains. *Nat Med* **6,** 991-997.

Peyron C, Tighe DK, van den Pol AN, de Lecea L, Heller HC, Sutcliffe JG & Kilduff TS. (1998). Neurons containing Hypocretin (Orexin) project to multiple neuronal systems. *J Neurosci* **18,** 9996-10015.

Phillips JK, Goodchild AK, Dubey R, Sesiashvili E, Takeda M, Chalmers J, Pilowsky PM & Lipski J. (2001). Differential expression of catecholamine biosynthetic enzymes in the rat ventrolateral medulla. *J Comp Neurol* **432,** 20-34.

Pick J. (1970). *The Autonomic Nervous System: Morphological, Comparative, Clinical and Surgical Aspects*. Philadelphia: J.B. Lippincott Company

Pickering AE, Simms AE & Paton JF. (2008). Dominant role of aortic baroreceptors in the cardiac baroreflex of the rat in situ. *Autonomic neuroscience : basic & clinical* **142,** 32-39.

Pieribone VA & Aston-Jones G. (1991). Adrenergic innervation of the rat nucleus locus coeruleus arises predominantly from the C1 adrenergic cell group in the rostral medulla. *Neuroscience* **41,** 525-542.

Pilowsky P. (1995). Good vibrations? Respiratory rhythms in the central control of blood pressure. *Clin Exp Pharmacol Physiol* **22,** 594-604.

Pilowsky P, Arnolda L, Chalmers J, Llewellyn-Smith I, Minson J, Miyawaki T & Sun QJ. (1996). Respiratory inputs to central cardiovascular neurons. *Ann N Y Acad Sci* **783,** 64-70.

Pilowsky P, Llewellyn-Smith IJ, Arnolda L, Minson J & Chalmers J. (1994a). Intracellular recording from sympathetic preganglionic neurons in cat lumbar spinal cord. *Brain Res* **656,** 319-328.

Pilowsky P, Llewellyn-Smith IJ, Lipski J & Chalmers J. (1992). Substance P immunoreactive boutons form synapses with feline sympathetic preganglionic neurons. *J Comp Neurol* **320,** 121-135.

Pilowsky P, Llewellyn-Smith IJ, Lipski J, Minson J, Arnolda L & Chalmers J. (1994b). Projections from inspiratory neurons of the ventral respiratory group to the subretrofacial nucleus of the cat. *Brain Res* **633,** 63-71.

Pilowsky P, Minson J, Hodgson A, Howe P & Chalmers J. (1986). Does substance P coexist with adrenaline in neurones of the rostral ventrolateral medulla in the rat? *Neurosci Lett* **71,** 293-298.

Pilowsky P, West M & Chalmers J. (1985). Renal sympathetic nerve responses to stimulation, inhibition and destruction of the ventrolateral medulla in the rabbit. *Neurosci Lett* **60,** 51-55.

Pilowsky PM, Abbott SB, Burke PG, Farnham MM, Hildreth CM, Kumar NN, Li Q, Lonergan T, McMullan S, Spirovski D & Goodchild AK. (2008). Metabotropic neurotransmission and integration of sympathetic nerve activity by the rostral ventrolateral medulla in the rat. *Clin Exp Pharmacol Physiol* **35,** 508-511.

Pilowsky PM & Goodchild AK. (2002). Baroreceptor reflex pathways and neurotransmitters: 10 years on. *J Hypertens* **20,** 1675-1688.

Pilowsky PM, Jiang C & Lipski J. (1990). An intracellular study of respiratory neurons in the rostral ventrolateral medulla of the rat and their relationship to catecholamine-containing neurons. *J Comp Neurol* **301,** 604-617.

Pilowsky PM, Lung MSY, Spirovski D & McMullan S. (2009). Differential regulation of the central neural cardiorespiratory system by metabotropic neurotransmitters. *Philos Trans R Soc Lond B Biol Sci* **364,** 2537-2552.

Pilowsky PM, Miyawaki T, Minson JB, Sun QJ, Arnolda LF, Llewellyn-Smith IJ & Chalmers JP. (1995). Bulbospinal sympatho-excitatory neurons in the rat caudal raphe. *J Hypertens* **13,** 1618-1623.

Pilowsky PM, Morris MJ, Minson JB, West MJ, Chalmers JP, Willoughby JO & Blessing WW. (1987). Inhibition of vasodepressor neurons in the caudal ventrolateral medulla of the rabbit increases both arterial pressure and the release of neuropeptide Y-like immunoreactivity from the spinal cord. *Brain Res* **420,** 380-384.

Polson JW, Halliday GM, McAllen RM, Coleman MJ & Dampney RA. (1992). Rostrocaudal differences in morphology and neurotransmitter content of cells in the subretrofacial vasomotor nucleus. *J Auton Nerv Syst* **38,** 117-137.

Poree LR & Schramm LP. (1992). Interaction between medullary and cervical regulation of renal sympathetic activity. *Brain Res* **599,** 297-301.

Porter JP & Brody MJ. (1985). Neural projections from paraventricular nucleus that subserve vasomotor functions. *Am J Physiol* **17,** R271-281.

Potts JT & Mitchell JH. (1998). Synchronization of somato-sympathetic outflows during exercise: role for a spinal rhythm generator. *J Physiol (Lond)* **508,** 646.

Poulat P, Marlier L, Rajaofetra N & Privat A. (1992). 5-Hydroxytryptamine, substance P and thyrotropin-releasing hormone synapses in the intermediolateral cell column of the rat thoracic spinal cord. *Neurosci Lett* **136,** 19-22.

Powley TL, Wang XY, Fox EA, Phillips RJ, Liu LW & Huizinga JD. (2008). Ultrastructural evidence for communication between intramuscular vagal mechanoreceptors and interstitial cells of Cajal in the rat fundus. *Neurogastroenterol Motil* **20,** 69-79.

Prabhakar NR & Peng YJ. (2004). Peripheral chemoreceptors in health and disease. *J Appl Physiol* **96,** 359-366.

Putnam RW, Filosa JA & Ritucci NA. (2004). Cellular mechanisms involved in CO2 and acid signaling in chemosensitive neurons. *Am J Physiol* **287,** C1493-C1526.

Pyner S & Coote JH. (1994). Evidence that sympathetic preganglionic neurones are arranged in target- specific columns in the thoracic spinal cord of the rat. *J Comp Neurol* **342,** 15-22.

Pyner S & Coote JH. (1998). Rostroventrolateral medulla neurons preferentially project to target-specified sympathetic preganglionic neurons. *Neuroscience* **83,** 617-631.

Rahman AA, Shahid IZ, Fong AY, Hammond AM & Pilowsky PM. (2012a). Vasostatin I (CgA_{17-76}) vasoconstricts rat splanchnic vascular bed but does not affect central cardiovascular function. *Auton Neurosci* **166,** 22-28.

Rahman AA, Shahid IZ & Pilowsky PM. (2011). Intrathecal neuromedin U induces biphasic effects on sympathetic vasomotor tone, increases respiratory drive and attenuates sympathetic reflexes in rat. *Br J Pharmacol* **164,** 617-631.

Rahman AA, Shahid IZ & Pilowsky PM. (2012b). Differential cardiorespiratory and sympathetic reflex responses to microinjection of neuromedin U in rat rostral ventrolateral medulla. *J Pharmacol Exp Ther* **341,** 213-224.

Rahmouni K, Correia MLG, Haynes WG & Mark AL. (2005). Obesity-associated hypertension: new insights into mechanisms. *Hypertension* **45,** 9-14.

Ramirez JM, Tryba AK & Pena F. (2004). Pacemaker neurons and neuronal networks: an integrative view. *Curr Opin Neurobiol* **14,** 665-674.

Randeva HS, Karteris E, Grammatopoulos D & Hillhouse EW. (2001). Expression of Orexin-A and Functional Orexin Type 2 Receptors in the Human Adult Adrenals: Implications for Adrenal Function and Energy Homeostasis. *J Clin Endocrinol Metab* **86,** 4808-4813.

Reja V, Goodchild AK, Phillips JK & Pilowsky PM. (2002a). Tyrosine hydroxylase gene expression in ventrolateral medulla oblongata of WKY and SHR: A quantitative real-time polymerase chain reaction study. *Auton Neurosci* **98,** 79-84.

Reja V, Goodchild AK & Pilowsky PM. (2002b). Catecholamine-related gene expression correlates with blood pressures in SHR. *Hypertension* **40,** 342-347.

Renaud B, Joh TH & Reis DJ. (1979). An abnormal regulation of tyrosine hydroxylase restricted to one catecholamine nucleus in the brain stem of spontaneously hypertensive rats. *Brain Res* **173,** 164-167.

Richardson RJ, Grkovic I, Allen AM & Anderson CR. (2006). Separate neurochemical classes of sympathetic postganglionic neurons project to the left ventricle of the rat heart. *Cell Tissue Res* **324,** 9-16.

Richter DW. (1982). Generation and maintenance of the respiratory rhythm. *J Exp Biol* **100,** 93-107.

Richter DW, Bischoff A, Anders K, Bellingham M & Windhorst U. (1991). Response of the medullary respiratory network of the cat to hypoxia. *J Physiol* **443,** 231-256.

Richter DW & Spyer KM. (2001). Studying rhythmogenesis of breathing: comparison of in vivo and in vitro models. *Trends Neurosci* **24,** 464-472.

Riphagen CL & Pittman QJ. (1989). Mechanisms underlying the cardiovascular responses to intrathecal vasopressin administration in rats. *Can J Physiol Pharmacol* **67,** 269-275.

Ripley B, Fujiki N, Okura M, Mignot E & Nishino S. (2001). Hypocretin Levels in Sporadic and Familial Cases of Canine Narcolepsy. *Neurobiol Dis* **8,** 525-534.

Rodgers RJ, Halford JCG, Nunes de Souza RL, Canto de Souza AL, Piper DC, Arch JRS, Upton N, Porter RA, Johns A & Blundell JE. (2001). SB-334867, a selective orexin-1 receptor antagonist, enhances behavioural satiety and blocks the hyperphagic effect of orexin-A in rats. *Eur J Neurosci* **13,** 1444-1452.

Rosin DL, Chang DA & Guyenet PG. (2006). Afferent and efferent connections of the rat retrotrapezoid nucleus. *J Comp Neurol* **499,** 64-89.

Ross CA, Armstrong DM, Ruggiero DA, Pickel VM, Joh TH & Reis DJ. (1981). Adrenaline neurons in the rostral ventrolateral medulla innervate thoracic spinal cord: a combined immunocytochemical and retrograde transport demonstration. *Neurosci Lett* **25,** 257-262.

Ross CA, Ruggiero DA, Joh TH, Park DH & Reis DJ. (1984a). Rostral ventrolateral medulla: selective projections to the thoracic autonomic cell column from the region containing C1 adrenaline neurons. *J Comp Neurol* **228,** 168-185.

Ross CA, Ruggiero DA, Park DH, Joh TH, Sved AF, Fernandez-Pardal J, Saavedra JM & Reis DJ. (1984b). Tonic vasomotor control by the rostral ventrolateral medulla: effect of electrical or chemical stimulation of the area containing C1 adrenaline neurons on arterial pressure, heart rate, and plasma catecholamines and vasopressin. *J Neurosci* **4,** 474-494.

Ross CA, Ruggiero DA & Reis DJ. (1985). Projections from the nucleus tractus solitarii to the rostral ventrolateral medulla. *J Comp Neurol* **242,** 511-534.

Ruggiero DA, Cravo SL, Arango V & Reis DJ. (1989). Central control of the circulation by the rostral ventrolateral reticular nucleus: Anatomical substrates. *Prog Brain Res* **81,** 49-79.

Ruggiero DA, Cravo SL, Golanov E, Gomez R, Anwar M & Reis DJ. (1994). Adrenergic and non-adrenergic spinal projections of a cardiovascular-active pressor area of medulla oblongata: quantitative topographic analysis. *Brain Res* **663,** 107-120.

Rumantir MS, Kaye DM, Jennings GL, Vaz M, Hastings JA & Esler MD. (2000). Phenotypic evidence of faulty neuronal norepinephrine reuptake in essential hypertension. *Hypertension* **36,** 824-829.

Russell SH, Kim MS, Small CJ, Abbott CR, Morgan DGA, Taheri S, Murphy KG, Todd JF, Ghatei MA & Bloom SR. (2000). Central Administration of Orexin A Suppresses Basal and Domperidone Stimulated Plasma Prolactin. *J Neuroendocrinol* **12,** 1213-1218.

Rybak IA, Shevtsova NA, Paton JF, Dick TE, St-John WM, Morschel M & Dutschmann M. (2004). Modeling the ponto-medullary respiratory network. *Resp Physiol Neurobiol* **143,** 307-319.

Saito Y, Tanaka I & Ezure K. (2002). Morphology of the decrementing expiratory neurons in the brainstem of the rat. *Neurosci Res* **44,** 141-153.

Sakao S, Tatsumi K & Voelkel NF. (2009). Endothelial cells and pulmonary arterial hypertension: Apoptosis, proliferation, interaction and transdifferentiation. *Respir Res* **10,** 95.

Sakima A, Yamazato M, Sesoko S, Muratani H & Fukiyama K. (2000). Cardiovascular and sympathetic Effects of L-glutamate and glycine injected into the rostral ventrolateral medulla of conscious rats. *Hypertens Res* **23,** 633-641.

Sakurai T. (2005). Reverse pharmacology of orexin: from an orphan GPCR to integrative physiology. *Regul Pept* **126,** 3-10.

Sakurai T. (2007). The neural circuit of orexin (hypocretin): maintaining sleep and wakefulness. *Nat Rev Neurosci* **8,** 171-181.

Sakurai T, Amemiya A, Ishii M, Matsuzaki I, Chemelli RM, Tanaka H, Williams SC, Richarson JA, Kozlowski GP, Wilson S, Arch JR, Buckingham RE, Haynes AC, Carr SA, Annan RS, McNulty DE, Liu WS, Terrett JA, Elshourbagy NA, Bergsma DJ & Yanagisawa M. (1998). Orexins and orexin receptors: a family of hypothalamic neuropeptides and G protein-coupled receptors that regulate feeding behavior. *Cell* **92**.

Sakurai T, Moriguchi T, Furuya K, Kajiwara N, Nakamura T, Yanagisawa M & Goto K. (1999). Structure and Function of Human Prepro-orexin Gene. *J Biol Chem* **274,** 17771-17776.

Sakurai T, Nagata R, Yamanaka A, Kawamura H, Tsujino N, Muraki Y, Kageyama H, Kunita S, Takahashi S, Goto K, Koyama Y, Shioda S & Yanagisawa M. (2005). Input of Orexin/Hypocretin Neurons Revealed by a Genetically Encoded Tracer in Mice. *Neuron* **46,** 297-308.

Samson WK, Gosnell B, Chang JK, Resch ZT & Murphy TC. (1999). Cardiovascular regulatory actions of the hypocretins in brain. *Brain Res* **831,** 248-253.

Sapru HN & Krieger AJ. (1977). Carotid and aortic chemoreceptor function in the rat. *Journal of applied physiology* **42,** 344-348.

Sartor DM & Verberne AJ. (2003). Phenotypic identification of rat rostroventrolateral medullary presympathetic vasomotor neurons inhibited by exogenous cholecystokinin. *J Comp Neurol* **465,** 467-479.

Sasek CA & Helke CJ. (1989). Enkephalin-immunoreactive neuronal projections from the medulla oblongata to the intermediolateral cell column: Relationship to substance P-immunoreactive neurons. *J Comp Neurol* **287,** 484-494.

Sato A & Schmidt RF. (1973). Somatosympathetic reflexes: afferent fibers, central pathways, discharge characteristics. *Physiol Rev* **53,** 916-947.

Sawchenko PE & Swanson LW. (1982). The organization of noradrenergic pathways from the brainstem to the paraventricular and supraoptic nuclei in the rat. *Brain Res* **257,** 275-325.

Sawchenko PE, Swanson LW, Grzanna R, Howe PR, Bloom SR & Polak JM. (1985). Colocalization of neuropeptide Y immunoreactivity in brainstem catecholaminergic neurons that project to the paraventricular nucleus of the hypothalamus. *J Comp Neurol* **241,** 138-153.

Schafer MK, Eiden LE & Weihe E. (1998). Cholinergic neurons and terminal fields revealed by immunohistochemistry for the vesicular acetylcholine transporter. II. The peripheral nervous system. *Neuroscience* **84,** 361-376.

Schmidt RF & Schönfuss K. (1970). An analysis of the reflex activity in the cervical sympathetic trunk induced by myelinated somatic afferents. *Pflugers Arch* **314,** 175-198.

Schouenborg J & Kalliomaki J. (1990). Functional organization of the nociceptive withdrawal reflexes. I. Activation of hindlimb muscles in the rat. *Exp Brain Res* **83,** 67-78.

Schramm LP, Strack AM, Platt KB & Loewy AD. (1993). Peripheral and central pathways regulating the kidney: a study using pseudorabies virus. *Brain Res* **616,** 251-262.

Schreihofer AM & Guyenet PG. (1997). Identification of C1 presympathetic neurons in rat rostral ventrolateral medulla by juxtacellular labeling in vivo. *J Comp Neurol* **387,** 524-536.

Schreihofer AM & Guyenet PG. (2000). Sympathetic reflexes after depletion of bulbospinal catecholaminergic neurons with anti-DBH-saporin. *Am J Physiol* **279,** R729-742.

Schreihofer AM & Guyenet PG. (2002). The baroreflex and beyond: control of sympathetic vasomotor tone by gabaergic neurons in the ventrolateral medulla. *Clin Exp Pharmacol Physiol* **29,** 514-521.

Schreihofer AM & Guyenet PG. (2003). Baro-activated neurons with pulse-modulated activity in the rat caudal ventrolateral medulla express GAD67 mRNA. *J Neurophysiol* **89,** 1265-1277.

Schreihofer AM, Stornetta RL & Guyenet PG. (1999). Evidence for glycinergic respiratory neurons: Botzinger neurons express mRNA for glycinergic transporter 2. *J Comp Neurol* **407,** 583-597.

Schreihofer AM, Stornetta RL & Guyenet PG. (2000). Regulation of sympathetic tone and arterial pressure by rostral ventrolateral medulla after depletion of C1 cells in rat. *J Physiol* **529 Pt 1,** 221-236.

Seedat YK. (2009). Perspectives on research in hypertension. *Cardiovasc J Afr* **20,** 39–42.

Seller H. (1996). Carl Ludwig and the localization of the medullary vasomotor center: old and new concepts of the generation of sympathetic tone. *Pflugers Arch* **432,** R94-98.

Seyedabadi M, Li Q, Padley JR, Pilowsky PM & Goodchild AK. (2006). A novel pressor area at the medullo-cervical junction that is not dependent on the RVLM: efferent pathways and chemical mediators. *J Neurosci* **26,** 5420-5427.

Shahid IZ & Pilowsky PM. (2010). Intrathecal orexin A increases sympathetic outflow and respiratory drive and modulates physiological reflexes. In *ANS/AuPS 2010, January 31-February 3*, pp. 132. Sydney, Australia.

Shahid IZ, Rahman AA & Pilowsky PM. (2011). Intrathecal orexin A increases sympathetic outflow and respiratory drive, enhances baroreflex sensitivity and blocks the somato-sympathetic reflex. *Br J Pharmacol* **162,** 961-973.

Shahid IZ, Rahman AA & Pilowsky PM. (2012a). Orexin A in rat rostral ventrolateral medulla is pressor, sympathoexcitatory, increases barosensitivity and attenuates the somatosympathetic reflex. *Br J Pharmacol* **165,** 2292–2303.

Shahid IZ, Rahman AA & Pilowsky PM. (2012b). Orexin and Central Regulation of Cardiorespiratory System. *Vitam Horm* **89,** 159-184.

Shcherbin YI & Tsyrlin VA. (2004). Comparison of the somatosympathetic reflex in normotensive and spontaneously hypertensive rats. *Neurosci Behav Physiol* **34,** 563-567.

Shen E & Dun NJ. (1990). Neonate rat sympathetic preganglionic neurons intracellularly labelled with lucifer yellow in thin spinal cord slices. *J Auton Nerv Syst* **29,** 247–254.

Sherin JE, Elmquist JK, Torrealba F & Saper CB. (1998). Innervation of histaminergic tuberomammillary neurons by GABAergic and galaninergic neurons in the ventrolateral preoptic nucleus of the rat. *J Neurosci* **18,** 4705-4721.

Shi H, Lewis DI & Coote JH. (1988). Effects of activating spinal alpha-adrenoreceptors on sympathetic nerve activity in the rat. *J Auton Nerv Syst* **23,** 69-78.

Shibahara M, Sakurai T, Nambu T, Takenouchi T, Iwaasa H, Egashira S-I, Ihara M & Goto K. (1999). Structure, tissue distribution, and pharmacological characterization of Xenopus orexins. *Peptides* **20,** 1169-1176.

Shih CD & Chuang YC. (2007). Nitric oxide and GABA mediate bi-directional cardiovascular effects of orexin in the nucleus tractus solitarii of rats. *Neuroscience* **149,** 625-635.

Shirasaka T, Nakazato M, Matsukura S, Takasaki M & Kannan H. (1999). Sympathetic and cardiovascular actions of orexins in conscious rats. *Am J Physiol* **277,** R1780-1785.

Simms AE, Paton JF & Pickering AE. (2007). Hierarchical recruitment of the sympathetic and parasympathetic limbs of the baroreflex in normotensive and spontaneously hypertensive rats. *J Physiol* **579,** 473-486.

Simms AE, Paton JF, Pickering AE & Allen AM. (2009). Amplified respiratory-sympathetic coupling in the spontaneously hypertensive rat: does it contribute to hypertension? *J Physiol* **587,** 597-610.

Smart D, Jerman JC, Brough SJ, Neville WA, Jewitt F & Porter RA. (2000). The hypocretins are weak agonists at recombinant human orexin-1 and orexin-2 receptors. *Br J Pharmacol* **129,** 1289-1291.

Smart D, Jerman JC, Brough SJ, Rushton SL, Murdock PR, Jewitt F, Elshourbagy NA, Ellis CE, Middlemiss DN & Brown F. (1999). Characterization of recombinant human orexin receptor pharmacology in a Chinese hamster ovary cell-line using FLIPR. *Br J Pharmacol* **128,** 1-3.

Smith JC, Abdala APL, Rybak IA & Paton JFR. (2009). Structural and functional architecture of respiratory networks in the mammalian brainstem. *Philos Trans R Soc Lond B Biol Sci* **364,** 2577-2587.

Smith JC, Butera RJ, Koshiya N, Del Negro C, Wilson CG & Johnson SM. (2000). Respiratory rhythm generation in neonatal and adult mammals: the hybrid pacemaker-network model. *Respir Physiol* **122,** 131-147.

Smith JC, Morrison DE, Ellenberger HH, Otto MR & Feldman JL. (1989). Brainstem projections to the major respiratory neuron populations in the medulla of the cat. *J Comp Neurol* **281,** 69-96.

Smith JE, Jansen AS, Gilbey MP & Loewy AD. (1998). CNS cell groups projecting to sympathetic outflow of tail artery: neural circuits involved in heat loss in the rat. *Brain Res* **786,** 153-164.

Smith PM, Connolly BC & Ferguson AV. (2002). Microinjection of orexin into the rat nucleus tractus solitarius causes increases in blood pressure. *Brain Res* **950,** 261-267.

Solomon IC. (2002). Modulation of expiratory motor output evoked by chemical activation of pre-Botzinger complex in vivo. *Respir Physiol Neurobiol* **130,** 235-251.

Solomon IC, Edelman NH & O'Neal MH, 3rd. (2000). CO(2)/H(+) chemoreception in the cat pre-Botzinger complex in vivo. *J Appl Physiol* **88,** 1996-2007.

Song K, Allen AM, Paxinos G & Mendelsohn FAO. (1992). Mapping of angiotensin II receptor subtype heterogeneity in rat brain. *J Comp Neurol* **316,** 467-484.

St-John WM. (1998). Neurogenesis of patterns of automatic ventilatory activity. *Prog Neurobiol* **56,** 97-117.

St-John WM & Bianchi AL. (1985). Responses of bulbospinal and laryngeal respiratory neurons to hypercapnia and hypoxia. *J Appl Physiol* **59,** 1201-1207.

Stas S, El-Atat F & Sowers J. (2004). Pathogenesis of hypertension in diabetes. *Rev Endocr Metab Disord* **5,** 221-225.

Stasinopoulos T, Goodchild AK, Christie MJ, Chalmers J & Pilowsky PM. (2000). Delta opioid receptor immunoreactive boutons appose bulbospinal CI neurons in the rat. *Neuroreport* **11,** 887-891.

Stocker SD, Simmons JR, Stornetta RL, Toney GM & Guyenet PG. (2006). Water deprivation activates a glutamatergic projection from the hypothalamic paraventricular nucleus to the rostral ventrolateral medulla. *J Comp Neurol* **494,** 673-685.

Stornetta RL, Akey PJ & Guyenet PG. (1999). Location and electrophysiological characterization of rostral medullary adrenergic neurons that contain neuropeptide Y mRNA in rat medulla. *J Comp Neurol* **415,** 482-500.

Stornetta RL, McQuiston TJ & Guyenet PG. (2004). GABAergic and glycinergic presympathetic neurons of rat medulla oblongata identified by retrograde transport of pseudorabies virus and in situ hybridization. *J Comp Neurol* **479,** 257-270.

Stornetta RL, Moreira TS, Takakura AC, Kang BJ, Chang DA, West GH, Brunet JF, Mulkey DK, Bayliss DA & Guyenet PG. (2006). Expression of Phox2b by brainstem neurons involved in chemosensory integration in the adult rat. *J Neurosci* **26,** 10305-10314.

Stornetta RL, Morrison SF, Ruggiero DA & Reis DJ. (1989). Neurons of rostral ventrolateral medulla mediate somatic pressor reflex. *Am J Physiol* **256,** R448-462.

Stornetta RL, Schreihofer AM, Pelaez NM, Sevigny CP & Guyenet PG. (2001). Preproenkephalin mRNA is expressed by C1 and non-C1 barosensitive bulbospinal neurons in the rostral ventrolateral medulla of the rat. *J Comp Neurol* **435,** 111-126.

Stornetta RL, Sevigny CP & Guyenet PG. (2002). Vesicular glutamate transporter DNPI/VGLUT2 mRNA is present in C1 and several other groups of brainstem catecholaminergic neurons. *J Comp Neurol* **444,** 191-206.

Stornetta RL, Sevigny CP & Guyenet PG. (2003). Inspiratory augmenting bulbospinal neurons express both glutamatergic and enkephalinergic phenotypes. *J Comp Neurol* **455,** 113-124.

Stornetta RL, Spirovski D, Moreira TS, Takakura AC, West GH, Gwilt JM, Pilowsky PM & Guyenet PG. (2009). Galanin is a selective marker of the retrotrapezoid nucleus in rats. *J Comp Neurol* **512,** 373-383.

Strack AM & Loewy AD. (1990). Pseudorabies virus: a highly specific transneuronal cell body marker in the sympathetic nervous system. *J Neurosci* **10,** 2139-2147.

Strack AM, Sawyer WB, Hughes JH, Platt KB & Loewy AD. (1989a). A general pattern of CNS innervation of the sympathetic outflow demonstrated by transneuronal pseudorabies viral infections. *Brain Res* **491,** 156-162.

Strack AM, Sawyer WB, Marubio LM & Loewy AD. (1988). Spinal origin of sympathetic preganglionic neurons in the rat. *Brain Res* **455,** 187-191.

Strack AM, Sawyer WB, Platt KB & Loewy AD. (1989b). CNS cell groups regulating the sympathetic outflow to adrenal gland as revealed by transneuronal cell body labeling with pseudorabies virus. *Brain Res* **491,** 274-296.

Sun MK. (1995). Central neural organization and control of sympathetic nervous system in mammals. *Prog Neurobiol* **47,** 157-233.

Sun MK & Guyenet PG. (1986a). Hypothalamic glutamatergic input to medullary sympathoexcitatory neurons in rats. *Am J Physiol* **251,** R798-810.

Sun MK & Guyenet PG. (1986b). Medullospinal sympathoexcitatory neurons in normotensive and spontaneously hypertensive rats. *Am J Physiol* **250,** R910-R917.

Sun MK, Hackett JT & Guyenet PG. (1988a). Sympathoexcitatory neurons of rostral ventrolateral medulla exhibit pacemaker properties in the presence of a glutamate-receptor antagonist. *Brain Res* **438,** 23-40.

Sun MK & Reis DJ. (1993a). Differential responses of barosensitive neurons of rostral ventrolateral medulla to hypoxia in rats. *Brain Res* **609,** 333-337.

Sun MK & Reis DJ. (1993b). Hypoxic excitation of medullary vasomotor neurons in rats are not mediated by glutamate or nitric oxide. *Neurosci Lett* **157,** 219-222.

Sun MK & Reis DJ. (1994). Intrathecal kynurenate but not benextramine blocks hypoxic sympathoexcitation in chemodenervated anesthetized rats. *J Auton Nerv Syst* **47,** 141-150.

Sun MK & Reis DJ. (1995). NMDA receptor-mediated sympathetic chemoreflex excitation of RVL-spinal vasomotor neurones in rats. *J Physiol* **482 (Pt 1),** 53-68.

Sun MK & Spyer KM. (1991). Responses of rostroventrolateral medulla spinal vasomotor neurones to chemoreceptor stimulation in rats. *J Auton Nerv Syst* **33,** 79-84.

Sun MK, Young BS, Hackett JT & Guyenet PG. (1988b). Reticulospinal pacemaker neurons of the rat rostral ventrolateral medulla with putative sympathoexcitatory function: An intracellular study in vitro. *Brain Res* **442,** 229-239.

Sun MK, Young BS, Hackett JT & Guyenet PG. (1988c). Rostral ventrolateral medullary neurons with intrinsic pacemaker properties are not catecholaminergic. *Brain Res* **451,** 345-349.

Sun QJ, Goodchild AK, Chalmers JP & Pilowsky PM. (1998). The pre-Botzinger complex and phase-spanning neurons in the adult rat. *Brain Res* **809,** 204-213.

Sun QJ, Minson J, Llewellyn-Smith IJ, Arnolda L, Chalmers J & Pilowsky P. (1997). Botzinger neurons project towards bulbospinal neurons in the rostral ventrolateral medulla of the rat. *J Comp Neurol* **388,** 23-31.

Sun QJ, Pilowsky P, Minson J, Arnolda L, Chalmers J & Llewellyn-Smith IJ. (1994). Close appositions between tyrosine hydroxylase immunoreactive boutons and respiratory neurons in the rat ventrolateral medulla. *J Comp Neurol* **340,** 1-10.

Sun Z & Zhang Z. (2005). Historic perspectives and recent advances in major animal models of hypertension. *Acta Pharmacologica Sinica* **26,** 295–301.

Sunanaga J, Deng BS, Zhang W, Kanmura Y & Kuwaki T. (2009). CO_2 activates orexin-containing neurons in mice. *Respir Physiol Neurobiol* **166,** 184-186.

Sunter D, Morgan I, Edwards CMB, Dakin CL, Murphy KG, Gardiner J, Taheri S, Rayes E & Bloom SR. (2001). Orexins: effects on behavior and localisation of orexin receptor 2 messenger ribonucleic acid in the rat brainstem. *Brain Res* **907,** 27-34.

Sutcliffe JG & De Lecea L. (2000). The hypocretins: Excitatory neuromodulatory peptides for multiple homeostatic systems, including sleep and feeding. *J Neurosci Res* **62,** 161-168.

Sved A, Ito S & Sved J. (2003). Brainstem mechanisms of hypertension: Role of the rostral ventrolateral medulla. *Curr Hypertens Rep* **5,** 262-268.

Sved AF, Ito S & Madden CJ. (2000). Baroreflex dependent and independent roles of the caudal ventrolateral medulla in cardiovascular regulation. *Brain Res Bull* **51,** 129-133.

Sved AF, Ito S, Madden CJ, Stocker SD & Yajima Y. (2001). Excitatory inputs to the RVLM in the context of the baroreceptor reflex. *Ann N Y Acad Sci* **940,** 247-258.

Sved AF, Mancini DL, Graham JC, Schreihofer AM & Hoffman GE. (1994). PNMT-containing neurons of the C1 cell group express c-fos in response to changes in baroreceptor input. *Am J Physiol* **266,** R361-367.

Sweerts BW, Jarrott B & Lawrence AJ. (1999). Expression of preprogalanin mRNA following acute and chronic restraint stress in brains of normotensive and hypertensive rats. *Mol Brain Res* **69,** 113-123.

Takakura AC, Colombari E, Menani JV & Moreira TS. (2011). Ventrolateral medulla mechanisms involved in cardiorespiratory responses to central chemoreceptor activation in rats. *Am J Physiol* **300,** R501-510.

Takakura AC, Moreira TS, Colombari E, West GH, Stornetta RL & Guyenet PG. (2006). Peripheral chemoreceptor inputs to retrotrapezoid nucleus (RTN) CO2-sensitive neurons in rats. *J Physiol* **572,** 503-523.

Takakura AC, Moreira TS, Stornetta RL, West GH, Gwilt JM & Guyenet PG. (2008). Selective lesion of retrotrapezoid Phox2b-expressing neurons raises the apnoeic threshold in rats. *J Physiol* **586,** 2975-2991.

Takeda K & Bunag RD. (1980). Augmented sympathetic nerve activity and pressor responsiveness in DOCA hypertensive rats. *Hypertension* **2,** 97-101.

Tan W, Pagliardini S, Yang P, Janczewski WA & Feldman JL. (2009). Projections of preBotzinger Complex neurons in adult rats. *J Comp Neurol* **518,** 1862-1878.

Taylor RF & Schramm LP. (1987). Differential effects of spinal transection on sympathetic nerve activities in rats. *Am J Physiol* **253**.

Teppema LJ, Veening JG, Kranenburg A, Dahan A, Berkenbosch A & Olievier C. (1997). Expression of c-fos in the rat brainstem after exposure to hypoxia and to normoxic and hyperoxic hypercapnia. *J Comp Neurol* **388,** 169-190.

Terada J, Nakamura A, Zhang W, Yanagisawa M, Kuriyama T, Fukuda Y & Kuwaki T. (2008). Ventilatory long-term facilitation in mice can be observed during both sleep and wake periods and depends on orexin. *J Appl Physiol* **104,** 499-507.

Thannickal TC, Moore RY, Nienhuis R, Ramanathan L, Gulyani S, Aldrich M, Cornford M & Siegel JM. (2000). Reduced Number of Hypocretin Neurons in Human Narcolepsy. *Neuron* **27,** 469-474.

Thorpe AJ & Kotz CM. (2005). Orexin A in the nucleus accumbens stimulates feeding and locomotor activity. *Brain Res* **1050,** 156-162.

Tian GF, Peever JH & Duffin J. (1998). Botzinger-complex expiratory neurons monosynaptically inhibit phrenic motoneurons in the decerebrate rat. *Exp Brain Res* **122,** 149-156.

Tian GF, Peever JH & Duffin J. (1999). Botzinger-complex, bulbospinal expiratory neurones monosynaptically inhibit ventral-group respiratory neurones in the decerebrate rat. *Exp Brain Res* **124,** 173-180.

Todorov LD, Mihaylova-Todorova ST, Bjur RA & Westfall DP. (1999). Differential cotransmission in sympathetic nerves: role of frequency of stimulation and prejunctional autoreceptors. *J Pharmacol Exp Ther* **290,** 241-246.

Touyz RM. (2000). Molecular and cellular mechanisms regulating vascular function and structure - Implications in the pathogenesis of hypertension. *Can J Cardiol* **16,** 1137-1146.

Toyama S, Sakurai T, Tatsumi K & Kuwaki T. (2009). Attenuated phrenic long-term facilitation in orexin neuron-ablated mice. *Respir Physiol Neurobiol* **168,** 295-302.

Trippodo NC & Frohlich ED. (1981). Similarities of genetic (spontaneous) hypertension: man and rat. *Circ Res* **48,** 309–319.

Trivedi P, Yu H, MacNeil DJ, Van Der Ploeg LHT & Guan XM. (1998). Distribution of orexin receptor mRNA in the rat brain. *FEBS Lett* **438,** 71-75.

Tsujino N & Sakurai T. (2009). Orexin/hypocretin: A neuropeptide at the interface of sleep, energy homeostasis, and reward system. *Pharmacol Rev* **61,** 162-176.

Tsujino N, Yamanaka A, Ichiki K, Muraki Y, Kilduff TS, Yagami K-i, Takahashi S, Goto K & Sakurai T. (2005). Cholecystokinin Activates Orexin/Hypocretin Neurons through the Cholecystokinin A Receptor. *J Neurosci* **25,** 7459-7469.

Tucker DC, Saper CB, Ruggiero DA & Reis DJ. (1987). Organization of central adrenergic pathways: I. Relationships of ventrolateral medullary projections to the hypothalamus and spinal cord. *J Comp Neurol* **259,** 591-603.

Uchino Y, Kudo N, Tsuda K & Iwamura Y. (1970). Vestibular inhibition of sympathetic nerve activities. *Brain Research* **22,** 195-206.

van den Pol AN. (1999). Hypothalamic Hypocretin (Orexin): Robust Innervation of the Spinal Cord. *J Neurosci* **19,** 3171-3182.

van den Pol AN, Gao X-B, Obrietan K, Kilduff TS & Belousov AB. (1998). Presynaptic and Postsynaptic Actions and Modulation of Neuroendocrine Neurons by a New Hypothalamic Peptide, Hypocretin/Orexin. *J Neurosci* **18,** 7962-7971.

van den Top M, Lee K, Whyment AD, Blanks AM & Spanswick D. (2004). Orexigen-sensitive NPY/AgRP pacemaker neurons in the hypothalamic arcuate nucleus. *Nat Neurosci* **7,** 493-494.

van den Top M, Nolan MF, Lee K, Richardson PJ, Buijs RM, Davies CH & Spanswick D. (2003a). Orexins induce increased excitability and synchronisation of rat sympathetic preganglionic neurones. *J Physiol* **549,** 809-821.

van den Top M, Nolan MF, Lee K, Richardson PJ, Buijs RM, Davies CH & Spanswick D. (2003b). Orexins induce increased excitability and synchronisation of rat sympathetic preganglionic neurones. *J Physiol* **549,** 809-821.

Vanni-Mercier G, Sakai K & Jouvet M. (1984). 'Waking-state specific' neurons in the caudal hypothalamus of the cat. *C R Acad Sci III*
298, 195-200.

Vardhan A, Kachroo A & Sapru HN. (1993). Excitatory amino acid receptors in commissural nucleus of the NTS mediate carotid chemoreceptor responses. *Am J Physiol* **264,** R41-R50.

Varner KJ, Rutherford DS, Vasquez EC & Brody MJ. (1992). Identification of cardiovascular neurons in the rostral ventromedial medulla in anesthetized rats. *Hypertension* **19,** 193-197.

Vasquez EC, Lewis SJ, Varner KJ & Brody MJ. (1992). Chronic lesion of rostral ventrolateral medulla in spontaneously hypertensive rats. *Hypertension* **19,** 154-158.

Veerasingham SJ & Raizada MK. (2003). Brain renin-angiotensin system dysfunction in hypertension: Recent advances and perspectives. *Br J Pharmacol* **139,** 191-202.

Vera PL, Holets VR & Miller KE. (1990a). Ultrastructural evidence of synaptic contacts between substance P-, enkephalin-, and serotonin-immunoreactive terminals and retrogradely labeled sympathetic preganglionic neurons in the rat: A study using a double-peroxidase procedure. *Synapse* **6,** 221-229.

Vera PL, Hurwitz BE & Schneiderman N. (1990b). Sympathoadrenal preganglionic neurons in the adult rabbit send their dendrites into the contralateral hemicord. *J Auton Nerv Syst* **30,** 193-198.

Verberne AJ, Stornetta RL & Guyenet PG. (1999). Properties of C1 and other ventrolateral medullary neurones with hypothalamic projections in the rat. *J Physiol* **517,** 477-494.

Volgin DV, Saghir M & Kubin L. (2002). Developmental changes in the orexin 2 receptor mRNA in hypoglossal motoneurons. *NeuroReport* **13,** 433-436.

Walling SG, Nutt DJ, Lalies MD & Harley CW. (2004). Orexin-A infusion in the locus ceruleus triggers norepinephrine (NE) release and NE-induced long-term potentiation in the dentate gyrus. *J Neurosci* **24,** 7421-7426.

Wang H, Stornetta RL, Rosin DL & Guyenet PG. (2001). Neurokinin-1 receptor-immunoreactive neurons of the ventral respiratory group in the rat. *J Comp Neurol* **434,** 128-146.

Wang L, Spary E, Deuchars J & Deuchars SA. (2008). Tonic GABAergic inhibition of sympathetic preganglionic neurons: A novel substrate for sympathetic control. *J Neurosci* **28,** 12445-12452.

Wayner MJ, Armstrong DL, Phelix CF & Oomura Y. (2004). Orexin-A (Hypocretin-1) and leptin enhance LTP in the dentate gyrus of rats in vivo. *Peptides* **25,** 991-996.

Wennergren G & Oberg B. (1980). Cardiovascular effects elicited from the ventral surface of medulla oblongata in the cat. *Pflugers Arch* **387,** 189-195.

Weston MC, Stornetta RL & Guyenet PG. (2004). Glutamatergic neuronal projections from the marginal layer of the rostral ventral medulla to the respiratory centers in rats. *J Comp Neurol* **473,** 73-85.

Widdop RE, Verberne AJM, Jarrott B & Louis WJ. (1990). Impaired arterial baroreceptor reflex and cardiopulmonary vagal reflex in conscious spontaneously hypertensive rats. *J Hypertens* **8,** 269-275.

Willette RN, Barcas PP, Krieger AJ & Sapru HN. (1983a). Vasopressor and depressor areas in the rat medulla. Identification by microinjection of L-glutamate. *Neuropharmacology* **22,** 1071-1079.

Willette RN, Krieger AJ, Barcas PP & Sapru HN. (1983b). Medullary gamma-aminobutyric acid (GABA) receptors and the regulation of blood pressure in the rat. *J Pharmacol Exp Ther* **226,** 893-899.

Williams RaH, Jensen LT, Verkhratsky A, Fugger L & Burdakov D. (2007). Control of hypothalamic orexin neurons by acid and CO2. *Proc Natl Acad Sci U S A* **104,** 10685-10690.

Willie JT, Chemelli RM, Sinton CM, Tokita S, Williams SC, Kisanuki YY, Marcus JN, Lee C, Elmquist JK, Kohlmeier KA, Leonard CS, Richardson JA, Hammer RE & Yanagisawa M. (2003). Distinct Narcolepsy Syndromes in Orexin Receptor-2 and Orexin Null Mice: Molecular Genetic Dissection of Non-REM and REM Sleep Regulatory Processes. *Neuron* **38,** 715-730.

Willie JT, Chemelli RM, Sinton CM & Yanagisawa M. (2001). To eat or to sleep? Orexin in the regulation of feeding and wakefulness. *Annu Rev Neurosci* **24,** 429-458.

Willis WD & Westlund KN. (1997). Neuroanatomy of the pain system and of the pathways that modulate pain. *J Clin Neurophysiol* **14,** 2-31.

Winsky-Sommerer Rl, Yamanaka A, Diano S, Borok E, Roberts AJ, Sakurai T, Kilduff TS, Horvath TL & de Lecea L. (2004). Interaction between the Corticotropin-Releasing Factor System and Hypocretins (Orexins): A Novel Circuit Mediating Stress Response. *J Neurosci* **24,** 11439-11448.

Winter SM, Fresemann J, Schnell C, Oku Y, Hirrlinger J & Hulsmann S. (2009). Glycinergic interneurons are functionally integrated into the inspiratory network of mouse medullary slices. *Pflugers Arch* **458,** 459-469.

Wittmann G, Liposits Z, Lechan RM & Fekete C. (2004). Medullary adrenergic neurons contribute to the cocaine- and amphetamine-regulated transcript-immunoreactive innervation of thyrotropin-releasing hormone synthesizing neurons in the hypothalamic paraventricular nucleus. *Brain Res* **1006,** 1-7.

Woodruff ML, Baisden RH, Whittington DL & Kelly JE. (1986). Inputs to the pontine A5 noradrenergic cell group: A horseradish peroxidase study. *Exp Neurol* **94,** 782-787.

Xie X, Crowder TL, Yamanaka A, Morairty SR, LeWinter RD, Sakurai T & Kilduff TS. (2006). GABAB receptor-mediated modulation of hypocretin/orexin neurones in mouse hypothalamus. *J Physiol* **574,** 399-414.

Xing T & Pilowsky PM. (2010). Acute intermittent hypoxia in rat in vivo elicits a robust increase in tonic sympathetic nerve activity that is independent of respiratory drive. *J Physiol* **588,** 3075-3088.

Xiong Y, Okada J, Tomizawa S, Takayama K & Miura M. (1998). Difference in topology and numbers of barosensitive catecholaminergic and cholinergic neurons in the medulla between SHR and WKY rats. *J Auton Nerv Syst* **70,** 200-208.

Yaksh TL & Rudy TA. (1976). Chronic catheterization of the spinal subarachnoid space. *Physiol Behav* **17,** 1031-1036.

Yamada H, Okumura T, Motomura W, Kobayashi Y & Kohgo Y. (2000). Inhibition of Food Intake by Central Injection of Anti-orexin Antibody in Fasted Rats. *Biochem Biophys Res Commun* **267,** 527-531.

Yamada KA, McAllen RM & Loewy AD. (1984). GABA antagonists applied to the ventral surface of the medulla oblongata block the baroreceptor reflex. *Brain Res* **297,** 175-180.

Yamada Y, Miyajima E, Tochikubo O, Matsukawa T, Shionoiri H, Ishii M & Kaneko Y. (1988). Impaired baroreflex changes in muscle sympathetic nerve activity in adolescents who have a family history of essential hypertension. *J Hypertens Suppl* **6,** S525-528.

Yamanaka A, Beuckmann CT, Willie JT, Hara J, Tsujino N, Mieda M, Tominaga M, Yagami K-i, Sugiyama F, Goto K, Yanagisawa M & Sakurai T. (2003a). Hypothalamic orexin neurons regulate arousal according to energy balance in mice. *Neuron* **38,** 701-713.

Yamanaka A, Kunii K, Nambu T, Tsujino N, Sakai A, Matsuzaki I, Miwa Y, Katsutoshi G & Sakurai T. (2000). Orexin-induced food intake involves neuropeptide Y pathway. *Brain Res* **859,** 404-409.

Yamanaka A, Muraki Y, Ichiki K, Tsujino N, Kilduff TS, Goto K & Sakurai T. (2006). Orexin Neurons Are Directly and Indirectly Regulated by Catecholamines in a Complex Manner. *J Neurophysiol* **96,** 284-298.

Yamanaka A, Muraki Y, Tsujino N, Goto K & Sakurai T. (2003b). Regulation of orexin neurons by the monoaminergic and cholinergic systems. *Biochem Biophys Res Commun* **303,** 120-129.

Yamanaka A, Tsujino N, Funahashi H, Honda K, Guan J-l, Wang Q-P, Tominaga M, Goto K, Shioda S & Sakurai T. (2002). Orexins Activate Histaminergic Neurons via the Orexin 2 Receptor. *Biochem Biophys Res Commun* **290,** 1237-1245.

Yamashita H, Kannan H, Kasai M & Osaka T. (1987). Decrease in blood pressure by stimulation of the rat hypothalamic paraventricular nucleus with L-glutamate or weak current. *J Auton Nerv Syst* **19,** 229-234.

Yang RH, Jin H, Wyss JM & Oparil S. (1992). Depressor effect of blocking angiotensin subtype 1 receptors in the anterior hypothalamus. *Hypertension* **19,** 475–481.

Yang Z-J, Meguid MM, Chai J-K, Chen C & Oler A. (1997). Bilateral Hypothalamic Dopamine Infusion in Male Zucker Rat Suppresses Feeding Due to Reduced Meal Size. *Pharmacol Biochem Behav* **58,** 631-635.

Yashpal K, Gauthier S & Henry JL. (1987). Substance P given intrathecally at the spinal T9 level increases arterial pressure and heart rate in the rat. *J Auton Nerv Syst* **18,** 93-103.

Yashpal K, Gauthier S & Henry JL. (1989). Angiotensin II stimulates sympathetic output by a direct spinal action. *Neuropeptides* **14,** 21-29.

Yin M & Sved AF. (1996). Role of gamma-aminobutyric acid B receptors in baroreceptor reflexes in hypertensive rats. *Hypertension* **27,** 1291-1298.

Yoshida K, McCormack S, España RA, Crocker A & Scammell TE. (2006). Afferents to the orexin neurons of the rat brain. *J Comp Neurol* **494,** 845-861.

Young JK, Wu M, Manaye KF, Kc P, Allard JS, Mack SO & Haxhiu MA. (2005). Orexin stimulates breathing via medullary and spinal pathways. *J Appl Physiol* **98,** 1387-1395.

Zagon A & Smith AD. (1993). Monosynaptic projections from the rostral ventrolateral medulla oblongata to identified sympathetic preganglionic neurons. *Neuroscience* **54,** 729-743.

Zaiman A, Fijalkowska I, Hassoun PM & Tuder RM. (2005). One hundred years of research in the pathogenesis of pulmonary hypertension. *Am J Respir Cell Mol Biol* **33,** 425-431.

Zanzinger J, Czachurski J, Offner B & Seller H. (1994). Somato-sympathetic reflex transmission in the ventrolateral medulla oblongata: Spatial organization and receptor types. *Brain Res* **656,** 353-358.

Zhang J & Mifflin SW. (1998). Differential roles for NMDA and non-NMDA receptor subtypes in baroreceptor afferent integration in the nucleus of the solitary tract of the rat. *J Physiol* **511,** 733-745.

Zhang Q, Yao F, Raizada MK, O'Rourke ST & Sun C. (2009). Apelin gene transfer into the rostral ventrolateral medulla induces chronic blood pressure elevation in normotensive rats. *Circ Res* **104,** 1421-1428.

Zhang TX & Ciriello J. (1985). Kainic acid lesions of paraventricular nucleus neurons reverse the elevated arterial pressure after aortic baroreceptor denervation in the rat. *Brain Res* **358,** 334-338.

Zhang W, Fukuda Y & Kuwaki T. (2005). Respiratory and cardiovascular actions of orexin-A in mice. *Neurosci Lett* **385,** 131-136.

Zheng Y, Riche D, Rekling JC, Foutz AS & Denavit-Saubie M. (1998). Brainstem neurons projecting to the rostral ventral respiratory group (VRG) in the medulla oblongata of the rat revealed by co-application of NMDA and biocytin. *Brain Res* **782,** 113-125.

Zhu Y, Miwa Y, Yamanaka A, Yada T, Shibahara M, Abe Y, Sakurai T & Goto K. (2003). Orexin Receptor Type-1 Couples Exclusively to Pertussis Toxin-Insensitive G-Proteins, While Orexin Receptor Type-2 Couples to Both Pertussis Toxin-Sensitive and -Insensitive G-Proteins. *J Pharmacol Sci* **92,** 259-266.

Zhuo M & Gebhart GF. (1990). Spinal cholinergic and monoaminergic receptors mediate descending inhibition from the nuclei reticularis gigantocellularis and gigantocellularis pars alpha in the rat. *Brain Res* **535,** 67-78.

List of suppliers for all items used in this thesis

Drug	Company	Country
Anaesthetics		
Sodium pentabarbital	Merial Australia Pty Ltd	Australia
Urethane	Sigma-Aldrich	Australia
Peptides		
Orexin A	Bachem AG	Switzerland
Other chemicals/agents		
10%CO_2:90%O_2	BOC Gas & Gear	Australia
[Ala11, D-Leu15]orexin B	Tocris Bioscience	UK
Atropine sulphate	Astra Pharmaceuticals Pty Ltd	Australia
Bupivacaine	Astra-Zeneca	Australia
Ethanol	Chem supply	Australia
Glucose	Sigma-Aldrich	Australia
Heparin sodium	Mayne Pharma Pty Ltd	Australia
L-glutamate	Sigma-Aldrich	Australia
Nitrogen (100%)	BOC Gas & Gear	Australia
Oxygen Gas	BOC Gas & Gear	Australia
Pancuronium bromide	Astra Pharmaceuticals Pty Ltd	Australia
Paraffin Oil	Faulding Pharmaceuticals	Australia
Paraformaldehyde	Sigma-Aldrich	Australia
Phenylephrine hydrochloride	Sigma-Aldrich	Australia
Phosphate buffered saline	Amresco	USA
Pontamine sky blue	Koch Laboratories Ltd	UK
Potassium chloride	Sigma-Aldrich	Australia
Rhodamine microbeads	Invitrogen	Australia
SB334867	Tocris Bioscience	UK
Silgel 612A & 612B	Wacker	Germany
Sodium chloride	Sigma-Aldrich	Australia
Sodium citrate	Sigma-Aldrich	Australia
Sodium nitroprusside	Sigma-Aldrich	Australia
Tween	Sigma-Aldrich	Australia
Ultramount	Fronine laboratories supplies	Australia
Vectashield	Vector Laboratories	Australia

Andibodies	Species	concentration	Company	Country
Primary				
Orexin-A	Rabiit	1:2000	Merck	Germany
Orexin 1 receptor	Rabit	1:50	Millipore	USA
Orexin 2 receptor	Goat	1:50	Santa Cruz Biotechnology, Inc.	USA

Tyrosine hydroxilase	Mouse	1:2500	Sigma-Aldrich	Australia
Secondary				
Alexa Fluor 488 anti-mouse	Donkey	1:500	Invitrogen	Australia
Cy3 anti-rabbit	Donkey	1:500	Jackson ImmunoResearch Laboratories	USA
Cy3 anti-sheep	Donkey	1:500	Jackson ImmunoResearch Laboratories	USA

Equipment	Model	Company	Country
3-way taps	#394600	BD-Connecta	Australia
Axiocam digital camera	MR3	Zeiss	Germany
AxioImager epiflourescence microscope	Z1	Zeiss	Germany
Bio pre-amplifier	830	CWE Inc.	USA
Blood gas analyser and cartridges	Vetstsat, IDEXX	IDEXX Laboratories	USA
Borosilicate glass capillary tubes		SDR Clinical Technology	Australia
Cambridge Electronic Design ADC system	1401	Cambridge Electronic Design	UK
CO_2 analyser	Capstar 100	CWE Inc.	USA
Cy3-4040B filter set		Semrock	USA
Glass Hamilton micro-syringe		Hamilton Company	USA
Homeothermic heating blanket		Harvard Apparatus	USA
Humbug (50/60 Hz –Line frequency filter)		Quest Scientific	Canada
Infusion pump	11 plus	Harvard Apparatus	USA
Laser puller	P2000	Sutter Instrument Company	USA
Micromanipulator		Narishige	Japan
Multi-pipette puller	PMP-100	Micro Data Instruments	USA
Needles	Multiple sizes	Terumo	Australia
Pressure transducer		IRMA Bayer Aust. Ltd	Australia
Polyethylene tubing (OD: 0.96 mm; ID 0.58 mm)		Critchley Electrical Products Pty Ltd	Australia
Polyethylene tubing (OD: 0.8 mm; ID 0.4 mm)		Critchley Electrical Products Pty Ltd	Australia
PowerLab 8/30		ADInstruments	Australia
Scaling amplifier	BMA-400 AC/DC Bioamplifier	CWE Inc.	USA

Saclpel blade	Blade#22	Swann-Mortin Limited	UK
Silastic tubing	OD: 0.94 mm x ID:0.51 mm	Dow Corning	USA
Silk sutures	5/0 & 2/0	Pearsalls	UK
Sphygmomanometer (mercury)	#605P	Yamsu Co Ltd	Japan
Stereotaxic frame		Macquarie Engineering & Technical Services	Australia
Stimulator		A.M.P.I.	Israel
Syringes	Multiple cc/ml	Terumo	Australia
Tracheal cannula	14G catheter plastic seatch	Johnson & Johnson medical	Australia
Two chamber wire myograph	DMT model 410A	Danish Myo Technology (DMT)	Denmark
Ventilator		Ugo Basile	Italy
Vibrating microtome	VT 1200 S	Leica	Australia

Software	Version	Company	Country
Axiovision	4.5	Carl Zeiss	Germany
CorelDRAW	X4	Corel Corporation	USA
Excel	2007	Microsoft Corporation	Australia
GraphPad Prism	5.0	GraphPad Software	USA
LabChart	7.2	ADInstruments	Australia
Spike 2	7.07	Cambridge Electronic Design	UK
Word	2007	Microsoft Corporation	Australia

Shahid, I. Z., Rahman, A. A., & Pilowsky, P. M. (2011). Intrathecal orexin A increases sympathetic outflow and respiratory drive, enhances baroreflex sensitivity and blocks the somato-sympathetic reflex. *British Journal of Pharmacology*, *162*(4), 961-973.

DOI: 10.1111/j.1476-5381.2010.01102.x

Shahid, I. Z., Rahman, A. A., & Pilowsky, P. M. (2012). Orexin A in rat rostral ventrolateral medulla is pressor, sympatho-excitatory, increases barosensitivity and attenuates the somato-sympathetic reflex. *British Journal of Pharmacology*, *165*(7), 2292-2303.

DOI: 10.1111/j.1476-5381.2011.01694.x

Shahid, I. Z., Rahman, A. A., & Pilowsky, P. M. (2012). Orexin and central regulation of cardiorespiratory system. In G. Litwack (Ed.), *Sleep hormones* (pp. 159-184).
(Vitamins and Hormones; Vol. 89). Elsevier. Vitamins and Hormones

DOI: 10.1016/B978-0-12-394623-2.00009-3

Rahman, A. A., Shahid, I. Z., & Pilowsky, P. M. (2011). Intrathecal neuromedin U induces biphasic effects on sympathetic vasomotor tone, increases respiratory drive and attenuates sympathetic reflexes in rat. *British Journal of Pharmacology*, *164*(2 B), 617-631.

DOI: 10.1111/j.1476-5381.2011.01436.x

Autonomic Neuroscience: Basic and Clinical 166 (2012) 22–28

Contents lists available at SciVerse ScienceDirect

Autonomic Neuroscience: Basic and Clinical

journal homepage: www.elsevier.com/locate/autneu

Vasostatin I ($CgA_{17–76}$) vasoconstricts rat splanchnic vascular bed but does not affect central cardiovascular function

Ahmed A. Rahman [a,b], Israt Z. Shahid [a,b], Angelina Y. Fong [a], Andrew M. Hammond [a], Paul M. Pilowsky [a,*]

[a] Australian School of Advanced Medicine, Macquarie University, Sydney, Australia
[b] Pharmacy Discipline, Life Science School, Khulna University, Khulna, Bangladesh

ARTICLE INFO

Article history:
Received 28 June 2011
Received in revised form 23 August 2011
Accepted 23 August 2011

Keywords:
Vasostatin I
Sympathetic nerve activity
Phrenic nerve discharge
Reflex
Rat mesenteric artery

ABSTRACT

Vasostatin I ($CgA_{1–76}$) is a naturally occurring biologically active peptide derived from chromogranin A (CgA), and is so named for its inhibitory effects on vascular tension. CgA mRNA is expressed abundantly in sympathoexcitatory catecholaminergic neurons of the rostral ventrolateral medulla (RVLM). CgA microinjection into the RVLM decreases blood pressure (BP), heart rate (HR) and sympathetic nerve activity (SNA). Proteolytic fragments of CgA are thought to be responsible for the cardiovascular effects observed. We hypothesised that vasostatin I is one of the fragments responsible for the central effects of CgA. We examined the role of a vasostatin I fragment, $CgA_{17–76}$ (VS-$I_{(CgA17–76)}$), containing the portion important for biological effects. The effects of VS-$I_{(CgA17–76)}$ delivered by intrathecal injection, or microinjection into the RVLM, on cardio-respiratory function in urethane anaesthetised, vagotomised, mechanically ventilated Sprague-Dawley rats ($n=21$) were evaluated. The effects of intrathecal VS-$I_{(CgA17–76)}$ on the somato-sympathetic, baroreceptor and peripheral chemoreceptor reflexes were also examined. At the concentrations used (10, 100 or 200 μM, intrathecal; or 5 μM, RVLM microinjection) VS-$I_{(CgA17–76)}$ produced no change in mean arterial pressure, HR, splanchnic SNA, phrenic nerve amplitude or phrenic nerve frequency. All reflexes examined were unchanged following intrathecal VS-$I_{(CgA17–76)}$. In the periphery, VS-$I_{(CgA17–76)}$ potentiated the contractile effects of noradrenaline on rat mesenteric arteries ($n=6$), with a significant left-shift in the dose response curve to noradrenaline (3.7×10^{-7} vs 7.7×10^{-7}). Our results indicate that VS-$I_{(CgA17–76)}$ is active in the periphery but not centrally, and is not a central modulator of cardiorespiratory function and physiological reflexes.

1. Introduction

Chromogranin A (CgA) is a 439 amino acid protein that was first identified in the secretory granules of chromaffin cells of bovine adrenal medulla (Banks and Helle, 1965), but is now known to be distributed in other neuroendocrine tissues, including adrenergic and noradrenergic neurons of the central nervous system (Somogyi et al., 1984; Woulfe et al., 1999). CgA is co-stored with an assortment of neuromodulators and hormones including amines and peptides and is co-released by exocytosis. Mice lacking the CgA gene are hypertensive with increased left ventricular mass, suggesting an important role for CgA in autonomic control of circulation (Mahapatra et al., 2005).

Tissue- and species- specific proteolytic processing of CgA produces several biologically active peptides including catestatin ($CgA_{344–364}$), vasostatin I ($CgA_{1–76}$), vasostatin II ($CgA_{1–113}$), and a variety of shorter vasostatin peptide fragments: $CgA_{1–40}$, $CgA_{7–57}$, $CgA_{47–66}$, $CgA_{67–76}$, that are found endogenously (Metz-Boutigue et al., 1993; Tota et al., 2008). Vasostatin I fragment ($CgA_{17–39}$) is found as a circulating peptide in mammals (Stridsberg et al., 2000) and can produce peripheral cardiovascular effects, including suppression of blood vessel contraction (Aardal and Helle, 1992; Aardal et al., 1993; Brekke et al., 2002). Recently both vasostatin I and catestatin were reported to induce a negative inotropic effect on the isolated rat heart under basal conditions and after β-adrenergic stimulation (Cerra et al., 2006; Angelone et al., 2008).

While CgA peptide products clearly have peripheral cardiovascular effects, the function of these peptides within the central nervous system is less clear. Recently we reported that CgA mRNA is expressed in sympathoexcitatory catecholaminergic neurons within the rostral ventrolateral medulla (RVLM), a region important in establishment and maintenance of basal sympathetic tone (Gaede et al., 2009). In addition, catestatin was also found in catecholaminergic RVLM neurons and microinjection of catestatin into RVLM increased both mean arterial pressure (MAP) and sympathetic nerve activity (SNA), as well as modulated a number of cardiorespiratory reflexes (Gaede and Pilowsky, 2010). In contrast, intrathecal catestatin had no effect on cardiovascular parameters (Gaede et al., 2009). However, the effects of other CgA cleavage products, including vasostatin remain unknown. We aimed to examine the effects of a vasostatin I fragment $CgA_{17–76}$ (VS-$I_{(CgA17–76)}$) in the splanchnic vascular bed by *in vitro* myograph

* Corresponding author at: The Australian School of Advanced Medicine, F10A, Macquarie University, Sydney, NSW 2109, Australia. Tel.: +61 2 9812 3560; fax: +61 2 9812 3600.
E-mail address: paul.pilowsky@mq.edu.au (P.M. Pilowsky).

1566-0702/$ – see front matter.
doi:10.1016/j.autneu.2011.08.023

Rahman, A. A., Shahid, I. Z., Fong, A. Y., Hammond, A. M., & Pilowsky, P. M. (2012). Vasostatin I (CgA17-76) vasoconstricts rat splanchnic vascular bed but does not affect central cardiovascular function. Autonomic Neuroscience: Basic and Clinical, 166(1-2), 22-28. https://doi.org/10.1016/j.autneu.2011.08.023

and on central cardiorespiratory function using intrathecal administration, or direct microinjection into the RVLM. This fragment of vasostatin I contains the disulfide-bridge region ($CgA_{17-38SS}$) that is important for biological effects (Tota et al., 2003). We hypothesised that vasostatin I and catestatin (Gaede et al., 2009; Gaede and Pilowsky, 2010) may act through similar mechanisms and both peptides might exert similar cardiorespiratory actions when delivered centrally.

2. Experimental procedures

All animal experiments in this study complied with the guidelines of the Australian Code of Practice for the Care and Use of Animals for Scientific Purposes (http://www.nhmrc.gov.au/publications/synopses/eal6syn.htm) and were approved by the Animal Ethics Committee of Macquarie University, Sydney, Australia.

2.1. General procedures

Surgical preparation was performed as described previously (Shahid et al., 2011; Rahman et al., 2011). Male Sprague-Dawley rats (350–500 g) were anaesthetized with urethane (1.2–1.4 g/kg, i.p.; supplemental doses of 30–40 mg, i.v. were given when necessary). The rectal temperature was maintained between 36°C and 37°C with a thermostatically controlled heating pad (Harvard Apparatus).

The left jugular vein and right carotid artery were cannulated with polyethylene tubing for administration of drugs and fluids, and for measurement of arterial blood pressure, respectively. In some experiments, both femoral veins were cannulated for the administration of sodium nitroprusside (SNP) and phenylephrine hydrochloride (PE) for baroreflex activation. The trachea was cannulated to permit artificial ventilation and ECG was recorded. The left greater splanchnic nerve and phrenic nerve were isolated, tied with silk thread and cut to permit recording (neurograms were sampled at 3 kHz, filtered (0.1–2 kHz) and amplified (×10,000)) of efferent sSNA and phrenic nerve activity (PNA), respectively. In an additional subset of animals, the sciatic nerve was isolated, tied and cut for the activation of somato-sympathetic reflex. The rats were secured in a stereotaxic frame, vagotomised, paralysed (pancuronium bromide; 0.8 mg initially, then 0.4 mg/h, Astra Pharmaceuticals) and artificially ventilated with oxygen enriched room air. End-tidal CO_2 was monitored and maintained between 4.0% and 4.5%. Arterial blood gas was analysed to maintain pH (7.35–7.45). Animals were infused with 5% glucose (1.0–2.0 ml/h) to ensure hydration. The depth of anaesthesia was assessed frequently by monitoring the absence of changes in arterial pressure and heart rate in response to pinching a hind paw. Nerve recordings were made with bipolar silver wire electrodes.

2.2. Activation of sympathetic reflexes

Reflexes were evoked as described previously (Miyawaki et al., 2002; Makeham et al., 2004). Activation of the somato-sympathetic reflex was achieved by electrical stimulation (10–20 V, 100 cycles at 1 Hz across 100 s) of the sciatic nerve with bipolar electrodes. Sympathetic baroreflex function curves were generated by sequential intravenous injection of SNP (10 μg/kg) and PE (10 μg/kg). Peripheral chemoreceptors were stimulated by a brief period of hypoxia evoked by ventilation with 100% N_2 for 12–14 s.

2.3. Experimental protocols

2.3.1. Intrathecal injection of VS-$I_{(CgA17-76)}$

The occipital crest of the skull was exposed, and the atlanto-occipital membrane was incised. A polyethylene catheter (ID, 0.4 mm; OD, 0.8 mm) was inserted through this slit into the intrathecal space and advanced caudally to the levels of T4–T6. The slit was then left open to avoid increased intrathecal pressure caused by the injection of agents or by flushing. Vehicle and volume control injections of 10 μl of 10 mM phosphate-buffered saline (PBS in 0.9% saline) flushed with 8 μl PBS were injected intrathecally. Thirty minutes after PBS injection, 10 μl of one dose of 10 μM (n = 5), 100 μM (n = 5) or 200 μM (n = 6) human VS-$I_{(CgA17-76)}$ (CgA_{17-76}, MW = 6811.83; Phoenix Pharmaceuticals, CA) was injected and flushed with a further 8 μl of PBS. Injections were made over a 15- to 20-s period. Responses were recorded for at least 30 min after the VS-$I_{(CgA17-76)}$ injections. The location of the catheter tip was confirmed by administering L-glutamate (100 mM, 10 μl). Sharp increases in BP (~20 mmHg), HR (~30 bpm) and sSNA (~30%) indicated a successful catheterization (Hong and Henry, 1992).

In a subset of animals (n = 6), the following cardio-respiratory reflexes were activated before and 15 min after intrathecal injection of VS-$I_{(CgA17-76)}$ (200 μM) or PBS: (a) somato-sympathetic reflex by sciatic nerve stimulation, (b) baroreflex by intravenous injection of SNP and PE, and (c) peripheral chemoreceptor reflex by brief hypoxia. The location of the injection site was marked by an injection of 10 μl of India ink flushed with 8 μl PBS. Following euthanasia (3 M KCl, 0.5 ml, i.v.) a laminectomy was performed to verify the location of the cannula tip. Each animal received only one treatment of VS-$I_{(CgA17-76)}$ in order to avoid the confounding effects of drug interactions and tachyphylaxis.

2.3.2. RVLM microinjection of VS-$I_{(CgA17-76)}$

The dorsal medulla was exposed after an occipital craniotomy. Single or multibarrel glass pipettes were used to microinject drugs to the RVLM. L-Glutamate (100 mM, 5 nmol in 50 nl; Sigma-Aldrich) and human VS-$I_{(CgA17-76)}$ (5 μM, 100 nl, Phoenix Pharmaceuticals, CA) were dissolved in PBS (10 mM, pH 7.4) and injected unilaterally into the RVLM in all rats (n = 5). PBS (100 nl) was also microinjected as a volume and vehicle control. The RVLM was first functionally identified by an increase of >30 mm Hg in MAP following microinjection of L-glutamate (100 mM, 5 nmol in 50 nl), as determined in previous studies (Abbott and Pilowsky, 2009). All variables were allowed to return to baseline (>30 min) before microinjection of PBS (100 nl) was performed. After a further 30 min, VS-$I_{(CgA17-76)}$ (5 μM, 100 nl) was microinjected into the same site and observation continued for a further 60 min. At the completion of each experiment, the injection site was marked with pontamine sky blue (1% in saline). Rats were then killed with 0.5 ml of 3 M KCl i.v., the brain stem was removed and placed in fixative (4% formaldehyde in 0.1 M PBS, pH 7.4). Histology was performed to identify injection sites.

2.4. In vitro myograph

The myograph protocol was adapted from (Mulvany and Halpern, 1977). In brief, gut mesenteric tissue was collected from adult male SD rats (n = 6, 400–500 g), euthanized with sodium pentobarbitone (300 mg/kg, i.v.), and stored on ice overnight in physiological saline solution (PSS). The following morning, two, third order, mesenteric arteries from each rat were dissected and threaded onto 40 μm diameter stainless steel wires mounted in a two chamber wire myograph (DMT model 410A). Vessels were warmed to 37 °C, bubbled with carbogen and rested for 30 min. The vessels were then stretched and their internal circumference set to 90% of that occurring at an effective transmural pressure of 100 mm Hg. The vessels were again rested for 30 min prior to reactivation using high potassium (60 mM) solution, KPSS. Vessels were reactivated by bathing for 2 min in the following solutions separated by 3 min washes with PSS: 2 times with 10 μM noradrenaline (NA) in KPSS, 10 μM NA in PSS, KPSS, and finally, 10 μM NA in PSS. Vessels were allowed to rest for a further 30 min in PSS before the start of the protocol.

Discrete concentration responses curve to NA (0.1–10 μM) were obtained for all vessels and the EC_{50} value for each vessel was calculated. The EC_{50} concentration of NA was re-applied a further two times, after 20–30 min rest periods, to ensure reproducibility of the response. Only vessels that produced consistent responses to EC_{50} concentrations of NA

were used in the following protocol. VS-$I_{(CgA17–76)}$ (200 nM) was added to one chamber and allowed to incubate for 15 min. A VS-$I_{(CgA17–76)}$ concentration of 200 nM was chosen based on the peak plasma concentration following intravenous infusion of vasostatin I (Roatta et al., 2011). VS-$I_{(CgA17–76)}$ was omitted from the other chamber, which acted as a time-control. Only one vessel from each rat was exposed to VS-$I_{(CgA17–76)}$. EC_{50} concentrations of NA were re-applied to all vessels a further 3 times, separated by washing and 20 min rest in PSS. A second concentration response curve to NA (0.1–10 μM) was repeated.

2.5. Data acquisition and analysis

Data from the *in vivo* experiments was acquired using a Cambridge Electronic Design ADC system (model 1401; Cambridge Electronic Design, Cambridge, UK) and Spike 2 acquisition and analysis software (version 6.09). Neurograms were rectified and smoothed (sSNA, 1 s time constant; PNA, 50 ms time constant). Zero sSNA was taken as the minimum background activity after death, and this value was subtracted from sSNA before analysis with off-line software (Spike 2 version 6.01). To analyse blood pressure, sSNA, HR, PNamp and PNf baseline values were obtained by averaging 60 s of data 5 min prior to drug or PBS injection. Maximum responses were expressed as absolute changes in MAP, HR and PNf, and percent changes in sSNA and PNamp from baseline values. sSNA was rectified and smoothed at 1 s and 5 ms time constants to analyse baroreceptor reflex and somatosympathetic reflex, respectively. sSNA was normalised against the pre-injection baseline. The sSNA response to sciatic nerve stimulation was analysed using peristimulus waveform averaging. The amplitude of sSNA from −100 to 0 ms before stimulation was taken as the baseline. The maximum response to stimulation was then expressed as a percentage change from the baseline. The response to hypoxia was quantified by comparing the average maximum sSNA for 10 s caused by the inhaled 100% N_2 as a percent change from a control period of 10 s average sSNA before 100% N_2 inhalation.

Data from *in vitro* myograph experiments was acquired using an ADInstruments ADC system (PowerLab 8/30; ADInstruments, Bella Vista, Australia) and LabChart software (ver 7.2). Responses to NA were measured at the plateau and calculated as the change in force (mN) from the baseline immediately before the drug was added. The responses to all concentrations of NA was normalised to 10 μM NA for each curve within each vessel. 10 μM NA was considered to be the maximal response (100%). Concentration-response curves to NA for *in vitro* myography experiments were plotted using GraphPad Prism (verson 5.0).

All statistical analysis was conducted with Graph Pad Prism (version 5.0). Paired *t*-test was used to analyse peak effects and reflexes for *in vivo* experiments. For the *in vitro* myograph experiments, two way ANOVA was conducted to compare the concentration-response curve to NA, and t-tests were conducted to compare the EC_{50} between the different groups. $P<0.05$ was considered significant in all cases. All values are expressed as means ± SE.

2.6. Solutions

Analyses provided by the manufacturer (Phoenix Pharmaceuticals Inc) included mass spectroscopy, high pressure/performance liquid chromatography (HPLC), and all assays confirmed the presence of VS-$I_{(CgA17–76)}$ at a purity of ≥95%.

Physiological saline solution (PSS), containing 119.0 mM NaCl, 4.7 mM KCl, 1.2 mM $MgSO_4$, 1.2 mM KH_2PO_4, 2.5 mM $CaCl_2$, 25.0 mM $NaHCO_3$, 0.03 mM EDTA and 5.5 mM glucose, was bubbled with carbogen (95% O_2/5% CO_2) before use to obtain a pH of 7.4. High potassium PSS (KPSS, 60 mM) was obtained by substitution of NaCl with equimolar KCl. NA (Sigma-Aldrich, St Louis, USA) was dissolved in distilled water, made immediately before use, and kept on ice, in the dark.

3. Results

3.1. Effects of intrathecal VS-$I_{(CgA17–76)}$

The baseline MAP and heart rate (HR) in anaesthetized rats were 98 ± 5 mm Hg and 457 ± 12 bpm (n = 16). Intrathecal VS-$I_{(CgA17–76)}$ (10, 100 and 200 μM) produced no change in any of the cardiovascular parameters (MAP, HR or splanchnic SNA (sSNA)), or respiratory parameters (phrenic nerve amplitude (PNamp), phrenic nerve frequency (PNf)). A representative experiment is shown in Fig. 1A. Intrathecal injection of PBS caused no significant change in any of the above parameters. The magnitude of change in MAP, HR, sSNA, PNamp and PNf following VS-$1_{(CgA17–76)}$ injections was non-significant compared to vehicle (PBS) and the group data is presented in Fig. 1B.

3.2. Effects of RVLM microinjection of VS-$I_{(CgA17–76)}$ on cardiorespiratory parameters

We also sought to determine whether VS-$I_{(CgA17–76)}$ has any effect when applied directly into the RVLM. In five animals (baseline MAP: 98 ± 9 mm Hg and HR: 499 ± 8 bpm), the RVLM was identified functionally by microinjection of L-glutamate prior to microinjection of VS-$I_{(CgA17–76)}$ (5 μM, Fig. 2A). VS-$I_{(CgA17–76)}$ microinjected into RVLM had no significant effect on MAP, HR, sSNA, PNf or PNamp compared to vehicle (PBS). Example traces from a representative experiment is shown in Fig. 2A and the group data illustrated in Fig. 2B.

3.3. Effects of intrathecal VS-$I_{(CgA17–76)}$ on sympathetic reflexes

Fig. 3 illustrates the effects of intrathecal VS-$I_{(CgA17–76)}$ (200 μM) on somato-sympathetic, baroreceptor and peripheral chemoreceptor reflexes. Sciatic nerve stimulation resulted in a characteristic two-peaked response in sSNA with the latencies of 75 ± 10 ms and 172 ± 4 ms (n = 6). These latencies were not significantly altered by intrathecal VS-$I_{(CgA17–76)}$ (89 ± 3 and 174 ± 5 ms, respectively). The excitatory response to sciatic nerve stimulation in the sSNA was unaffected by VS-$I_{(CgA17–76)}$ injection (first peak: 136 ± 46 to 135 ± 39%; second peak: 49 ± 11 to 50 ± 10%, of baseline, n = 6, Fig. 3A).

In five animals, intrathecal injection of VS-$I_{(CgA17–76)}$ had no effect on any of the variables (upper and lower plateaus, threshold, midpoint or saturation levels) of the baroreflex function curve or maximum gain compared to vehicle (Table 1, Fig. 3B).

Activation of peripheral chemoreceptors with brief hypoxia evoked an increase in MAP (65 ± 9 mm Hg), HR (32 ± 3 bpm) and sSNA (152 ± 25%, Fig. 3C). Peak effects occurred near the end of stimulus and recovered rapidly to baseline. The pressor, tachycardic and sympathoexcitatory responses to hypoxia were not affected by the intrathecal injection of VS-$I_{(CgA17–76)}$ (n = 6, Fig. 3C).

3.4. Effects of VS-$I_{(CgA17–76)}$ on noradrenergic responses in rat mesenteric arteries

The VS-$I_{(CgA17–76)}$ was tested in the *in vitro* myograph to verify its biological activity. NA produced concentration-dependent isometric contractions of the rat mesenteric artery prior to addition of VS-$I_{(CgA17–76)}$ (Fig. 4B − Baseline). Addition of VS-$I_{(CgA17–76)}$ alone produced no change in force, indicating that VS-$I_{(CgA17–76)}$ is not vasoactive (Fig. 4A). A subsequent application of an EC_{50} concentration of NA to vessels incubated with the VS-$I_{(CgA17–76)}$ revealed an increase in amplitude of response compared to the baseline response (Fig. 4A). VS-$I_{(CgA17–76)}$ (n = 6) produced a significant left-shift of the concentration-response curve to NA compared to the baseline (Fig. 4B), with a significantly lower EC_{50} value (Table 2).

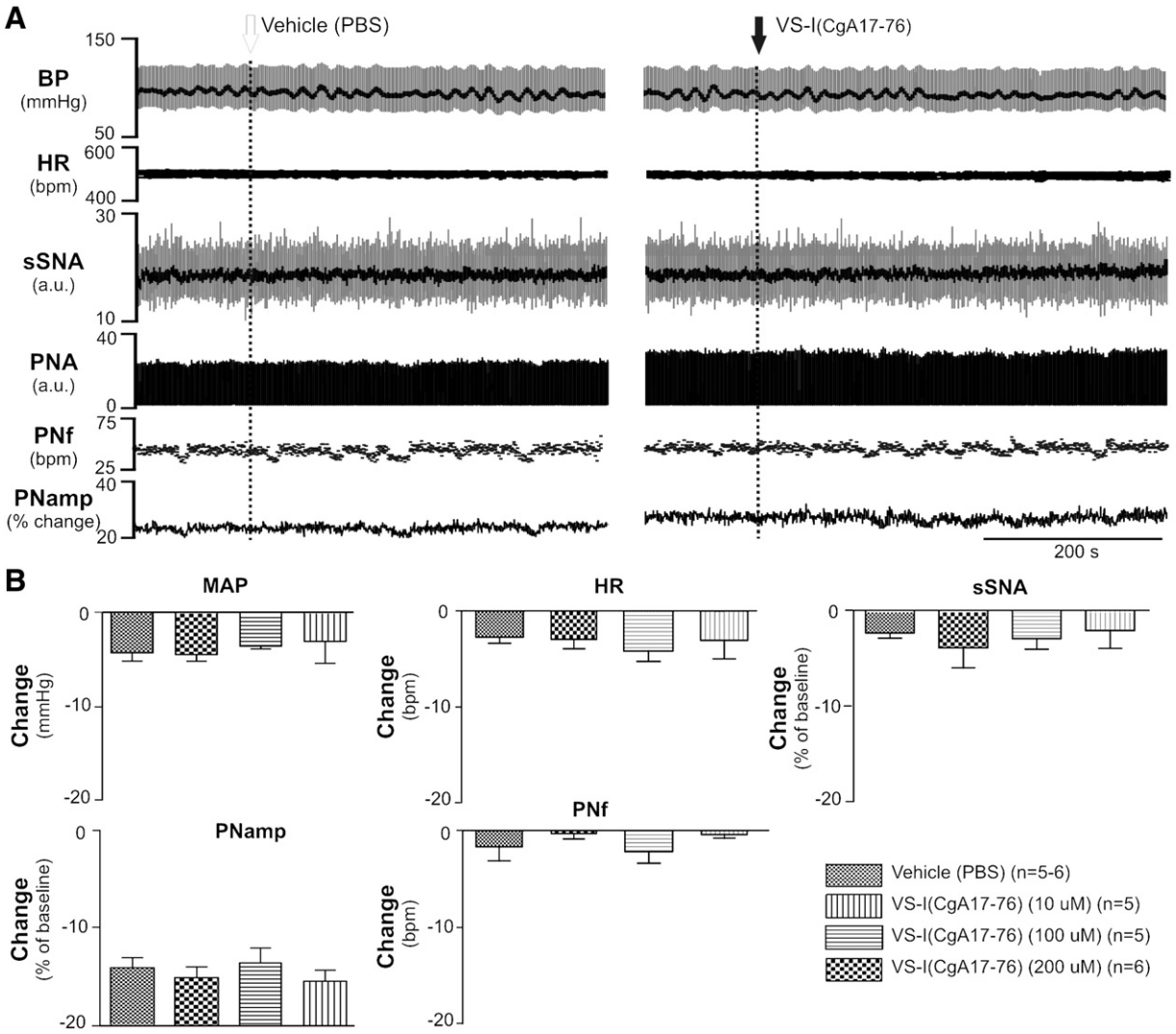

Fig. 1. Effect of intrathecal vasostatin I fragment, CgA_{17-76} (VS-$I_{(CgA17-76)}$) on mean arterial pressure (MAP), heart rate (HR), splanchnic sympathetic nerve activity (sSNA), phrenic nerve frequency (PNf) and phrenic nerve amplitude (PNamp). A: Representative traces following intrathecal injections of vehicle (PBS, open arrow) and VS-$I_{(CgA17-76)}$ (200 μM) (filled arrow). Traces from top to bottom represent blood pressure (BP), HR, integrated sSNA [arbitrary units (a.u.)], rectified phrenic nerve activity (PNA) [(a.u.)], PNf and PNamp. MAP (black) is superimposed on BP (grey) and integrated sSNA (black) is superimposed over raw sSNA (grey). B: comparison of peak cardiovascular and respiratory effects produced by vehicle (PBS, n = 5–6) and 10 μM (n = 5), 100 μM (n = 5) and 200 μM (n = 6) of VS-$I_{(CgA17-76)}$. All the effects were non-significant as compared to PBS. bpm, beats per minute for HR and bursts per minute for PNf.

In a subset of vessels, the NA concentration-response curve was repeated without the addition of VS-$I_{(CgA17-76)}$ (n = 4), resulting in no shift of the concentration-response curve, or change to the EC_{50} value (Fig. 4B, Table 2).

4. Discussion

To the best of our knowledge, this is the first study to examine the central effect of VS-$I_{(CgA17-76)}$ on cardiorespiratory systems and reflexes and the effect of VS-$I_{(CgA17-76)}$ on rat mesenteric arteries. Our data demonstrate that i) VS-$I_{(CgA17-76)}$ applied in the CNS produces no cardiorespiratory effects under the conditions reported here, ii) intrathecal VS-$I_{(CgA17-76)}$ does not modulate sympathetic reflexes examined, and iii) VS-$I_{(CgA17-76)}$ enhances the effect of NA on rat mesenteric arteries. The data suggests that VS-$I_{(CgA17-76)}$ acts through different mechanisms to catestatin, which does exhibit central cardiorespiratory effects when microinjected into the RVLM (Gaede and Pilowsky, 2010). Interestingly, the peripheral effects of VS-$I_{(CgA17-76)}$ appear to be dependent on the vascular bed examined since in human saphenous vein vasostatin I causes relaxation (Aardal and Helle, 1992).

Microinjection of VS-$I_{(CgA17-76)}$ into the RVLM did not elicit any cardiorespiratory changes. The RVLM is essential for the maintenance of the basal level of sympathetic nerve activity as well as resting MAP and reflex control of MAP. Earlier studies showed abundant CgA mRNA in catecholaminergic sympathoexcitatory neurons in the RVLM (Gaede et al., 2009) and CgA was functionally active within the RVLM (Krassioukov et al., 1994). Microinjection of another CgA fragment, catestatin, into the RVLM produced sympathoexcitation, elevates blood pressure and augments phrenic burst amplitude (Gaede and Pilowsky, 2010). In contrast, microinjection of VS-$I_{(CgA17-76)}$ into RVLM, or intrathecally, in the present study produced no cardiorespiratory changes. This suggests that VS-$I_{(CgA17-76)}$ acting on its own is not an active CgA fragment within the RVLM.

Sympathetic preganglionic neurones (SPN), located in intermediolateral cell column of the thoracolumbar spinal cord, receive inputs from a number of brain regions, including the RVLM and participate in controlling cardiovascular responses through their projections to the adrenal medulla and sympathetic autonomic ganglia (Pilowsky and Goodchild, 2002; Guyenet, 2006). The spinal cord is also integral in receiving and conveying afferent information to the brain, as well as relaying the integrated efferent signals of different

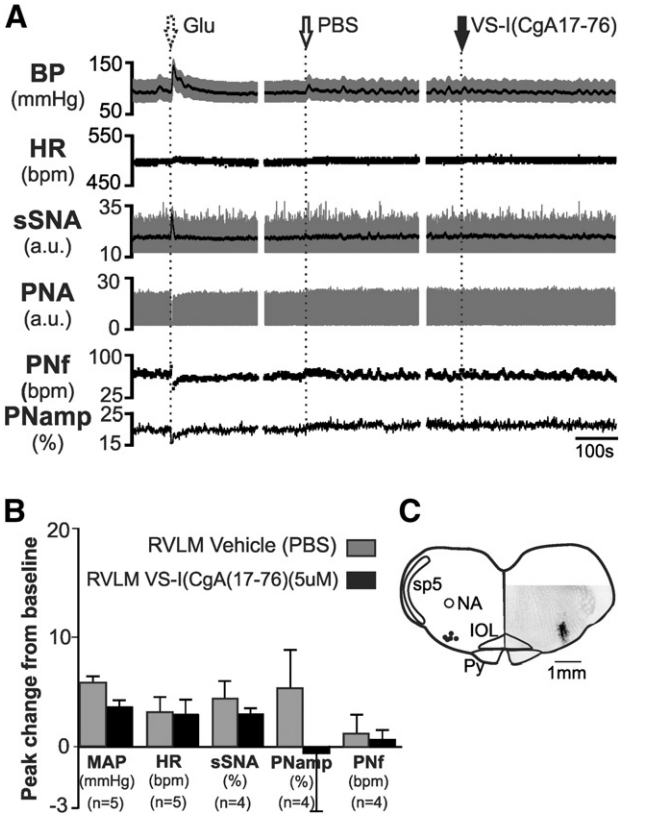

Fig. 2. Effect of unilateral microinjection of vasostatin I fragment, CgA_{17-76} ($VS\text{-}I_{(CgA17-76)}$) (5 μM) on mean arterial pressure (MAP), heart rate (HR), splanchnic sympathetic nerve activity (sSNA), phrenic nerve frequency (PNf) and phrenic nerve amplitude (PNamp). A: Representative traces of the effects of L-glutamate (dotted arrow), vehicle (PBS, open arrow) and $VS\text{-}I_{(CgA17-76)}$ (5 μM, filled arrow) microinjection into the RVLM. Traces from top to bottom represent blood pressure (BP), HR, integrated sSNA [arbitrary unit (a.u)], rectified PNA [(a.u)], PNf and PNamp. MAP (black) is superimposed on BP (grey) and integrated sSNA (black) is superimposed over rectified sSNA (grey). B: Comparison of peak cardiorespiratory effects produced by vehicle (PBS, n = 5) and $VS\text{-}I_{(CgA17-76)}$ (n = 5). C: Microinjection sites in the RVLM and a section showing an injection site labelled with pontamine sky blue. NA: nucleus ambiguus; sp5: spinal trigeminal tract; IOL: inferior olive; Py: pyramidal tract. All changes were non-significant. bpm, beats per minute for HR and bursts per minute for PNf.

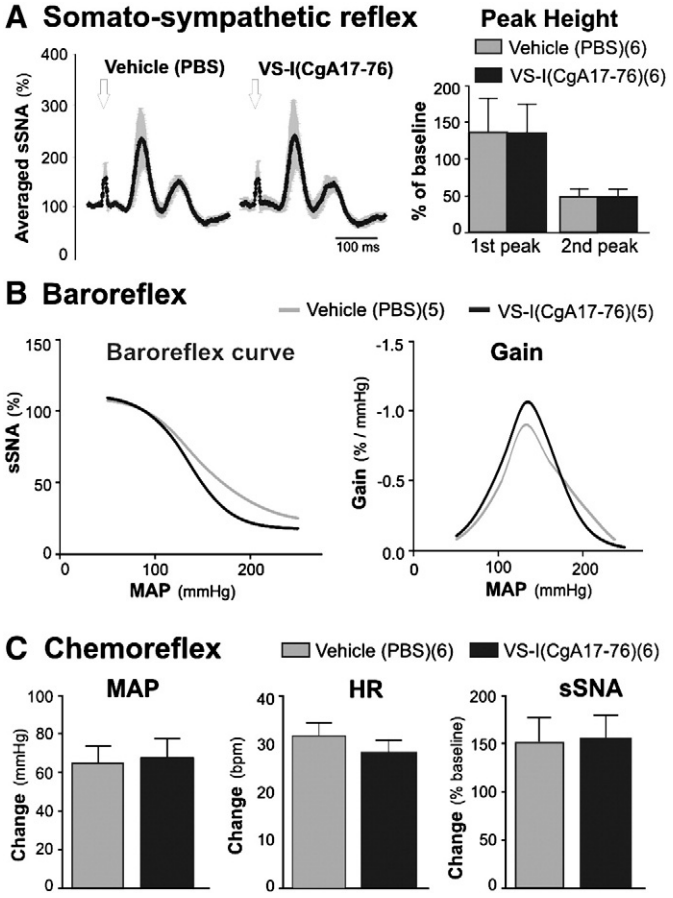

Fig. 3. Effect of intrathecal vasostatin I fragment, CgA_{17-76} ($VS\text{-}I_{(CgA17-76)}$) (200 μM) on somato-sympathetic, baroreceptor and chemoreceptor reflex. A: Effect on somato-sympathetic reflex evoked by sciatic nerve (SN) stimulation. Left 2 traces represent grouped effect of SN-stimulation evoked excitation of splanchnic sympathetic nerve activity (sSNA) after intrathecal injection of vehicle (PBS, n = 6) and $VS\text{-}I_{(CgA17-76)}$ (200 μM, n = 6). Black and grey data denote mean ± SE. Arrows indicate the times of stimulation. Graph on the right panel represents the comparison of peak height. B: Effect on baroreceptor reflex evoked by intravenous injection of phenylephrine hydrochloride and sodium nitroprusside. Left trace represents average sympathetic baroreflex functional curves generated for data after intrathecal injection vehicle (PBS, n = 5) and $VS\text{-}I_{(CgA17-76)}$ (200 μM, n = 5) injection. Right trace represents baroreflex gain for sSNA (error bars are omitted for clarity). C: Comparison of peak effects on mean arterial pressure (MAP), heart rate (HR) and sSNA after intrathecal injection of vehicle (PBS, n = 6) and $VS\text{-}I_{(CgA17-76)}$ (200 μM, n = 6) in response to brief hypoxia induced by ventilation of 100% N2 for 12–14 s. All the effects were non-significant as compared to PBS. bpm, beats per minute.

reflexes. For example, SPN are involved in the baroreflex mediated inhibition of vasomotor activity (Coote and Lewis, 1995; Lewis and Coote, 1996), and are the final relay centre for the integrated efferent signal of peripheral chemoreceptor activation (Sun and Reis, 1994) and the somato-sympathetic response (Stornetta et al., 1989; Makeham et al., 2005). We hypothesised that CgA containing neurons within the RVLM may release CgA, or its fragments, onto SPN to modulate cardiorespiratory functions and reflexes. Our study demonstrates that $VS\text{-}I_{(CgA17-76)}$ delivered intrathecally had no effect on cardiovascular or respiratory function. Previous works in our lab have shown that intrathecal administration of many peptides, including orexin A, neuromedin U and many others, can alter BP, sSNA and HR, indicating peptidergic modulation of cardiovascular functions at the level of the spinal cord (Pilowsky et al., 2009; Shahid et al., 2011; Rahman et al., 2011). Our current observation is similar to that previously shown for another CgA fragment, catestatin and suggests that CgA fragments may not participate in modulation of basal cardiorespiratory parameters at the level of the spinal cord. Furthermore, $VS\text{-}I_{(CgA17-76)}$ modulates neither the afferent nor the efferent pathway of somato-sympathetic, baroreceptors, or chemoreceptor reflex within the spinal cord. However, this does not preclude the possibility that other CgA fragments may be involved in the modulation of physiological reflexes at the level of the spinal cord.

The lack of central effect following $VS\text{-}I_{(CgA17-76)}$ application in this study is not likely due to insufficient peptide injected or the use of inactive fragments. Firstly, chromatographic assay (Section 2.6) confirmed the presence of $VS\text{-}I_{(CgA17-76)}$ in all injectate used in our experiments. Secondly, the fragment used in the current experiments contain two cysteine residues, at the 17th and 38th amino acid positions of vasostatin I to form a disulfide bridge loop ($CgA_{17-38ss}$) that is thought to be important for the biological activities (Tota et al., 2003). Other vasostatin I fragments that contain this disulfide-bridge loop, including CgA_{1-40} (Brekke et al., 2002), and CgA_{7-57} (Tota et al., 2003; Imbrogno et al., 2004), showed similar activity as vasostatin I. Furthermore, the *in vitro* myograph data in this study demonstrate that $VS\text{-}I_{(CgA17-76)}$ potentiated the contractile effects of noradrenaline on rat mesenteric arteries, indicating that this fragment is a biologically active derivative of the original vasostatin I (CgA_{1-76}). Taken together with the lack of effect after either intrathecal or microinjection of $VS\text{-}I_{(CgA17-76)}$, this supports the notion that $VS\text{-}I_{(CgA17-76)}$ does not directly modulate neuronal activity, but may modulate blood vessel tone in the periphery.

Table 1
Baroreflex control of sSNA after intrathecal injection of vehicle (PBS) or the vasostatin I fragment VS-I $_{(CgA17–76)}$, 200 μM.

	Lower plateau (%)	Upper plateau (%)	Mid point (mm Hg)	Max. gain	Range of SNA (%)	Threshold level (mm Hg)	Saturation level (mm Hg)	Operating range (mmHg)
PBS	22.5 ± 7.9	108.8 ± 5.9	143.5 ± 12.2	−0.83 ± 0.2	86.3 ± 11.9	91.6 ± 14.2	195.5 ± 11.5	103.8 ± 8.1

(continued on next page)

Three different methods of receptor independent activation by vasostatin I have been proposed. Vasostatin I can 1) exert potent negative inotrophy via NO-cGMP-PKG dependent mechanism, 2) is a non-competitive inhibitor of the β-adrenergic receptor on cardiomyocytes (Logothetis et al., 1987; Cappello et al., 2007; Cerra et al., 2008) or 3) induce vasodilatation via opening of GIRK channels as additional accessory proteins (Helle, 2010). As these mechanisms are present within the brainstem and spinal cord, the lack of effect of VS-I$_{(CgA17–76)}$ in the present study suggest that VS-I$_{(CgA17–76)}$ is not functionally active under the conditions examined. Another CgA fragment, catestatin, was also unable to modulate cardiovascular system when administered intrathecally (Gaede et al., 2009). However, as CgA is functionally active within the central nervous system, it remains possible that other proteolytic fragment of CgA, including catestatin (Gaede and Pilowsky, 2010), and others, such as chromostatin, pancreastatin or as yet unidentified fragments might be involved in the central effects of CgA. The effects of these fragments on central cardiovascular regulation remain to be determined.

The precursor for vasostatin I, CgA, is widely distributed in the brainstem and suggests that its fragments, including vasostatin I, have modulatory actions within the brain. While the present study demonstrated that vasostatin I, or its fragment, may not be involved in neuronal control of cardiorespiratory function or reflexes under normotensive condition, this does not preclude the possibility that vasostatin I may be involved in other local actions. Vasostation I is a significant factor in cardiovascular regulation in the periphery, including inhibition of vascular contractility, cardiac contractility, and vascular endothelial cell function (Helle, 2010). Intriguingly, our data demonstrates that vasostatin I may have different effects in different parts of the peripheral vasculature. Our current data indicates that the vasostatin I fragment, VS-I$_{(CgA17–76)}$, enhances noradrenaline evoked contractility in the rat mesenteric bed, and is in agreement with a recent study that demonstrated vasostatin I may induce α-adrenoreceptor mediated vasoconstriction (Roatta et al., 2011). Increased contractility of mesenteric artery will result in diversion of blood flow from the mesentery to other vascular beds and is consistent with the inhibitory effect of vasostatin I on gastric motility (Amato et al., 2005). However, this data is in contrast to previous studies in human saphenous vein and internal thoracic artery (Aardal and Helle, 1992; Aardal et al., 1993) and bovine coronary arteries (Brekke et al., 2002). This raises an interesting possibility that vasostatin I may have different modulatory actions on the different vascular beds. It is possible that although vasostatin I does not affect neuronal activity, it may have local effects on the vasculature. In addition, recent evidence indicates that the CgA gene may be involved in essential hypertension as ablation of the CgA gene resulted in hypertension (Sahu et al., 2010). The effects of vasostatin I on local blood flow and in hypertension deserve future study, and remain to be explored in detail. Nevertheless, it is tempting to speculate that vasostatin I could be involved simultaneously in redirecting blood flow from the gut towards the heart, brain and other vital organs in times of stress. Such a combination of effects would be consistent with the release of CgA from the adrenal gland in times of stress.

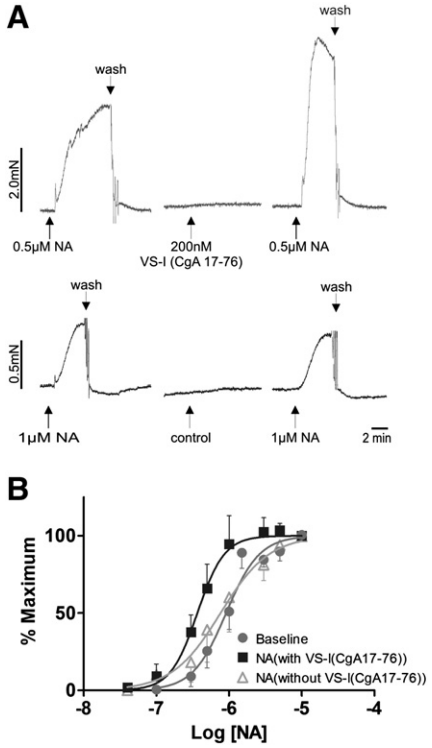

Fig. 4. Effect of noradrenaline (NA) on a third-order rat mesenteric artery. A: Representative traces showing addition of NA causes isometric contraction that is potentiated by pre-incubation with vasostatin I fragment, CgA$_{17–76}$ (VS-I$_{(CgA17–76)}$, top trace). VS-I$_{(CgA17–76)}$ alone had no effect. Repeat application of NA, without pre-incubation with VS-I$_{(CgA17–76)}$, was not different to earlier NA (lower trace). B: Comparison of NA concentration-response curves generated at the beginning of the experiment (baseline, n = 10), repeated following pre-incubation with VS-I$_{(CgA17–76)}$ (with VS-I$_{(CgA17–76)}$, n = 6), or equivalent time-control (without VS-I$_{(CgA17–76)}$, n = 4). Incubation with VS-I$_{(CgA17–76)}$ produced a significant left-shift of the concentration-response curve (* = two-way ANOVA, $P<0.05$).

Table 2
Noradrenaline concentration-response curve parameters for rat third-order mesenteric arteries in the presence and absence of vasostatin I fragment (VS-I $_{(CgA17–76)}$).

	Baseline	With VS-I$_{(CgA17–76)}$	Without VS-I$_{(CgA17–76)}$
EC_{50} (μM)	9.1×10^{-7}	$3.7\times10^{-7*}$	7.7×10^{-7}
Hill slope	1.9	2.3	1.3

*$P<0.0001$ vs baseline, $P<0.05$ vs 'without VS-I $_{(CgA17-76)}$', Student's *t* test. n = 10 for baseline, n = 6 for 'with VS-I $_{(CgA17-76)}$', n = 4 for 'without VS-I $_{(CgA17-76)}$'.

Abbreviations

CgA	Chromogranin A
ECG	electrocardiogram
HR	heart rate
IML	intermediolateral cell column
i.t.	intrathecal
KPSS	high potassium physiological saline solution
MAP	mean arterial pressure
NA	noradrenaline
PBS	phosphate buffered saline
PE	phenylephrine hydrochloride
PNA	phrenic nerve activity
PNamp	phrenic nerve amplitude

PNf	phrenic nerve frequency
PSS	physiological saline solution
RVLM	rostral ventrolateral medulla
SNP	sodium nitroprusside
SPN	sympathetic preganglionic neurons
sSNA	splanchnic sympathetic nerve activity
$VS\text{-}I_{(CgA17–76)}$	Vasostatin I fragment

Acknowledgments

Work in the Authors' laboratory is supported by grants from the National Health and Medical Research Council of Australia (457080, 457069), ARC (DP110102110), Macquarie University and the Garnett Passe and Rodney Williams Memorial Foundation. A.A.R. and I.Z.S. are recipients of Macquarie Research Excellence Scholarships. AMH is supported by a Coregas-Macquarie Research Excellence Scholarship. The authors have no conflicts of interest to declare.

References

Aardal, S., Helle, K.B., 1992. The vasoinhibitory activity of bovine chromogranin A fragment (vasostatin) and its independence of extracellular calcium in isolated segments of human blood vessels. Regul. Pept. 41, 9–18.

Aardal, S., Helle, K.B., Elsayed, S., Reed, R.K., Serck-Hanssen, G., 1993. Vasostatins, comprising the N-terminal domain of chromogranin A, suppress tension in isolated human blood vessel segments. J. Neuroendocrinol. 5, 405–412.

Abbott, S.B.G., Pilowsky, P.M., 2009. Galanin microinjection into rostral ventrolateral medulla of the rat is hypotensive and attenuates sympathetic chemoreflex. Am. J. Physiol. 296, R1019–R1026.

Amato, A., Corti, A., Serio, R., Mulè, F., 2005. Inhibitory influence of chromogranin A N-terminal fragment (vasostatin-1) on the spontaneous contractions of rat proximal colon. Regul. Pept. 130, 42–47.

Angelone, T., Quintieri, A.M., Brar, B.K., Limchaiyawat, P.T., Tota, B., Mahata, S.K., Cerra, M.C., 2008. The antihypertensive Chromogranin A peptide catestatin acts as a novel endocrine/paracrine modulator of cardiac inotropism and lusitropism. Endocrinology 149, 4780–4793.

Banks, P., Helle, K., 1965. The release of protein from the stimulated adrenal medulla. Biochem. J. 97, 40C–41C.

Brekke, J.F., Osol, G.J., Helle, K.B., 2002. N-terminal chromogranin-derived peptides as dilators of bovine coronary resistance arteries. Regul. Pept. 105, 93–100.

Cappello, S., Angelone, T., Tota, B., Pagliaro, P., Penna, C., Rastaldo, R., Corti, A., Losano, G., Cerra, M.C., 2007. Human recombinant chromogranin A-derived vasostatin-1 mimics preconditioning via an adenosine/nitric oxide signaling mechanism. Am. J. Physiol. 293, H719–H727.

Cerra, M.C., De Iuri, L., Angelone, T., Corti, A., Tota, B., 2006. Recombinant N-terminal fragments of chromogranin-A modulate cardiac function of the Langendorff-perfused rat heart. Basic Res. Cardiol. 101, 43–52.

Cerra, M.C., Gallo, M.P., Angelone, T., Quintieri, A.M., Pulera, E., Filice, E., Guerold, B., Shooshtarizadeh, P., Levi, R., Ramella, R., Brero, A., Boero, O., Metz-Boutigue, M.H., Tota, B., Alloatti, G., 2008. The homologous rat chromogranin A ($rCGA_{1-64}$) modulates myocardial and coronary function in rat heart to counteract adrenergic stimulation indirectly via endothelium-derived nitric oxide. FASEB J. 22, 3992–4004.

Coote, J.H., Lewis, D.I., 1995. The spinal organisation of the baroreceptor reflex. Clin. Exp. Hypertens. 17, 295–311.

Gaede, A.H., Pilowsky, P.M., 2010. Catestatin in rat RVLM is sympathoexcitatory, increases barosensitivity, and attenuates chemosensitivity and the somatosympathetic reflex. Am. J. Physiol. 299, R1538–R1545.

Gaede, A.H., Lung, M.S., Pilowsky, P.M., 2009. Catestatin attenuates the effects of intrathecal nicotine and isoproterenol. Brain Res. 1305, 86–95.

Guyenet, P.G., 2006. The sympathetic control of blood pressure. Nat. Rev. Neurosci. 7, 335–346.

Helle, K.B., 2010. The chromogranin A-derived peptides vasostatin-I and catestatin as regulatory peptides for cardiovascular functions. Cardiovasc. Res. 85, 9–16.

Hong, Y., Henry, J.L., 1992. Glutamate, NMDA and NMDA receptor antagonists: cardiovascular effects of intrathecal administration in the rat. Brain Res. 569, 38–45.

Imbrogno, S., Angelone, T., Corti, A., Adamo, C., Helle, K.B., Tota, B., 2004. Influence of vasostatins, the chromogranin A-derived peptides, on the working heart of the eel (*Anguilla anguilla*): negative inotropy and mechanism of action. Gen. Comp. Endocrinol. 139, 20–28.

Krassioukov, A.V., Munoz, D.G., Yang, J.P., Weaver, L.C., 1994. Effect of chromogranin A on central autonomic control of blood pressure. J. Auton. Nerv. Syst. 50, 61–71.

Lewis, D.I., Coote, J.H., 1996. Baroreceptor-induced inhibition of sympathetic neurons by GABA acting at a spinal site. Am. J. Physiol. 270, H1885–H1892.

Logothetis, D.E., Kurachi, Y., Galper, J., 1987. The beta gamma subunits of GTP-binding proteins activate the muscarinic K+ channel in heart. Nature 325, 321–326.

Mahapatra, N.R., O Connor, D.T., Vaingankar, S.M., Hikim, A.P.S., Mahata, M., Ray, S., Staite, E., Wu, H., Gu, Y., Dalton, N., Kennedy, B.P., Ziegler, M.G., Ross, J., Mahata, S.K., 2005. Hypertension from targeted ablation of chromogranin A can be rescued by the human ortholog. J. Clin. Invest. 115, 1942–1952.

Makeham, J.M., Goodchild, A.K., Costin, N.S., Pilowsky, P.M., 2004. Hypercapnia selectively attenuates the somato-sympathetic reflex. Respir. Physiol. Neurobiol. 140, 133–143.

Makeham, J.M., Goodchild, A.K., Pilowsky, P.M., 2005. NK1 receptor activation in rat rostral ventrolateral medulla selectively attenuates somato-sympathetic reflex while antagonism attenuates sympathetic chemoreflex. Am. J. Physiol. 288, R1707–R1715.

Metz-Boutigue, M.-H., Garcia-Sablone, P., Hogue-Angeletti, R., Aunis, D., 1993. Intracellular and extracellular processing of chromogranin A. Determination of cleavage sites. Eur. J. Biochem. 217, 247–257.

Miyawaki, T., Goodchild, A.K., Pilowsky, P.M., 2002. Activation of mu-opioid receptors in rat ventrolateral medulla selectively blocks baroreceptor reflexes while activation of delta opioid receptors blocks somato-sympathetic reflexes. Neuroscience 109, 133–144.

Mulvany, M.J., Halpern, W., 1977. Contractile properties of small arterial resistance vessels in spontaneously hypertensive and normotensive rats. Circ. Res. 41, 19–26.

Pilowsky, P.M., Goodchild, A.K., 2002. Baroreceptor reflex pathways and neurotransmitters: 10 years on. J. Hypertens. 20, 1675–1688.

Pilowsky, P.M., Lung, M.S., Spirovski, D., McMullan, S., 2009. Differential regulation of the central neural cardiorespiratory system by metabotropic neurotransmitters. Philos. Trans. R. Soc. B 364, 2537–2552.

Rahman, A.A., Shahid, I.Z., Pilowsky, P.M., 2011. Intrathecal neuromedin U induces biphasic effects on sympathetic vasomotor tone, increases respiratory drive and attenuates sympathetic reflexes in rat. Br. J. Pharmacol. 164, 617–631.

Roatta, S., Passatore, M., Novello, M., Colombo, B., Dondossola, E., Mohammed, E., Losano, G., Corti, A., Helle, K.B., 2011. The chromogranin A- derived N-terminal peptide vasostatin-I: in vivo effects on cardiovascular variables in the rabbit. Regul. Pept. 168, 10–20.

Sahu, B., Sonawane, P., Mahapatra, N., 2010. Chromogranin A: a novel susceptibility gene for essential hypertension. Cell. Mol. Life Sci. 67, 861–874.

Shahid, I.Z., Rahman, A.A., Pilowsky, P.M., 2011. Intrathecal orexin A increases sympathetic outflow and respiratory drive, enhances baroreflex sensitivity and blocks the somato-sympathetic reflex. Br. J. Pharmacol. 162, 961–973.

Somogyi, P., Hodgson, A.J., DePotter, R.W., Fischer-Colbrie, R., Schober, M., Winkler, H., Chubb, I.W., 1984. Chromogranin immunoreactivity in the central nervous system. Immunochemical characterisation, distribution and relationship to catecholamine and enkephalin pathways. Brain Res. 320, 193–230.

Stornetta, R.L., Morrison, S.F., Ruggiero, D.A., Reis, D.J., 1989. Neurons of rostral ventrolateral medulla mediate somatic pressor reflex. Am. J. Physiol. 256, R448–R462.

Stridsberg, M., Angeletti, R., Helle, K., 2000. Characterisation of N-terminal chromogranin A and chromogranin B in mammals by region-specific radioimmunoassays and chromatographic separation methods. J. Endocrinol. 165, 703–714.

Sun, M.K., Reis, D.J., 1994. Intrathecal kynurenate but not benextramine blocks hypoxic sympathoexcitation in chemodenervated anesthetized rats. J. Auton. Nerv. Syst. 47, 141–150.

Tota, B., Mazza, R., Angelone, T., Nullans, G., Metz-Boutigue, M.H., Aunis, D., Helle, K.B., 2003. Peptides from the N-terminal domain of chromogranin A (vasostatins) exert negative inotropic effects in the isolated frog heart. Regul. Pept. 114, 123–130.

Tota, B., Angelone, T., Mazza, R., Cerrav, M.C., 2008. The chromogranin A-derived vasostatins: new players in the endocrine heart. Curr. Med. Chem. 15, 1444–1451.

Woulfe, J., Deng, D., Munoz, D., 1999. Chromogranin A in the central nervous system of the rat: pan-neuronal expression of its mRNA and selective expression of the protein. Neuropeptides 33, 285–300.

Rahman, A. A., Shahid, I. Z., & Pilowsky, P. M. (2012). Differential cardiorespiratory and sympathetic reflex responses to microinjection of neuromedin U in rat rostral ventrolateral medulla. *Journal of Pharmacology and Experimental Therapeutics*, *341*(1), 213-224.

DOI: 10.1124/jpet.111.191254

Peptides 44 (2013) 15–24

Contents lists available at SciVerse ScienceDirect

Peptides

journal homepage: www.elsevier.com/locate/peptides

Neuromedin U causes biphasic cardiovascular effects and impairs baroreflex function in rostral ventrolateral medulla of spontaneously hypertensive rat

Ahmed A. Rahman[a,b,c], Israt Z. Shahid[a,b], Paul M. Pilowsky[a,*]

[a] Australian School of Advanced Medicine, Macquarie University, Sydney, NSW 2112, Australia
[b] Pharmacy Discipline, Life Science School, Khulna University, Khulna 9208, Bangladesh
[c] College of Health and Biomedicine, Victoria University, Melbourne, Australia

ARTICLE INFO

Article history:
Received 4 January 2013
Received in revised form 15 March 2013
Accepted 15 March 2013
Available online 25 March 2013

Keywords:
Sympathetic vasomotor tone
Phrenic nerve activity
Somatosympathetic reflex
Spinal cord

ABSTRACT

Neuromedin U (NMU) causes biphasic cardiovascular and sympathetic responses and attenuates adaptive reflexes in the rostral ventrolateral medulla (RVLM) and spinal cord in normotensive animal. However, the role of NMU in the pathogenesis of hypertension is unknown. The effect of NMU on baseline cardiorespiratory variables in the RVLM and spinal cord were investigated in urethane-anaesthetized, vagotomized and artificially ventilated male spontaneously hypertensive rats (SHR) and Wistar–Kyoto rats (WKY). Experiments were also conducted to determine the effects of NMU on somatosympathetic and baroreceptor reflexes in the RVLM of SHR and WKY. NMU injected into the RVLM and spinal cord elicited biphasic response, a brief pressor and sympathoexcitatory response followed by a prolonged depressor and sympathoinhibitory response in both hypertensive and normotensive rat models. The pressor, sympathoexcitatory and sympathoinhibitory responses evoked by NMU were exaggerated in SHR. Phrenic nerve amplitude was also increased following intrathecal or microinjection of NMU into the RVLM of both strains. NMU injection into the RVLM attenuated the somatosympathetic reflex in both SHR and WKY. Baroreflex sensitivity was impaired in SHR at baseline and further impaired following NMU injection into the RVLM. NMU did not affect baroreflex activity in WKY. The present study provides functional evidence that NMU can have an important effect on the cardiovascular and reflex responses that are integrated in the RVLM and spinal cord. A role for NMU in the development and maintenance of essential hypertension remains to be determined.

1. Introduction

Neuromedin U (NMU) was originally purified from porcine spinal cord and named because of its potent contractile activity on uterine smooth muscle [19]. NMU is implicated not only in uterine smooth muscle contraction, but also in other functions such as feeding, blood pressure (BP) regulation and regional blood flow, ion transport in the gut, adrenocortical function, anxiety-related behavior, nociception, inflammation, bone-remodeling and, more recently even in cancer, suggesting differential physiological and pharmacological roles of NMU (reviewed in [20]). NMU acts at two GPCRs ($G_{q/11}$ and/or $G_{i/0}$), NMU receptor 1 (NMU1) and NMU receptor 2 (NMU2) [1]. NMU1 is predominantly expressed in peripheral tissues while NMU2 in the central nervous system [12,31,43,48].

The presence of NMU immunoreactive neurons in key cardiovascular areas of the brainstem and spinal cord including the nucleus tractus solitarius (NTS), dorsal motor nucleus of the vagus, inferior olive and area postrema [12], raising the possibility that NMU may participate in the central control of cardiovascular function. NMU increases sympathetic nerve activity (SNA), BP, heart rate (HR) and plasma noradrenaline when given by intracerebroventricular injection [5,44]. Microinjection of NMU into the NTS decreases BP and HR [45]. Recently we demonstrated that NMU delivered intrathecally or microinjected into the RVLM, shows biphasic effects on sympathetic vasomotor tone and differentially modulates sympathetic reflexes [33,34]. However, whether the NMU system in the RVLM and/or in the spinal cord contributes to the pathogenesis of hypertension is unknown. These data, along with those concerning the role of NMU in the modulation of

Abbreviations: AUC, area under the curve; BP, blood pressure; HR, heart rate; i.t., intrathecal; MAP, mean arterial pressure; NMU, neuromedin U; NMU1, neuromedin U receptor 1; NMU2, neuromedin U receptor 2; NTS, nucleus tractus solitarius; PBS, phosphate buffered saline; PE, phenylephrine hydrochloride; PNA, phrenic nerve activity; PNamp, phrenic nerve amplitude; PNf, phrenic nerve frequency; RVLM, rostral ventrolateral medulla; SD, Sprague-Dawley rats; SHR, spontaneously hypertensive rats; SPN, sympathetic preganglionic neurons; sSNA, splanchnic sympathetic nerve activity; WKY, Wistar–Kyoto rats.

* Corresponding author at: The Australian School of Advanced Medicine, F10A, Macquarie University Sydney, NSW 2109, Australia. Tel.: +61 2 9812 3560; fax: +61 2 9812 3600.
E-mail addresses: paul.pilowsky@mq.edu.au, ppilowsky@gmail.com (P.M. Pilowsky).

0196-9781/$ – see front matter.
http://dx.doi.org/10.1016/j.peptides.2013.03.017

Rahman, A. A., Shahid, I. Z., & Pilowsky, P. M. (2013). Neuromedin U causes biphasic cardiovascular effects and impairs baroreflex function in rostral ventrolateral medulla of spontaneously hypertensive rat. Peptides, 44, 15-24. https://doi.org/10.1016/j.peptides.2013.03.017

cardiovascular function and sympathetic reflexes in normotensive rats, led us to hypothesize that altered NMU activity in the RVLM and spinal cord contribute to the pathogenesis of hypertension in SHR. The objectives of the present study were 1) to investigate the cardiovascular and respiratory effects of NMU following microinjection into the RVLM, and intrathecal (i.t.) injection at the T5–T7 level of thoracic spinal cord in SHR and normotensive Wistar–Kyoto rats (WKY), and 2) to evaluate the effects of NMU on somatosympathetic, and baroreceptor reflexes in the RVLM.

2. Materials and methods

All procedures in the present study were approved by the Animal Ethics Committee of Macquarie University, Sydney, Australia and conducted in accordance with the guidelines of the Australian Code of Practice for the Care and Use of Animals for Scientific Purposes (http://www.nhmrc.gov.au/guidelines/publications/ea16).

2.1. General procedures

Experiments were performed in 18–20 weeks, age-matched adult male SHR (310–375 g) and WKY (355–385 g). Rats were anaesthetized with an initial dose (1.2–1.4 g kg^{-1}, i.p.) of urethane. Supplemental doses of urethane (20–30 mg, i.v.) were given if BP rose more than 10 mmHg in response to hind paw pinch at every 30 min. Body temperature was monitored and maintained at $37 \pm 0.5\,^{\circ}C$ by placing rats on a feedback-controlled heating blanket for the duration of the experiment (Harvard Apparatus, Holliston, MA, USA).

The left carotid artery and right jugular vein were cannulated for measurement of BP and regular injections of drugs and fluids, respectively. In 5 animals, the left femoral vein was cannulated for administration of phenylephrine hydrochloride (PE). HR was derived from the arterial BP. The trachea was cannulated to permit artificial ventilation and end-tidal CO_2 monitoring. Nerve recordings were obtained from the splanchnic and phrenic nerves. The left greater splanchnic nerve was isolated and dissected through a retroperitoneal approach. The phrenic nerve was accessed from a dorsolateral approach after retraction of the left shoulder blade. The distal end of the nerves were tied with 5/0 silk thread and cut to permit recording of efferent nerve activity. In 5 experiments, the sciatic nerve was isolated, tied and cut. Once the nerves were isolated, they were covered with saline soaked cotton wool for the duration of the remainder of surgical preparation to prevent desiccation.

Animals were secured in a stereotaxic frame and the head tilted downwards at a 45° angle to the horizontal. All animals were paralyzed (pancuronium bromide; 0.8 mg i.v. initially, then 0.4 mg h^{-1}, i.v.), artificially ventilated with oxygen-enriched room air and bilaterally vagotomized to prevent entrainment of the phrenic nerve discharge to the ventilator. End-tidal CO_2 and pH were maintained at 4.0–4.5% and 7.35–7.45, respectively, by adjusting the rate and depth of ventilation after arterial blood gas analysis (pH 7.4 ± 0.05, $PaCO_2$ 40.4 ± 0.6). Animals were infused with 5% glucose in water (1.0–2.0 ml h^{-1}) to ensure hydration. Nerve recordings were made with bipolar silver wire electrodes. The recording electrodes were immersed in a pool of liquid paraffin oil to prevent dehydration and for electrical insulation. After nerves were placed on the recording electrodes, rats were allowed to stabilize for 30–60 min. The neurograms were amplified (10,000×; CWE Inc., Ardmore, PA, USA), band pass filtered (0.1–2 kHz), sampled at 3 kHz (1401 plus, CED Ltd., Cambridge, UK) and recorded on computer using Spike2 software (v7, CED Ltd., Cambridge, UK).

2.2. RVLM microinjections

To enable microinjection into the RVLM, the dorsal surface of the medulla was exposed by partial occipital craniotomy. The dura was cut and reflected laterally. The brainstem was kept moist using phosphate buffered saline (PBS) soaked cotton wool until the experiment protocol began. Brain microinjection, and functional identification of the RVLM, was performed as described previously [32,38]. Briefly, bilateral microinjection of test agents into the RVLM, at a fixed volume of 50 nl, was carried out stereotaxically and sequentially with single barrel glass pipettes over a 10-s period. At the beginning of each experiment, RVLM was identified functionally on either side by an increase of >30 mmHg in MAP following microinjection of L-glutamic acid (5 nmol). The preliminary coordinates used to find the RVLM were 1.8 mm rostral, 1.8 mm lateral, and 3.5 mm ventral to calamus scriptorius. Vehicle solutions, PBS contained 2% rhodamine beads to aid in subsequent histological verification of the injection site. Following euthanasia (3 M KCl, 0.5 ml, i.v.) the brain was removed from the skulls, fixed in 4% paraformaldehyde and sectioned at 100 μm to verify the microinjection sites. Only rats with microinjection sites within the boundaries of the RVLM were used for data analysis.

2.3. I.t. drug administration

I.t. drug injection was performed as described previously [34,37]. Briefly, an i.t. catheter was inserted into the sub-arachnoid space and advanced caudally to the levels of T5–T7 following exposure of the occipital crest and incision of the atlanto-occipital membrane. The patency of the catheter was examined immediately after insertion by withdrawal of cerebrospinal fluid. The slit was left open to prevent increase in i.t. pressure caused by the injection of agents or by flushing. Drug (NMU; 2 mM) and vehicle (10 mM PBS; pH 7.4) were administered i.t. in a total volume of 10 μl using a 25-μl Hamilton syringe. The volume of each catheter was measured before insertion (range 6–8 μl) into i.t. space and this volume was then used to flush the catheter. Injections were made over a 15- to 20-s period. Successful catheterization was confirmed by injecting L-glutamic acid (100 mM, 10 μl). Sharp increases in BP (~20 mmHg), HR (~30 bpm) and sSNA (~30%) indicated a successful catheterization [e.g. 11, 34]. At the end of experiment the location of the injection site was marked by an injection of 10 μl of India ink flushed with PBS. Following euthanasia (3 M KCl, 0.5 ml, i.v.) a laminectomy was performed to verify the location of the cannula tip.

2.4. Sympathetic reflex activation

Baroreflexes were evoked as described previously [6,34]. The sciatic nerve (somatosympathetic reflex) was stimulated intermittently (0.2 ms pulse width; 50 pulses, 1 Hz) at a voltage that was sufficient to generate 2 distinct peaks in the rectified, averaged sSNA trace over the stimulus period (6–18 V) before and after microinjection of NMU. Baroreceptors were activated by intravenous injection of PE (0.1 mg kg^{-1}) before and after microinjection of NMU.

2.5. Experimental protocol

To investigate the effects of NMU on cardiovascular and respiratory responses in the RVLM, NMU (2 mM equivalent to 100 pmol per side, 50 nl) was injected into the RVLM. The dose of NMU was chosen according to dose response curves done in previous experiments [33,34]. PBS was microinjected as a volume and vehicle control 30 min after the completion of glutamate application. This time lag was adopted to ensure complete recovery from the glutamate-induced pressor response before bilateral microinjection into the RVLM of vehicle. Another gap of 30 min was given before injection of NMU. In another set of animals, the somatosympathetic and arterial baroreflexes were evoked before and after

bilateral microinjection of NMU. As the inhibitory effect of NMU was more prominent, reflexes were induced at this phase.

NMU (2 mM equivalent to 20 nmol, 10 μl) and PBS were also injected i.t. at T5–T7 level to determine the effects of NMU in cardiorespiratory parameters in the spinal cord. In both RVLM microinjection and i.t. injection experiments, each animal received only one treatment and vehicle to avoid tachyphylaxis. The effect of NMU on basal MAP, HR, sSNA or phrenic nerve activity (PNA) was evaluated for 60 min post-treatment.

2.6. Data acquisition and analysis

Data were analyzed using Spike 2 version 7 software (CED, UK). Neurograms were rectified and smoothed (sSNA 1 s time constant; PNA, 50 ms). Zero sSNA value was obtained from the minimum background activity after death and was subtracted from sSNA. Baseline values were obtained by averaging 60 s of data 5 min prior to NMU or PBS injection and maximum changes were expressed as absolute (MAP, HR, phrenic nerve frequency (PNf)), or percentage (sSNA and phrenic nerve amplitude (PNamp)) changes from baseline values. sSNA was rectified and smoothed at 5 ms and 1 s time constants to analyze somatosympathetic reflex and baroreceptor reflex, respectively. To analyze reflexes, sSNA was normalized between the activity of sSNA before NMU injection (100%) and the sSNA after death (0%). The sSNA response to sciatic nerve stimulation was analyzed using peristimulus waveform averaging. The area under the curve (AUC) of the sympathoexcitatory peaks was analyzed. To normalize the difference in baseline values, efficiency of the somatosympathetic reflex was assessed by calculating percent change from the control (pre-drug administration). The percentage changes for somatosymapthetic reflex were calculated according to Eq. (1).

$$\left(\frac{\text{Response to drug or control}}{\text{control response}}\right) \times 100\% \quad (1)$$

To analyze the data from the baroreflex function tests, mean MAP was divided into 1 s consecutive bins and the average sSNA during each bin was determined; successive values were tabulated and graphed as XY plots, taking MAP as the abscissa and sSNA as the ordinate. Each data set was then analysed to determine the sigmoidal curve of best fit [15], which is described by Eq. (2).

$$y = \frac{A1}{[1 + \exp(A2(x - A3))] + A4} \quad (2)$$

where y is sSNA, x is MAP, $A1$ is the y range (y at the upper plateau − y at the lower plateau), $A2$ is the gain coefficient, $A3$ is the value of x at the midpoint (which is also the point of maximum gain), and $A4$ is y at the lower plateau. The computed baroreflex function curves were differentiated to determine the gain of SNA of the baroreflex across the full range of MAP and the peak gain of each curve were determined. The range of sSNA was calculated as the difference between the values at the upper and lower plateaus of the curve. The threshold and saturation values for MAP were defined [18] as the values of MAP at which y was 5% (of the y range) below and above the upper and lower plateaus, respectively.

2.7. Statistics

Statistical analysis was conducted with GraphPad Prism (version 5.0) (GraphPad, La Jolla, CA, USA). Grouped data are expressed as mean ± SE. Paired t-test was used to analyze peak effects and reflexes. One-way ANOVA with Bonferroni's correction was used to compare the drug responses between the strains. Differences were considered significant when the P value was less than 0.05.

2.8. Drugs

NMU (MW = 2643; Cat. No: 2421; Lot No: 30955) was obtained from Auspep (Australia). Urethane, L-glutamic acid, glucose, PE were purchased from Sigma–Aldrich (Sydney, Australia), pancuronium bromide from AstraZeneca Pty Ltd. (Sydney, Australia), rhodamine microbeads from Molecular Probes (NSW, Australia) and PBS (10 mM in 0.9% NaCl) tablets from AMRESCO Inc. (Solon, OH, USA). NMU and rhodamine (2%, v/v) were dissolved and further diluted in PBS (10 mM; pH 7.4). PBS and PE were prepared in deionised water. Urethane was dissolved in 0.9% NaCl and L-glutamic acid in PBS.

3. Results

3.1. Cardiovascular and sympathetic responses to microinjection of NMU into the RVLM

NMU (100 pmol per side, 50 nl) was microinjected bilaterally into the functionally identified and histologically verified sites within the RVLM to determine its effect on MAP, HR and sSNA. The baseline MAP, HR and integrated sSNA in anaesthetized WKY ($n = 6$) and SHR ($n = 6$) were 84 ± 4 and 127 ± 9 mmHg, 444 ± 13 and 451 ± 9 bpm, and 4.3 ± 0.6 and 8.9 ± 0.8 μV, respectively. Baseline MAP and integrated sSNA in SHR were significantly higher ($P < 0.05$) than those recorded in WKY. Bilateral microinjection of NMU into the RVLM elicited a short-term hypertensive, tachycardiac and sympathoexcitatory response followed by a prolonged hypotensive, bradycardiac and sympathoinhibitory response in both SHR ($n = 6$) and WKY ($n = 6$) (Fig. 1A–C). The effects were almost immediate and peaked about 30 seconds after bilateral administration of the peptide (Fig. 1A and B). The excitatory response lasted for ≈5 min when the inhibitory response started that returned to baseline in about 30 min (Fig. 1A and B). The hypertensive (39 ± 4 mmHg vs 16 ± 2 mmHg, $P < 0.01$), sympathoexcitatory (35 ± 4% vs 24 ± 1% of baseline, $P < 0.05$) and sympathoinhibitory (−32 ± 4% vs −12 ± 2% of baseline, $P < 0.05$) responses were significantly higher in SHR as compared with WKY (Fig. 1C).

Microscopic examination of microinjection sites, marked with rhodamine microbeads, confirmed that all injections used in this study were within 500 μm of the caudal end of the facial nucleus (Fig. 1D).

3.2. Respiratory response to microinjection of NMU into the RVLM

NMU injected bilaterally (100 pmol per side, 50 nl) into the RVLM evoked a significant increase in PNamp without any effect on PNf in both SHR ($n = 6$) and WKY ($n = 6$) (Fig. 1A–C). No significant difference was observed in the PNamp increase between SHR (28 ± 4% of baseline, $P < 0.05$) and WKY (24 ± 2% of baseline, $P < 0.001$) (Fig. 1C).

3.3. Somatosympathetic reflex response to microinjection of NMU into the RVLM

Intermittent stimulation of the sciatic nerve resulted in two characteristic excitatory peaks in sSNA of both SHR and WKY. The latencies of the peaks at control period did not differ significantly in the two strains (SHR: 84 ± 3 and 165 ± 5 ms; WKY: 80 ± 1 and 157 ± 3 ms) (Fig. 2A). However the baseline of sSNA was shifted to higher level at SHR compared to WKY (Fig. 2A), and the AUC of first excitatory peak was significantly smaller in SHR ($n = 5$) than that in WKY ($n = 5$) ($P < 0.05$) (Fig. 2B). Bilateral NMU injection (100 pmol per side, 50 nl) in the RVLM markedly attenuated the AUC of both excitatory peaks of sSNA at both hypertensive and normotensive rats as compared to control (Fig. 2B–F). However the latencies of

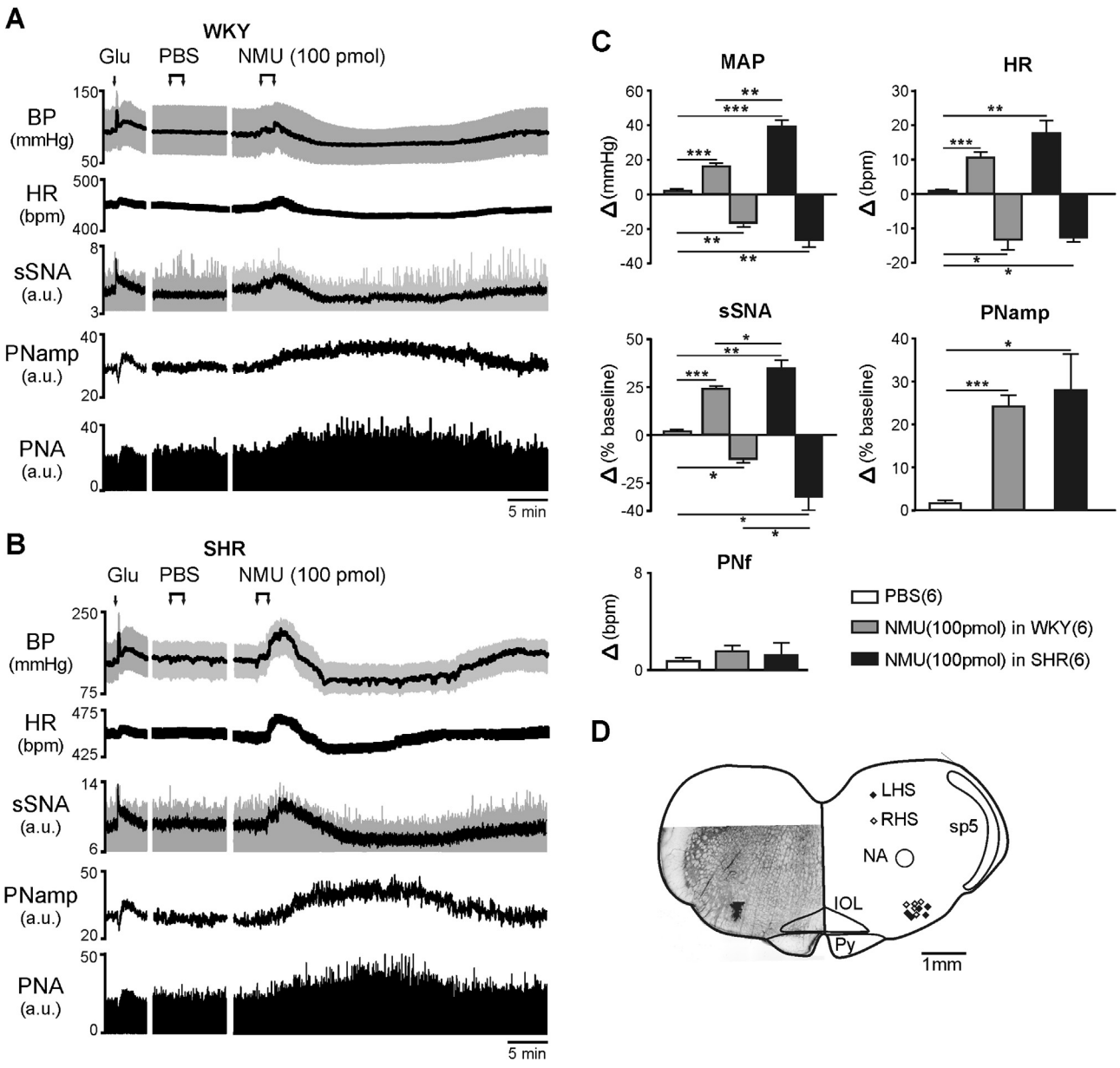

Fig. 1. Effect of bilateral microinjection of neuromedin U (NMU) into the rostral ventrolateral medulla (RVLM) of spontaneously hypertensive rats (SHR) and Wistar–Kyoto rats (WKY). (A) and (B) representative recording of blood pressure (BP) (gray – pulsatile and black – mean), heart rate (HR), splanchnic sympathetic nerve activity (sSNA) (gray – rectified and black – rectified and integrated) [arbitrary unit (a.u.)], phrenic nerve amplitude (PNamp) and rectified phrenic nerve activity (PNA) [arbitrary unit (a.u.)] before and after injection of L-glutamic acid (Glu), phosphate buffered saline (PBS) or NMU (100 pmol) in WKY (A) and SHR (B). (C) Grouped data of maximum cardiorespiratory effects following PBS or NMU. Peak effects are shown as absolute (mean arterial pressure (MAP), HR, phrenic nerve frequency (PNf)) or percentage (sSNA, PNamp) change from respective basal values. (D) Microinjection sites in the RVLM and a section showing an injection site stained following an injection of rhodamine microbeads. Data are expressed as mean ± SE. Number of animals are shown in parentheses. $^{***}P < 0.001$, $^{**}P < 0.01$, $^{*}P < 0.05$ compared with PBS or compared between SHR and WKY. bpm, beats per minute for HR or bursts per minute for PNf.

the peaks of sSNA were not significantly altered by NMU injection in any strain (data not shown).

3.4. Baroreflex response to microinjection of NMU into the RVLM

Changes in sSNA were plotted against changes in MAP evoked by i.v. injection of PE in both SHR ($n = 5$) and WKY ($n = 5$). During the control period baroreflex sensitivity was reduced in SHR, as indicated by a decrease in maximum gain, when compared to WKY. Bilateral microinjection of NMU (100 pmol per side, 50 nl) into RVLM significantly inhibited the reflex sympathoinhibitory responses evoked by PE in SHR. NMU significantly decreased the maximum gain, range of sSNA, the threshold level, midpoint and the saturation level of MAP without significantly altering the lower plateau, upper plateau and operating range as compared with control (Fig. 3A and Table 1). In contrast, NMU failed to change the baroreflex sensitivity of sSNA in WKY (Fig. 3B and Table 2).

3.5. Cardiovascular and sympathetic responses to i.t. injection of NMU

To elucidate the role of NMU in the spinal cord on MAP, HR and sSNA, NMU was injected i.t. at T5–T7 level of the spinal cord. In both SHR ($n = 5$) and WKY ($n = 5$), i.t. injection of NMU (20 nmol) evoked a biphasic response consisting of a rapid transient increase followed by a marked prolonged decrease in MAP and sSNA, that reached

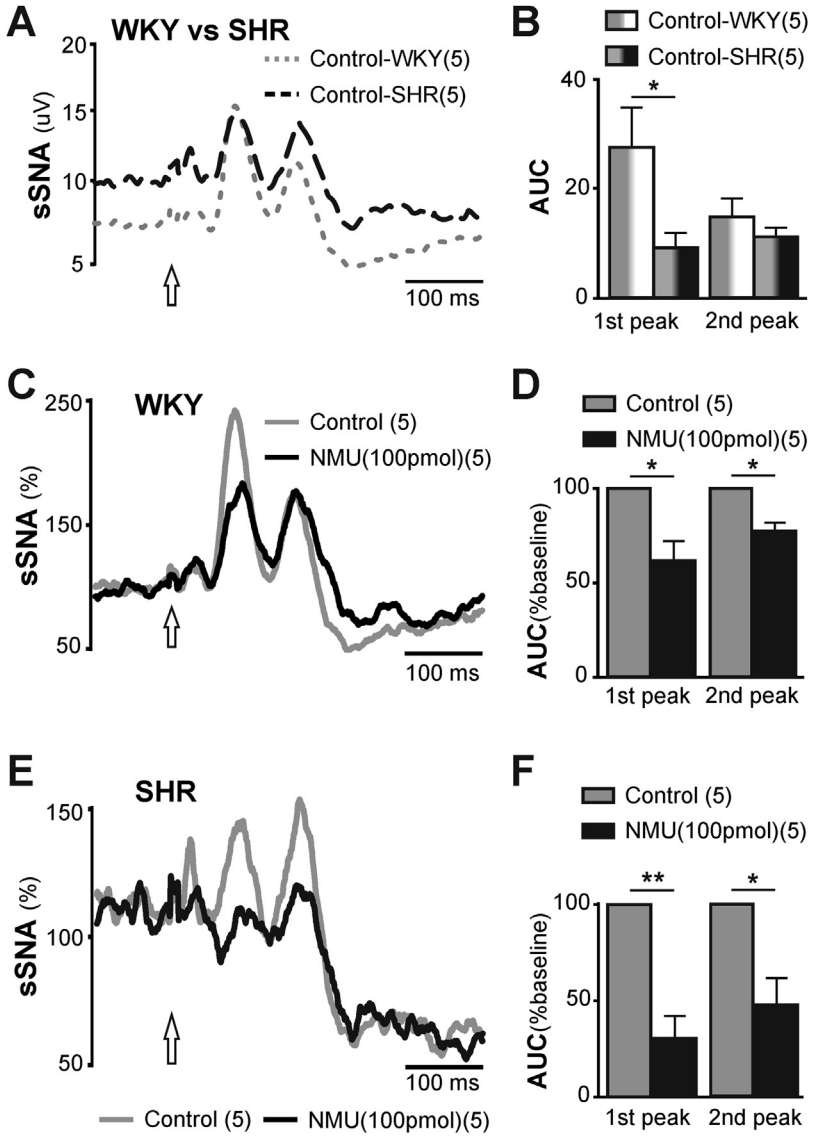

Fig. 2. Effect of bilateral microinjection of neuromedin U (NMU) on somatosympathetic reflex in spontaneously hypertensive rats (SHR) and Wistar–Kyoto rats (WKY). (A) Grouped effect of sciatic nerve-evoked stimulation of splanchnic sympathetic nerve activity (sSNA) (in μV unit) at control period in SHR and WKY. (C) and (E) Grouped effect of sciatic nerve-evoked stimulation of sSNA (%) at control period and after injection of NMU in WKY (C) and SHR (E). Error bars are omitted for clarity. Arrows indicate the time of stimulation. (B) Grouped data comparing the AUC of 1st and 2nd sympathoexcitatory peaks between WKY and SHR during control (pre-drug administration) period. (D) and (F) Grouped data illustrating the effects of NMU (100 pmol, $n = 5$ for each strain) on the AUC of 1st and 2nd sympathoexcitatory peaks in WKY (D) and SHR (F). $^{**}P < 0.01$, $^{*}P < 0.05$ compared with control or compared between SHR and WKY.

a maximum inhibition ≈10 min after the injection (Fig. 4A–C). Peak of the pressor response and sympathoexcitation was reached within 2–3 min after injection (Fig. 4A and B). All variables returned toward basal values after 30 min. The magnitude of increase in MAP and decrease in sSNA evoked by NMU was significantly higher in SHR than in WKY (ΔMAP, 39 ± 6 vs. 9 ± 5 mmHg, $P < 0.01$; ΔsSNA, −48 ± 8% vs −27 ± 5% of baseline, $P < 0.05$; $n = 5$ for each strain; Fig. 4C). NMU did not cause any significant change in HR in both strains (Fig. 4A–C). Vehicle (PBS) ($n = 5$ for each strain) had no effect on MAP, HR or sSNA (Fig. 4A–C).

3.6. Respiratory response to i.t. injection of NMU

I.t. injection of NMU evoked moderate increase in PNamp in both SHR ($n = 5$) and WKY ($n = 5$), that peaked at ≈15 min post-injection and returned gradually to baseline in 30 min (Fig. 4A and B). The change in PNamp evoked by NMU was significantly higher in SHR than in WKY (38 ± 8% vs 20 ± 3% of baseline; $n = 5$ for each strain; $P < 0.05$) (Fig. 4C). In contrast, NMU did not induce any significant change in PNf in any strain. I.t injection of PBS also had no effect on PNamp and PNf (Fig. 4A–C).

4. Discussion

The main findings of the present study are first, that NMU causes biphasic cardiovascular and sympathetic responses consisting of an initial pressor and sympathoexcitatory phase followed by a sustained hypotensive and sympathoinhibitory phase when administered intrathecally, or when microinjected into the RVLM, in both SHR and WKY. Secondly, that NMU increases PNamp following injection intrathecally or into the RVLM, of both hypertensive and normotensive rats. Thirdly, that NMU impairs the sympathetic baroreflex in the RVLM of SHR, but not in normotensive animals. Fourthly, that the excitatory peaks of sSNA evoked by sciatic nerve stimulation – somatosympathetic reflex – are attenuated by NMU injection into the RVLM in both SHR and WKY.

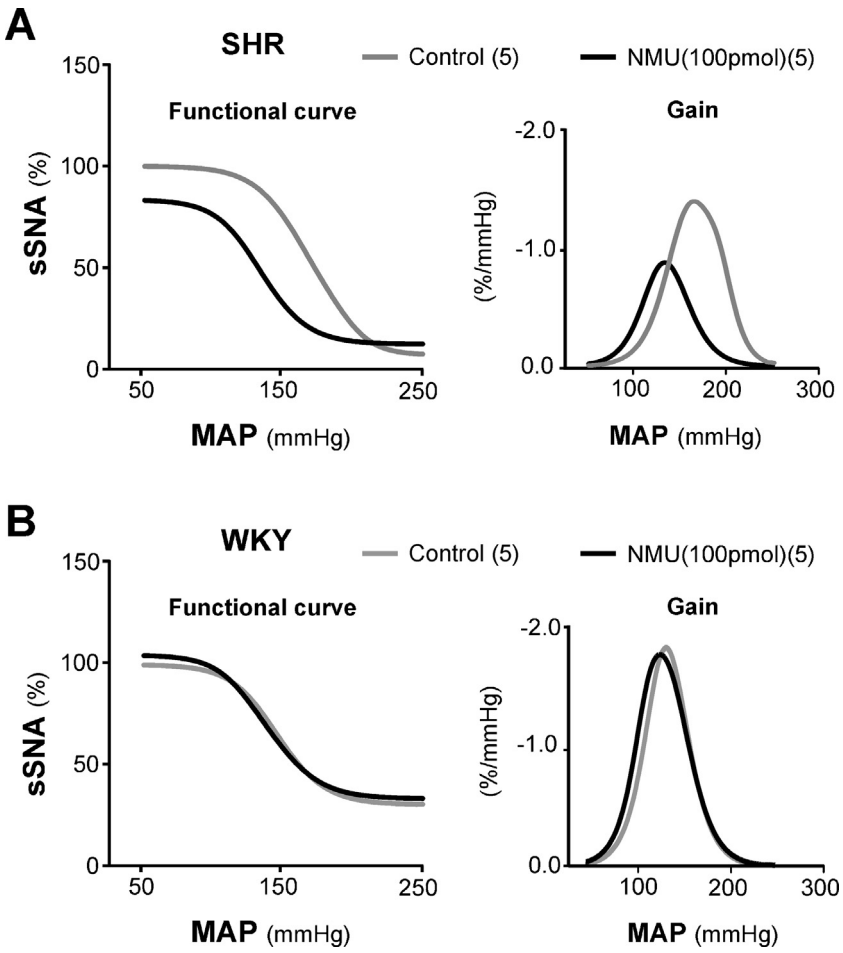

Fig. 3. Effect of bilateral microinjection of neuromedin U (NMU) in the rostral ventrolateral medulla on the arterial baroreflex evoked by intravenous injection of phenylephrine hydrochloride (PE) in spontaneously hypertensive rats (SHR) and Wistar–Kyoto rats (WKY). (A) and (B) Average splanchnic sympathetic baroreflex function curves generated for data before (control) or after NMU (100 pmol, $n = 5$ for each strain) injection in SHR (A) and WKY (B). Traces at right represent baroreflex gain for sSNA (error bars are omitted for clarity – see Table 1 for SHR and Table 2 for WKY).

Consistent with our previous findings in Sprague-Dawley rats (SD) [33], bilateral microinjection of NMU into the RVLM causes a biphasic response consisting of an initial brief hypertension, tachycardia and sympathoexcitation followed by a prolonged hypotension, bradycardia and sympathoinhibition in both WKY and SHR. These data suggest that NMU receptors are present on RVLM neurons in WKY and SHR, and that activation of these receptors profoundly alters the function of cardiorespiratory neurons in the RVLM. Considerable evidence indicates that increased RVLM neuronal activity leading to increased basal SNA is a critical mechanism for the development and maintenance of hypertension [4,16,23]. In SHR, excitation of RVLM vasomotor neurons is mainly due to increased glutamate mediated excitation and decreased GABA mediated inhibition [10,42]. The mechanism of the effect of NMU on neuronal activity in the RVLM of SHR and WKY is unclear. A lack of availability of potent and selective NMU receptor antagonists and/or a good antibody for NMU receptors further restricts our ability to elucidate the precise mechanism of the NMU mediated modulation of cardiovascular function in RVLM. Recently we suggested that the excitatory effect is due to the activation of NMU2 whereas the inhibitory effect is due to the activation of NMU1 [33]. However, involvement of other unknown or unidentified receptors for NMU cannot be excluded [24,50]. Further studies are necessary to clarify the precise mechanisms involved.

In this study we find that the pressor, sympathoexcitatory and sympathoinhibitory responses evoked by NMU are significantly higher in SHR compared to WKY. This augmented sympathoinhibitory effect in SHR is likely due to the higher level of sympathetic activity present in SHR as seen here and in previous work [13]. The effects of NMU microinjection into the RVLM of SD, WKY and SHR strongly suggest a role of NMU and the presence of NMU receptors in the RVLM. NMU1 and NMU2 are both coupled to phospholipase C stimulation via a Gq-type G protein, resulting in the release of the inositol triphosphate (IP_3) second messenger and increased intracellular Ca^{2+} [3,30,47]. Phosphatidylinositol-3 kinase-sensitive pathway in the RVLM is considered to be an important cause of the elevated arterial pressure in SHR [36,46]. These data seem to indicate that NMU receptors are either more sensitive or greater in number in the RVLM of SHR. Further studies are needed to clarify this mechanism.

Here we show that in anesthetized and vagotomized SHR and WKY, discrete application of exogenous NMU in the RVLM increases respiratory drive as indicated by an increase in PNamp without any effect on PNf as previously noted in SD [33]. The respiratory changes in response to NMU occurred immediately after the microinjections into the RVLM suggesting that these effects are not due to the drug diffusion to other respiratory (ventral respiratory column) regions of the brainstem. The RVLM is a functionally heterogeneous region in which cardiovascular and respiratory (Bötzinger and pre-Bötzinger) neurons are intermingled [14,28]. This close relationship, and likely synaptic input from respiratory neurons to RVLM neurons [26,40], along with close appositions between

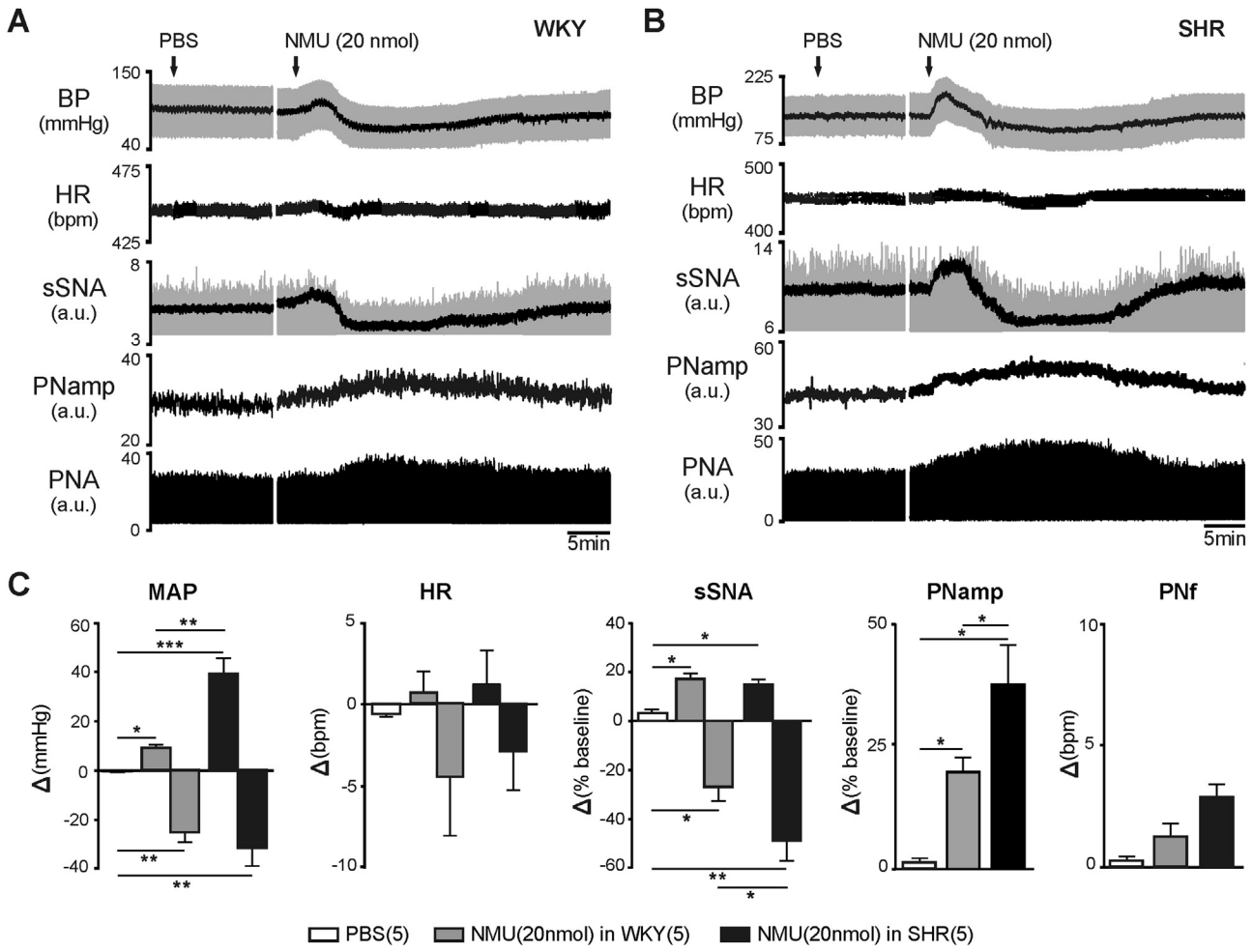

Fig. 4. Effect of intrathecal (i.t.) injection of neuromedin U (NMU) on cardiorespiraory function in spontaneously hypertensive rats (SHR) and Wistar–Kyoto rats (WKY). (A) and (B) Representative recording of blood pressure (BP) (gray – pulsatile and black – mean), heart rate (HR), splanchnic sympathetic nerve activity (sSNA) (gray – rectified and black – rectified and integrated) [arbitrary unit (a.u.)], phrenic nerve amplitude (PNamp) and rectified phrenic nerve activity (PNA) [arbitrary unit (a.u.)] before and after injection of phosphate buffered saline (PBS) or NMU (20 nmol) in WKY (A) and SHR (B). (C) Grouped data of maximum cardiorespiratory effects following PBS or NMU. Peak effects are shown as absolute (mean arterial pressure (MAP), HR, phrenic nerve frequency (PNf)) or percentage (sSNA, PNamp) change from respective basal values. Data are expressed as mean ± SE. Number of animals are shown in parentheses. $^{***}P < 0.001$, $^{**}P < 0.01$, $^{*}P < 0.05$ compared with PBS or compared between SHR and WKY. bpm, beats per minute for HR or bursts per minute for PNf.

bulbospinal tyrosine hydroxylase immunoreactive neurons of the C1 cell group and boutons from identified Bötzinger neurons [41] suggests a possible interaction between the two systems [8,25]. It remains to be determined if the effect of NMU on sympathetic activity is due to effects on antecedent respiratory neurons, or direct effects, or a combination of both.

Neurons in the RVLM integrate information from diverse inputs, including baroreceptors, chemoreceptors and nociceptors [17,27,29]. The sympathetic baroreflex is one of the most important regulatory mechanisms in the cardiovascular system, and baroreflex dysfunction is associated with many forms of hypertension, and may contribute to the development and maintenance of the disease [7,9,49]. Central NMU plays an important role in modulating sympathetic outflow and baroreflex [33,34]. Before experimental application of NMU, we observed a significantly higher resting blood pressure and a reduced barosensitivity, as indicated by a decrease in maximum gain, in SHR relative to age-matched WKY. Interestingly, in the present study, we found that microinjection of NMU into the RVLM impairs the baroreflex in SHR but not in the WKY. Neurochemical alterations in hypertension might alter afferent and efferent signaling or integration of baroreceptor information within the RVLM and might be the underlying cause of the impaired baroreflex observed here. Since NMU impairs the baroreflex selectively in SHR, the NMU system may, at least in part, be associated with the development and maintenance of hypertension in SHR.

In the present study we report for the first time the direct effects of NMU in the RVLM on somatosympathetic reflex in SHR and WKY. Electrical stimulation of sciatic nerve evokes an early and late excitatory peaks in sSNA of both SHR and WKY, as commonly observed in normotensive rats [21,22]. An interesting finding of this study is that the early peak in the control period is significantly lower in SHR compared with WKY. The increased baseline value of sSNA in SHR and the possibility of saturation of the excitability of sSNA cannot be excluded as a reason for this reduction in the early peak in SHR compared with WKY. Although the organization of the somatosympathetic reflex is identical in hypertensive and normotensive animals, the reflex excitability of the splanchnic sympathetic nerve, at least the early response, is decreased in SHR. This finding contradicts an earlier study where Scherbin and Tsyrlin [39] reported that the reflex excitability of the cervical sympathetic nerve was increased in SHR. Our data also show that NMU induces a significant decrease in the AUC of both peaks of somatosympathetic reflex in both SHR and WKY and mimics that which we have described previously in SD [33].

Table 1
Parameters describing baroreflex control of sSNA after bilateral microinjection of NMU (100 pmol) in the RVLM of SHR.

	Lower plateau (%)	Upper plateau (%)	Mid point (mmHg)	Max. gain (%/mmHg)	Range of SNA (%)	Threshold level (mmHg)	Saturation level (mmHg)	Operating range (mmHg)
Control	6.6 ± 3.5	99.3 ± 2.3	169.6 ± 9.2	−1.5 ± 0.2	92.6 ± 4.5	125.2 ± 13.8	214.1 ± 5.3	88.9 ± 9.9
NMU	12.0 ± 1.6 (ns)	82.8 ± 10.2 (ns)	135.0 ± 3.5 (*)	−0.9 ± 0.1 (**)	70.8 ± 10.7 (*)	87.22 ± 3.5 (*)	182.7 ± 6.2 (*)	95.5 ± 7.1 (ns)

Values are mean ± SE ($n = 5$). Maximum (Max.) gain is the slope of the sigmoid curve of best fit at the MAP corresponding to steepest part of the curve. ns, non-significant; $^{**}P < 0.01$, $^{*}P < 0.05$ compared with control.

Table 2
Parameters describing baroreflex control of sSNA after bilateral microinjection of NMU (100 pmol) in the RVLM of WKY.

	Lower plateau (%)	Upper plateau (%)	Mid point (mmHg)	Max. gain (%/mmHg)	Range of SNA (%)	Threshold level (mmHg)	Saturation level (mmHg)	Operating range (mmHg)
Control	30.0 ± 9.5	99.1 ± 5.1	113.4 ± 2.4	−1.9 ± 0.1	68.9 ± 14.5	81.3 ± 1.2	145.5 ± 5.0	64.1 ± 5.4
NMU	33.0 ± 12.8 (ns)	103.8 ± 10.4 (ns)	107.5 ± 5.1 (ns)	−1.8 ± 0.1 (ns)	70.7 ± 12.4 (ns)	76.4 ± 0.9 (ns)	138.5 ± 9.5 (ns)	62.1 ± 8.7 (ns)

Values are mean ± SE ($n = 5$). Maximum (Max.) gain is the slope of the sigmoid curve of best fit at the MAP corresponding to steepest part of the curve. ns, non-significant; compared with control.

Here we investigated the possibility that differences in the NMU system in the spinal cord contribute to the pathogenesis of hypertension in SHR. The data show that i.t. injection of NMU induces a biphasic vasomotor response, consisting of an initial pressor response along with sympathoexcitation followed by a prolonged vasodepression and sympathoinhibition both in SHR and WKY that was also observed in SD [34]. Our findings also show that the pressor response evoked by NMU is exaggerated in SHR, although not mediated by excessive increase in splanchnic sympathoexcitation. Interestingly sympathoinhibition by NMU is of a higher magnitude in SHR compared to WKY. Although we favor the mechanism underlying the biphasic effects of NMU described in an earlier study [34], another explanation for the exaggerated hypertensive and sympathoinhibitory response in the SHR is that NMU-receptor expressing SPN in SHR may be more sensitive to NMU. The adrenal medulla is important in the pathogenesis of hypertension in the SHR [2,35]. The possibility of an increase in the number of NMU-receptors expressed in SPN projecting to adrenal medulla in SHR or differences in the resting level of excitability of SPN in SHR cannot be ruled out and needs further investigation.

5. Conclusion

Exogenous NMU, administered i.t. or into the RVLM, has a biphasic effect on cardiovascular and sympathetic function. The NMU response includes a rapid transient increase followed by a prolonged intense inhibition of BP and sSNA in both SHR and WKY. Additionally, NMU increases respiratory drive. Our results also show that NMU attenuates somatosymapthetic reflex in both hypertensive and normotensive rats, and baroreflex in SHR. This study suggests a novel role of NMU in the central regulation of the autonomic nervous system and adaptive reflexes in both SHR and WKY. However the physiological role of NMU in each of these places deserves future study and remains to be explored. In conclusion, we speculate that NMU induces an exaggerated pressor response and baroreflex impairement in SHR suggesting that NMU might be partially responsible for the development of hypertension in SHR.

Acknowledgements

The authors are grateful to Dr Angelina Y Fong for helpful discussions. Work in the Authors' laboratory is supported by grants from the: National Health and Medical Research Council of Australia [1024489], Australian Research Council [DP110102110, DE120100992], National Heart Foundation [G 11S 5957]. A.A. Rahman and I.Z. Shahid are supported by Macquarie University Research Excellence Scholarships.

References

[1] Alexander SP, Mathie A, Peters JA. Guide to receptors and channels (GRAC). Br J Pharmacol 2011;164:S1–324.
[2] Borkowski KR. Effect of adrenal demedullation and adrenaline on hypertension development and vascular reactivity in young spontaneously hypertensive rats. J Auton Pharmacol 1991;11:1–14.
[3] Brighton PJ, Szekeres PG, Wise A, Willars GB. Signaling and ligand binding by recombinant neuromedin U receptors: evidence for dual coupling to $G\alpha_{q/11}$ and $G\alpha_i$ and an irreversible ligand–receptor interaction. Mol Pharmacol 2004;66:1544–56.
[4] Campese VM, Krol E. Neurogenic factors in renal hypertension. Curr Hypertens Rep 2002;4:256–60.
[5] Chu C, Jin Q, Kunitake T, Kato K, Nabekura T, Nakazato M, et al. Cardiovascular actions of central neuromedin U in conscious rats. Regul Pept 2002;105:29–34.
[6] Ciriello J, Li Z, De Oliveira CVR. Cardioacceleratory responses to hypocretin-1 injections into rostral ventromedial medulla. Brain Res 2003;991:84–95.
[7] Gonzalez E, Krieger A, Sapru H. Central resetting of baroreflex in the spontaneously hypertensive rat. Hypertension 1983;5:346–52.
[8] Haselton JR, Guyenet PG. Central respiratory modulation of medullary sympathoexcitatory neurons in rat. Am J Physiol 1989;256:R739–50.
[9] Head GA, Adams MA. Characterization of the baroreceptor heart rate reflex during development in spontaneously hypertensive rats. Clin Exp Pharmacol Physiol 1992;19:587–97.
[10] Hirooka Y, Sagara Y, Kishi T, Sunagawa K. Oxidative stress and central cardiovascular regulation – pathogenesis of hypertension and therapeutic aspects. Circ J 2010;74:827–35.
[11] Hong Y, Henry JL. Glutamate, NMDA and NMDA receptor antagonists: cardiovascular effects of intrathecal administration in the rat. Brain Res 1992;569:38–45.
[12] Howard AD, Wang R, Pong SS, Mellin TN, Strack A, Guan XM, et al. Identification of receptors for neuromedin U and its role in feeding. Nature 2000;406:70–4.
[13] Judy WV, Watanabe AM, Henry DP, Besch Jr HR, Murphy WR, Hockel GM. Sympathetic nerve activity: role in regulation of blood pressure in the spontaenously hypertensive rat. Circ Res 1976;38:II21–9.
[14] Kanjhan R, Lipski J, Kruszewska B, Rong W. A comparative study of presympathetic and Botzinger neurons in the rostral ventrolateral medulla (RVLM) of the rat. Brain Res 1995;699:19–32.
[15] Kent BB, Drane JW, Blumenstein B, Manning JW. A mathematical model to assess changes in the baroreceptor reflex. Cardiology 1972;57:295–310.
[16] Leenen FHH. Cardiovascular consequences of sympathetic hyperactivity. Can J Cardiol 1999;15:2A–7A.
[17] Mayorov DN, Head GA. Influence of rostral ventrolateral medulla on renal sympathetic baroreflex in conscious rabbits. Am J Physiol 2001;280:R577–87.
[18] McDowall LM, Dampney RAL. Calculation of threshold and saturation points of sigmoidal baroreflex function curves. Am J Physiol 2006;291:H2003–7.
[19] Minamino N, Kangawa K, Matsuo H. Neuromedin U-8 and U-25: novel uterus stimulating and hypertensive peptides identified in porcine spinal cord. Biochem Biophys Res Commun 1985;130:1078–85.
[20] Mitchell JD, Maguire JJ, Davenport AP. Emerging pharmacology and physiology of neuromedin U and the structurally related peptide neuromedin S. Br J Pharmacol 2009;158:87–103.
[21] Miyawaki T, Goodchild AK, Pilowsky PM. Activation of mu-opioid receptors in rat ventrolateral medulla selectively blocks baroreceptor reflexes while activation of delta opioid receptors blocks somato-sympathetic reflexes. Neuroscience 2002;109:133–44.
[22] Morrison SF, Reis DJ. Reticulospinal vasomotor neurons in the RVL mediate the somatosympathetic reflex. Am J Physiol 1989;256:R1084–97.
[23] Palatini P. Sympathetic overactivity in hypertension: a risk factor for cardiovascular disease. Curr Hypertens Rep 2001;3:S3–9.
[24] Peier A, Kosinski J, Cox-York K, Qian Y, Desai K, Feng Y, et al. The antiobesity effects of centrally administered neuromedin U and neuromedin S are mediated predominantly by the neuromedin U receptor 2 (NMUR2). Endocrinology 2009;150:3101–9.
[25] Pilowsky P. Good vibrations? Respiratory rhythms in the central control of blood pressure. Clin Exp Pharmacol Physiol 1995;22:594–604.
[26] Pilowsky P, Llewellyn-Smith IJ, Lipski J, Minson J, Arnolda L, Chalmers J. Projections from inspiratory neurons of the ventral respiratory group to the subretrofacial nucleus of the cat. Brain Res 1994;633:63–71.
[27] Pilowsky PM, Goodchild AK. Baroreceptor reflex pathways and neurotransmitters: 10 years on. J Hypertens 2002;20:1675–88.
[28] Pilowsky PM, Jiang C, Lipski J. An intracellular study of respiratory neurons in the rostral ventrolateral medulla of the rat and their relationship to catecholamine-containing neurons. J Comp Neurol 1990;301:604–17.
[29] Pilowsky PM, Lung MSY, Spirovski D, McMullan S. Differential regulation of the central neural cardiorespiratory system by metabotropic neurotransmitters. Philos Trans R Soc Lond B Biol Sci 2009;364:2537–52.
[30] Qiu DL, Chu CP, Shirasaka T, Nabekura T, Kunitake T, Kato K, et al. Neuromedin U depolarizes rat hypothalamic paraventricular nucleus neurons in vitro by enhancing I_H channel activity. J Neurophysiol 2003;90:843–50.
[31] Raddatz R, Wilson AE, Artymyshyn R, Bonini JA, Borowsky B, Boteju LW, et al. Identification and characterization of two neuromedin U receptors differentially expressed in peripheral tissues and the central nervous system. J Biol Chem 2000;275:32452–9.
[32] Rahman AA, Shahid IZ, Fong AY, Hammond AM, Pilowsky PM. Vasostatin I (CgA_{17-76}) vasoconstricts rat splanchnic vascular bed but does not affect central cardiovascular function. Auton Neurosci 2012;166:22–8.
[33] Rahman AA, Shahid IZ, Pilowsky PM. Differential cardiorespiratory and sympathetic reflex responses to microinjection of neuromedin U in rat rostral ventrolateral medulla. J Pharmacol Exp Ther 2012;341:213–24.
[34] Rahman AA, Shahid IZ, Pilowsky PM. Intrathecal neuromedin U induces biphasic effects on sympathetic vasomotor tone, increases respiratory drive and attenuates sympathetic reflexes in rat. Br J Pharmacol 2011;164:617–31.
[35] Schramm LP, Chornoboy ES. Sympathetic activity in spontaneously hypertensive rats after spinal transection. Am J Physiol 1982;243:R506–11.
[36] Seyedabadi M, Goodchild AK, Pilowsky PM. Differential role of kinases in brain stem of hypertensive and normotensive rats. Hypertension 2001;38:1087–92.
[37] Shahid IZ, Rahman AA, Pilowsky PM. Intrathecal orexin A increases sympathetic outflow and respiratory drive, enhances baroreflex sensitivity and blocks the somato-sympathetic reflex. Br J Pharmacol 2011;162:961–73.
[38] Shahid IZ, Rahman AA, Pilowsky PM. Orexin A in rat rostral ventrolateral medulla is pressor, sympathoexcitatory, increases barosensitivity and attenuates the somatosympathetic reflex. Br J Pharmacol 2012;167:2292–303.
[39] Shcherbin YI, Tsyrlin VA. Comparison of the somatosympathetic reflex in normotensive and spontaneously hypertensive rats. Neurosci Behav Physiol 2004;34:563–7.

[40] Sun Q-J, Minson J, Llewellyn-Smith IJ, Arnolda L, Chalmers J, Pilowsky P. Bötzinger neurons project towards bulbospinal neurons in the rostral ventrolateral medulla of the rat. J Comp Neurol 1997;388:23–31.
[41] Sun QJ, Pilowsky P, Minson J, Arnolda L, Chalmers J, Llewellyn-Smith IJ. Close appositions between tyrosine hydroxylase immunoreactive boutons and respiratory neurons in the rat ventrolateral medulla. J Comp Neurol 1994;340:1–10.
[42] Sved A, Ito S, Sved J. Brainstem mechanisms of hypertension: role of the rostral ventrolateral medulla. Curr Hypertens Rep 2003;5:262–8.
[43] Szekeres PG, Muir AI, Spinage LD, Miller JE, Butler SI, Smith A, et al. Neuromedin U is a potent agonist at the orphan G protein-coupled receptor FM3. J Biol Chem 2000;275:20247–50.
[44] Tanida M, Satomi J, Shen J, Nagai K. Autonomic and cardiovascular effects of central neuromedin U in rats. Physiol Behav 2009;96:282–8.
[45] Tsubota Y, Kakimoto N, Owada-Makabe K, Yukawa K, Liang XM, Mune M, et al. Hypotensive effects of neuromedin U microinjected into the cardiovascular-related region of the rat nucleus tractus solitarius. Neuroreport 2003;14:2387–90.
[46] Veerasingham SJ, Yamazato M, Berecek KH, Wyss JM, Raizada MK. Increased PI3-kinase in presympathetic brain areas of the spontaneously hypertensive rat. Circ Res 2005;96:277–9.
[47] Wang F, Zhang Y, Jiang X, Zhang Y, Zhang L, Gong S, et al. Neuromedin U inhibits T-type Ca^{2+} channel currents and decreases membrane excitability in small dorsal root ganglia neurons in mice. Cell Calcium 2011;49:12–22.
[48] Westfall TD, McCafferty GP, Pullen M, Gruver S, Sulpizio AC, Aiyar VN, et al. Characterization of neuromedin U effects in canine smooth muscle. J Pharmacol Exp Ther 2002;301:987–92.
[49] Widdop RE, Verberne AJM, Jarrott B, Louis WJ. Impaired arterial baroreceptor reflex and cardiopulmonary vagal reflex in conscious spontaneously hypertensive rats. J Hypertens 1990;8:269–75.
[50] Zeng H, Gragerov A, Hohmann JG, Pavlova MN, Schimpf BA, Xu H, et al. Neuromedin U receptor 2-deficient mice display differential responses in sensory perception, stress, and feeding. Mol Cell Biol 2006;26:9352–63.

Four (4) pages have removed from Open Access version as they may contain sensitive/confidential content.